# Dissertation

# Tracking the trace: Factors contributing to tumor dissemination

submitted by

**Katja Sallinger, BSc., MSc.**

for the Academic Degree of

**Doctor of Medical Science**

**(Dr. scient. med.)**

at the

Medical University of Graz

Division of Cell Biology, Histology and Embryology,
Gottfried Schatz Research Center for Cell Signaling, Metabolism and Aging

and

Center for Biomarker Research in Medicine (CBmed)

under the supervision of

**Research Prof. PD Amin El-Heliebi, MSc, PhD**

2023

# Statutory declaration

I hereby declare that this thesis is my own original work and that I have fully acknowledged by name all of those individuals and organizations that have contributed to the research constituting this thesis. Due acknowledgement has been made to all other material used. Throughout this thesis and in all related publications I followed the “Standards of Good Scientific Practice and Ombuds Committee at the Medical University of Graz “.

Graz, July 2023 e.h. Katja Sallinger

# Disclosures

Please note that parts of this thesis and work related to this thesis have been published in:

> **Sallinger, K**., *et al.* (2023). Spatial tumour gene signature discriminates neoplastic from non-neoplastic compartments in colon cancer: unravelling predictive biomarkers for relapse. Journal of Translational Medicine, 21(1), 528. https://doi.org/10.1186/s12967-023-04384-0



All co-authors who contributed to these publications are listed below and gave their explicit permission to use the published data in this thesis.

**Michael Gruber,** Division of Cell Biology, Histology and Embryology, Gottfried Schatz Research Center, Medical University of Graz, Austria

**Christin-Therese Müller,** Division of Cell Biology, Histology and Embryology, Gottfried Schatz Research Center, Medical University of Graz, Austria

**Lilli Bonstingl,** Division of Cell Biology, Histology and Embryology, Gottfried Schatz Research Center, Medical University of Graz, Austria
Center for Biomarker Research in Medicine (CBmed), Graz, Austria

**Elisabeth Pritz,** Division of Cell Biology, Histology and Embryology, Gottfried Schatz Research Center, Medical University of Graz, Austria

**Karin Pankratz,** Division of Cell Biology, Histology and Embryology, Gottfried Schatz Research Center, Medical University of Graz, Austria

**Armin Gerger,** Division of Oncology, Department of Internal Medicine, Medical University of Graz, Graz, Austria

**Maria Anna Smolle,** Department of Orthopaedics and Trauma, Medical University of Graz, Austria

**Ariane Aigelsreiter,** Diagnostic and Research Institute of Pathology, Medical University of Graz, Graz, Austria

**Olga Surova,** Science for Life Laboratory, Department of Biochemistry and Biophysics, Stockholm University, 17165 Solna, Sweden

**Jessica Svedlund,** Science for Life Laboratory, Department of Biochemistry and Biophysics, Stockholm University, 17165 Solna, Sweden
10x Genomics,Life City, Solnavagen 3H, 113 63 Stockholm, Sweden

**Mats Nilsson,** Science for Life Laboratory, Department of Biochemistry and Biophysics, Stockholm University, 17165 Solna, Sweden

**Thomas Kroneis,** Division of Cell Biology, Histology and Embryology, Gottfried Schatz Research Center, Medical University of Graz, Austria
Center for Biomarker Research in Medicine (CBmed), Graz, Austria

**Amin El-Heliebi**, Division of Cell Biology, Histology and Embryology, Gottfried Schatz Research Center, Medical University of Graz, Austria
Center for Biomarker Research in Medicine (CBmed), Graz, Austria

# Acknowledgements

Dr.sci.med student Katja Sallinger received funding from the Medical University of Graz through the Doctoral Program Translational Molecular and Cellular Biosciences and the Center for Biomarker Research in Medicine (CBmed).

The K1 COMET Competence Center CBmed was funded by the Federal Ministry of Transport, Innovation and Technology (BMVIT), the Federal Ministry of Science, Research and Economy (BMWFW), Land Steiermark (Department 12, Business and Innovation), the Styrian Business Promotion Agency (SFG), and the Vienna Business Agency. The COMET program is executed by the Austrian Research Promotion Agency (FFG).

This work was performed in collaboration with Stefan Kühberger under the supervision of Ellen Heitzer (Institute of Human Genetics, Diagnostic & Research Center for Molecular BioMedicine, Medical University of Graz, Austria) and Sebastian Tiesmeyer under the supervision of Naveed Ishaque (Digital Health Center, Berlin Institute of Health (BIH) at Charité - Universitätsmedizin Berlin, Germany). The collaboration with Berlin was supported by the ”Forschungsfeld Krebsforschung” through the grant of a Travel Fellowship.

I want to acknowledge the team of Mats Nilsson at SciLifeLab from Stockholm University and the company CARTANA, for sharing their expertise and setting up the *in situ* sequencing panel with us, the Biobank Graz and the LKH Graz West for providing the tissues, as well as Daniel Kummer at the Medical University of Graz for the technical support.

I am grateful to everyone at the Division of Cell Biology, Histology, and Embryology for their professional expertise and emotional support throughout the challenging phases of my thesis, which resulted in the development of strong friendships. I especially want to express my gratitude to my supervisor, Amin El-Heliebi, for providing me with the opportunity to join his team, placing trust in me to establish a new methodology, and his enthusiasm to challenge me to step out of my comfort zone and surpass my personal limits. Next, I would like to extend my gratitude to my co-supervisor, Thomas Kroneis, for giving me with the opportunity to join his team after my three-year PhD journey and enabling me to complete my dissertation.

I express my appreciation to my thesis committee members, Ellen Heitzer and Thomas Bauernhofer, for their priceless input at the committee meetings.

I want to give a special thanks to Lilli for her support, both professionally and emotionally, throughout all the ups and downs we've experienced together. Her motivation during times when I couldn't push on was invaluable. This entire project wouldn't have been possible without her knowledge, patience, and human empathy.

I also want to thank Michael for his participation in this project. Without his computational expertise, we wouldn't have been able to carry out the analyses and couldn't have successfully finished the project.

Next, I want to thank my former colleague and friend, Lissi, for always providing me with valuable advice, standing by my side, and offering helpful guidance during emotionally challenging phases, as well as motivating me.

Karin, thanks a lot for consistently being a willing listener and for offering diverse perspectives and solutions. I truly value our conversations.

I truly thank Hillary Rebernig for proofreading the thesis.

I want to thank my long-time friends for their support, understanding, and willingness to help me take a break from work to clear my mind, which allowed me to refocus on my tasks again.

Finally, I would like to express my gratitude to my family, particularly my parents and my aunt, for their unwavering love and support throughout my entire life, especially during the challenging past years. They have always believed in me and motivated me when I was on the brink of failure.

# Table of contents

## List of figures

# List of tables

## List of supplementary figures



## List of supplementary tables

## Abbreviations

| | |
|---|---|
| AP | Adapter probe |
| ASCO | Adjuvant Therapy for Stage II Colon Cancer |
| ACT | Adjuvant chemotherapy |
| CEA | Carcinoembryonic antigen |
| CRC | Colorectal cancer |
| ctDNA | Cell-free circulating tumor DNA |
| CT | Computed tomography |
| CTCs | Circulating tumor cells |
| Cy3 | Cyanine 3 |
| Cy7 | Cyanine 7 |
| DAPI | 4’,6-diamidino-2-phenylindole |
| DEPC | Diethyl pyrocarbonate |
| DO | Detection oligonucleotides |
| DNA | Deoxyribonucleic acid |
| dRNA-HybISS | Direct RNA - Hybridization based *in situ* sequencing |
| EFI | Extended focus imaging |
| EMT | Epithelial-mesenchymal transition |
| ESMO | European Society for Medical Oncology |
| FFPE | Formalin-fixed, paraffin-embedded |
| FIT | Faecal immunochemical testing |
| FITC | Fluorescein isothiocyanate |
| FU | Fluorouracil |
| H&E | Haematoxylin and eosin stain |
| HybISS | Hybridization based *in situ* sequencing |
| LED | Light-emitting diode |
| ISS | *In situ* sequencing |

| | |
|---|---|
| IS | *In situ* |
| KDE | Kernel Density Estimation |
| mRNA | Messenger ribonucleic acid |
| MMR/MSI | Mismatch repair/ Microsatellite instability |
| MSS | Microsatellite stability |
| nt | nucleotide |
| PBS | Phosphate buffered saline |
| PBS-Tween | 0.05 % Tween-20 in PBS |
| PCA | Principal Component Analysis |
| PCR | Polymerase chain reaction |
| PLP | Padlock probe |
| RCA | Rolling circle amplification |
| RCP | Rolling circle product |
| RM | Reaction mix |
| RNA | Ribonucleic acid |
| RNAseq | RNA sequencing |
| scRNAseq | single cell RNA sequencing |
| SP | Sequencing probe |
| t-SNE | t-distributed Stochastic Neighbour Embedding |
| TSO500 | TruSight Oncology 500 |
| UICC | Union for International Cancer Control |
| WB | Wash buffer |

# Abstract

Therapeutic management of stage II colon cancer remains difficult regarding the decision to either opt for or against the administration of adjuvant chemotherapy (Sallinger et al., 2023). Recurrence of cancer within five years after tumor resection is of significant concern as it is related with a high risk of cancer-associated deaths. Predictive biomarkers are urgently needed. We, therefore, hypothesize that the spatial tissue composition of relapsed and non-relapsed colon cancer stage II patients after tumor resection reveals relevant biomarkers (Sallinger et al., 2023).

The spatial tissue composition of stage II colon cancer patients was examined by a novel cutting-edge spatial transcriptomic technology, namely *in situ* sequencing, with single cell and sub-cellular resolution. A panel of 176 genes was designed to investigate various cancer-associated processes and components of the tumor microenvironment. Based on spatial expression patterns generated by *in situ* sequencing (GTC-tool – Genes-To-Count), we identified a tumor gene signature to subclassify tissue into neoplastic and non-neoplastic tissue structures. Three differentially expressed genes (*FGFR2, MMP11* and *OTOP2*) in the neoplastic tissue compartments of patients who developed a relapse in comparison to non-relapsed patients were identified, which predict recurrence in stage II colon cancer (Sallinger et al., 2023). Additionally, to confirm the specificity of the used technology, cell-phenotyping of one patient sample was performed by using the *in situ* sequencing generated data.

In conclusion, this thesis highlights the importance of understanding the biological processes that contribute to tumor dissemination and provides insight into the underlying mechanisms. We were the first to apply a direct RNA-hybridization based *in situ* sequencing approach in colon cancer for the purpose of identifying new potential biomarkers. This could lead to more effective and precise therapies for colon cancer stage II patients.

# Zusammenfassung

Die therapeutische Behandlung von Darmkrebspatienten im Stadium II bleibt herausfordernd hinsichtlich der Entscheidung, ob eine adjuvante Chemotherapie verabreicht werden sollte oder nicht. Das Wiederauftreten von Tumoren innerhalb von fünf Jahren nach der Tumorresektion bleibt von erheblicher Bedeutung, da es mit einem hohen Risiko für krebsbedingte Todesfälle verbunden ist. Daher ist es von dringender Notwendigkeit prädiktive Biomarker zu identifizieren, welche die Wahrscheinlichkeit des Wiederauftretens prognostizieren. In dieser Arbeit wurde die räumliche Gewebezusammensetzung von Patienten mit Darmkrebs im Stadium II untersucht und Patienten die einen Rückfall erlitten hatten mit denjenigen, die keinen Rückfall hatten, verglichen. Ziel der Arbeit war es in den verschiedenen Patientengruppen relevante Biomarker zu benennen.

Die räumliche Gewebezusammensetzung von Patienten mit Darmkrebs im Stadium II wurde mit einer neuen, hochmodernen, räumlichen Transkriptomik-Technologie untersucht. Die Methodik, welche auch *In-situ* Sequenzierung (ISS) genannt wird, erlaubt die räumliche Zuordnung von RNA Transkripten mit Einzelzell- und subzellulärer Auflösung. Ein Panel von 176 Genen wurde entworfen, um verschiedene krebsassoziierte Prozesse und Komponenten der Tumorumgebung zu untersuchen. Basierend auf den räumlichen Expressionsmustern, welche durch die dRNA-HybISS-Analyse erhalten wurden, konnte eine Tumorgen-Signatur zur Unterscheidung von neoplastischen und nicht-neoplastischen Gewebekompartimenten identifiziert werden (GTC-Tool – Genes-To-Count). Drei differentiell exprimierte Transkripte (*FGFR2, MMP11* und *OTOP2*) in den neoplastischen Gewebekompartimenten von Patienten, die einen Rückfall erlitten hatten, verglichen zu Patienten ohne Rückfall wurden als Prädiktoren für ein Wiederauftreten von Darmkrebs im Stadium II identifiziert. Zusätzlich wurde zur Bestätigung der Spezifität der verwendeten Technologie die Zell-Phänotypisierung einer Patientenprobe mit den durch dRNA-HybISS generierten Daten durchgeführt.

Zusammenfassend zeigt diese Arbeit die enorme Relevanz des Verständnisses von biologischen Prozessen, die zur Tumorausbreitung beitragen, und bietet Einblicke in deren zugrundeliegenden Mechanismen. Hierbei wurde zum ersten Mal ein direkter RNA-ISS-Hybridisierungsansatz auf Darmkrebsgewebe angewandt, um neue potenzielle Biomarker zu identifizieren, die zu effektiveren und präziseren Therapien für Darmkrebs - Patienten im Stadium II führen könnten.

.

# 1. Introduction

## 1.1. Colorectal cancer

In the year 2020 approximately 1.9 million cases of colorectal cancer (CRC) and 935.000 CRC related deaths were predicted worldwide, making CRC the third most common malignancy and the second highest ranked cancer in cancer associated mortality (Sung et al., 2021). The incidence of CRC among adults aged 20-49 years in the European Union is on the rise, while factors such as consumption of alcohol, unhealthy diets, lack of exercise, obesity and aging of the population are to blame for this yearly increase in incidence (Vuik et al., 2019). The overall survival strongly depends on the stage at diagnosis with a 90% overall 5-year survival rate at stage I and a 10% overall survival rate at metastatic stages, the latter figure highlighting the importance of early detection (Cardoso et al., 2022). Although therapeutic management has improved significantly in the last years, management of stage II colon cancer remains challenging in deciding for or against the administration of adjuvant chemotherapy (ACT) (Rebuzzi et al., 2020).

### 1.1.1. Histology of the colon

The colon belongs to the gastrointestinal tract and therefore is characterized by the following fundamental structures: mucosa, submucosa, muscularis and the serosa (Lüllmann-Rauch & Asan, 2015). The mucosa consists of the epithelium, the lamina propria and muscularis mucosae containing crypts with enteroendocrine cells producing hormones and goblet cells that are responsible for the production of mucus for the transport of faeces (Lüllmann-Rauch & Asan, 2015). The submucosa is comprised of loose connective tissue, encompassing blood- and lymphatic vessels, nerve plexuses and adipose tissue structures (Lüllmann-Rauch & Asan, 2015). The muscularis is composed of an inner circular (stratum circulare) and an outer longitudinal (stratum longitudinale) layer and the plexus myentericus located in between those two layers (Lüllmann-Rauch & Asan, 2015).The serosa, a thin layer of tissue, covers the exterior of the colon in order to provide protection (Lüllmann-Rauch & Asan, 2015).

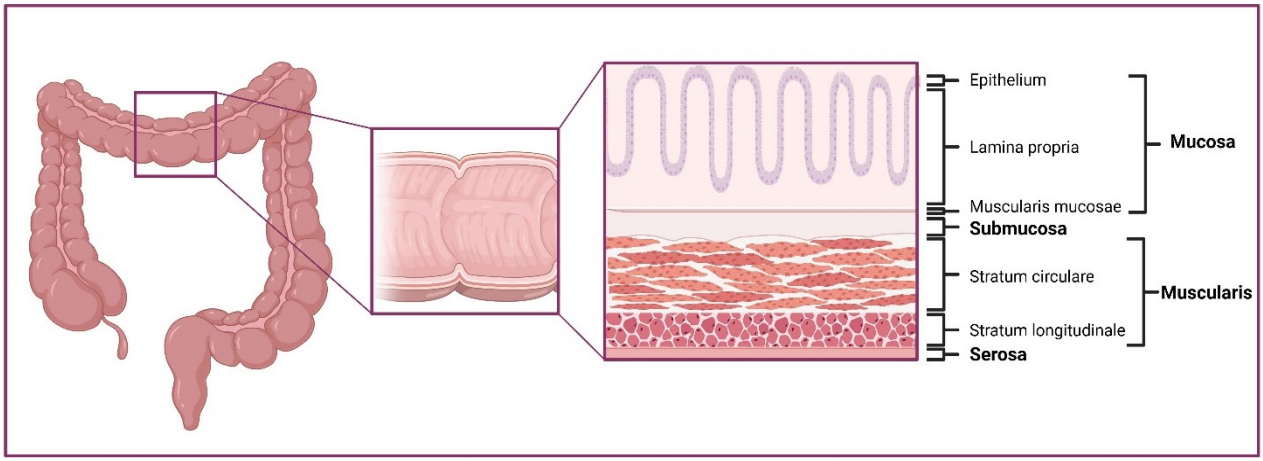


***Figure 1: Histology of the colon***

*Basic tissue structures of the colon are depicted which can be divided into the mucosa, the submucosa, the muscularis and the serosa.*

*Created with BioRender.com*

### 1.1.2. CRC development

CRC often develops slowly without symptoms until it reaches a considerable size, in centimetres, at which point it leads to a blockage of faeces, cramps or bleeding (Simon, 2016). In most cases, the development is a multi-step process, which involves morphological and genetical changes over time (Lochhead et al., 2014). Typically, CRC evolves from a benign polyp, which is a cluster of abnormal cells located in the mucosa and stretches into the lumen of the intestine (American Cancer Society, 2011; Simon, 2016). Over time, cells within these polyps undergo specific genetic changes and gain the ability to invade the bowel wall (Simon, 2016). Some cells undergo even further alterations and spread to local lymph nodes later on invading different metastatic sites (Simon, 2016). Only very few polyps obtain malignant character and those that do take several years (Simon, 2016). Two different types of polyps that could develop into malignant structures exist: adenomas and sessile serrated polyps (SSP) (Simon, 2016). 60-70% of CRCs develop from adenomas and the remaining percent from SSPs (Simon, 2016). When polyps start to proliferate, their size increases and a series of genetic changes, either inherited or acquired, take place (Simon, 2016). Inherited mutations such as the *MLH1, MSH2, MLH6, APC*, *PMS1* and *PMS2* gene mutations are very uncommon and account for roughly only 5% of all CRC cases (Mármol et al., 2017). Traditionally, two different pathways are known to be involved in the development of CRC; -the gatekeeper and the caretaker pathway. The first is responsible for approximately 85% of sporadic CRC cases (Weitz et al., 2005). According to this pathway, the first mutations take place in the *APC* gene, activating the transcription of genes involved in invasion and tumorigenesis,

followed by mutations in the *KRAS* and *PI3K* oncogenes (Mármol et al., 2017). These gene alterations affect survival, differentiation, and cell growth and further lead to a loss of function in *TP53,* which plays a key role in cellular functions such as apoptosis and transcription, ultimately resulting in carcinogenesis (Mármol et al., 2017; Simon, 2016). Caretaker pathway characteristics are epigenetic changes such as histone acetylation and DNA methylation or mutations of genes responsible for genetic stability such as mismatch repair (MMR) genes (Weitz et al., 2005). 15% of sporadic CRCs as well as hereditary nonpolyposis CRCs (HNPCC) are caused by this pathway (Weitz et al., 2005). Together with the familial adenomatous polyposis (FAP), HNPCC belongs to the subtype of hereditary cancer syndromes and is associated with approximately 5-10% of CRCs (Weitz et al., 2005). These two pathways cannot be completely separated from each other, as MMR genes can influence cell proliferation and the *APC* gene could act as a caretaker (Weitz et al., 2005).

### 1.1.3. Screening

CRC screening is recommended for individuals from the age of 50 as it can prevent cancer mortality and high treatment costs by detecting lesions prior to malignancy and early-stage cancer prior to becoming metastatic (Mariotto et al., 2011; Simon, 2016). Several different screening procedures are available, whereby colonoscopy, sigmoidoscopy, computed tomography (CT) colonography and faecal immunochemical testing (FIT) procedures are the most common (Simon, 2016). Colonoscopies are the gold standard as they allow for the detection of precancerous and cancerous CRC lesions of the entire colon with a sensitivity of more than 95% (Avid et al., 2000; Simon, 2016) . Even though sigmoidoscopies do not require sedation and also have a sensitivity of 95%, this procedure is less frequently used as they only allow for the examination of the distal half of the colon (Joe V. Selby, 1992; Simon, 2016). CT colonographies are used for suboptimal colonoscopy candidate patients and allow for the identification of 90% of CRC patients with cancers and adenomas by generating a three-dimensional image of the colon (Johnson et al., 2008). FIT tests detect haemoglobin in the stool of patients, are non-invasive and can be performed at home. This diagnostic method, however, can lead to false-negative results due to sporadic bleedings from lesions (Simon, 2016).

### 1.1.4. Staging

Staging of cancers is used to describe the severity of the disease und provides a basis for prognosis and therapy decisions (Su et al., 2022). According to the Union for International Cancer Control Tumor-Lymph Node-Metastasis (TNM) staging system, malignancies can be divided into

5 different stages: 0, I, II, III and IV. These stages give information on the localisation and the size of the tumor, how much nearby tissue is affected and the spread to lymph nodes or other organs (Su et al., 2022).

#### 1.1.4.1. Tumor (T) Staging

The T-stage is used to indicate the size of the malignancy and its invasiveness (Rosen RD & Sapra A., 2023). While T0 describes the absence of a tumor, T1-T4 are used to characterize the size of the neoplastic tissue and the involved histological structures: In T1 classified tumors the submucosa is invaded, whereas T2 tumors show an invasion of the muscularis propria (Rosen RD & Sapra A., 2023). In T3 cancers the subserosa is affected and T4 tumors indicate an invasion of all layers of colonic structures in addition to the peritoneum (Rosen RD & Sapra A., 2023). In general, a higher T-stage is associated with poorer overall survival and disease-free survival of the patient. Additionally, with a higher T-stage, the risk of nodal metastasis and distant metastasis increases (Chen et al., 2021).

#### 1.1.4.2. Nodal (N) Staging

The N-stage is used to characterize the involvement of regional lymph nodes (Rosen RD & Sapra A., 2023). N0 indicates that no lymph nodes have been affected by the spread, N1 describes the involvement of 1-3 regional nodes, in N2 4-6 nodes have been affected, while for N3 7 or more regional nodes are involved (Rosen RD & Sapra A., 2023). In general, an increased count of involved nodes and a low lymph node yield (i.e. a low number of resected lymph nodes) are associated with a worse overall survival rate (K. Chen et al., 2021).

#### 1.1.4.3. Metastasis (M) Staging

The M-stage describes the absence or presence of metastases of the primary neoplastic tissue (Rosen RD & Sapra A., 2023). M0 indicates the absence of distant metastasis, while M1 describes evidence of metastasis (Rosen RD & Sapra A., 2023). For a more detailed diagnosis the classification can be subdivided, whereby M1a identifies tumors that have spread to one area, M1b cancers have spread to 2 or more areas and M1c tumors have spread to the surface of the peritoneum (Rosen RD & Sapra A., 2023). The M-staging represents the strongest prediction factor for prognosis, whereby patients with distant metastasis have a 5-year overall survival rate of less than 10% (K. Chen et al., 2021).

### 1.1.5. CRC stage II subtypes

CRC stage II can be subcategorized into three stages: IIA, IIB and IIC (Church et al., 2013; Mahul B. Amin & Stephen B. Edge, 2017).

In stage IIA CRC patients, the tumor has spread through the muscle layer (muscularis) into the serosa without infiltrating the visceral peritoneum (Church et al., 2013; Mahul B. Amin & Stephen B. Edge, 2017). In stage IIB CRC, the tumor has spread through the serosa to the visceral peritoneum and in stage IIC, the cancer has infiltrated the serosa to the visceral peritoneum and has spread to nearby organs (Church et al., 2013; Mahul B. Amin & Stephen B. Edge, 2017).

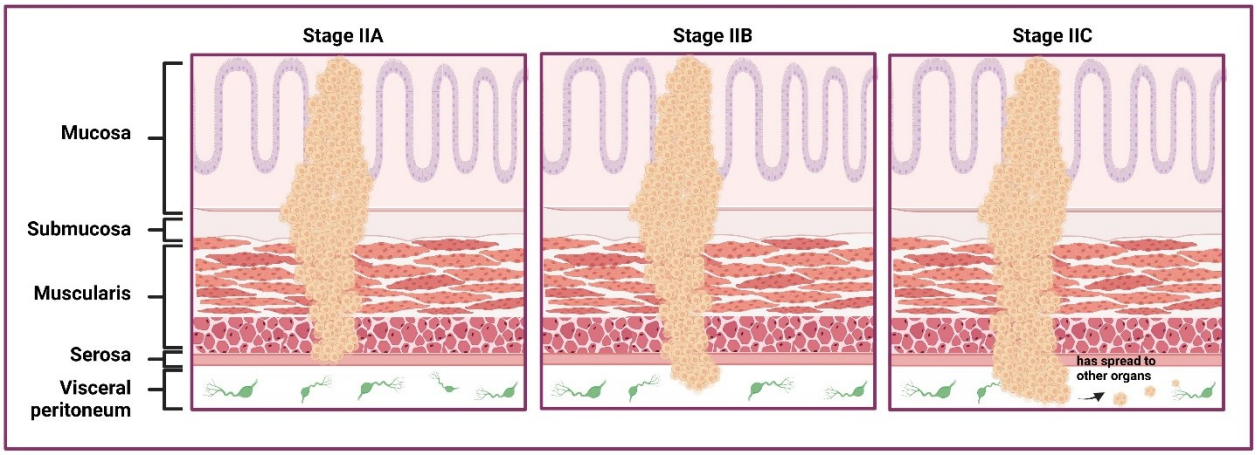


***Figure 2: Colorectal cancer stage II subtypes: IIA, IIB and IIC.***

*CRC stage II cancer can be divided into three subtypes: IIA, IIB and IIC. IIA CRC spread through the muscularis to the serosa whereas stage IIB tumors infiltrate through the serosa into the visceral peritoneum. In stage IIC CRC the cancer has spread to the visceral peritoneum and additionally infiltrated nearby organs.*

*Created with BioRender.com*

### 1.1.6. Relapse

For two-thirds of all CRC patients surgical resection of the neoplastic tissue remains the best treatment option with curative intent at time of diagnosis (Ryuk et al., 2014). Recurrence of disease, however, is of significant concern as it relates with a high risk of tumor-associated deaths (Ryuk et al., 2014). Recurrence, commonly referred to as relapse, emerges in 30-50% of patients within two years after surgery, whereby survival, especially for early relapsed patients, remains poor (Ryuk et al., 2014). Additionally, time to recurrence differs by TNM stage (Kobayashi et al., 2007). For stage I patients, cumulative recurrence rate was found to increase constantly for 5 years, whereas for patients with stage II and III CRC diagnosis, a rapid increase was observed for the first 3 years, followed by a slow elevation for the following 2 years (Kobayashi et al., 2007).

Recurrence can develop at different sites of the body, whereby the liver and the lung being most frequently affected, followed by local and anastomotic tumor relapses (Kobayashi et al., 2007).
A variety of different factors such as gender, age, tumor stage, genetic predisposition, vascular invasion, perineural invasion, postoperative carcinoembryonic antigen (CEA) levels and the presence of micrometastasis at the time of surgery can attribute to the development of a relapse (Desch et al., 2005; Tsai et al., 2009).
Therefore, identification of these high-risk Union for International Cancer Control stage I–III CRC patients with early relapse is important, as defining patients with this tumor entity could allow for an enhanced follow-up and therapeutic program (Tsai et al., 2009).

## 1.2. Therapeutic management of CRC

Treatment of CRC highly depends on the stage of disease (Ahmed, 2020). Stage I tumors can be treated by surgical resection of the neoplastic tissue and local lymph nodes, whereby correct staging depends on the precise examination of lymph nodes (Ahmed, 2020). For stage II, surgical resection of the tumor without administration of adjuvant chemotherapy treatment (ACT), excluding patients indicating high risk features such as positive margins, localized perforation, less than 12 lymph nodes, lymphovascular invasion or differentiated cancer, is recommended (Ahmed, 2020). Stage III patients are treated by surgical resection of the tumor, followed by ACT with 6 cycles of 5-flurouracil with leucovorin and oxaliplatin (FOL-FOX) or capecitabine and oxaliplatin (Capox) (Ahmed, 2020). Stage IV CRC is treated by a combination of palliative surgery, chemotherapy, immunotherapy, checkpoint inhibitor therapy and radiotherapy (Ahmed, 2020).

Due to the improvement of therapeutic treatment and the development of screening procedures, death rates in the USA, as compared to those in 1970, decreased by approximately 50% in 2016, while survival time increased (Xie et al., 2020). Although, chemotherapy in stage III and IV remains the backbone of treatment, the development of new treatment approaches is essential, due to its drawbacks such as unsatisfying response rate and systemic toxicity (Xie et al., 2020).

### 1.2.1. Treatment of stage II CRC patients

When deciding whether or not patients should receive ACT to reduce the risk of recurrence, the risk estimation of relapse is of great importance (Argilés et al., 2020). For stage III CRC treatment administration of ACT after resection of the tumor is the gold standard, as it provides a long-term survival gain of 8.7% to 21.5% (Rebuzzi et al., 2020).

According to various studies, however, this survival benefit is not realized for stage II CRC, resulting in contradicting conclusions regarding the advantageous nature of chemotherapy after resection (Rebuzzi et al., 2020). The overall survival rate in those trials shows very little improvement - an outcome, which could, furthermore, only be a side effect as the majority of stage II CRC patients are predicted to have a good long-term survival anyway (Rebuzzi et al., 2020).

### 1.2.2. ESMO versus ASCO guidelines for the treatment of stage II CRC

According to the ESMO (European Society for Medical Oncology) guidelines published in 2020, risk of tumor recurrence after resection for stage II CRC patients is assessed by integrating a combination of the mismatch repair/ microsatellite instability (MMR/MSI) status and clinicopathological features (figure 3a) (Argilés et al., 2020). Major clinicopathological factors, such as the presence of <12 lymph nodes or pT4 stage, present an elevated risk of relapse in comparison to minor factors, which are less related with an increased risk of recurrence (Argilés et al., 2020). Follow-up is recommended for low-risk stage patients, whereas patients with an intermediate- or high-risk are recommended to receive ACT (Argilés et al., 2020). For patients with an intermediate-risk, defined by microsatellite stability (MSS) plus risk factors except the presence of <12 lymph nodes or pT4 stage such as perineural invasion, vascular invasion, lymphatic invasion or tumor obstruction, the administration of fluoropyrimidine for 6 months is recommended (Argilés et al., 2020). High-risk patients should additionally receive oxaliplatin for 3-6 months after 6 months of fluoropyrimidine treatment (Argilés et al., 2020). Timing of ACT is, furthermore, of great importance, as a delay of more than 8 weeks after surgery is related with a higher risk of death (Argilés et al., 2020).

According to the ASCO (Adjuvant Therapy for Stage II Colon Cancer) guidelines ACT should not be offered to patients with low-risk features, including patients with stage IIA diagnosis with a minimum of 12 sampled lymph nodes, tumors without lymphovascular and perineural invasion, tumor perforation or poor tumor grade (figure 3b) (Baxter et al., 2021). It may be offered to IIA CRC patients with high-risk of recurrence, including patients with a lower number of 12 sampled lymph nodes, tumors with lymphovascular and perineural invasion, tumor perforation or poor tumor grade (Baxter et al., 2021). For patients with stage IIB and IIC CRC administration of fluoropyrimidine for 6 months is recommended and potential benefits and risks of adding oxaliplatin for 3-6 months should be discussed (Baxter et al., 2021).

.

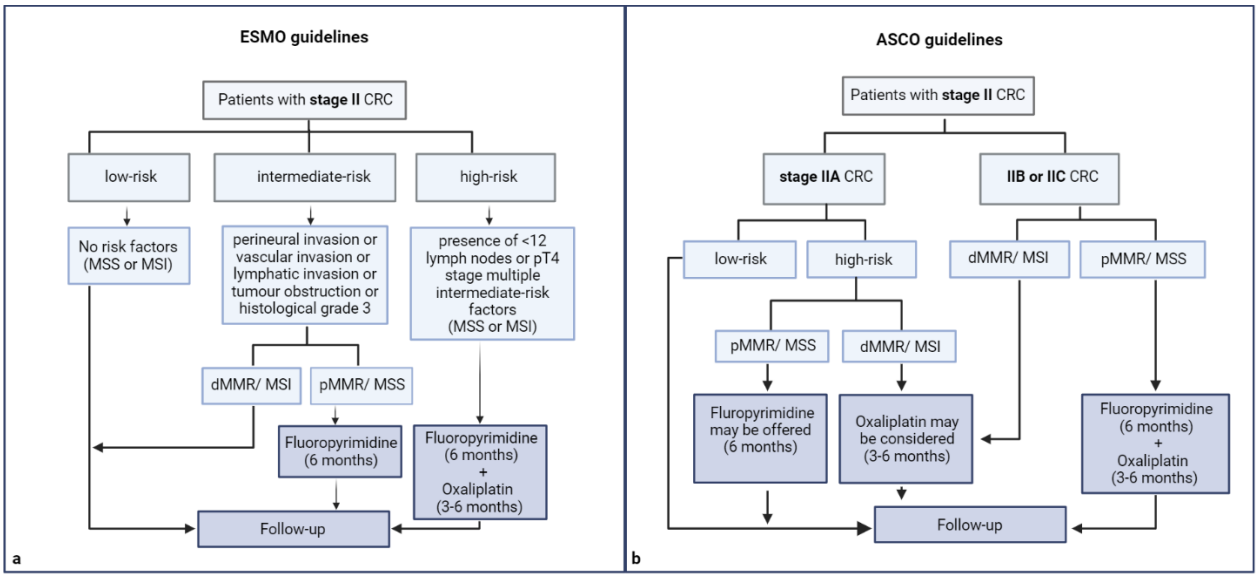


***Figure 3: Overview of the ESMO versus ASCO guidelines for the treatment of CRC stage II patients.*** *In the ESMO guidelines patients are subcategorized into 3 groups (low-risk, intermediate-risk and high-risk patients) by using a combination of the MMR/MSS status and clinicopathological features. Low-risk and intermediate-risk patients with dMMR/MSI status should not receive adjuvant chemotherapy (ACT), whereas patients with high-risk and intermediate-risk and pMMR/MSI status should be treated with ACT. According to the ASCO guidelines patients are categorized into two subgroups (stage IIA and stage IIB or IIC). No ACT is recommended for stage IIA patients with low-risk, whereas ACT should be considered for high-risk stage IIA tumors, as well as for stage IIB or IIC patients with dMMR/MSI status. Patients with stage IIB or IIC and pMMR/MSS status should be treated with ACT. Created with BioRender.com*

In the case of the guidelines mentioned above, there exist diverse treatment recommendations due to the categorization of stage II CRC patients into different subgroups. An additional risk stratification allowing precise estimation of recurrence risk for the identification of stage II adjuvant therapy benefiting CRC patients in the clinics is urgently needed (Rebuzzi et al., 2020). Additionally, factors such as lymphovascular invasion, tumor perforation, undifferentiated grade of tumors and T4 tumors are unreliable in the predication of treatment benefit and even some low-risk patients develop recurrence after surgery (Baxter et al., 2021).

### 1.2.3. Side effects of chemotherapy

As chemotherapy treatment is significantly related with side effects such as insomnia, fatigue, pain and potential toxicity, factors such as all-cause mortality and quality of life must also be taken into consideration when deciding for or against the administration of chemotherapy (Lewis et al., 2016). As an example, fluorouracil (FU) causes side effects such as vomiting, diarrhoea and an increase of white blood cells and 50% of patients treated with oxaliplatin suffer from neurotoxicity which can last years after treatment (Lewis et al., 2016). Therefore, ACT treatment of all stage II patients

would be an overtreatment, as its administration provides patients with only few benefits and poses a real risk in reduction of quality of life (Lewis et al., 2016; Sallinger et al., 2023).

## 1.3. Blood- and tissue-based biomarkers for risk stratification

### 1.3.1. Technologies to identify stage II CRC specific biomarkers

A study performed by the Cancer Genome Atlas Network in 2012 provided key insights into the main basic molecular processes that contribute to the development of colon cancer and further identified potential therapeutic and prognostic targets (Morley-Bunker et al., 2019).

Even still, more precise biomarkers, especially for the prediction of recurrence in stage II CRC patients, are urgently needed (Tie et al., 2022). Pages et al. (2018) developed an immunoscore based on the immunohistochemistry staining of CD3+ and CD8+ cells in tumor tissue (Pagès et al., 2018). For this, 2681 patients, after quality and clinical data control, with TNM stage I-III were included in the analysis and divided into three subgroups: patients with a high-, intermediate-, and low immunoscore (Pagès et al., 2018). Based on this classification, patients with a high immunoscore showed the lowest risk of tumor recurrence and high overall survival and disease-free survival (Pagès et al., 2018). Yamanaka et al. (2016), used a 12-gene OncotypeDX recurrence score assay based on tissue lysates analyzed by reverse transcription-polymerase chain reaction (RT-PCR) to identify patients with a high recurrence risk and who would, therefore, benefit from the ACT administration (Yamanaka et al., 2016). Similarly, Kopetz et al. (2015), applied an 18-gene expression-based classifier called ColoPrint on stage II CRC patients to predict high tumor recurrence risk patients, who should be considered for additional chemotherapy treatment (Kopetz et al., 2015; Sallinger et al., 2023).

Due to limitations in the applied technologies, such as immunohistochemistry and polymerase chain reaction (PCR)-based approaches, combined with the nature of tumor heterogeneity, which includes genetic, molecular, and cellular differences within a single tumor, there exists a lack of markers implemented in clinical practice (Morley-Bunker et al., 2019). Immunohistochemistry, known as an integral method for protein expression level measurement, in comparison to other molecular technologies shows limitations in the quantification of results and validated antibodies are available for only approximately 25% of human proteins (Morley-Bunker et al., 2019). Quantitative PCR-based approaches, which, due to high specificity, are considered to be the gold standard for gene expression level measurements, show limited sensitivity if performed on heterogeneous multicellular cancer samples, whereby results can be influenced by non-neoplastic cells (Morley-Bunker et al., 2019).

Our knowledge of CRC biology has increased significantly through the analytical and technical progresses made within the last decade and has further transformed through applications enabling analysis of genome wide expression, such as different sequencing approaches and microarrays (Morley-Bunker et al., 2019).

Nevertheless, molecular analyses, such as OncotypeDX recurrence score and next generation sequencing, are performed on bulk cell tissue lysates, which involves the mixture of cells from a whole tissue, rather than examining specific regions (Svedlund et al., 2019). Tumor heterogeneity may not be depicted with bulk tissue analysis, as it provides an average of the genetic and molecular features of all cells within the tumor, which can mask the presence of distinct subpopulations with unique characteristics (Svedlund et al., 2019). Therefore, sub-grouping of patients will be biased towards the largest clones present and rare cell populations within the tumor, which could have a significant impact on the behaviour and response to treatment, might not be identified (Svedlund et al., 2019). Single cell RNA sequencing (scRNAseq) could be used to indicate the transcriptomic diversity of all cell types within a tissue sample and to further expand the understanding of molecular basic mechanisms in CRC (Gyllborg et al., 2020). As mentioned, however, this requires the dissociation of tissue structures (Gyllborg et al., 2020), whereby the spatial histological context between cells in bulk analysis as well as scRNAseq approaches is lost (El-Heliebi et al., 2017; Gyllborg et al., 2020). Thereby, cancer associated biological processes such as inflammation, tissue remodelling, proliferation and epithelial cell differentiation identified by RNAseq can only be measured without their spatial correlations within the tissue (Xu et al., 2017).

### 1.3.2. The evolution of spatial transcriptomics

To overcome this loss of spatial context within tissues, spatial transcriptomic technologies have been developed to examine the gene expression profile of tissues and to, furthermore, locate the transcripts at their original location (Wang et al., 2021).

In 1998, Femino et al. demonstrated the ability of FISH technology to visualize single mRNA molecules by using 50 nucleotide (nt) long fluorophore labelled probes that bind to mRNA sequences (Femino Andrea M. & Fay Fredric S., 1998). This allowed for the identification of individual transcripts, with fluorescence signals correlating directly to mRNA levels (Femino Andrea M. & Fay Fredric S., 1998). smFISH offers quantitative analysis with a near 100% detection sensitivity (Lein et al., n.d.). However, its capability to detect multiple genes is limited by the number of spectrally resolvable fluorophores (Femino Andrea M. & Fay Fredric S., 1998). To overcome this limitation, new approaches that utilize a combination of multiple colors and

hybridization cycles have been created to enhance the analysis color spectrum (Moses & Pachter, 2022). The introduction of seqFISH marked a significant shift, allowing for the encoding of 12 genes by applying a combination of 4 colors across 2 hybridization rounds (Lubeck et al., 2014). To reduce the detection of false positives, the procedure involved three iterations of the two hybridization rounds filtering out any non-matching signals between the repeated cycles (Lubeck et al., 2014). In 2015, an advanced seqFISH variant, called multiplexed error-robust FISH (MERFISH), was introduced (K. H. Chen et al., 2015). MERFISH utilizes 30 nt long encoding probes targeting the transcript, combined with a 20 nt readout sequences (K. H. Chen et al., 2015). Singly labelled readout probes then attach to these sequences on the encoding probes (K. H. Chen et al. 2015). In a series of hybridization and imaging cycles, the specific readout probes were identified to decode the target (K. H. Chen et al., 2015). Theoretically, this method of combinatorial labelling is designed to exponentially increase the number of detectable targets with each additional round of hybridization (K. H. Chen et al., 2015). However, this results in a corresponding exponential increase in the potential for detection errors (K. H. Chen et al., 2015). Therefore, modified Hamming code schemes are used to detect and correct errors (K. H. Chen et al., 2015). Binary barcode systems with fluorescence are used ("1" for presence, "0" for absence) that requires a minimum of 4 differences (Hamming distance of 4 = HD4) between each other (K. H. Chen et al., 2015; Moses & Pachter, 2022). Each barcode contains four "1"s to allow unique gene identification even if one signal is lost (Moses & Pachter, 2022). However, two missing signals lead to an uncorrectable error due to indistinguishable barcodes (K. H. Chen et al., 2015). Approximately 80% efficiency was achieved in RNA detection, and a strong correlation was noted between the RNA copy numbers detected by MERFISH and those derived from smFISH analyses (K. H. Chen et al. 2015). HD2 codes used for detecting around 10000 RNA targets can identify but not correct errors (K. H. Chen et al., 2015). This leads to a total RNA count per cell that is about 1/3 of what was obtained using HD4 coding (K. H. Chen et al. 2015). SeqFISH+ is an advanced method that allows for super-resolution imaging and the analysis of up to 10,000 genes (Eng et al., 2019). It extends the range of detectable colors beyond the typical four or five to a much larger number of 'pseudo-colors' through multiple rounds of hybridization (Eng et al., 2019). This technique distributes mRNA molecules across 60 pseudo-color channels over separate images, which enables the precise localization of each mRNA molecule (Eng et al., 2019).

Split-FISH is a methodology that was developed to reduce off-target hybridization and background noise (Goh et al., 2020). This technique combines the concept of split probes with multiplexed FISH (Goh et al., 2020). By utilizing a bridge sequence that lies between a pair of encoding probes it is only capable of binding when these probes are hybridized adjacent to each other on the target sequence (Goh et al., 2020). To encode 317 genes, the system selects two "1"s out of 26 binary

barcode positions, creating 325 possible barcodes, with 8 left blank to manage false positives (Goh et al., 2020).

In smFISH, it is common to use numerous singly labelled probes to enhance the signal (Moses & Pachter, 2022). However, not every transcript is long enough to allow for the attachment of this many probes (Moses & Pachter, 2022). One commonly used way to boost the signals without increasing the number of probes is rolling circle amplification (RCA) (Moses & Pachter, 2022). Here, padlock probes with a barcode, specifically hybridize to transcribed cDNA (Gyllborg et al., 2020). The amplification of probes allows for the visualization of amplicons using a conventional fluorescence microscope that enables high-throughput analysis (Moses & Pachter, 2022).

The advanced dRNA-HybISS method provided by CARTANA directly targets RNA, eliminating the need for reverse transcription. This approach is based on rolling circle amplification (RCA) of padlock probes (PLPs) after their hybridization to the RNA targets of interest directly on the tissue (figure 5) (Lee et al., 2022). By directly targeting RNA, the reverse transcription step of cDNA-based ISS approaches can be avoided, resulting in a fivefold increased transcript detection efficacy (Lee et al., 2022). Each PLP is provided with a unique barcode which can be sequentially decoded by adding so called “bridge probes” and fluorescently labelled detection oligonucleotides (DO) over several cycles (Lee et al., 2022). Each cycle is visualized with a fluorescent microscope followed by stripping and rehybridization of the next bridge probes and DOs (Lee et al., 2022). Computational analysis of the images is performed in CellProfiler (Broad Institute, MA, United States) and MATLAB (Mathworks, Sweden) and results in multiplexed spatial mapping of gene transcripts by preserving the tissue architecture (Gyllborg et al., 2020; Kamentsky et al., 2011; Lee et al., 2022).

### 1.3.3. Comparison of an NGS-based approach (Visium) and dRNA-HybISS

In 2018, the commercially available technology Visium provided by 10x Genomics (California, USA) became the leading technology in the era of next-generation sequencing (NGS) - barcoding approaches (Wang et al., 2021). The methodology targets transcripts from tissue sections that have been placed on a spatial array, followed by a permeabilization step in order to perform RNA-sequencing (RNA-seq) (Gracia Villacampa et al., 2021). Visium provides an enhanced spatial resolution, utilizing a hexagonal pattern of spots that are 55 µm wide and separated by 100 µm, which enables the mapping of sequencing data back to spatially arranged spots (figure 4a,c) (Moses & Pachter, 2022; Wang et al., 2021).

This technology, however, does not allow single transcripts to be assigned to their originating cells, a drawback that could lead to the loss of key information of rare cells between spots (Wang et al.,

2021; Sallinger et al., 2023). To overcome this limitation, dRNA-HybISS technology can be used, which allows for the detection of up to 300 transcripts of interest with single cell and subcellular resolution (Gyllborg et al., 2020; Lee et al., 2022; Sallinger et al., 2023)

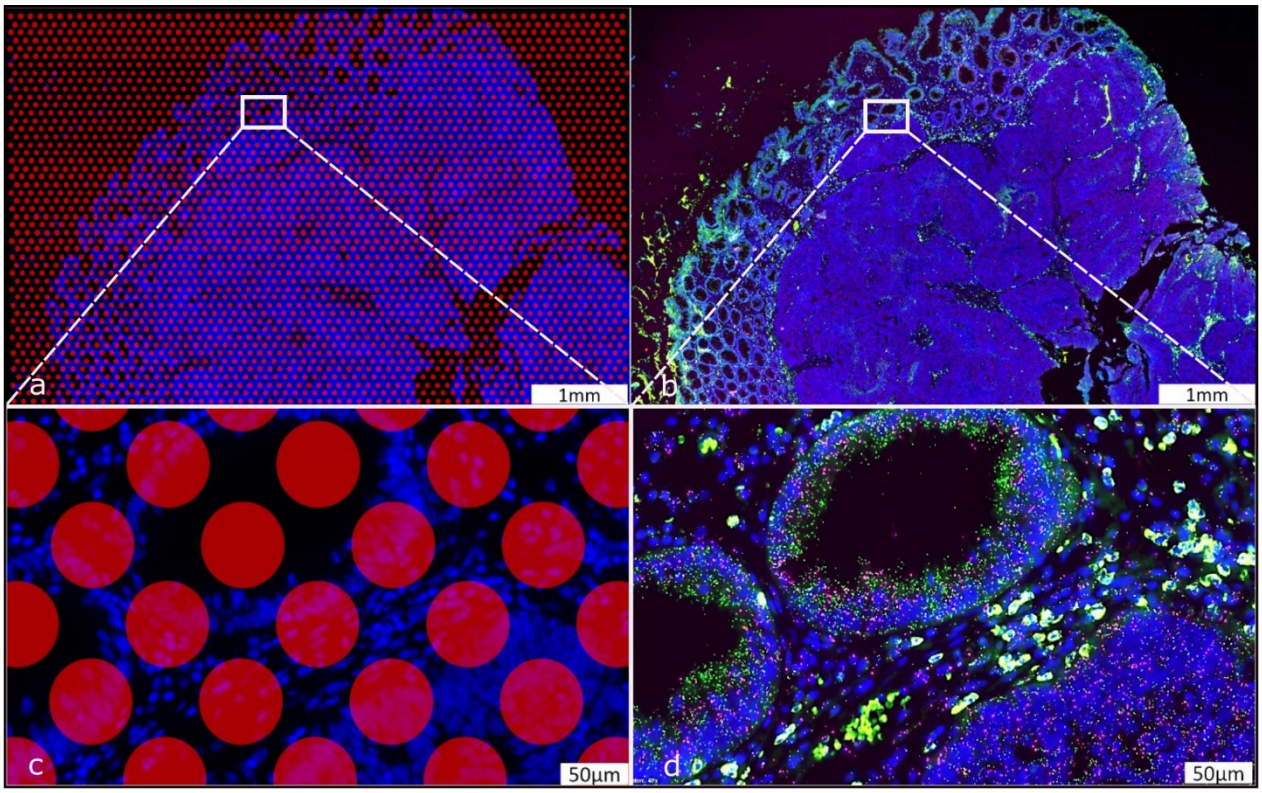


***Figure 4: Spatial transcriptomic technologies: Visium vs. dRNA-hybridization-based in situ sequencing.***
*a) Visium technology provided by 10x Genomics (California, USA) with a magnification of a specific area in c) shows the spot-based design of the approach. b) dRNA-Hybridization-based in situ sequencing provided by CARTANA (now part of 10x Genomics) with a magnification of a specific area in d).*

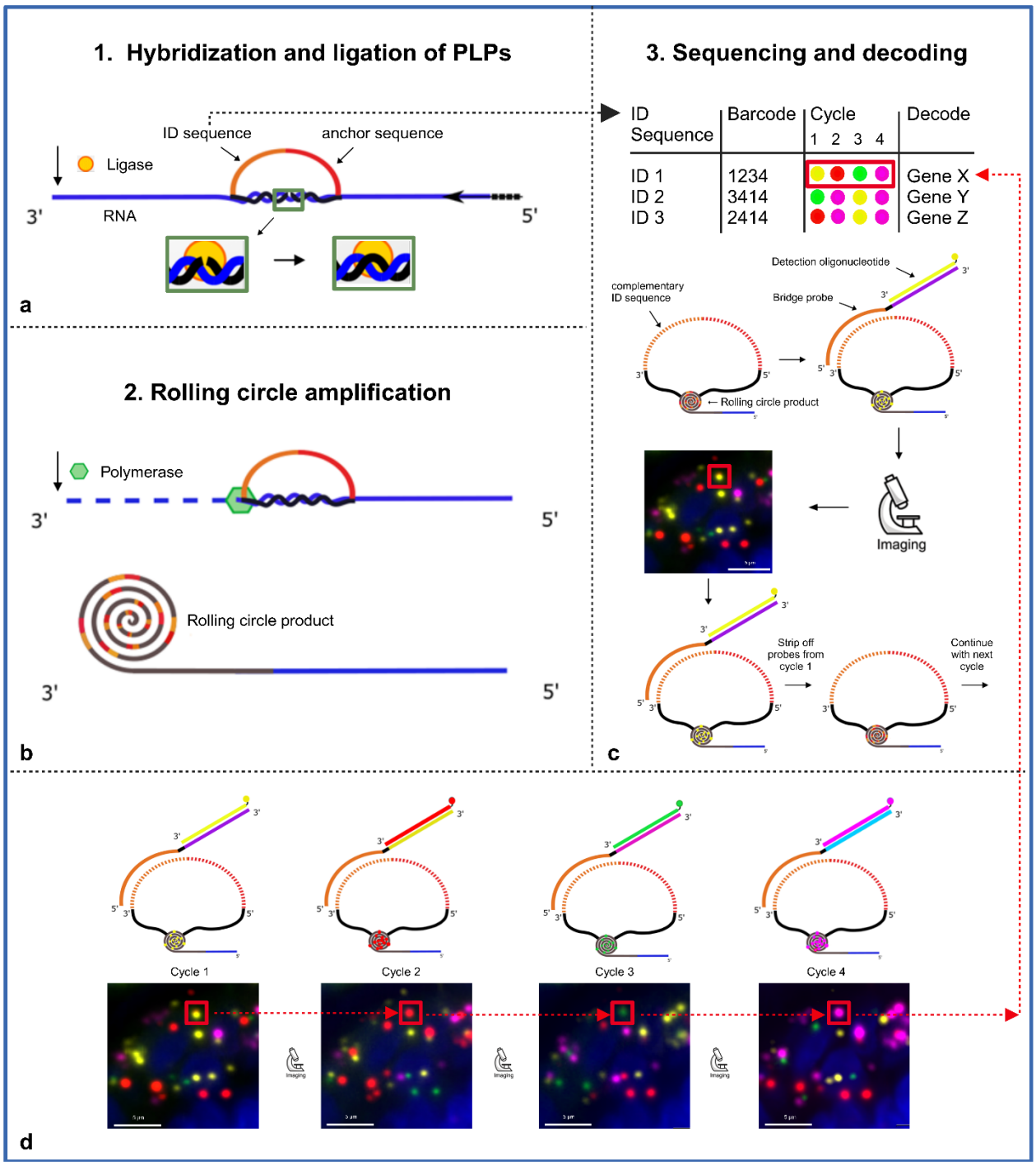


***Figure 5: Overview of ISS technology***.

*a) Padlock probes (PLPs) directly bind to RNA targets of interest and the nick between the arms is ligated* (Lee et al., 2022). *b) PLPs are amplified by a rolling circle amplification which result in rolling circle products (RCPs)* (Lee et al., 2022). *c) All PLPs contain a unique ID sequence, which is associated with a unique color code* (Lee et al., 2022). *c, d) Decoding is performed sequentially by adding bridge- and detection oligonucleotide probes specific for each cycle. Computational analysis is performed in CellProfiler and MATLAB* (Lee et al., 2022).

### 1.3.4. Detection efficiencies and limitations of different spatial transcriptomic approaches.

SmFISH technologies are highly efficient for detecting transcripts, achieving nearly 100% detection efficiency (Lein et al., n.d.; Lubeck et al., 2014). Huge differences in the efficiency of spatial transcriptomic methodologies have been observed, with different methods used to estimate it (Moses & Pachter, 2022). Typically, smFISH, serving as a gold standard, is compared with newly developed techniques by evaluating the average number of transcripts detected per gene per cell to draw comparisons (Moses & Pachter, 2022). This approach has been applied to achieve the efficiencies of methods such as MERFISH, seqFISH+, and was used to compare the performance in detecting transcripts in HybISS, and dRNA-HybISS (Moses & Pachter, 2022). While MERFISH is capable of reaching a detection efficiency of up to 80% for 140 genes using approximately 90 probes each, its efficiency drops to about 30% when employing codes designed to handle nearly 10,000 genes without error correction features (K. H. Chen et al., 2015) (table 1). SeqFISH+ demonstrates an efficiency of approximately 49% efficiency for 60 genes (Eng et al., 2019) (table 1). After CARTANA commercialized HybISS, the method was optimized by utilizing chimeric padlock probes for direct mRNA targeting, avoiding the reverse transcription step. As a result, the direct targeting of RNA led to a fivefold improvement in the efficiency of detecting transcripts in comparison to the HybISS approach, which targets cDNA (Magoulopoulou et al., 2023) (table 1).

Sometimes the enhancement of signal intensity is required through the application of a large number of singly labelled probes (Moses & Pachter, 2022). An average number of 50-100 probes per target are recommended to receive robust signals (Safieddine et al., 2023). The technique's applicability is restricted to RNAs with approximately 1400 nts length, due to the average hybridization sequence being roughly 30 nts in length (Safieddine et al., 2023). Not all transcripts are long enough to accommodate the required number of probes and thus detecting transcripts under 500 bases proves to be theoretically impossible (Moses & Pachter, 2022; Safieddine et al., 2023). To increase signal intensity without adding more probes, elaborate tissue clearing procedures are required, though these do not always yield clearly distinguishable signals (Moses & Pachter, 2022). When performing HybISS and dRNA-HybISS technology, 4-5 probes per transcript are used to generate a robust signal through rolling circle amplification (Lee et al., 2022; Moses & Pachter, 2022). To analyze the RNA expression of a huge number of genes using FISH-based technologies, it is necessary to design a vast number of probes, especially when using multiple probes per gene to boost signal strength (Moses & Pachter, 2022). Additionally, probes

tagged with fluorophores are costly, and their demand increases with the need for signal amplification (Moses & Pachter, 2022).

Hence, for researchers aiming to establish a FISH-based spatial transcriptomics method, the challenges go beyond just acquiring new images processing tools (Moses & Pachter, 2022). Additionally, for some methods they face the task of building a custom fluidics system that can be integrated to a microscope (Moses & Pachter, 2022). However, the situation is changing with commercially available kits like those offered by CARTANA (Lee et al., 2022). Moreover, even more advanced platforms are emerging, such as Vizgen MERFISH and 10X Xenium (Moses & Pachter, 2022). These platforms not only provide reagent kits but also feature integrated automated imaging systems (Moses & Pachter, 2022). Notably, 10X Xenium represents an advanced technology that has been optimized from CARTANA's original technology, enhancing its detection efficiency (Salas et al., n.d.).

***Table 1: Comparison of different spatial transcriptomic approaches***

*Parameters such as the detection efficiency, pros and cons of different spatial transcriptomic approaches (smFISH, seqFISH+, MERFISH, splitFISH, HybISS, dRNA-HybISS and Visium) were compared and summarized.*

| Method | Description | Pros | Cons | Detection Efficiency |
|---|---|---|---|---|
| smFISH (Femino Andrea M. & Fay Fredric S., 1998) | Uses fluorescent probes to visualize individual mRNA molecules in cells. | High specificity, single-molecule resolution. | Limited by the number of detectable fluorophores. | Nearly 100% |
| seqFISH+ (Eng et al., 2019) | Multiplexed FISH with sequential barcoding to detect up to 10000 genes by utilizing 60 pseudo-color channels. | Multiplexing capacity, detection of up to 10000 genes. | Numerous rounds (80) of hybridization. | ~49%. |
| MERFISH (K. H. Chen et al., 2015) | Multiplexing and error-robust barcoding to quantify ~140 genes with HD4 codes or 10000 genes with HD2 codes. | High throughput, high sensitivity (HD4). | Complex setup and analysis. | ~80% with HD4 code.<br>~30% with HD2 code. |
| splitFISH (Goh et al., 2020) | Combines the concept of split probes with multiplexed FISH. | Reduces off-target hybridization and background noise. | Increased complexity in probe design | not reported |
| HybISS (Gyllborg et al., 2020) | Padlock probes are used to target cDNA and amplify the signal by RCA. | Only 5 padlock probes used, can detect SNPs. | Low detection efficacy | ~1% |
| dRNA-HybISS (Lee et al., 2022) | Padlock probes are used to directly target RNA and amplify the signal by RCA. | Higher detection efficacy than HybISS due to direct targeting of RNA | Probe sequences are proprietary to CARTANA | ~5% |
| Visium (Gracia Villacampa et al., 2021) | Spot-based untargeted spatial transcriptomics approach. | Untargeted approach (transcriptome-wide) | no single cell resolution | not reported |

### 1.3.5. Tumor dissemination and circulating cell free tumor DNA

Aside from normal cells, tumor cells can also shed DNA fragments and other components into the blood circulation (Filice & Ruiz-Cabello, 2019). These cellular components describe the genetic landscape of the tumor, and the analysis of these cancer-derived components is known as a liquid biopsy (Filice & Ruiz-Cabello, 2019). Tumor components, such as circulating tumor cells (CTCs), provide information at a cellular level, whereby cell-free circulating tumor DNA (ctDNA) mirrors the entire genetic landscape (Filice & Ruiz-Cabello, 2019). Considerable effort has been made in the last years to overcome limited detection sensitivities to allow the detection of rare events. Non-metastatic disease states, however, remains challenging (Filice & Ruiz-Cabello, 2019). The exact mechanism of ctDNA release into the blood circulation is still widely unknown, although mechanisms such as heart injury, inflammation, heavy smoking, and advanced disease states have been proven to increase their release into the systemic circulation (Filice & Ruiz-Cabello, 2019).

The remarkable liquid biopsy technology is already being used as part of clinical practise by applications such as the early detection of cancer and resistances for therapies, prediction of response to targeted therapy and immunotherapy, such as CAR-T cell therapy, the assessment of DNA from different metastatic sites, analysis of tumor burden after surgery to identify minimal residual disease and evaluation of cancer patients with difficult biopsy sites (Nikanjam et al., 2022).

### 1.3.6. ctDNA in CRC stage II patients

Based on the presence of detectable ctDNA after surgery, the evaluation of tumor recurrence risk through analysis of peripheral blood would be a promising strategy in deciding for or against administration of ACT for stage II CRC patients. In the DYNAMIC (Circulating Tumor DNA Analysis Informing Adjuvant Chemotherapy in Stage II Colon Cancer) trial by Tie et al. (2022) a ctDNA based approach was compared with the standard management procedure for stage II patients (Tie et al., 2022). Utilizing the ctDNA guided approach, the number of patients who received adjuvant therapy decreased, while no increase in the recurrence risk could be observed. Additionally, stage II CRC patients who did not receive ACT with the absence of ctDNA after surgical resection of the tumor showed a low risk of recurrence (Tie et al., 2022). The association of ctDNA to the risk of recurrence was also examined in a trial conducted by Reinert et al. (2019) (Reinert et al., 2019). In this study, the plasma of 94 patients after surgery was collected and analyzed, resulting in 84 patients being ctDNA negative, while 10 showing detectable values of ctDNA (Reinert et al., 2019). Patients who tested positive for ctDNA indicated a higher recurrence

rate than those who were ctDNA negative (Reinert et al., 2019). Patients with the presence of ctDNA in the blood are classified as shedders in this thesis, whereas patients with no detectable ctDNA in drawn blood are categorized as non-shedders.

## 1.4. Aim of the thesis

The standard procedure for patients diagnosed with stage II CRC, apart from those that are high-risk, is surgical resection of the neoplastic tissue without additional chemotherapy (Ahmed, 2020). Opting for or against the administration of ACT in the therapeutic management of stage II CRC patients remains challenging (Ahmed, 2020). Studies set out to answer the question of the necessity of additional chemotherapeutic treatment for stage II patients, show contradicting results with very little survival benefits for patients. Further results also point to the potential side effects of overtreatment, which lead to an unnecessary exposure to chemotherapy-induced toxicities and reduced quality of life (Lewis et al., 2016; Sallinger et al., 2023). Recurrence of cancer within five years after tumor resection remains of significant concern, as it relates to a high risk of cancer-associated deaths especially for early relapsed patients (Ryuk et al., 2014). A variety of factors, such as genetic predisposition, perineural invasion, tumor stage, gender, age and the presence of micrometastasis can influence the potential development of a relapse (Desch et al., 2005; Tsai et al., 2009).

The analysis of cancer-derived components, such as CTCs and ctDNA in blood samples, referred to as liquid biopsies, is a powerful tool to describe the genetic landscape of tumors and could further add information regarding the disease progression (Filice & Ruiz-Cabello, 2019a).
In the DYNAMIC study by Tie et al. (2022) the standard management procedure for stage II patients was compared with a ctDNA-based approach. Their results showed an increased risk of developing cancer recurrence in patients with detected ctDNA after surgery whereas patients with an absence of ctDNA showed a low risk of developing a relapse after surgical resection (Tie et al., 2022). A multitude of ctDNA-based diagnostic applications for molecular tumor profiling in the field of precision medicine is already available (Nikanjam et al., 2022). This includes applications such as early detection and prediction of therapy resistances and the detection of DNA from different metastatic locations to understand the heterogeneity of tumors (Nikanjam et al., 2022).

Although the analysis of cancer-derived components in blood samples has gained interest within the last years, the underlying mechanisms contributing to tumor dissemination in the blood, potentially causing a relapse of disease, is poorly understood. Similarly, processes such as

proliferation, apoptosis, necrosis, and inflammation are known to play an essential role in the release of tumor DNA into the bloodstream, although the exact mechanisms remain unclear (Filice & Ruiz-Cabello, 2019b).

Different studies on biomarker panels have been performed to predict early recurrence, such as the 12-gene recurrence score assay OncotypeDX (Yamanaka et al., 2016), the 18-gene expression-based classifier called ColoPrint (Kopetz et al., 2015) and various next generation sequencing approaches (Wang et al., 2021). All these methodologies are based on analysis of bulk tissue lysates, which only inform on the average composition of all sub-clones. This average composition, in turn, creates a bias towards the largest clones that are present in the tumor and can, in addition, be influenced by non-neoplastic cells (Svedlund et al., 2019). As a consequence, information of small clones as well as the spatial histological architecture of cells within the tissue is lost in such approaches, due to the required lysis (Svedlund et al., 2019). Factors that contribute to tumor dissemination, such as metabolic dysregulations, apoptosis or proliferation can, therefore, only be measured without their spatial context within their respective tissue structures. Hence, the knowledge of expression patterns with preservation of their spatial architecture within neoplastic tissues and their surrounding microenvironment would contribute to an increase in the understanding of disease recurrence (El-Heliebi et al., 2017; Sallinger et al., 2023; Xu et al., 2017).

For this reason, we investigated the spatial tissue composition of stage II CRC patients by a novel spatial transcriptomics technology on a single cell resolution level. By designing a panel of 176 genes, we aimed to examine different biological processes that could contribute to tumor dissemination such as apoptosis, proliferation, angiogenesis, stemness, oxidative stress, hypoxia, invasion and markers for components of the tumor microenvironment (TME) (Sallinger et al., 2023). We hypothesize that spatial histological expression patterns differ between relapsed patients versus non-relapsed patients (Sallinger et al., 2023). For this, a hybridization-based *in situ* sequencing approach (dRNA-HybISS) was established and optimized to provide novel insights into biological processes that contribute to tumor dissemination in stage II CRC patients.

# 2. Methods and materials

A list of used of reagents, buffers, solutions, and kits is included in the appendix (Supplementary table 4).

## 2.1. Study design

### 2.1.1. Relapse project

Patients were monitored for 3 years after tumor resection and divided into two groups: patients that relapsed (5 patients) and those who did not (5 patients) (Sallinger et al., 2023). All patients were diagnosed with stage T3 (tumor growth through muscularis propria and into subserosa) without chemotherapy administration after tumor resection. Detailed patient characteristics can be found in table 2. Tissue of patients was formalin-fixed and paraffin-embedded (FFPE) and stored in the Biobank Graz. The Ethics Committee of the Medical University of Graz granted approval for the study protocol (29-187 ex 16/17) and written informed consent was provided by all patients. The study adheres to the ethical principles described in the declaration of Helsinki and good clinical practice.

***Table 2: Characteristics of 10 diagnosed stage II colon cancer patients included into the retrospective relapse project study.***

*Parameters such as age, gender, weight, date of tumor resection, tumor location, T classification, histological characterisation, stage and ACT administration were collected from each patient and depicted in the table.*

| ID | Recurrence 0=No 1=Yes | Age (at Surgery, in years) | Gender 0=Male 1=Female | Weight (in kg) | Date of Tumor OP | Tumor Location | T | Histo | Stage | Adjuvant CTX 0=No 1=Yes |
|---|---|---|---|---|---|---|---|---|---|---|
| Patient 1 | 1 | 70 | 1 | 63 | 18.04.2010 | Flexura coli sinistra | 3 | Adenocarcioma | 2 | 0 |
| Patient 2 | 1 | 80 | 0 | 80 | 12.12.2012 | Colon transversum | 3 | Adenocarcioma | 2a | 0 |
| Patient 3 | 1 | 76 | 0 | 78 | 13.02.2013 | Rectum | 3 | Adenocarcioma | 2a | 0 |
| Patient 4 | 1 | 60 | 0 | 72 | 21.07.2010 | Caecum | 3 | Adenocarcioma | 2a | 0 |
| Patient 5 | 1 | 56 | 0 | 63 | 08.02.2010 | Colon transversum | 3 | Adenocarcioma | 2a | 0 |
| Patient 6 | 0 | 64 | 0 | 89 | 08.11.2010 | Left flexura | 3 | Adenocarcioma | 2a | 0 |
| Patient 7 | 0 | 74 | 1 | 77 | 12.05.2011 | Sigmoid | 3 | Adenocarcioma | 2a | 0 |
| Patient 8 | 0 | 27 | 0 | 77 | 26.03.2010 | Sigmoid | 3 | Adenocarcioma | 2a | 0 |
| Patient 9 | 0 | 73 | 1 | 80 | 10.07.2012 | Sigmoid | 3 | Adenocarcioma | 2a | 0 |
| Patient 10 | 0 | 70 | 1 | 61 | 20.12.2010 | Colon transversum | 3 | Adenocarcioma | 2 | 0 |

### 2.1.2. Shedder project

In a prospective study 21 diagnosed stage I and II CRC patients were recruited. Blood samples before tumor resection were collected and corresponding FFPE tissue after surgery was available. Plasma and tissues of patients will be sequenced at the Institute of Human Genetics, Diagnostic & Research Center for Molecular BioMedicine, Medical University of Graz by Stefan Kühberger under supervision of Ellen Heitzer by using the TruSight Oncology 500 (TSO500) kit (Illumina, San Diego, California, USA). Based on the occurrence of the same somatic variants in the plasma and resected tissue, patients will be grouped as either non/low shedders or shedders. The Ethics Committee of the Medical University of Graz granted approval for the study protocol (32-489 ex 19/20) and written informed consent was provided by all patients. The study adheres to the ethical principles described in the declaration of Helsinki and good clinical practice.

***Table 3: Characteristics of patients included into the shedder project study.***

*Parameters such as year of birth, gender, date of tumor resection, tumor location, TNM classification, histological characterisation and stage were collected from each patient and are depicted in the table.*

| ID | Year of birth | Gender 0=Male 1=Female | Date of Tumor OP | Tumor Location | T | N | M | Histo | Stage |
|---|---|---|---|---|---|---|---|---|---|
| **Patient 1** | 1942 | f | 01.09.2021 | C.ascendens | T3a | N0 | M0 | Adenocarcinoma | 2 |
| **Patient 2** | 1962 | ? | 25.05.2021 | NA | T4a | N0 | M0 | NA | 2 |
| **Patient 3** | 1953 | f | 17.05.2022 | C.transversum | T2 | N0 | M0 | Adenocarcinoma | 1 |
| **Patient 4** | 1943 | m | 26.01.2022 | Rectum | T1 | N0 | M0 | Adenocarcinoma | 1 |
| **Patient 5** | 1954 | m | 30.07.2021 | C.sigmoideum | T3a | N0 | M0 | Adenocarcinoma | 2 |
| **Patient 6** | 1954 | m | 27.07.2021 | C.descendens | T2 | N0 | M0 | Adenocarcinoma | 1 |
| **Patient 7** | 1952 | f | 19.07.2021 | C.ascendens | T2 | N0 | M0 | Adenocarcinoma | 1 |
| **Patient 8** | ? | ? | 22.06.2021 | NA | T4a | N0 | M0 | NA | 2 |
| **Patient 9** | 1949 | f | 10.01.2022 | C.sigmoideum | T3b | N0 | M0 | Adenocarcinoma | 2 |
| **Patient 10** | 1953 | f | 05.04.2022 | C.ascendens | T4a | N0 | M0 | Adenocarcinoma | 2 |
| **Patient 11** | 1951 | f | 24.03.2021 | C.ascendens | T3a | N0 | M0 | Adenocarcinoma | 2 |
| **Patient 12** | 1946 | f | 24.08.2021 | Rectum | T3 | N0 | M0 | Adenocarcinoma | 2 |
| **Patient 13** | ? | ? | 21.05.2021 | NA | T3a | N0 | M0 | NA | 2 |
| **Patient 14** | 1953 | m | 11.05.2021 | C.sigmoideum | T2 | N0 | M0 | Adenocarcinoma | 1 |
| **Patient 15** | 1964 | f | 31.05.2021 | C.sigmoideum | T3a | N0 | M0 | Adenocarcinoma | 2 |
| **Patient 16** | NA | NA | 21.03.2022 | C.sigmoideum | T3 | N0 | M0 | Adenocarcinoma | 2 |
| **Patient 17** | 1959 | m | 28.05.2021 | C.sigmoideum/Rectum | T3b | N0 | M0 | Adenocarcinoma | 2 |
| **Patient 18** | 1944 | m | 12.07.2021 | C.sigmoideum | T4 | N0 | M0 | Adenocarcinoma | 2 |
| **Patient 19** | NA | NA | 06.05.2021 | NA | T3a | N0 | M0 | NA | 2 |
| **Patient 20** | 1959 | f | 02.03.2022 | C.sigmoideum / Rectum | T2 | N0 | M0 | Adenocarcinoma | 1 |
| **Patient 21** | 1973 | m | 28.06.2021 | C.ascendens | T2 | N0 | M0 | Adenocarcinoma | 1 |

## 2.2. Haematoxylin and eosin (H&E) staining

Before staining FFPE tissue slides were deparaffinized 4 times in HistoLab Clear (Sanova Pharma, Vienna, Austria) for 5 min each (HistoLab Clear 1a, 1b, 2a and 2b) and dehydrated in a descending ethanol series for 2 min each (100%, 95%, 70%, 50%). Samples were transferred to diethylpyrocarbonate (DEPC) treated water (Sigma-Aldrich, Vienna, Austria) for 2 min and incubated in Mayer's hematoxylin (Merck, Darmstadt, Germany) for 10 min. Slides were washed in deionized water and shortly submersed into acid water (Merck, Darmstadt, Germany) for a few seconds until the nuclei stain appeared blue. This was followed by a washing step in deionized water. Samples were incubated in eosin (Merck, Darmstadt, Germany) for approximately 30 sec and shortly submersed in an ascending ethanol series for 5 sec each (96%, 96%, 100%, HistoLab Clear/100% 1:1). Tissue sections were incubated in HistoLab Clear 2b (Sanova Pharma, Vienna, Austria) for 10 min, layered with Tissue-Tek mounting medium (Sakura, Umkirch, Germany) and covered with a coverslip (20x20, Roth, Karlsruhe, Germany).

## 2.3. Panel design

To examine different biological processes within the neoplastic tissue and its environment, a padlock probe panel was designed for direct targeting 176 transcripts of interest. Markers for different pathways such as apoptosis, autophagy, necrosis, angiogenesis, proliferation, energy metabolism, stemness, invasion, hypoxia, oxidative stress, epithelial-mesenchymal transition (EMT), as well as markers targeting epithelial cells in colon, immune cells and tumor associated stromal cells were included in the panel (table 4) (Sallinger et al., 2023). The final panel list was sent to CARTANA (Stockholm, Sweden, now part of 10x Genomics, California, USA). As the PLPs were designed by the company, the structure of probes and exact target sequences were not known. Additionally, two pre-designed panels, the Immune General I1A 0.2 (supplementary table 1) and the Immune Oncology I2B 0.2 (supplementary table 2) panel from CARTANA (Stockholm, Sweden, now part of 10x Genomics, California, USA) were ordered.

***Table 4: Pathway gene panel with genes associated to their biological group and subgroup.***

*For the examination of different biological pathways (apoptosis, autophagy, necrosis, angiogenesis, proliferation, energy metabolism, stemness, invasion, hypoxia, oxidative stress, epithelial-mesenchymal transition) and different celltypes (epithelial cells, immune cells and tumor associated stromal cells) a panel with 176 markers was designed. For each marker the associated biological process and the ENS number (derived from Ensembl) is depicted in the table (Sallinger et al., 2023).*

| Biological process/group | Subgroups | Gene (according to Human protein atlas) | ENS number (derived from Ensembl genome browser) |
|---|---|---|---|
| Angiogenesis | | ANGPT1 | ENSG00000154188 |
| | | ANGPT2 | ENSG00000091879 |
| | | FLT4 | ENSG00000037280 |
| | | KDR (VEGFR-2) | ENSG00000128052 |
| | | TIE1 | ENSG00000066056 |
| | | EREG | ENSG00000124882 |
| | | ENG (CD105) | ENSG00000106991 |
| | | MET | ENSG00000105976 |
| | | CD248 (TEM1) | ENSG00000174807 |
| | | ADGRA2 (TEM5) | ENSG00000020181 |
| | | PLXDC1 (TEM7) | ENSG00000161381 |
| | | ANTXR1 (TEM8) | ENSG00000169604 |
| | | TEK | ENSG00000120156 |
| | | F8 | ENSG00000185010 |
| Apoptosis | Pro-apoptotic | BBC3 (PUMA) | ENSG00000105327 |
| | | TNFSF10 (TRAIL) | ENSG00000121858 |
| | | BID | ENSG00000015475 |
| | | BIK | ENSG00000100290 |
| | | BCL2L11 (Bim) | ENSG00000153094 |
| | | BAK1 | ENSG00000030110 |
| | Inhibitors | CFLAR (cFLIP) | ENSG00000003402 |
| | | BCL2L1 (BCLX) | ENSG00000171552 |
| | | MCL1 | ENSG00000143384 |
| | Receptors | TNFRSF10A (DR4) | ENSG00000104689 |
| | | TNFRSF10B (DR5) | ENSG00000120889 |
| | Caspases | CASP8 | ENSG00000064012 |
| | | CASP9 | ENSG00000132906 |
| | | CASP7 | ENSG00000165806 |
| | | CASP3 | ENSG00000164305 |
| Autophagy | | MAP1LC3A (LC3) | ENSG00000101460 |
| | | ATG5 | ENSG00000057663 |
| | | BECN1 (Beclin 1) | ENSG00000126581 |
| Necrosis | | RIPK3 | ENSG00000129465 |
| | | MLKL | ENSG00000168404 |
| | | HMGB1 | ENSG00000189403 |

| | | | |
|---|---|---|---|
| | | RIPK1 | ENSG00000137275 |
| | | PPIF | ENSG00000108179 |
| Proliferation | Proliferation | PCNA | ENSG00000132646 |
| | | MCM2 | ENSG00000073111 |
| | | CNTD2 | ENSG00000105219 |
| | | EXOSC5 | ENSG00000077348 |
| | | E2F1 | ENSG00000101412 |
| | | MYBL2 | ENSG00000101057 |
| | | CCND1 | ENSG00000110092 |
| | | CCNE1 | ENSG00000105173 |
| | | GRB7 | ENSG00000141738 |
| | | RPS6KB1 | ENSG00000108443 |
| | | AURKA | ENSG00000087586 |
| | | SAAL1 | ENSG00000166788 |
| | | TGFA | ENSG00000163235 |
| | | EGFR | ENSG00000146648 |
| | | KIT | ENSG00000157404 |
| | | URGCP | ENSG00000106608 |
| | Inhibitors | BOP1 | ENSG00000261236 |
| | | BTG2 | ENSG00000159388 |
| | | FRK | ENSG00000111816 |
| Oxidative stress | | SOD1 | ENSG00000142168 |
| | | GPX1 | ENSG00000233276 |
| | | CAT | ENSG00000121691 |
| | | GSR | ENSG00000104687 |
| | | NOS2 | ENSG00000007171 |
| | | TXNL1 | ENSG00000091164 |
| | | PRDX2 | ENSG00000167815 |
| | | OSER1 | ENSG00000132823 |
| Hypoxia | | HIF1A | ENSG00000100644 |
| | | HIF3A | ENSG00000124440 |
| | | EGLN3 | ENSG00000129521 |
| | | PDK1 | ENSG00000152256 |
| | | SLC2A1 (GLUT1) | ENSG00000117394 |
| | | HYOU1 | ENSG00000149428 |
| Stemness/Differentiation | | ALDH1A1 | ENSG00000165092 |
| | | NANOG | ENSG00000111704 |
| | | SALL4 | ENSG00000101115 |
| | | CD44 | ENSG00000026508 |
| | | PROM1 (CD133) | ENSG00000007062 |
| | | BMI1 | ENSG00000168283 |
| | | MPL (CD110) | ENSG00000117400 |
| | | EPHB2 | ENSG00000133216 |
| | | LGR5 | ENSG00000139292 |

| | | | |
|---|---|---|---|
| | | IL6 | ENSG00000136244 |
| | | POU5F1 | ENSG00000204531 |
| | | SOX2 | ENSG00000181449 |
| Invasion | | LAMC2 (Laminin-5, γ2) | ENSG00000058085 |
| | | ITGAV | ENSG00000138448 |
| | | L1CAM | ENSG00000198910 |
| | | MMP7 | ENSG00000137673 |
| | | ENAH (MENA) | ENSG00000154380 |
| | | FGFR2 | ENSG00000066468 |
| | | SCAI | ENSG00000173611 |
| | | MIEN1 | ENSG00000141741 |
| | | TIAM1 | ENSG00000156299 |
| Epithelial-Mesenchymal Transition | | TJP1 | ENSG00000104067 |
| | | FN1 (Fibronectin) | ENSG00000115414 |
| | | TWIST1 | ENSG00000122691 |
| | | FOXC2 | ENSG00000176692 |
| | | ZEB1 | ENSG00000148516 |
| | | FAM3C | ENSG00000196937 |
| Energy metabolism | | SLC2A1 (GLUT1) (already in table 3, other biological process) | ENSG00000117394 |
| | | HK1 | ENSG00000156515 |
| | | HK2 | ENSG00000159399 |
| | | PKM2 | ENSG00000067225 |
| | | LDHA | ENSG00000134333 |
| | | GLS | ENSG00000115419 |
| | | GLUD1 | ENSG00000148672 |
| OncotypeDX genes | Cell cycle genes | MYBL2 (already in table 3, other biological process) | ENSG00000101057 |
| | Stromal genes | BGN | ENSG00000182492 |
| | | INHBA | ENSG00000122641 |
| | Early response gene | GADD45B | ENSG00000099860 |
| Epithelial cells | Colonocytes (Enterocytes) | ANPEP | ENSG00000166825 |
| | | CA1 | ENSG00000133742 |
| | | CA2 | ENSG00000104267 |
| | | FABP1 | ENSG00000163586 |
| | | BEST4 | ENSG00000142959 |
| | | OTOP2 | ENSG00000183034 |
| | | GUCA2B | ENSG00000044012 |
| | | SLC26A3 | ENSG00000091138 |
| | Goblet cells | MUC2 | ENSG00000198788 |
| | | MUC5AC | ENSG00000215182 |

| | | | | |
|---|---|---|---|---|
| | | | SPDEF | ENSG00000124664 |
| | | | KLF4 | ENSG00000136826 |
| | | | TFF1 | ENSG00000160182 |
| | | | TFF3 | ENSG00000160180 |
| | | Enteroendocrine cells | CHGA | ENSG00000100604 |
| | | | TBXT | ENSG00000164458 |
| | | | ZGLP1 | ENSG00000220201 |
| | | | GIP | ENSG00000159224 |
| | | | SST | ENSG00000157005 |
| | | | NTS | ENSG00000133636 |
| | | | PYY | ENSG00000131096 |
| | | | GAST | ENSG00000184502 |
| | | | MLN | ENSG00000096395 |
| | | Tuft cells | DCLK1 | ENSG00000133083 |
| | | | TRPM5 | ENSG00000070985 |
| | | | POU2F3 | ENSG00000137709 |
| | | | GFI1B | ENSG00000165702 |
| | | Stem cells | OLFM4 | ENSG00000102837 |
| | | | CD44 (already in table 3, other biological process) | ENSG00000026508 |
| | | | PROM1 (CD133) (already in table 3, other biological process) | ENSG00000007062 |
| | | | LGR5 (already in table 3, other biological process) | ENSG00000139292 |
| | | | ALDH1A1 (already in table 3, other biological process) | ENSG00000165092 |
| Tumor-associated stromal cells (TASC) | Cancer- associated fibroblasts (CAFs) | Mesenchymal stem cell-like | CD105 (already in table 3, other biological process) | ENSG00000106991 |
| | | | THY1 (CD90) | ENSG00000154096 |
| | | | NT5E (CD73) | ENSG00000135318 |
| | | | CD44 (already in table 3, other biological process) | ENSG00000026508 |
| | | Endothelial-like | ICAM1 (CD54) | ENSG00000090339 |
| | | | TEK (TIE2) | ENSG00000120156 |
| | | | VCAM1 (CD106) | ENSG00000162692 |
| | | | CDH5 (CD144) | ENSG00000179776 |
| | | MyoFibroblast-like | TNC | ENSG00000041982 |
| | | | TAGLN | ENSG00000149591 |
| | | | PDGFA | ENSG00000197461 |
| | | | TGFB3 | ENSG00000119699 |
| | | Pericyte-like | CSPG4 (NG2) | ENSG00000173546 |

| | | | | |
|---|---|---|---|---|
| | | Matrix remodelling | S100A4 (FSP1) | ENSG00000196154 |
| | | | MMP2 | ENSG00000087245 |
| | | | DCN | ENSG00000011465 |
| | | | COL1A2 | ENSG00000164692 |
| | | others | FSTL1 | ENSG00000163430 |
| | | | TIMP1 | ENSG00000102265 |
| | | | LIF | ENSG00000128342 |
| | | | IL11 | ENSG00000095752 |
| | Cancer-associated adipocytes (CAAs) | | IGFBP2 | ENSG00000115457 |
| | | | MMP11 | ENSG00000099953 |
| | | | IL6 (already in table 3, other biological process) | ENSG00000136244 |
| | | | IL1B | ENSG00000125538 |
| | | | IL8 | ENSG00000169429 |
| | | | FABP4 | ENSG00000170323 |
| | Cancer-associated endothelial cells (CAECs) | | S100A4 (FSP1) (already in table 3, other biological process) | ENSG00000196154 |
| | | | CXCL1 | ENSG00000163739 |
| | | | CD248 (TEM1) (alredy in list) | ENSG00000174807 |
| | | | ADGRA2 (TEM5) (already in table 3, other biological process) | ENSG00000020181 |
| | | | PLXDC1 (TEM7) (already in table 3, other biological process) | ENSG00000161381 |
| | | | ANTXR1 (TEM8) (already in table 3, other biological process) | ENSG00000169604 |
| | metastasis-associated fibroblasts (MAFs) | | CXCL12 (SDF1) | ENSG00000107562 |
| Th1 response | | | TNF | ENSG00000232810 |
| Macrophages /MDSC gene profile | | | NOS1 | ENSG00000089250 |
| | | | IL8 (already in table 3, other biological process) | ENSG00000169429 |
| | | | CD83 | ENSG00000112149 |
| | | | CD86 | ENSG00000114013 |
| T cell inhibition | | | IDO2 | ENSG00000188676 |
| | | | IL7R | ENSG00000168685 |
| | | | BTLA | ENSG00000186265 |
| | | | NCAM1 | ENSG00000149294 |
| General immunosuppression | | | BTLA (already in table 3, other biological process) | ENSG00000186265 |

| | | |
|---|---|---|
| | IDO2 (already in table 3, other biological process) | ENSG00000188676 |
| Inflammatory | NOS2 (already in table 3, other biological process) | ENSG00000007171 |
| | CD83 (already in table 3, other biological process) | ENSG00000112149 |
| Natural killer cells | NCR1 | ENSG00000189430 |
| | MICA | ENSG00000204520 |
| | MICB | ENSG00000204516 |
| | KLRK1 | ENSG00000213809 |
| | NCAM1 (already in table 3, other biological process) | ENSG00000149294 |
| Dendritic cells | ITGAM | ENSG00000169896 |

## 2.4. Sequencing of plasma and tissue samples of shedder project

Plasma and tissue samples of 21 recruited patients were sequenced at the Institute of Human Genetics, Diagnostic & Research Center for Molecular BioMedicine, Medical University of Graz in collaboration with Stefan Kühberger under supervision of Ellen Heitzer by using the TSO500 kit (Illumina, San Diego, California, USA). FFPE tissue blocks were cut into 5 µm thick sections and stained with H&E at the Division of Cell Biology, Histology and Embryology, Gottfried Schatz Research Center, Medical University of Graz. Neoplastic areas of slides were marked by a histologist and handed over to the Institute of Human Genetics, Diagnostic & Research Center for Molecular BioMedicine, Medical University of Graz for DNA extraction of the marked areas. 80 ng of DNA per sample were used for sequencing to reach a median exon coverage of >150. For plasma sequencing the total amount of collected plasma (8 ml) was used and a minimum of 1300 median exon coverage was required to confirm sequencing efficacy. To control and confirm the same origin of plasma and tissue samples, germline mutations of both sample types were matched.

Next, somatic mutations were identified and used to group patients into shedders (occurrence of variants in plasma and tissue) and non/low shedders (absence or very low occurrence of variants in plasma and tissue).

## 2.5. dRNA-HybISS

The lab work of dRNA-HybISS contains two main parts: library preparation and a sequencing procedure that consists of six cycles in addition to one stripping step for background imaging. An overview with detailed steps of both parts is depicted in figure 6 with additional optimization steps that were performed for the permeabilization, the hybridization of fluorescent labels and imaging.

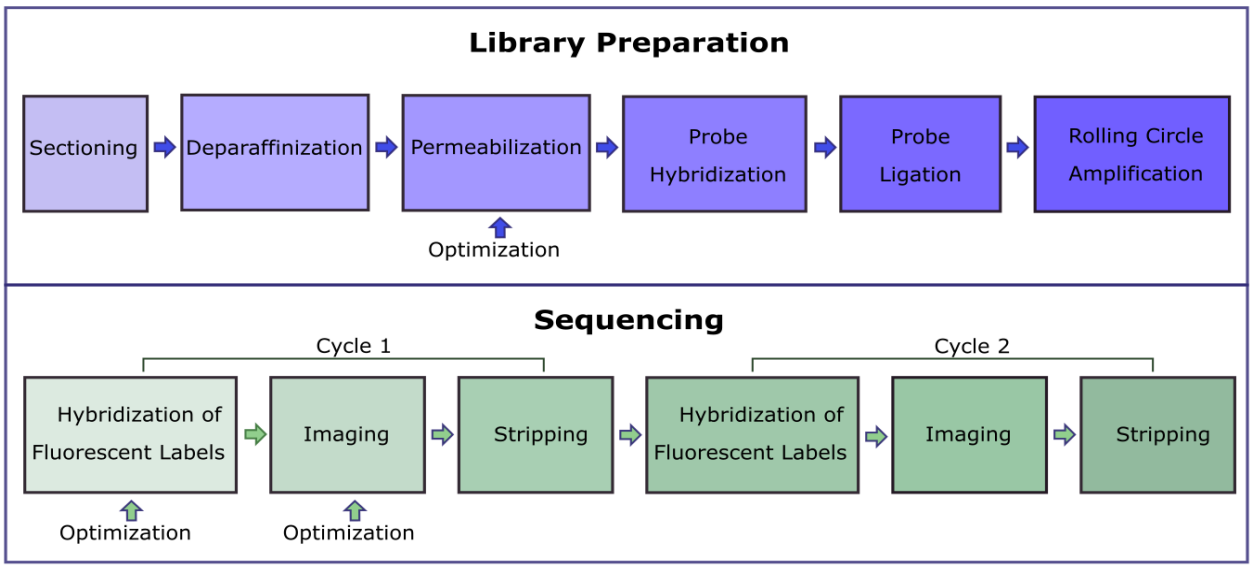


***Figure 6: Schematic overview of wet lab part of dRNA-HybISS technology with all the optimized steps.*** *Optimization experiments were performed for the permeabilization step, the hybridization of fluorescent labels and for the imaging step.*

### 2.5.1. Sectioning of tissue

Tissue samples from colon/ CRC stage II patients were FFPE embedded and stored at +4°C until use. Sample characteristics of both studies can be found in table 2 and 3. FFPE tissue blocks were pre-cooled on a cooling plate (TUC-1, Pathisto, Garbsen, Germany) set to -20°C and 5 µm tissue sections were cut by using the rotary microtome HM 355S (HM 355S, ThermoFischer Scientific, Massachusetts, USA). Slides with attached freshly cut FFPE tissue samples were dried overnight at room temperature, baked at 60°C for 20 min and stored at -80°C until use.

### 2.5.2. Library Preparation

Tissue sections were processed according to the manufacturer's protocols (Cartana, Stockholm, Sweden now 10xGenomics). RNA-degradation during tissue processing was kept to a minimum by adding 0.1% v/v diethylpyrocarbonate (=DEPC, Sigma-Aldrich, Vienna, Austria) to all buffers and reagents that were not provided by the manufacturer.

#### 2.5.2.1. Deparaffinization and Rehydration

Tissue sections were baked on a heating plate (Slide Stretching Tables OTS 40, Medite, Burgdorf, Germany) at 60°C for one hour and incubated 4 times in HistoLab Clear (Sanova Pharma, Vienna, Austria) at room temperature for 5 min each. Slides were then rehydrated in a descending ethanol series (100%, 95%, 70%, 50%; 2 min each), transferred to DEPC treated water (Sigma-Aldrich, Vienna, Austria) for 2 min and washed with washing buffer WB1 for 1 min.

#### 2.5.2.2. Permeabilization

In order to optimize permeabilization protocols for colon tissue samples, different conditions were tested using high- (*MALAT1*) and medium- expressed (*RPLP0*) control probes before using the final probe panels.

##### 2.5.2.2.1. First optimization experiment

The first optimization experiment was performed on four consecutive colon tissue samples by targeting *MALAT1*. The first slide was treated with 0.5 mg/ml pepsin (Sigma-Aldrich, Vienna, Austria) in phosphate buffered saline (PBS) for 30 min at 37°C, the second slide with 0.5 mg/ml pepsin (Sigma-Aldrich, Vienna, Austria) in PBS for 10 min at 37°C, the third slide was incubated in citrate buffer (pH = 6) (Merck, Darmstadt, Germany) for 45 min at 93°C in a microwave (Miele, Gütersloh, Deutschland) and the fourth slide was incubated in citrate buffer (pH = 6) (Merck, Darmstadt, Germany) for 45 min in a cooking steamer (Intellisteam compact, Morphy richards, Mexborough, Great Britain) at a temperature range between 95-100°C recommended by CARTANA.

##### 2.5.2.2.2. Second optimization experiment

The second optimization experiment was performed on four consecutive colon tissue samples by targeting *RPLP0*. The same conditions mentioned in the first optimization experiment were used to repeatedly examine the best permeabilization condition.

##### 2.5.2.2.3. CellProfiler pipeline for quantification of optimization

To analyze the images of the permeabilization experiment, a CellProfiler (Broad Institute, MA, United States) pipeline was created including the following steps: Nuclei were detected based on DAPI staining and expanded in order to recognize all tissue structures for inclusion in analysis (Stirling et al., 2021). Next, a threshold for truly positive signals was set to exclude false positive signals caused by autofluorescence. Additionally, a mask for the detected tissue area was generated to exclude all signals outside the tissue borders. The module

“MeasureObjectSizeShape” was used to measure the size of detected nuclei. By using the module “MeasureObjectIntensity” the number and intensity of the detected signals was measured. The next step included “masking” truly positive signals to enable measurement of background intensity within tissue boarders. All images and measured values were exported and saved in csv. files. The total number of detected cells was divided by the total pixel area of the DAPI stained nuclei. Additionally, the maximum signal/background ratio was calculated by dividing the average maximum signal intensities of all detected signals by the mean intensity of the background without signals. A detailed description of the used CellProfiler (Broad Institute, MA, United States) pipeline can be seen in the appendix under 6.6.1 (Stirling et al., 2021).

#### 2.5.2.2.4. Final permeabilization protocol

Slides were incubated in citrate buffer with pH = 6 (Merck, Darmstadt, Germany) for 45 min at temperatures between 95-100°C using a cooking steamer (Intellisteam compact, Morphy richards, Mexborough, Great Britain). They were then washed twice in fresh washing buffer WB1 and dehydrated in an ascending ethanol series (70%, 85%, 100%; 2 min each) to allow completion of all following steps using SecureSeal hybridization chambers (Secure Seal®, ThermoFischer Scientific, Massachusetts, USA) with a diameter of 9 mm achieving a hybridization area of 63,62 mm².

### 2.5.2.3. Probe Hybridization

For the rehydration of samples washing buffer WB3 was added no longer than 10 min, while the reaction mix (RM) was prepared (40 µl of RM1 and 10 µl of the used probes). After gently pipetting the RM up and down, WB3 was removed, and the RM was added to each section. Slides were placed in a RNAse free humidity chamber and incubated overnight at 37°C in a hybridization oven (HB-1D Hybridizer, Bibby Scientific US (Techne Inc.), Burlington, USA).

### 2.5.2.4. Probe Ligation

The following day the slides were washed twice with WB2, treated with WB4 for 30 min at 37°C and washed 3 times with WB2. RM2 was prepared (46.25 µl RM2 + 1.25µl Enzyme 1 + 2.5 µl Enzyme 2) and added to each tissue section for 2 hours at 37°C in a hybridization oven (HB-1D Hybridizer, Bibby Scientific US (Techne Inc.), Burlington, USA).

### 2.5.2.5. Rolling circle amplification

After washing twice with WB2, RM3 (40 µl RM3 + 10 µl Enzyme 3) was added to each sample and incubated overnight at 30°C in a hybridization oven (HB-1D Hybridizer, Bibby Scientific US (Techne Inc.), Burlington, USA).

### 2.5.3. Sequencing

#### 2.5.3.1. Hybridization of fluorescent labels

Sections were washed three times with WB2 and incubated with the Adapter Probe (AP) (=bridge probe) mix (40µl buffer A + 10 µl APx) for each cycle for 1 hour at 37°C in a hybridization oven (HB-1D Hybridizer, Bibby Scientific US (Techne Inc.), Burlington, USA). Slides were washed shortly with WB2 and treated with the Sequencing Probe (SP) (=detection oligonucleotide) mix including DAPI for nuclei counterstaining (40µl buffer A + 10 µl SP) for 30 min at 37°C in a hybridization oven (HB-1D Hybridizer, Bibby Scientific US (Techne Inc.), Burlington, USA). After removing the SP mix, tissue sections were dehydrated in an ascending ethanol series (70%, 85%, 100%; 2 min each), air-dried, mounted with SlowFade Gold Antifade (Invitrogen, ThermoFischer Scientific, Massachusetts, USA) and covered with a small coverslip (20x20 Roth, Karlsruhe, Germany).

#### 2.5.3.2. Imaging

The imaging of dRNA-HybISS-stained samples required a standard fluorescent microscope which allows for crosstalk-free detection of signals in 4',6-diamidino-2-phenylindole (DAPI), fluorescein isothiocyanate (FITC), Cyanine 3 (Cy3), Cyanine 5 (Cy5) and Cyanine 7 (Cy7).
Two different microscopes were tested and compared in parameters such as: applicability, scanning time, quality of signals in scanned areas and post-processing of images.

#### 2.5.3.3. Stripping

To perform further sequencing cycles after imaging, the fluorescent labels of each cycle were removed by using 100% Formamide (Sigma-Aldrich, Vienna, Austria). For this, sections with coverslips were incubated in DEPC-PBS water (Sigma-Aldrich, Vienna, Austria) until the coverslips detached from the samples. Slides were dehydrated in an ascending ethanol series (70%, 85%, 100%; 2 min each) to enable mounting of the SecureSeal hybridization chambers (Secure Seal®, ThermoFischer Scientific, Massachusetts, USA) and to perform the next sequencing cycle. Six cycles of sequencing were performed in total.

### 2.5.4. Microscope testing

#### 2.5.4.1. Testing the AxioObserver.Z1

The AxioObserver.Z1 inverted microscope from Zeiss (Jena, Germany) with an 40x objective, an HXP-120 light source, Zeiss filter sets 01, 17, 20 and 26 and an Axiocam 702 mono microscope

camera was used to image sections in the 5 channels mentioned above. The entire circular hybridized spot with a diameter of 9 mm was selected for scanning. The exposure times were set to 15 ms in the DAPI channel, 80 ms in the FITC channel, 200 ms in the Cy3 channel, 400 ms in the Cy5 channel and 400 ms in the Cy7 channel. Z-stacks of 10 slices with 1 µm intervals were used to detect all signals located in different cellular focal planes. Orthogonal projection was applied on the generated Z-stack to display all signals in one plane by setting the parameters to a thickness of 10 slices and to “Maximum Intensity”.

#### 2.5.4.2. Testing the scanner VS200

The same section was imaged in the same 5 channels by using the digital slide scanner VS200 from Evident with an 40x objective (Slideview VS200, Evident, Tokio, Japan) connected to an external Light-emitting diode (LED) source (Excelitas Technologies, X-Cite Xylis, Mississauga, Canada), a fluorescent pentafilter (AHF), a sCMOS camera (ORCA-Fusion C14440-20UP, 16 bit, Hamamatsu, Japan) and an universal-plan super apochromat 40× (0.95 NA/air, Evident, Tokio, Japan). The entire circular hybridized spot with a diameter of 8 mm was selected for scanning. The exposure times were set to 3.5 ms in the DAPI channel, 50 ms in the FITC channel, 50 ms in the Cy3 channel, 100 ms in the Cy5 channel and 200 ms in the Cy7 channel. For each cycle an image in DAPI, FITC, Cy3, Cy5 and Cy7 was captured, whereby the exact X- and Y coordinates of the scanned areas were saved to allow repetitive cycle imaging. For automatic rejection of unfocused Z-stack planes, the “Extended focus imaging (EFI)” function was used in which focused, bright signals were received.

#### 2.5.4.3. Testing exposure times at the VS200 scanner

Fluorescent-labelled *in situ* (IS) slides were used to determine the best exposure time to achieve the maximum signal/background ratio for signals in each channel. To perform the following steps in SecureSeal chambers with a diameter of 9 mm, slides were incubated in PBS (Sigma-Aldrich, Vienna, Austria), to remove remaining coverslips, and dehydrated in an ascending ethanol series (70%, 85%, S100%; 2 min each) and SecureSeals were mounted (Secure Seal®, ThermoFischer Scientific, Massachusetts, USA). Fluorescent labels were stripped by incubating the samples with 100% formamide three times (Sigma-Aldrich, Vienna, Austria) for 1 min, followed by a washing step with DEPC-PBS-Tween (Sigma-Aldrich, Vienna, Austria). For each tested fluorescent dye a separate spot was used (3 slides with two spots each) to avoid bleaching effects. Detection probe mixes for each slide were prepared by diluting the detection oligonucleotides (DO) (labelled with FITC, Cy3, Cy5 and Cy7) with 25 µl 2x Hybridization buffer (4x SSC (Invitrogen, ThermoFischer Scientific, Massachusetts, USA), 40% Formamide (Sigma-Aldrich, Vienna, Austria)) and 23.5 µl

DEPC $H_20$ (Sigma-Aldrich, Vienna, Austria) and applied to the samples at 37°C for 30 min. After removal of the detection probe mix, samples were dehydrated in an ascending ethanol series (70%, 85%, 100%; 2 min each), air-dried, mounted with SlowFade Gold Antifade (Invitrogen, ThermoFischer Scientific, Massachusetts, USA) and covered with a coverslip (20x20 Roth, Karlsruhe, Germany). Slides were imaged with the VS200 scanner by using different exposure times (25 ms, 50 ms, 100 ms, 150 ms, 200 ms, 400 ms, 600 ms, 800 ms, 1000 ms and 1500 ms).

#### 2.5.4.4. CellProfiler pipeline to analyze the exposure time experiment.

To analyze exposure time experiment images, a CellProfiler (Broad Institute, MA, United States) pipeline was created including the following steps: nuclei were detected based on DAPI staining and cell boarders were identified based on the autofluorescence in the FITC channel (Stirling et al., 2021). Signals with a feature size of 10 in all channels were enhanced to improve the identification of truly positive signals. After signal identification signals were related to their originating cell. With the use of the “MaskObjects” module only signals within cell boarders were detected. The modules “MeasureObjectSizeShape” and “MeasureObjectIntensity” were used to measure the number and the intensity of detected signals. To measure the background intensity within cell boarders, detected signals in each channel were masked by using the “MaskImage” module. All images and measured values were exported and saved in .csv files.

#### 2.5.4.5. Calculation of the maximum signal/background ratio

The measured values that were generated in the pipeline above were used to calculate the maximum signal/background ratio. To clarify the reason behind calculating and using the maximum signal/background ratio instead of the standard signal/background ratio, it is important to note that the decision was based on the subsequent dRNA-HybISS analysis, in which the maximum values of each signal are measured and used for decoding.

Therefore, the maximum signal/background ratios were calculated by dividing the average of maximum pixel intensity values of all signals in a channel by the mean intensity of the background. A schematic drawing of three different signals is depicted in figure 7, where signal 1 exhibits the highest maximum intensity values, followed by signal 2, and signal 3 with the lowest maximum intensity values. Consequently, we receive the highest maximum signal/background ratio for signal 1, followed by signals 2 and 3.

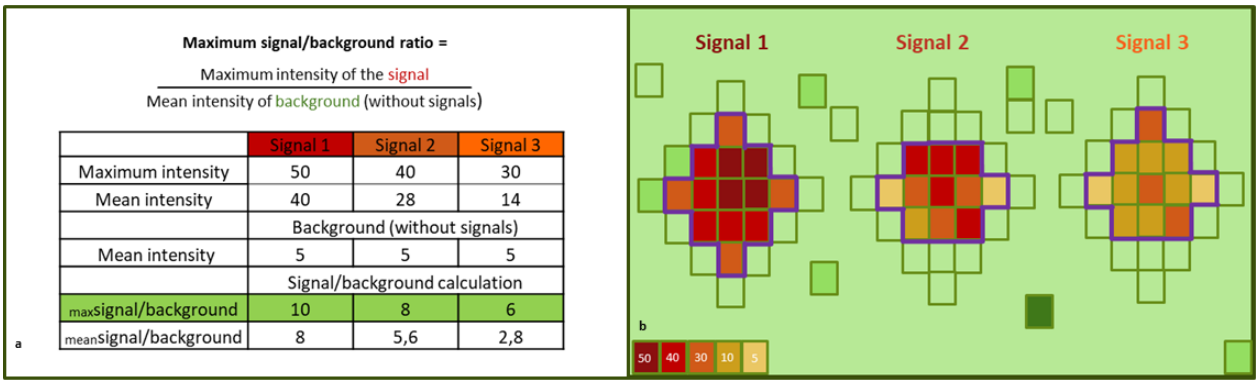


***Figure 7: Maximum signal/background calculation scheme***

*a) The maximum signal/background ratio was calculated by dividing the average maximum intensity of all signals in a channel by the mean intensity of the background without signals. This was schematically done for 3 signals with different signal intensities, whereat the intensities used for the mean signal intensity calculation are highlighted by a purple line enclosing them as depicted in b).*

### 2.5.5. Analysis pipeline

Analysis of dRNA-HybISS comprises 6 steps, which are performed in the VS200 Desktop software, MATLAB (Mathworks, Sweden) and CellProfiler (Broad Institute, MA, United States) with plugins from ImageJ. A schematic overview of the workflow is depicted in figure 8.

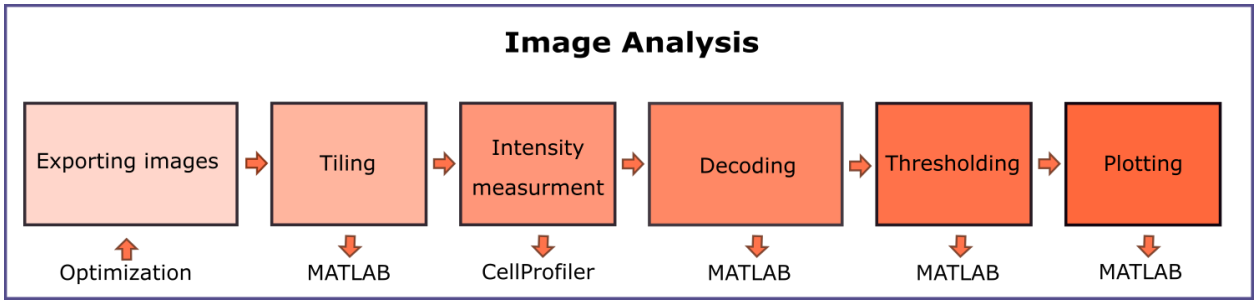


***Figure 8: Schematic overview of dRNA-HybISS image analysis workflow.***

*The exporting procedure was optimized to export .vsi files (Olympus format) to .tiff images. Image analysis was performed in MATLAB and CellProfiler which requires plugins for ImageJ.*

#### 2.5.5.1. Exporting images: VS200 scanner

Generated .vsi image files were converted to .tiff images by using the Olympus VS200 Desktop version (Evident, Tokio, Japan). For this, the function “Convert Virtual Slide Images” was used to select the correct export parameters (figure 9): Images to be exported were chosen by selecting the path for each image and saved by creating a target folder. Images were converted to .tiff formats for which only detail scans were used and a binning of 2x2 was selected to reduce the

size of the images. Multichannel images were split into separate images to receive one .tiff image per channel. Additionally, the “no tilling required” function was used before generating the converted files.

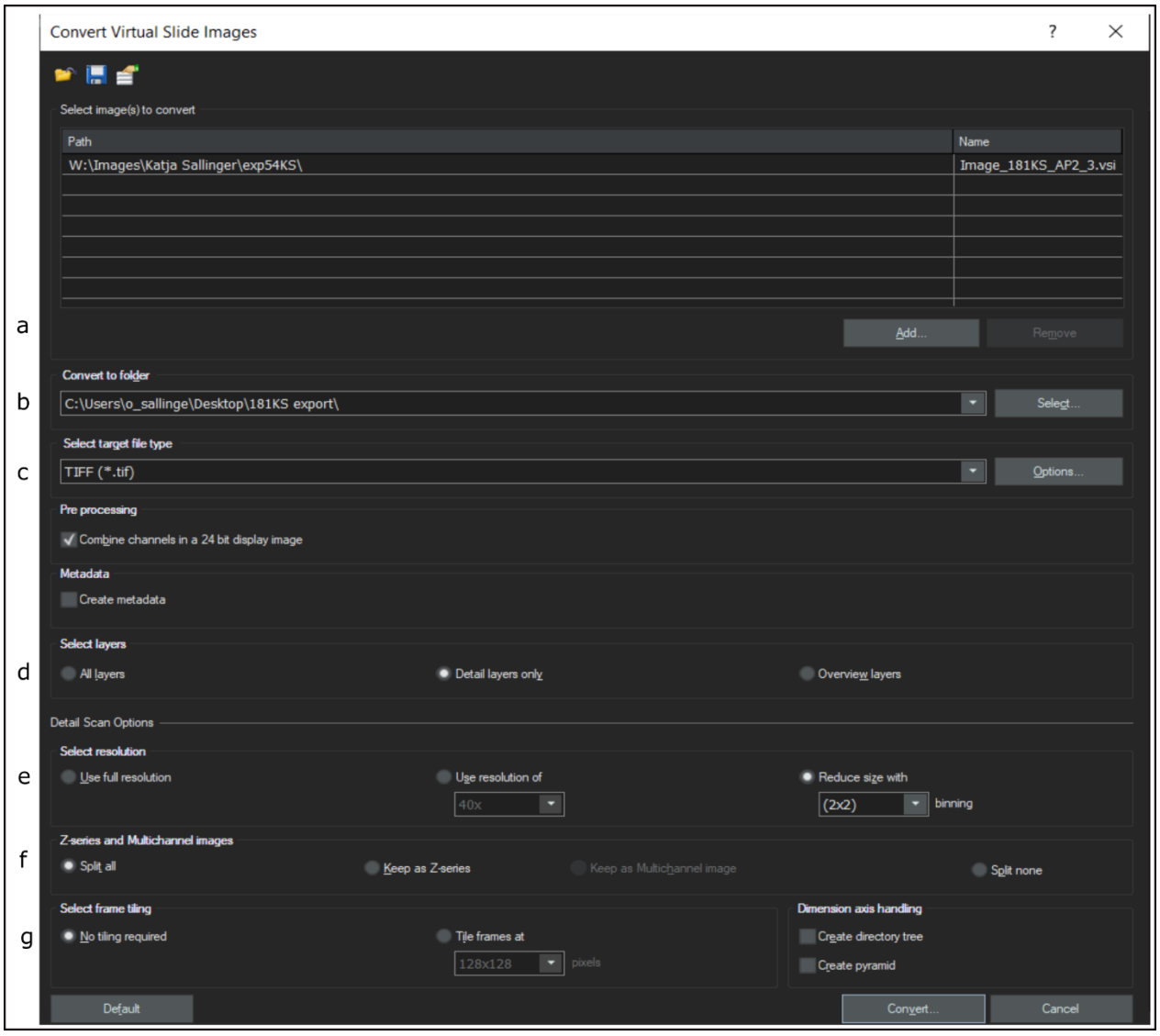


***Figure 9: Exporting scheme for converting .vsi images to .tiff files.***

*Different parameters were selected to convert the .vsi images to .tiff images: a) Images that should be exported were selected. b) A folder was selected, in which converted images were saved and c) A target file type was selected. d) Only detailed layers were selected (overview was excluded). e) The size of the images was reduced with a 2x2 binning. f) Multichannel images were split by using the function “Split all”. g) “No tiling required” was chosen for the tiling options.*

#### 2.5.5.2. Analysis in MATLAB part 1 (tiling)

The provided MATLAB (Mathworks, Sweden) script (CARTANA (Stockholm, Sweden, now part of 10x Genomics, California, USA)) contains a main script which is linked with different background scripts. Once analysis is established, only the main script must be adjusted for each sample

analysis (figure 10). In line 10 an output directory for the analyzed sample was created. Line 13 defined the number of performed dRNA-HybISS cycles, which in most cases was set to 6 or 5 cycles, depending on the quality of the cycles. E.g: if one cycle displayed very poor signal quality, it was excluded from analysis and analysis was performed with the 5 cycles that showed good quality signals. For the optimization of dRNA-HybISS analysis two additional modules were added to the pipeline that were defined in line 16 and 17. If the “real” general stain based on Cy5 staining of all signals was used, the imaging position of the Cy5 channel was selected in line 27. This procedure should be carried out before the first sequencing cycle and is essential for identifying all transcripts detected by the technique. The general stain transcripts that are identified indicate the positions at which the intensities of the four channels will be measured in each subsequent cycle.

As the same imaging procedure for the order of imaged channels was used for all the experiments, general stain signals were detected in Cy5. Therefore, adjustment of this value was not needed.

In line 30 the number of DAPI channels that were used during analysis in total was adjusted, which includes all DAPI images that were taken during the sequencing cycles (6 sequencing cycles = 6x number 1) plus the DAPI image that was taken during the background imaging.

In our setting, instead of using the real general stain in Cy5, we decided to computationally generate a pseudo-general stain, whereby detected signals across all 4 channels (FITC, Cy3, Cy5 and Cy7) of the first cycle were merged. Therefore, when using a pseudo-general stain, one additional number 1 was added to the specific line. If, for example, one performs 6 sequencing cycles + background subtraction step + generation of a pseudo-general stain, one must add the number 1 8 times.

The path to all images and cycles was adjusted in line 44 according to the channel order-DAPI, FITC, Cy3, Cy5 and Cy7. After defining the path to the images generated during the sequencing cycles, the path to the background images and the pseudo-general stain was added. By running the script, DAPI channels of each cycle were aligned with the DAPI channel of sequencing cycle one. Results of the alignment can be visualized in the folder “Aligned” that is created automatically. Next, images are tiled and saved in the folder “Tiled”. Csv. files containing the pathways to the tiled images are created and serve as the input files for the CellProfiler (Broad Institute, MA, United States) pipeline.

```
8     % Initiate
9 -   ctn = cartana;
10 -  ctn.OutputDirectory = 'W:\Analysis\Katja Sallinger\exp60KS\203KS_AP1';
11
12    % How many rounds of ISS cycles
13 -  ctn.nRounds = 6;
14
15    % EDIT: =1 if background channels present else 0
16 -  ctn.BackgroundChannels = 1;
17 -  ctn.extraChannel = 1;
18
19    % Whether library prep image is provided and required to be used as reference
20    % If no library preparation image was taken, the value is 0, and ISS cycle 1
21    % images will be used as reference instead
22 -  ctn.isLibraryPrep = 0;
23
24    % The channel number of anchor stain in library prep image
25    % If library prep image anchor and DAPI images are provided, this image
26    % will be used as reference ISS spots
27 -  ctn.AnchorChannel = 2;
28
29    % DAPI channel, one for each ISS cycle, Lirary Prep is the first
30 -  ctn.DAPIChannel = [1 1 1 1 1 1 1];
31
32    % ISS channels
33    % One row for one cycle of ISS, 4 channels in each cycle
34    % Cycle order: AlexFluor750, Cy3, Cy5, AlexFluor488 (same in all cycles)
35 -  ctn.ISSChannels = repmat([5 3 4 2], 6 + ctn.BackgroundChannels + ctn.extraChannel, 1
36
37
38    %% Pre-align stitched images
39    % To compensate for inaccuracy in microscope stage repositioning
40    % EDIT: add background channels as last Round(line) and set ctn.BackgroundChannels t
41
42
43 -  ctn.StitchedImages = {...
44    'W:\Analysis\Katja Sallinger\exp60KS\203KS_AP1\203KS_AP1_DAPI.tif', 'W:\Analysis\Kat
45    'W:\Analysis\Katja Sallinger\exp60KS\203KS_AP1\203KS_AP2_DAPI.tif', 'W:\Analysis\Kat
46    'W:\Analysis\Katja Sallinger\exp60KS\203KS_AP1\203KS_AP3_DAPI.tif', 'W:\Analysis\Kat
47    'W:\Analysis\Katja Sallinger\exp60KS\203KS_AP1\203KS_AP4_DAPI.tif', 'W:\Analysis\Kat
48    'W:\Analysis\Katja Sallinger\exp60KS\203KS_AP1\203KS_AP5_DAPI.tif', 'W:\Analysis\Kat
49    'W:\Analysis\Katja Sallinger\exp60KS\203KS_AP1\203KS_AP6_DAPI.tif', 'W:\Analysis\Kat
50    'W:\Analysis\Katja Sallinger\exp60KS\203KS_AP1\203KS_BG_DAPI.tif', 'W:\Analysis\Kat
51    'W:\Analysis\Katja Sallinger\exp60KS\203KS_AP1\203KS_AP1_DAPI.tif', 'W:\Analysis\Kat
52
53    };
```

***Figure 10: MATLAB main script used for tiling, decoding, thresholding and plotting***.

*In line 10 an output directory was created, whereas in line 13 the number of performed cycles was defined. The number of used DAPI images needs to be adjusted in line 30 and for line 44 the path to all images of all cycles must be added.*

#### 2.5.5.3. Multiplication factor and background subtraction step

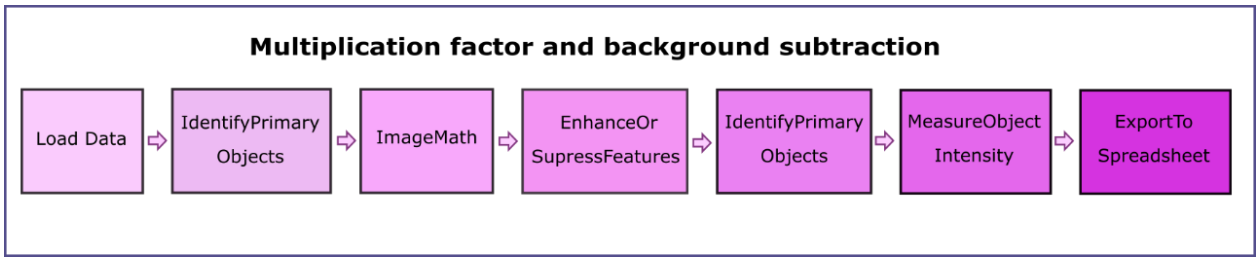


***Figure 11: Schematic overview of the developed "Multiplication factor and background subtraction" steps that were included in the dRNA-HybISS analysis workflow.***

Due to prior determination of the best exposure times for an optimal signal/background ratio in each color (as described in 2.5.4.4), the mean pixel intensity values of signals differed across channels for example 700 for FITC, 1500 for Cy3, 1700 for Cy5 and 1000 for Cy7. Therefore, the intensity values were normalized to 10000 by using a multiplication factor specific for each channel. To assess this factor for each color, a CellProfiler (Broad Institute, MA, United States) pipeline was developed which additionally included a background subtraction step to reduce autofluorescence of specific structures especially present in FITC and Cy3 for example erythrocytes and collagen fibres (Kamentsky et al., 2011). The individual steps of the pipeline can be seen in figure 11. First, the input.csv file was loaded into the pipeline and the rows to process were chosen. As intensity values for each channel possibly differed between sequencing cycles, each cycle was analyzed separately. For all samples in this study the same imaging size was defined. This resulted in 169 tiles after the tiling step in MATLAB (Mathworks, Sweden). To confirm the number of tiles per cycle (dependant on the total size of the scanned area) the folder "Tiled" can be opened. By using the "IdentifyPrimaryObjects" and "ExpandOrShrinkObjects" modules, the cytoplasm based on the FITC channel was detected and expanded by a pixel number of 7. To subtract the background autofluorescence in each channel the module "ImageMath" was used. Importantly, the order and annotations for the channels must stay the same: DO1=Cy7, DO2=Cy3, DO3=Cy5 and DO4=FITC. To avoid the loss of real signals due to excessive background subtraction, the "ImageMath" module was performed for each channel separately. To regulate the amount of background subtraction, the parameter "Multiply the second image by" was adjusted. This parameter influences the intensity of the background image: e.g: By multiplying the background image (second image) by a factor of 0.8, 80% of the background intensity will be subtracted. Signals in each channel with a feature size of 10 were enhanced and detected by using the module „IdentifyPrimaryObjects". Lower and upper bounds of the threshold were adjusted for each channel to avoid detecting false positive signals caused by autofluorescence.

The module “MeasureObjectIntensity” was used to measure the intensities of detected signals. The last module “ExportToSpreadsheet” saved and exported the measured values to a .csv file. A detailed description of the used CellProfiler (Broad Institute, MA, United States) pipeline can be seen in the appendix under 6.6.1 (Stirling et al., 2021). The pipeline generated different intensity values (mean, median and maximum intensities), whereby the maximum intensity value of each signal was used for further calculations. The mean value of all measured maximum signal intensities was calculated, multiplied by the number of pixels of the microscope (65335), normalized to 10000 and integrated into the main CellProfiler (Broad Institute, MA, United States) pipeline to analyze the dRNA-HybISS images.

#### 2.5.5.4. Generation of a “pseudo-general stain”

As the CellProfiler version 2. 1. 1 is compatible with ImageJ plugins included in the pipeline, all further analysis steps carried out in CellProfiler (Broad Institute, MA, United States) were performed in version 2.1.1 (Kamentsky et al., 2011).

A pseudo-general stain was generated by merging all 4 channels of sequencing cycle one to avoid performing an additional staining and imaging step in which all signals would be labelled with one color (called a general stain). For this, data was loaded in CellProfiler (Broad Institute, MA, United States) version 2.1.1, and background subtraction of each channel from sequencing cycle one was performed by using the “ImageMath” module. The received multiplication factors (described in 2.5.5.3) were integrated in the same module under the parameter “Multiply the result by”. This was done for all channels in addition to enhance signals in all channels with a feature size of 10. The merged image, called the pseudo-general stain, was created by the module “ImageMath” with the operation parameter “Maximum”. This allows for the selection of the channel with the maximum value at every pixel.

#### 2.5.5.5. Profiler pipeline

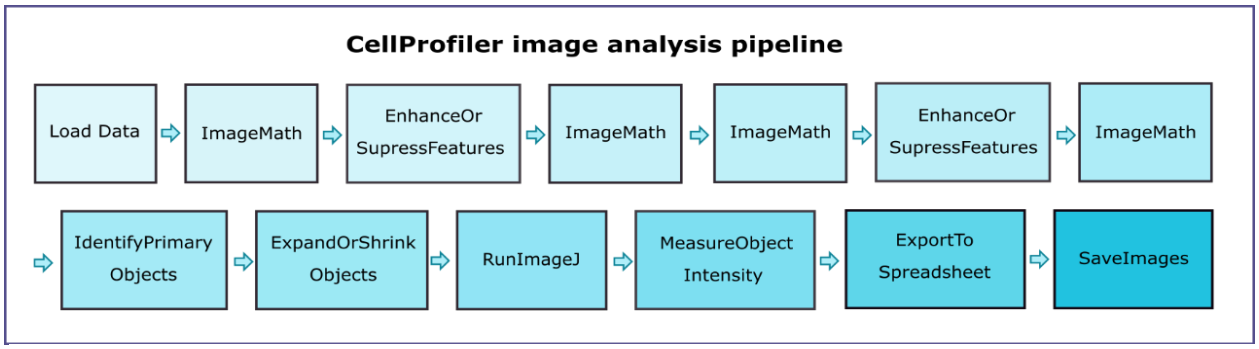


***Figure 12: Overview of the CellProfiler pipeline for dRNA-HybISS image analysis.*** *CellProfiler version 2.1.1. must be used, as only this version is compatible with the required ImageJ plugins (MultiStackReg, StackReg and TurboReg).*

As mentioned above, the following analysis steps were performed in CellProfiler (Broad Institute, MA, United States) 2.1.1 as this is the only version compatible with ImageJ (Kamentsky et al., 2011). Prior to running the pipeline, plugins for ImageJ (MultiStackReg, StackReg and TurboReg) must be downloaded and added to the preferences. The input .csv file was uploaded in the pipeline, rows to process were chosen for cycle one and the pseudo-general stain was created by using the modules “ImageMath”, “EnhanceOrSupressFeatures” and “ImageMath” as described above. The pseudo-general stain was generated only once per sample whereby the parameters in the specified modules must not be changed during analysis. The same set of modules was run to create a pseudo-anchor of each sequencing cycle. This was used for a second, more precise alignment to the pseudo-general stain (Sallinger et al., 2023). The parameters for the generation of the pseudo-anchor were adjusted in each cycle. By running the modules “IdentifyPrimaryObjects” and “ExpandOrShrinkObjects”, signals of the pseudo-general stain and the pseudo-anchor were detected by adjusting the manual thresholds and were expanded by a size of 2 pixels. All processed images were than loaded to ImageJ, which enables aligning of the pseudo-anchor of each cycle to the pseudo-general stain. The transformation matrix was saved and applied on all images in all channels to transform all images accordingly. The positions (x- and y- coordinates) of the pseudo-general stained signals were used to measure the pixel intensities across all channels (FITC, Cy3, Cy5 and Cy7) which were saved and exported to a .csv file. A detailed description of the modified CellProfiler (Broad Institute, MA, United States) pipeline modules can be seen in the appendix under 6.6.2 (Kamentsky et al., 2011). To control the efficacy of alignment, the aligned images of the pseudo-general stain and pseudo-anchor were saved. This procedure was performed separately for each sequencing cycle. Therefore, a MATLAB (Mathworks, Sweden) script was developed combining the output files of each cycle.

#### 2.5.5.6. Analysis in MATLAB part 2 (decoding and plotting)

For the decoding of detected signals, the codebook file path was added in line 92 of the MATLAB (Mathworks, Sweden) script containing barcode sequences and names of the genes in the used panel. The highest intensity value for each signal in each cycle was determined to be a real signal which was then used for decoding based on the barcode sequences in the codebook file. For visualization of the analysis, all decoded transcripts were plotted on the DAPI-stained image.

#### 2.5.5.7. Evaluation of alignment efficacy

After running dRNA-HybISS analysis in MATLAB (Mathworks, Sweden) and CellProfiler (Broad Institute, MA, United States), the alignment efficacy must be verified for each aligned tile. For each sequencing cycle a separate folder was generated automatically in which aligned tiles were saved. Tiles must be manually checked for correct alignment of the pseudo-general stain (red signals) and the pseudo anchor (green signals) of each sequencing cycle (overlap leads to yellow signals) to avoid decoding of false positive transcripts. Misaligned tiles (red) or tiles with tissue damage (orange) were marked in an overview image for each cycle and were possibly excluded from further analysis.

## 2.6. Cell segmentation

For the segmentation of cells, a provided MATLAB (Mathworks, Sweden) script (CARTANA (Stockholm, Sweden, now part of 10x Genomics, California, USA)) was used in which DAPI stained images of the pseudo-general stain were used to segment the cells. Additionally, the file with x and y coordinates of transcripts was needed to run the script and an output folder had to be defined. Depending on the RAM capacity of the used computer two possible outcomes occur, either RAM is sufficient to process the full image or not in which case the image must be tiled before segmentation can be performed. The Otsu method, an automatic thresholding technique, was used. It calculates the histogram of pixel intensities in a grayscale image to analyze the distribution of pixel intensities. The method then iterates through all possible thresholds and calculates the variance between the pixel intensities that would be categorized into different classes (foreground and background) by that threshold (Dong, 2014). It then selects the threshold value that maximizes the variance between the foreground and background, thus most effectively distinguishing cells (or similar foreground elements) from the background (Dong, 2014). This optimal threshold is then applied to segment the image into binary form, achieving a more effective separation of cells from the background than manual thresholding (Dong, 2014).

## 2.7. GTC-tool and statistical testing

To quantify the transcripts detected by dRNA-HybISS, an in-house developed tool, the genes-to-count tool (in short GTC-tool) was used that is available at the repository (https://github.com/spatialhisto/GTC). Based on the observation that some transcripts were mainly expressed in the neoplastic area sections, a set of specific transcripts overexpressed in these areas was identified, referred to as tumor gene signature. The dot like signals were expanded by 50-180 pixels to form connected areas which were subsequently used to automatically classify the tumor into its main compartments: neoplastic and non-neoplastic. For the quantification of signals, the number of signals per transcript were counted and normalized to the number of detected cells for each patient sample (see 2.6 cell segmentation). To test the statistical differences of the normalized transcripts between neoplastic and non-neoplastic areas, a two-tailed paired t-test was applied (Sallinger et al., 2023). In order to perform statistical testing of the normalized transcripts in the neoplastic areas of relapsed versus non-relapsed patients, a two-tailed independent t-test was used (Sallinger et al., 2023). For both statistical tests a significance level of $\alpha=0.05$ was chosen.

## 2.8. Gaussian heatmap plot

The in-house developed GTC-tool was used to generate gaussian heatmap plots. Each transcript is represented as a two-dimensional distribution with identical sigma values. The plot, furthermore, shows the cumulative distribution of the transcripts, by highlighting dense transcript area in lighter color and thinner area in darker color. By employing this approach, intricate patterns become more apparent.

## 2.9. Virtual H&E staining

Virtual H&E images of the dRNA-HybISS hybridized tissue slides were generated according to DAPI and FITC background images, taken during the sequencing procedure (Sallinger et al., 2023). This methodology was first described by Giacomelli et al. (2023) and allowed us to use the morphological structure identical to the tissue section that had been used for dRNA-HybISS transcript detection (Giacomelli MG, 2016; Sallinger et al., 2023). The evaluation of the virtual H&E images of all patients was performed by a pathologist, who sub-classified the patient samples into neoplastic and non-neoplastic areas.

## 2.10. Cell-phenotyping with DeNovo SSAM

As a proof of concept, cell-phenotyping of one patient sample was performed by using a tool named DeNovo SSAM, developed and published by Park et al. (Park et al., 2021). All scripts are written in python and can be accessed via an Ubuntu environment on Windows with a Windows Subsystem for Linux. The tool allows for cell-phenotyping of tissues, without prior need of segmenting cells. Therefore, an automatic run-script was used, requiring the adjustment of sample parameters (figure 13) and processing parameters (figure 14). To configure the sample parameters the path of the sample csv.file was specified in line 46 and an output directory was defined in line 52. For the processing parameters, specific settings were modified within the respective subsections, including the bandwidth for kernel density plots; the minimal cluster size, principle component analysis (PCA) dimensions, and vector resolution for clustering; as well as the spot size for t-distributed Stochastic Neighbour Embedding (t-SNE) plots (figure 14).

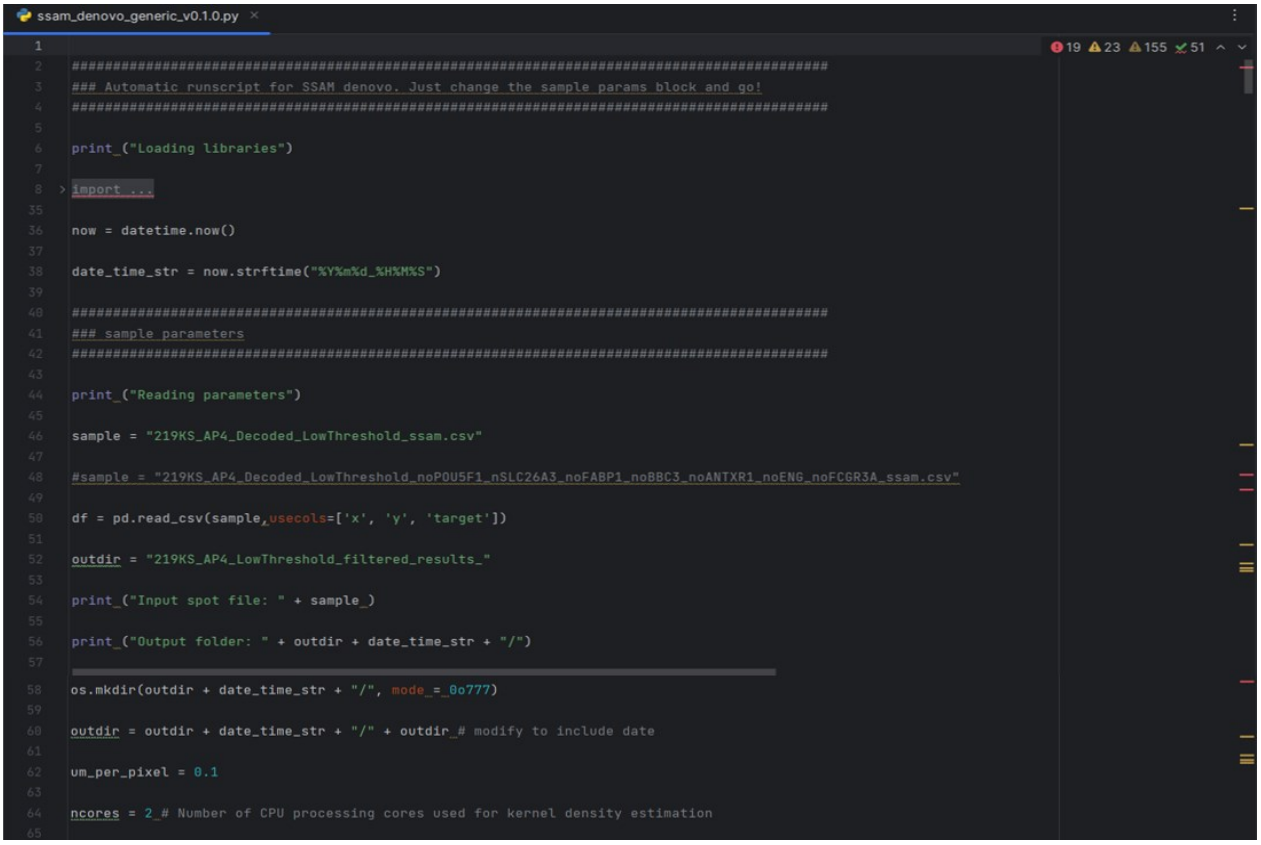


***Figure 13: DeNovo SSAM script part 1 _ sample parameters***

*In the first part of the script, the path to the csv.file for analysis was defined in line 46 and an output directory was specified in line 52.*

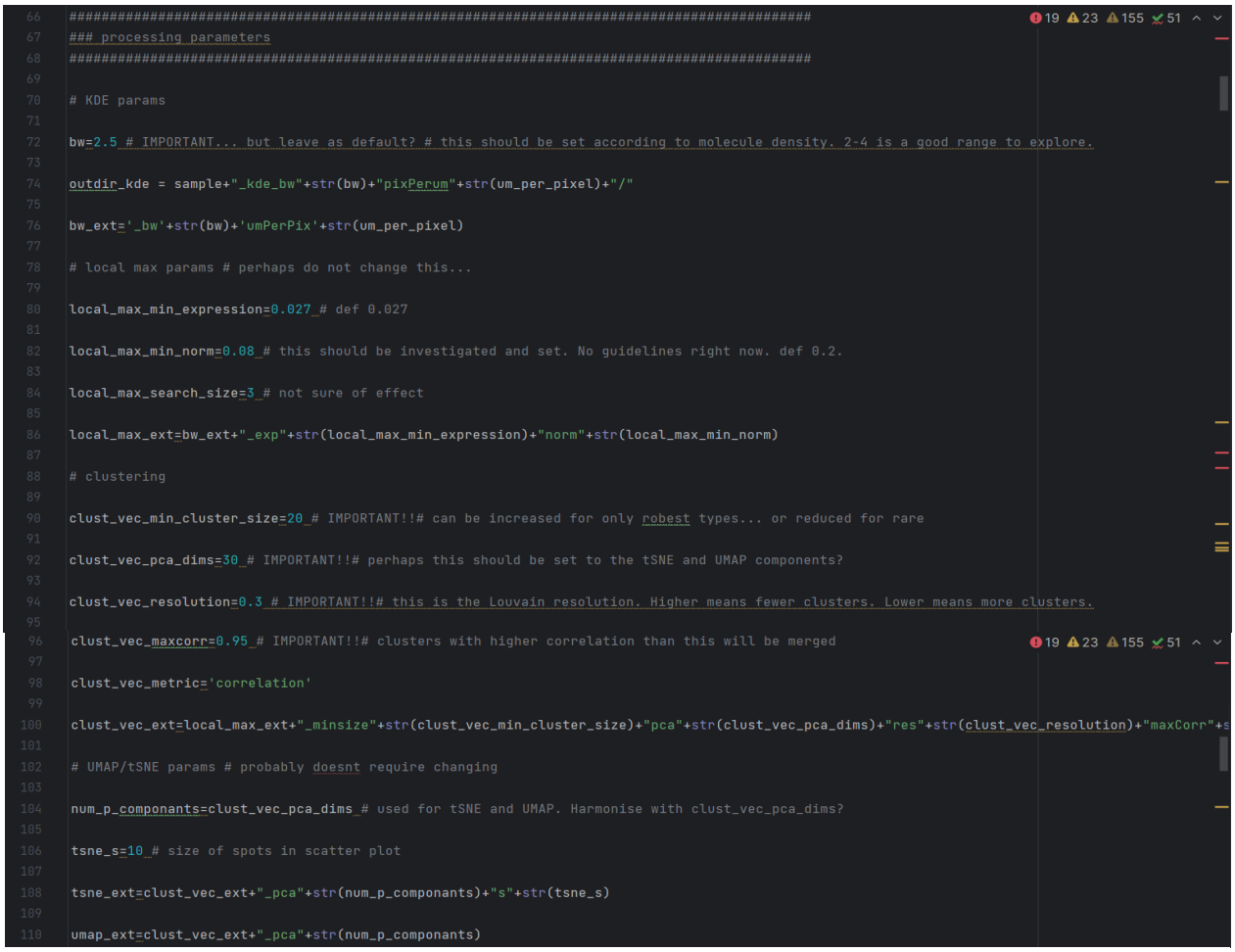

```
##############################################################################################
### processing parameters
##############################################################################################

# KDE params

bw=2.5 # IMPORTANT... but leave as default? # this should be set according to molecule density. 2-4 is a good range to explore.

outdir_kde = sample+"_kde_bw"+str(bw)+"pixPerum"+str(um_per_pixel)+"/"

bw_ext='_bw'+str(bw)+'umPerPix'+str(um_per_pixel)

# local max params # perhaps do not change this...

local_max_min_expression=0.027 # def 0.027

local_max_min_norm=0.08 # this should be investigated and set. No guidelines right now. def 0.2.

local_max_search_size=3 # not sure of effect

local_max_ext=bw_ext+"_exp"+str(local_max_min_expression)+"norm"+str(local_max_min_norm)

# clustering

clust_vec_min_cluster_size=20 # IMPORTANT!!# can be increased for only robest types... or reduced for rare

clust_vec_pca_dims=30 # IMPORTANT!!# perhaps this should be set to the tSNE and UMAP components?

clust_vec_resolution=0.3 # IMPORTANT!!# this is the Louvain resolution. Higher means fewer clusters. Lower means more clusters.

clust_vec_maxcorr=0.95 # IMPORTANT!!# clusters with higher correlation than this will be merged

clust_vec_metric='correlation'

clust_vec_ext=local_max_ext+"_minsize"+str(clust_vec_min_cluster_size)+"pca"+str(clust_vec_pca_dims)+"res"+str(clust_vec_resolution)+"maxCorr"+s

# UMAP/tSNE params # probably doesnt require changing

num_p_componants=clust_vec_pca_dims # used for tSNE and UMAP. Harmonise with clust_vec_pca_dims?

tsne_s=10 # size of spots in scatter plot

tsne_ext=clust_vec_ext+"_pca"+str(num_p_componants)+"s"+str(tsne_s)

umap_ext=clust_vec_ext+"_pca"+str(num_p_componants)
```

***Figure 14: DeNovo SSAM script part 2_processing parameters***

*Specific adjustments were made in the corresponding sub-sections of the processing parameters script, including the bandwidth of kernel density plots; minimum cluster size, dimensions of PCA, and resolution of vectors for clustering; along with the spot size for UMAP and t-SNE visualizations.*

Initially, kernel density estimation (KDE) plots of each gene in the dataset were generated and used for the creation of a gene expression vector field (figure 15a). Next, the vectors of the field were down-sampled by performing principle component analysis (figure 15b) and the Louvain clustering algorithm was used to create clusters of genes with similar expression patterns (figure 15c). By combining step 1 and 2, cell-type specific maps of the samples were generated that were subsequently annotated based on the histological structure of the tissue (figure 15c). Additionally, t-SNE plots were generated to show the location of each identified cluster in relation to the other clusters (figure 15d). Results were optimized by removing unspecific genes of the gene expression matrix. For this, heatmaps of the expression matrices were created, a z-normalization of the datasets was performed, clusters were combined to subgroups and finally unspecific markers were identified and removed from the matrix.


***Figure 15: DeNovo SSAM script part 3_KDE, Cluster vectors, t-SNE and cell-type map***

*a) Kernel density plots for each gene were produced, used for the creation of a gene expression vector field. b) PCA down-samples the field vectors and c) the Louvain clustering algorithm identified clusters of genes with similar expression patterns and cell-type specific maps were generated. d) t-SNE plots were created.*

# 3. Results

## 3.1. Optimization of library preparation: Citrate buffer in a steamer for 45 min at 95-100°C

To examine the best permeabilization condition for colon tissue, 4 different conditions (pepsin for 30 min, pepsin for 10 min, citrate buffer in a microwave and citrate buffer in a cooking steamer) were tested by using high- (*MALAT1*) and medium- expressed (*RPLP0*) control probes.
The number of detected signals per pixel area and the maximum signal to background ratio was calculated for each condition, to quantify the received results.

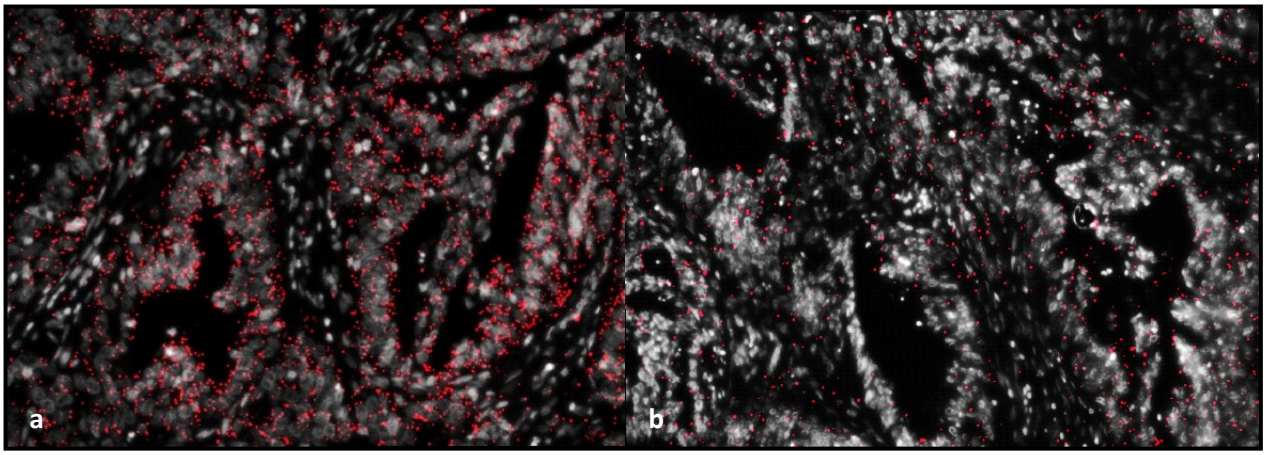


***Figure 16: Detected MALAT1 transcripts.***
*Tissue permeabilization was performed by using (a) citrate buffer in a steamer for 45 min at 95-100°C (b) pepsin for 10 min.*

Optimal results for MALAT1, in terms of signal density per area and signal to background ratio, were achieved by permeabilizing with citrate buffer for 45 minutes in a steamer at a temperature range tightly controlled between 95°C and 100°C (3858 signals/area and a signal/background ratio of 3.89) depicted in figure 16a. Using pepsin for 30 min, 10 min (figure 16b) and citrate buffer for 45 min in a microwave resulted in 2327, 1317 and 2294 detected signals per area and signal to background ratios of 2.51, 3.87 and 3.41 (table 5).

***Table 5: Signals/area and signal/background ratio of detected MALAT1 transcripts.***

*The parameters were calculated for four different permeabilization conditions: pepsin for 30 min, pepsin for 10 min, citrate buffer in a microwave and citrate buffer in a cooking steamer.*

| ***Malat1*** | **Signals/area (1*10^6 pixel)** | **Signal/background ratio** |
|---|---|---|
| **pepsin 30min** | 2327 | 2.51 |
| **pepsin 10min** | 1317 | 3.87 |
| **citrate buffer + microwave - 45min** | 2294 | 3.41 |
| **citrate buffer + steamer - 45min** | **3858** | **3.89** |

Testing the same conditions with the transcript *RPLP0* showed the best result in number of signals per area through permeabilization with citrate buffer for 45 min in a steamer at a temperature range between 95-100°C, leading to 272 detected signals per area. Permeabilization with pepsin for 30 min yielded the highest signal to background ratio (4.54).

Using pepsin for 30 min, 10 min and citrate buffer for 45 min in a microwave resulted in 272, 101 and 283 detected signals per area. The signal to background ratio for treatment with pepsin for 10 min, citrate buffer for 45 min in a microwave and citrate buffer for 45 min in a steamer was 4.37, 3.36 and 4.46 (table 6).

***Table 6: Signals/area and signal/background ratio of detected RPLP0 transcripts.***

*The parameters were calculated for 4 different permeabilization conditions: pepsin for 30 min, pepsin for 10 min, citrate buffer in a microwave and citrate buffer in a cooking steamer.*

| ***RPLP0*** | **Signals/area (1*10^6 pixel)** | **Signal/background ratio** |
|---|---|---|
| **pepsin 30mins** | 272 | 4.54 |
| **pepsin 10min** | 101 | 4.37 |
| **citrate buffer + microwave - 45min** | 283 | 3.36 |
| **citrate buffer + steamer - 45min** | **315** | **4.46** |

## 3.2. Imaging performance of VS200 versus AxioObserver.Z1 from Zeiss

The same sample and scanning area (diameter of 9 mm, 63,62 $mm^2$) was chosen to compare the imaging performances of the AxioObserver.Z1 from Zeiss (Jena, Germany) and the VS200 from Evident (Tokio, Japan). The slide was scanned in the following 5 channels for both microscopes: DAPI, FITC, Cy3, Cy5 and Cy7. Whereas for VS200 the provided autofocusing function was used, manual focus points had to be set for the entire scanning area for the Observer to avoid out-of-focus images. Approximately 20 hours were needed to image the chosen area with the Observer, whereas the same spot was scanned within 3 hours using the Evident (Tokio, Japan) microscope. Additionally, the VS200 Scanner was equipped with a batch function to serially image 6 slides. This function enabled overnight imaging of samples. When evaluating the imaging quality of both microscopes, higher pixel intensities of autofluorescent structures, especially present in FITC and Cy3, were seen by using the Observer in comparison to the VS200, resulting in lower signal to background ratios.

## 3.3. Defining the best exposure time for each channel

Slides specifically labelled for each channel were imaged with 10 different exposure times (25, 50, 100, 150, 200, 400, 600, 800, 1000, 1500 ms). The resulting images were then exported and subsequently analyzed in a CellProfiler (Broad Institute, MA, United States) pipeline. For each exposure time and channel, the signal to background values were calculated, depicted in table 7 and figure 17. For Atto488 the highest signal/background ratio was observed with an exposure time of 50 ms. For Cy3 the highest signal/background ratio was observed with an exposure time of 100 ms and Cy5 and Cy7 displayed the highest signal/background ratio with exposure times of 400 and 600 ms. In table 7 the optimal exposure times for each channel are highlighted in blue. Measurements for Cy5 at 25, 50 and 100 ms and for Cy7 at 25, 50, 100 and 150 ms were excluded from analysis (shown as “na” in table 7), as CellProfiler (Broad Institute, MA, United States) was not able to distinguish real signals from background, resulting in the detection of false positive signals.

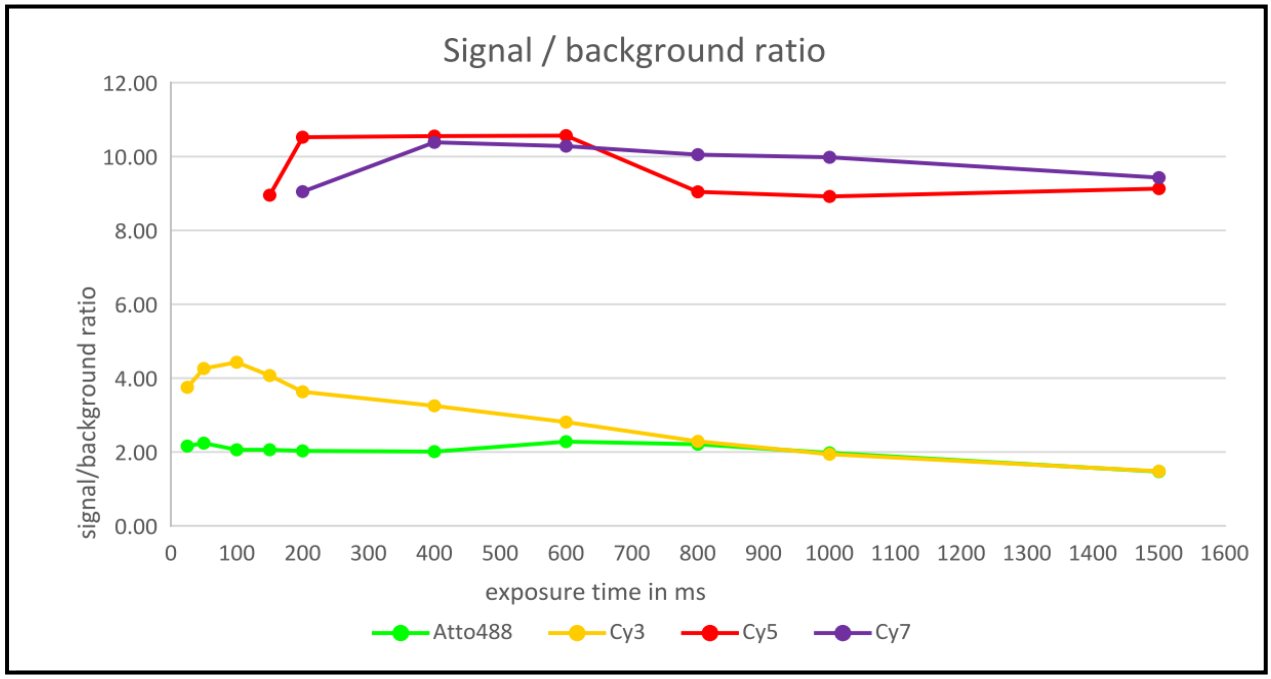


***Figure 17: Line graph of signal/background ratios at different exposure times for each channel.***

*The figure represents a line graph of signal/background ratios of the channels Atto488 (green), Cy3 (yellow), Cy5 (red) and Cy7 (violet) calculated for 10 different exposure times (25, 50, 100, 150, 200, 400, 600, 800, 1000 and 1500 ms).*

***Table 7: Calculated signal/background ratios for different exposure times and each channel.***

*The table represents signal/background ratios of the channels Atto488 (green), Cy3 (yellow), Cy5 (red) and Cy7 (violet) calculated for 10 different exposure times (25, 50, 100, 150, 200, 400, 600, 800, 1000 and 1500 ms). The highest (=best) value/values for each channel are highlighted in blue. "na" represents values, that were excluded from analysis, as real signals were not able be differentiated from the background.*

| 40x | | | | |
|---|---|---|---|---|
| | **Atto488** | **Cy3** | **Cy5** | **Cy7** |
| **Exposure time in ms** | s/b ratio | s/b ratio | s/b ratio | s/b ratio |
| 25 | 2,16 | 3,75 | na | na |
| 50 | 2,24 | 4,26 | na | na |
| 100 | 2,06 | 4,43 | na | na |
| 150 | 2,06 | 4,07 | 8,95 | na |
| 200 | 2,03 | 3,63 | 10,52 | 9,05 |
| 400 | 2,01 | 3,25 | 10,55 | 10,38 |
| 600 | 2,28 | 2,81 | 10,57 | 10,28 |
| 800 | 2,21 | 2,29 | 9,04 | 10,05 |
| 1000 | 1,98 | 1,94 | 8,92 | 9,98 |
| 1500 | 1,47 | 1,48 | 9,13 | 9,43 |

## 3.4. Calculation of the multiplication factor

A CellProfiler (Broad Institute, MA, United States) pipeline was used to calculate the multiplication factor of each channel, whereby the signal pixel intensity was measured. Figure 18 shows the different pipeline modules used for the measurement of FITC signal pixel intensity values. The same pipeline was used to measure pixel intensities of Cy3, Cy5 and Cy7 signals. To include signals located within the nuclei as well as signals in the cytoplasm, nucleic boarders were identified with the DAPI images and expanded to cover the whole tissue section (figure 18a). To remove autofluorescent structures, especially for FITC and Cy3, the background image of each channel was subtracted from each of the six performed sequencing cycles (figure 18b). Signals with a feature size of 10 were enhanced and identified by adjusting the threshold (figure 18c, d). Various intensity parameters such as the median, mean and maximum intensity of each signal were measured and saved in an excel sheet (figure 18e). The mean of all FITC maximum intensity signals was calculated separately for each cycle, then multiplied by the number of microscope pixels (65535) and finally normalized to a pixel intensity value of 10000 (table 8). The same CellProfiler (Broad Institute, MA, United States) pipeline and calculation procedure that is described in figure 18 was used to measure the pixel intensities for Cy3 (table 9), Cy5 (table 10) and Cy7 (table 11). Table 12 shows a list of the used “Multiply second image by” values and the calculated “multiplication factors” for all channels and performed cycles.

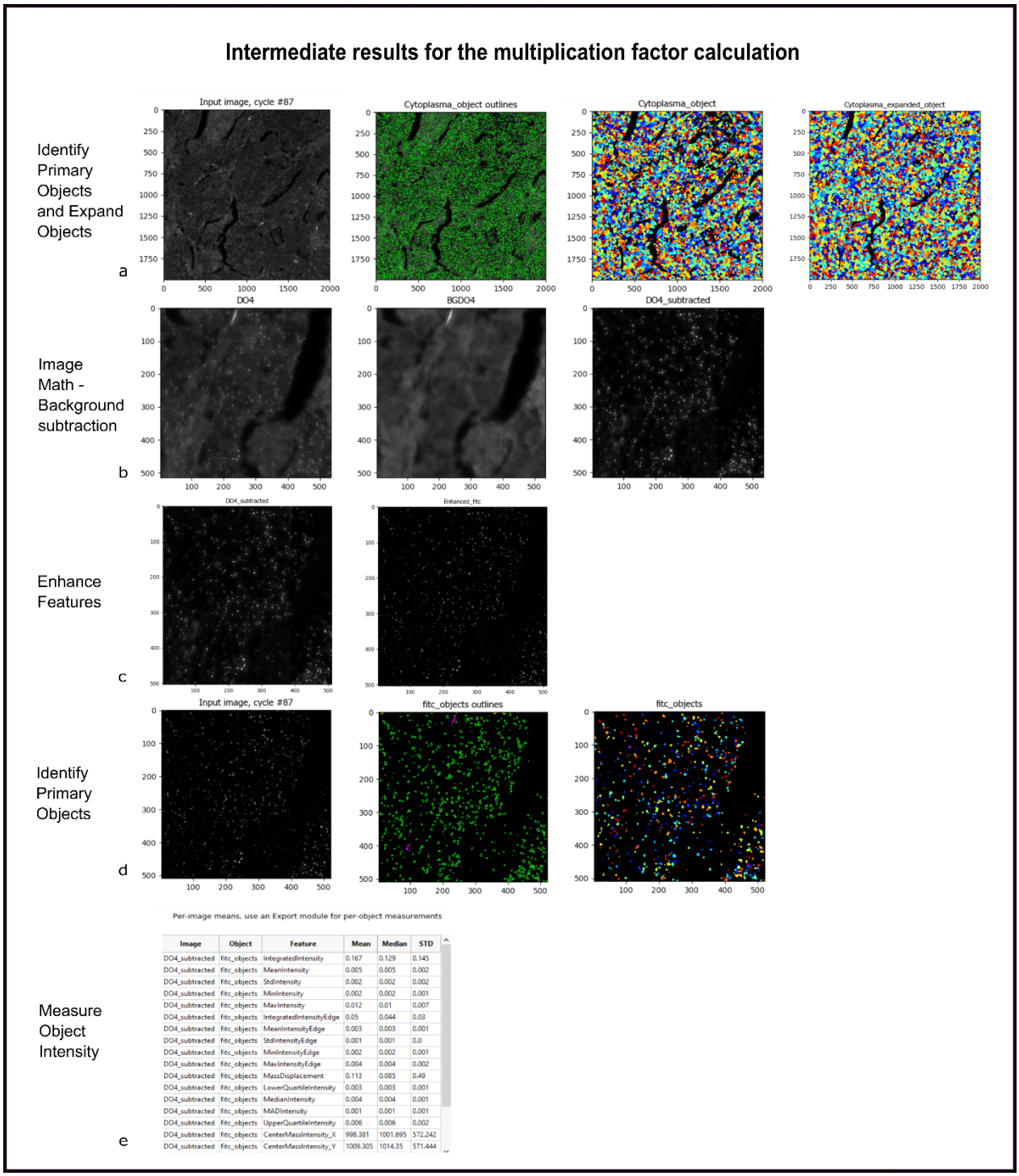


***Figure 18: Intermediate results produced by the CellProfiler pipeline to measure pixel intensity values of FITC signals***.

*a) Cell nuclei were identified based on DAPI staining and expanded. b) The background from each channel was subtracted from each cycle to remove autofluorescent structures. c) Signals with a feature size of 10 were enhanced, d) signals were identified by adjusting the threshold, e) different intensity parameters were measured and saved.*

***Table 8: Results from the multiplication factor calculation for the FITC channel.***

*The calculation was performed separately for each cycle. The table shows the mean value calculated from all measured maximum intensity FITC object values. The mean value for each cycle is multiplied by the number of microscope pixels (65535) and normalized to a pixel intensity value of 10000.*

| | | |
|---|---|---|
| **Cycle 1** | | **Maximum intensity_FITC_objects** |
| | Mean | 0,012 |
| | Pixel intensity | 800 |
| | Multiplication factor | **12,5** |
| | | |
| **Cycle 2** | | **Maximum intensity_FITC_objects** |
| | Mean | 0,013 |
| | Pixel intensity | 868 |
| | Multiplication factor | **11,5** |
| | | |
| **Cycle 3** | | **Maximum intensity_FITC_objects** |
| | Mean | 0,012 |
| | Pixel intensity | 777 |
| | Multiplication factor | **12,9** |
| | | |
| **Cycle 4** | | **Maximum intensity_FITC_objects** |
| | Mean | 0,017 |
| | Pixel intensity | 1092 |
| | Multiplication factor | **9,2** |
| | | |
| **Cycle 5** | | **Maximum intensity_FITC_objects** |
| | Mean | 0,012 |
| | Pixel intensity | 787 |
| | Multiplication factor | **12,7** |
| | | |
| **Cycle 6** | | **Maximum intensity_FITC_objects** |
| | Mean | 0,011 |
| | Pixel intensity | 714 |
| | Multiplication factor | **14** |

***Table 9: Results from the multiplication factor calculation for the Cy3 channel.***

*The calculation was performed separately for each cycle. The table shows the mean value calculated from all measured maximum intensity Cy3 object values. The mean value for each cycle is multiplied by the number of microscope pixels (65535) and normalized to a pixel intensity value of 10000.*

| | | |
|---|---|---|
| **Cycle 1** | | **Maximum intensity_Cy3_objects** |
| | Mean | 0,032 |
| | Pixel intensity | 2112 |
| | Multiplication factor | **4,7** |
| | | |
| **Cycle 2** | | **Maximum intensity_Cy3_objects** |
| | Mean | 0,025 |
| | Pixel intensity | 1624 |
| | Multiplication factor | **6,2** |
| | | |
| **Cycle 3** | | **Maximum intensity_Cy3_objects** |
| | Mean | 0,024 |
| | Pixel intensity | 1587 |
| | Multiplication factor | **6,3** |
| | | |
| **Cycle 4** | | **Maximum intensity_Cy3_objects** |
| | Mean | 0,032 |
| | Pixel intensity | 2081 |
| | Multiplication factor | **4,8** |
| | | |
| **Cycle 5** | | **Maximum intensity_Cy3_objects** |
| | Mean | 0,027 |
| | Pixel intensity | 1748 |
| | Multiplication factor | **5,7** |
| | | |
| **Cycle 6** | | **Maximum intensity_Cy3_objects** |
| | Mean | 0,022 |
| | Pixel intensity | 1455 |
| | Multiplication factor | **6,9** |

***Table 10: Results from the multiplication factor calculation for the Cy5 channel.***

*The calculation was performed separately for each cycle. The table shows the mean value calculated from all measured maximum intensity Cy5 object values. The mean value for each cycle is multiplied by the number of microscope pixels (65535) and normalized to a pixel intensity value of 10000.*

| | | |
|---|---|---|
| **Cycle 1** | | **Maximum intensity_Cy5_objects** |
| | Mean | 0,031 |
| | Pixel intensity | 2052 |
| | Multiplication factor | **4,9** |
| | | |
| **Cycle 2** | | **Maximum intensity_Cy5_objects** |
| | Mean | 0,022 |
| | Pixel intensity | 1448 |
| | Multiplication factor | **6,9** |
| | | |
| **Cycle 3** | | **Maximum intensity_Cy5_objects** |
| | Mean | 0,027 |
| | Pixel intensity | 1793 |
| | Multiplication factor | **5,6** |
| | | |
| **Cycle 4** | | **Maximum intensity_Cy5_objects** |
| | Mean | 0,032 |
| | Pixel intensity | 2103 |
| | Multiplication factor | **4,8** |
| | | |
| **Cycle 5** | | **Maximum intensity_Cy5_objects** |
| | Mean | 0,024 |
| | Pixel intensity | 1604 |
| | Multiplication factor | **6,2** |
| | | |
| **Cycle 6** | | **Maximum intensity_Cy5_objects** |
| | Mean | 0,03 |
| | Pixel intensity | 1935 |
| | Multiplication factor | **5,2** |

***Table 11: Results from the multiplication factor calculation for the Cy7 channel.***

*The calculation was performed separately for each cycle. The table shows the mean value calculated from all measured maximum intensity Cy7 object values. The mean value for each cycle is multiplied by the number of microscope pixels (65535) and normalized to a pixel intensity value of 10000.*

| | | |
|---|---|---|
| **Cycle 1** | | **Maximum intensity_Cy7_objects** |
| | Mean | 0,016 |
| | Pixel intensity | 1061 |
| | Multiplication factor | **9,4** |
| | | |
| **Cycle 2** | | **Maximum intensity_Cy7_objects** |
| | Mean | 0,013 |
| | Pixel intensity | 836 |
| | Multiplication factor | **12** |
| | | |
| **Cycle 3** | | **Maximum intensity_Cy7_objects** |
| | Mean | 0,014 |
| | Pixel intensity | 943 |
| | Multiplication factor | **10,6** |
| | | |
| **Cycle 4** | | **Maximum intensity_Cy7_objects** |
| | Mean | 0,018 |
| | Pixel intensity | 1203 |
| | Multiplication factor | **8,3** |
| | | |
| **Cycle 5** | | **Maximum intensity_Cy7_objects** |
| | Mean | 0,015 |
| | Pixel intensity | 979 |
| | Multiplication factor | **10,2** |
| | | |
| **Cycle 6** | | **Maximum intensity_Cy7_objects** |
| | Mean | 0,018 |
| | Pixel intensity | 1194 |
| | Multiplication factor | **8,4** |

***Table 12: List of "Multiply second image by" values and "Multiplication factors" for all cycles and all channels.*** *The table depicts the chosen "Multiply second image by" and the calculated "Multiplication factors" for each cycle and channel (Cy7= violet, Cy3= orange, Cy5= red and FITC= green).*

| | Cycle 1 | | Cycle 2 | |
|---|---|---|---|---|
| | Multiply second image by | Multiplication factor | Multiply second image by | Multiplication factor |
| Cy7 | 0,9 | 9,4 | 0,8 | 12,0 |
| Cy3 | 0,5 | 4,7 | 0,8 | 6,2 |
| Cy5 | 1,4 | 4,9 | 1,4 | 6,9 |
| FITC | 0,8 | 12,5 | 0,9 | 11,5 |

| | Cycle 3 | | Cycle 4 | |
|---|---|---|---|---|
| | Multiply second image by | Multiplication factor | Multiply second image by | Multiplication factor |
| Cy7 | 0,8 | 10,6 | 0,8 | 8,3 |
| Cy3 | 0,9 | 6,3 | 0,9 | 4,8 |
| Cy5 | 1,4 | 5,6 | 1,4 | 4,8 |
| FITC | 0,9 | 12,9 | 0,7 | 9,2 |

| | Cycle 5 | | Cycle 6 | |
|---|---|---|---|---|
| | Multiply second image by | Multiplication factor | Multiply second image by | Multiplication factor |
| Cy7 | 0,8 | 10,2 | 0,8 | 8,4 |
| Cy3 | 0,8 | 5,7 | 0,8 | 6,9 |
| Cy5 | 1,4 | 6,2 | 1,4 | 5,2 |
| FITC | 0,9 | 12,7 | 0,8 | 14,0 |

## 3.5. Generation of a "pseudo-general stain"

A pipeline for the generation of the pseudo-general stain was developed including modules for the background subtraction for each channel and each separate sequencing cycle. Additionally, signals with a feature size of 10 were enhanced. Figure 19 shows the background subtraction (Extrax_subtracted) and the enhancement of signals (Filtered:Extra_X), whereby a) indicates results from Cy7, b) from Cy3, c) from Cy5 and d) from FITC. To create the pseudo-general stain, output images from each channel were superimposed into one merged image (Enhanced_newgeneralstain), shown in 19e.

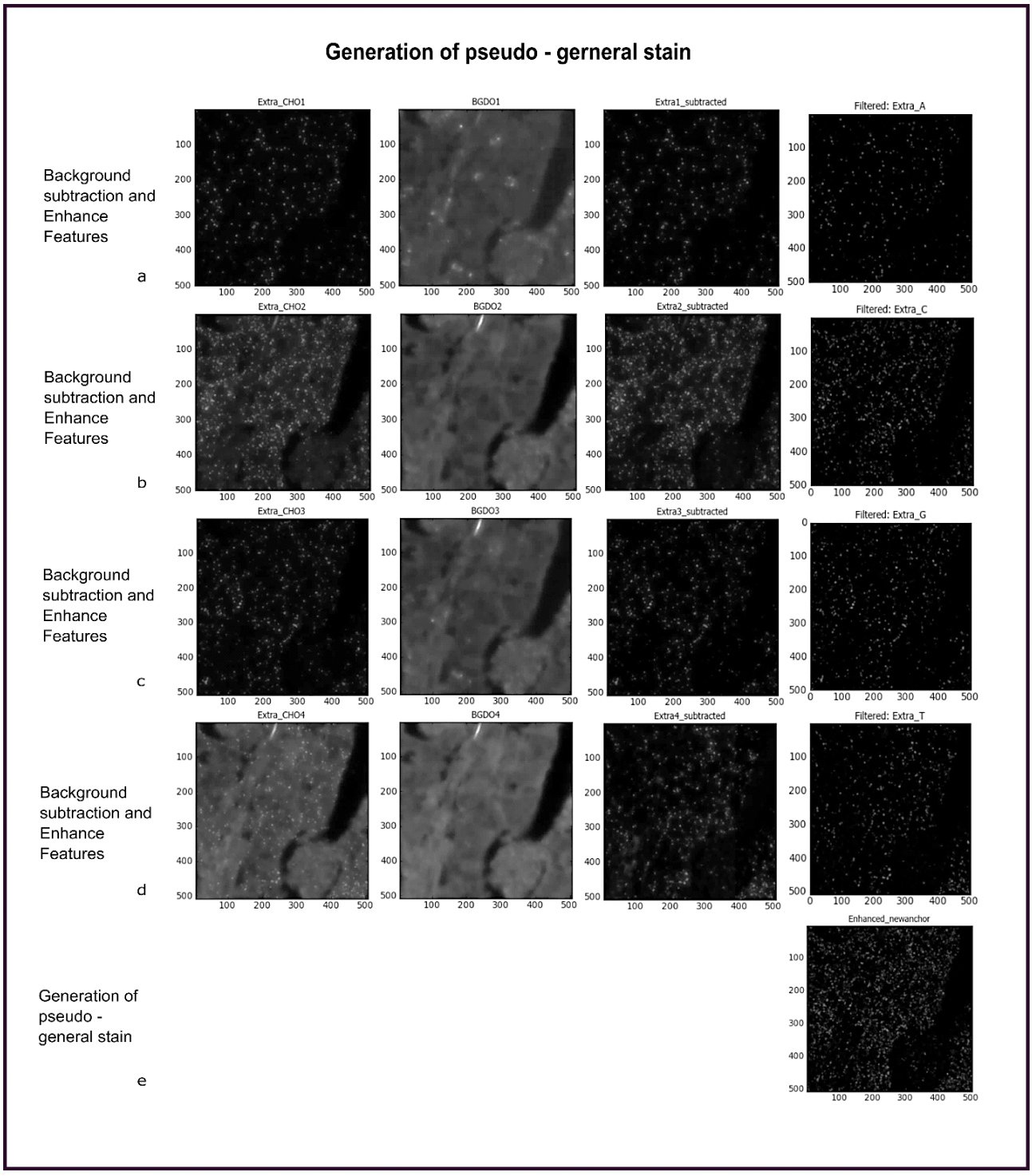


***Figure 19: Intermediate results produced by the CellProfiler pipeline to create the pseudo-general stain.*** *The background from each channel (BGD0x) was subtracted from each sequencing cycle image (Extra_CH0x) to remove autofluorescent structures (Extrax_subtracted)* (Sallinger et al., 2023)*. Additionally, signals with a feature size of 10 were enhanced, which was done separately for each channel (Filtered:Extra_X). Results for Cy7 can be seen in a) for Cy3 in b) for Cy5 in c) and for FITC in d). For the generation of the pseudo-general stain, subtracted and enhanced images of each channel were combined into one merged image ( e) enhanced_newanchor).*

## 3.6. Background subtraction increases number of expected reads.

A background subtraction step was included in the CellProfiler (Broad Institute, MA, United States) pipeline to avoid the detection of false positive signals caused by autofluorescent structures of specific tissue regions especially in FITC and Cy3. For this, the background of all channels used during the sequencing procedure (DAPI, FITC, Cy3, Cy5 and Cy7) was imaged after the last sequencing cycle, shown in figure 20a. Figure 20b indicates the detected signals plotted on a DAPI stained image after background subtraction. Truly positive signals only were detected after running the background subtraction module whereby autofluorescent structures that would have resulted in false positive signals were excluded from analysis.

To test the efficacy of the background subtraction step, ISS analysis was performed on a small autofluorescent region with and without the CellProfiler (Broad Institute, MA, United States) background subtraction module. Running the analysis without background subtraction resulted in 4159 (figure 21a) expected reads, whereas including the background subtraction module led to 5736 (figure 21b) expected reads. For this chosen test area, the background subtraction step resulted in an ~27% increase of expected reads.

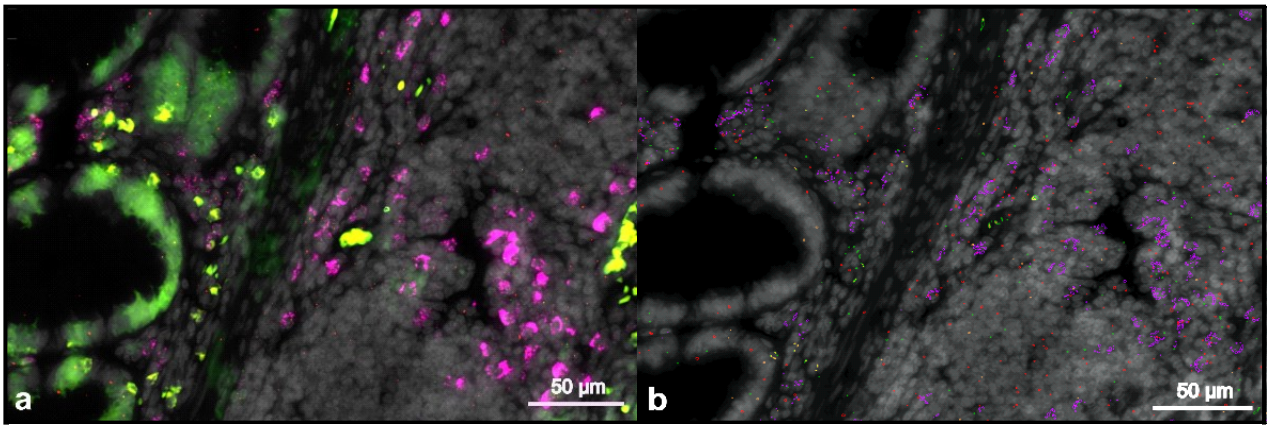


***Figure 20: Background subtraction of autofluorescent structures.***

*a) Image area scanned in DAPI, FITC, Cy3, Cy5 and Cy7 channel. Autofluorescent structures can be observed in FITC and Cy3 channel. b) After background subtraction of the autofluorescent structures only truly positive signals were detected.*

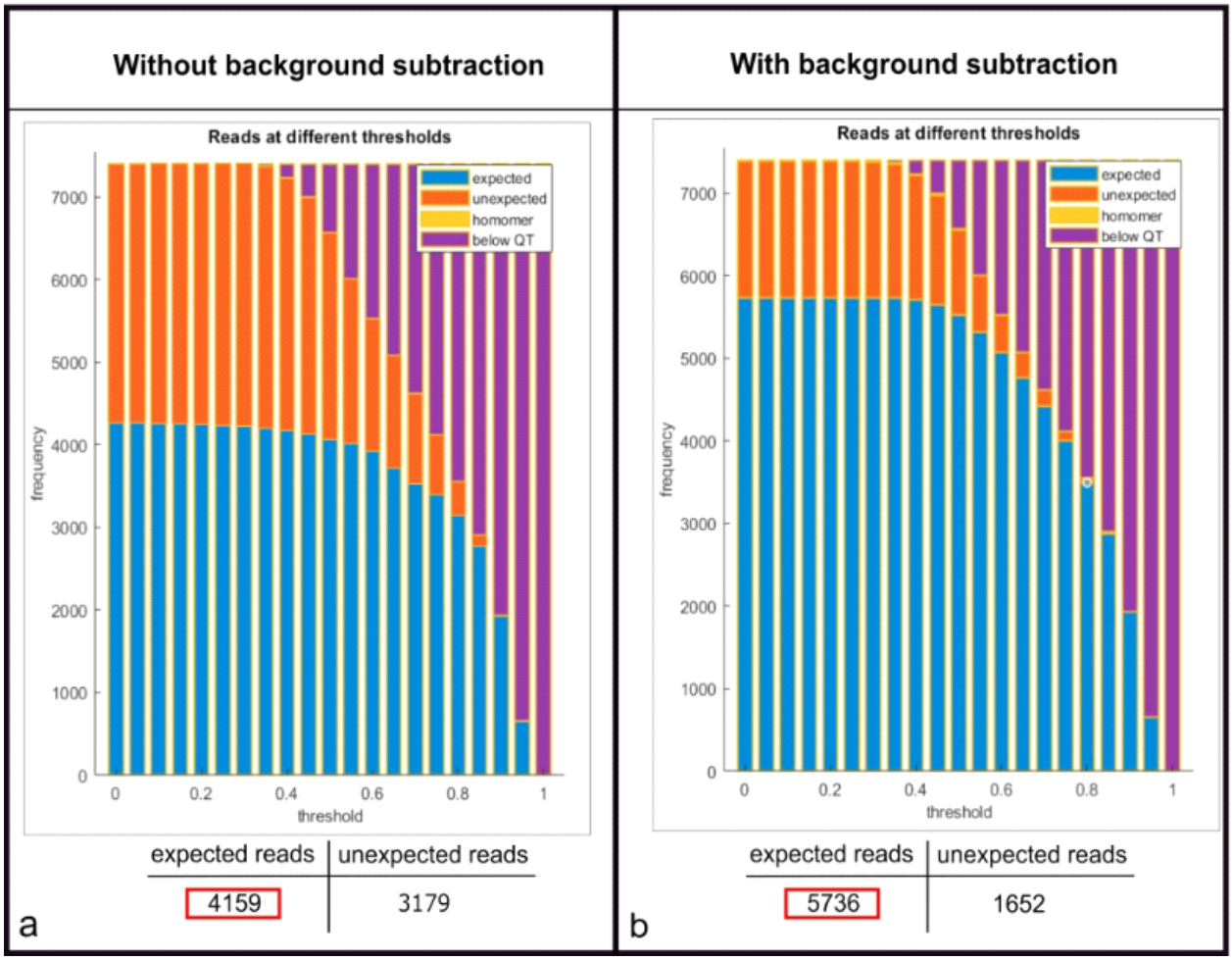


***Figure 21: ISS analysis output – quality bar.***

*The quality bar shows the ratio of expected (blue bars) to unexpected reads (orange bars). The higher the expected reads bar and the lower the unexpected reads bar, the better the efficacy of the analysis. Without performing the background subtraction step 4159 expected reads (a) were detected in comparison to 5736 (b) expected reads when including the background subtraction step.*

## 3.7. Misaligned tiles must be excluded from further analysis.

After running ISS analysis in MATLAB and CellProfiler (Broad Institute, MA, United States), the alignment efficacy must be verified for each aligned tile. Images of each aligned tile are automatically saved in separate folders for each sequencing cycle during analysis. Figure 22a represents a perfectly aligned tile, as the signals from the pseudo-general stain (red) and the pseudo-anchor (green) are perfectly aligned (yellow). In some specific areas as in tile 22b and c, signals mainly from the pseudo-general stain (red) are visible, indicating tissue damage during rehybridization of the sequencing cycle. These tiles are marked in orange in the alignment

overview of the cycle in figure 23b. Figure 22d shows a misaligned tile as only green and red signals can be seen and no overlap (yellow) of the pseudo-general stain and the pseudo anchor is observed. Such tiles are marked red in the overview and must be excluded from further analysis (figure 23a).

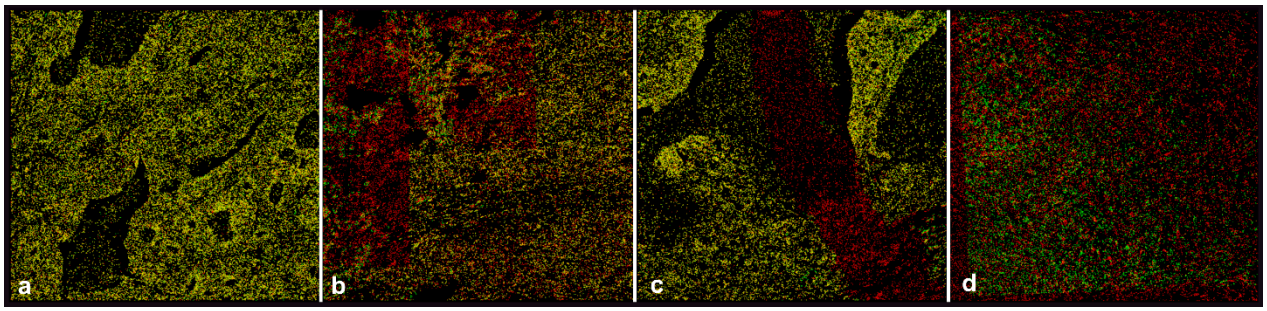


***Figure 22: Alignment of tiles***

*a) Shows a correctly aligned tile, whereas b) and c) indicate tiles with damaged tissue areas which are aligned correctly but could also cause issues during decoding by potential false positive detected transcripts depending on the appearance of the tissue damage. d) Represents a misaligned tile that must be excluded from further analysis.*

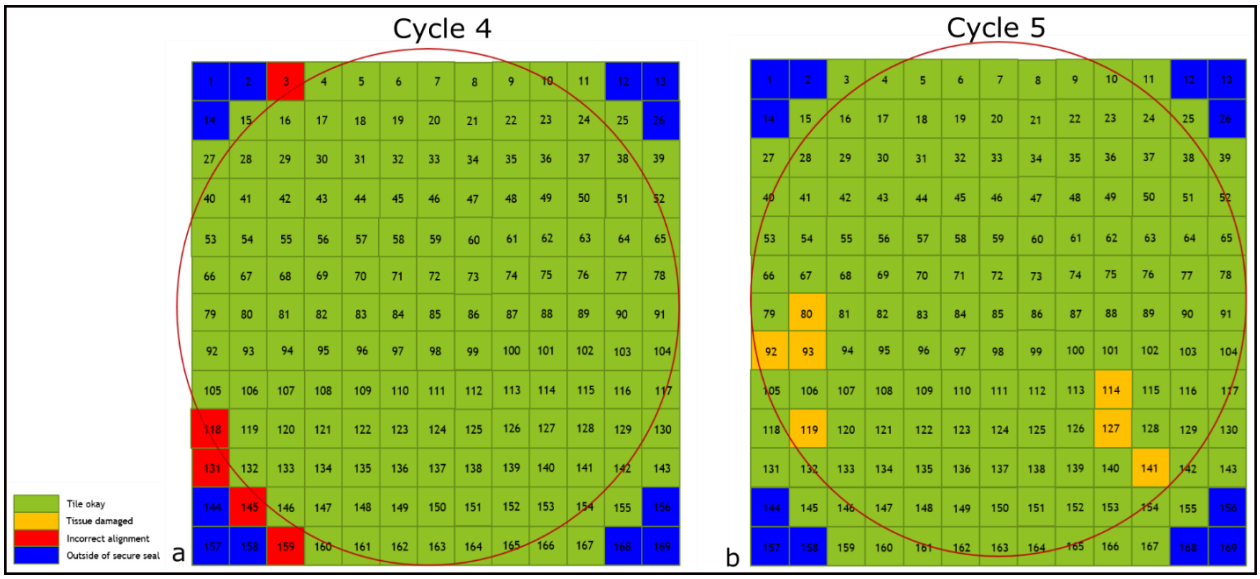


***Figure 23: Overview of alignment for each cycle.***

*For each cycle an overview map of the aligned tiles was created to observe which tiles were misaligned and to exclude these tiles from further analysis. a) Shows the alignment overview of cycle 4 of a sample, which only includes perfectly aligned tiles (green), whereas b) shows cycle 5 of the same sample that indicates 5 incorrectly aligned tiles (red) to be excluded. Blue tiles represent areas that are located outside of the hybridization chamber. (Orange tiles represent areas with damaged tissue, which could also lead to false positive decoded transcripts depending on the cycle.)*

## 3.8. Output of dRNA-HybISS analysis

dRNA-HybISS detected transcripts are plotted on the DAPI image of the pseudo-general stain, whereby each transcript is shown with a different symbol and color (figure 24a). Furthermore, a quality bar is generated (figure 24b) for each dRNA-HybISS analyzed sample, showing the number of detected transcripts on the y-axis and the used threshold on the x-axis. The quantity of expected transcripts (=correct decoded transcripts) is depicted by blue bars, the number of unexpected transcripts is shown as orange bars and homomers are indicated as yellow bars. In figure 24b the number of detected transcripts (expected, unexpected and homomers) can be seen for different thresholds. E.g.: with a threshold of 0.2 1184588 expected reads, 303963 unexpected reads and 158143 homomers were detected.

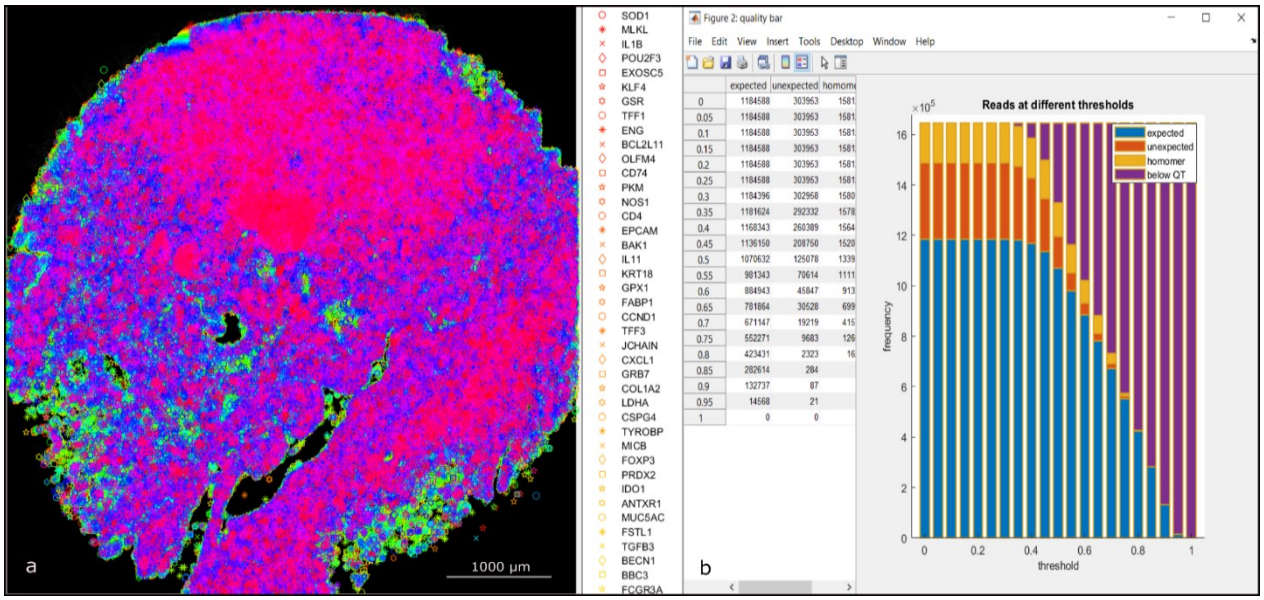


***Figure 24: MATLAB results from dRNA-HybISS analysis***

*a) Shows all detected transcripts (each transcript has a different symbol and color) plotted on DAPI. b) Represents the quality bar of analysis, wherein expected (=correct) reads are shown as blue, unexpected reads as dark orange and homomers as yellow bars.*

## 3.9. Quality control of dRNA-HybISS data

To assess the quality of RNA and the efficacy of dRNA-HybISS technology, the expected decoded reads (=transcripts) of the dRNA-HybISS raw data were quantified. This data is generated during the MATLAB (Mathworks, Sweden) analysis and was normalized to the total reads per analysis. All samples passed the quality control that was set at a threshold of 65% for the expected reads and is depicted in table 13.

***Table 13: Quality control of in situ sequencing data.***
*The list contains the number and percentages of expected reads, unexpected reads and homomers of each patient sample calculated with a threshold of 0.1 from the MATLAB script* (Sallinger et al., 2023)*. Adapted "table S3", Sallinger et al., 2023, licensed under CC BY 4.0.*

| | total counts with threshold 0.1 | | | Percentage distribution (%) | | | reads in total |
|---|---|---|---|---|---|---|---|
| | expected reads | unexpected reads | homomer | expected reads | unexpected reads | homomer | |
| **Patient 1** | 891999 | 254404 | 62085 | 74 | 21 | 5 | 1208488 |
| **Patient 2** | 985008 | 390797 | 105300 | 67 | 26 | 7 | 1481105 |
| **Patient 3** | 942977 | 365210 | 20150 | 71 | 27 | 2 | 1328337 |
| **Patient 4** | 992282 | 269708 | 31233 | 77 | 21 | 2 | 1293223 |
| **Patient 5** | 723538 | 277071 | 33743 | 70 | 27 | 3 | 1034352 |
| **Patient 6** | 1072757 | 372653 | 124511 | 68 | 24 | 8 | 1569921 |
| **Patient 7** | 1684402 | 756442 | 120427 | 66 | 30 | 5 | 2561271 |
| **Patient 8** | 1697772 | 624136 | 116621 | 70 | 26 | 5 | 2438529 |
| **Patient 9** | 1337611 | 556580 | 21780 | 70 | 29 | 1 | 1915971 |
| **Patient 10** | 804678 | 251427 | 17182 | 75 | 23 | 2 | 1073287 |

## 3.10. Segmenting cells

Cells are segmented based on the DAPI nuclear stain, whereby cell boarders are plotted on the DAPI image. Segmentation efficacy strongly depends on the structure of the tissues, e.g.: cells in loose tissue areas, especially in non-neoplastic areas (figure 25a and 25b), can be separated from each other clearly, whereas cell boarders in dense tissue structures, mainly in neoplastic areas and lymphoid structures (figure 25c and 25d), can hardly be recognized due to the cellular boarder overlap. A magnification of the lymphoid tissue structure of figure 25c is shown in figure 25d, indicating the differences of cell densities within tissues. Lymphoid structures are densely packed with immune cells, whereby single cells can hardly be distinguished from their neighbouring cells. For each sample, different fields of view were visually examined to assess the performance of the segmentation.

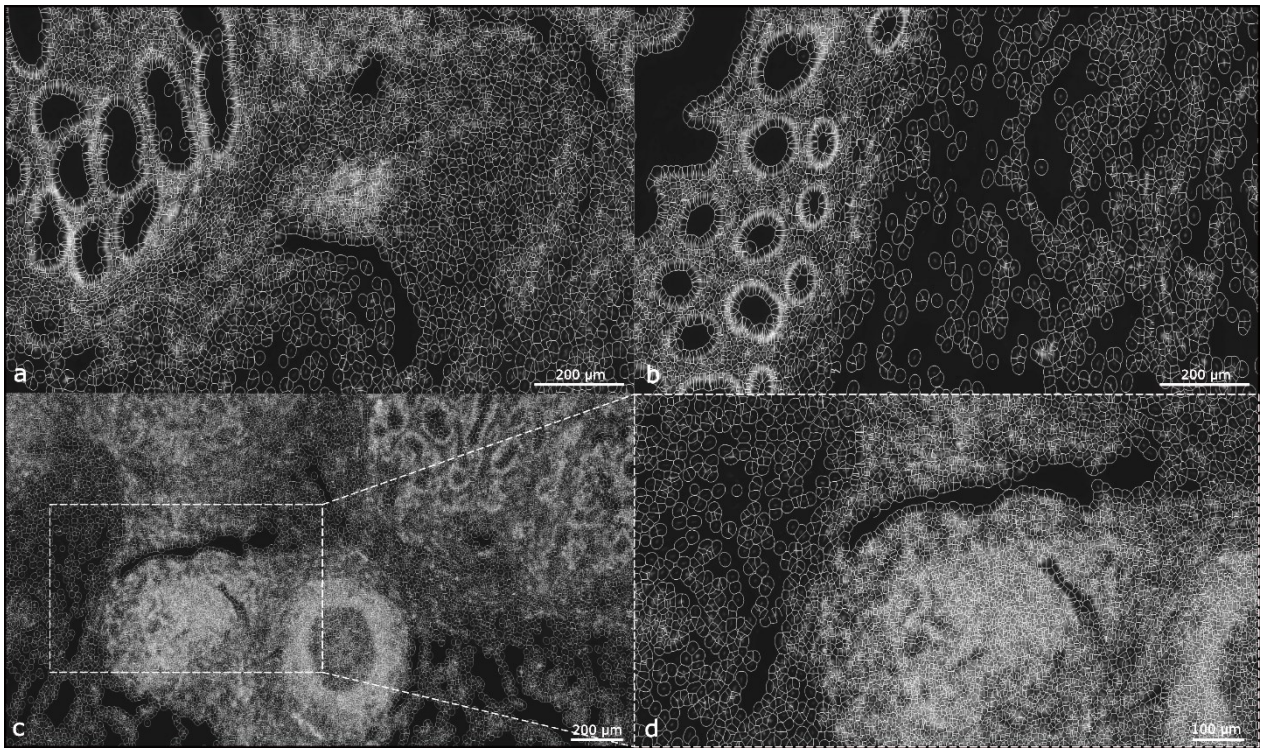


***Figure 25: Segmentation of cells in loose and dense tissues plotted on DAPI images.*** *a) and b) Represent areas of loose tissue in non-neoplastic and the transition to neoplastic tissue areas. c) Indicates a dense lymphoid tissue structure within the neoplastic tissue and d) shows the magnification of the lymphoid tissue structure.*

## 3.11. Gaussian heatmap plots enable the visualisation of gene expression patterns.

To localize “hot” expression areas and gene expression patterns of transcripts (area with a high density of expressed transcripts), Gaussian heatmap plots were generated by using the GTC tool. Figure 26 shows the distribution of the transcripts *ENG, MET* and *MUC2* for patient samples 220KS and 233KS. *ENG* and *MET* are highly expressed transcripts in neoplastic tissues, whereas *MUC2* is a gene expressed in cancer- and non-neoplastic epithelial cells. In patient 220KS a hotspot of *ENG* was observed in the neoplastic tissue structure next to the border region to the non-neoplastic area, whereas a hotspot of *MUC2* could be observed in the non-neoplastic compartment in the same patient.

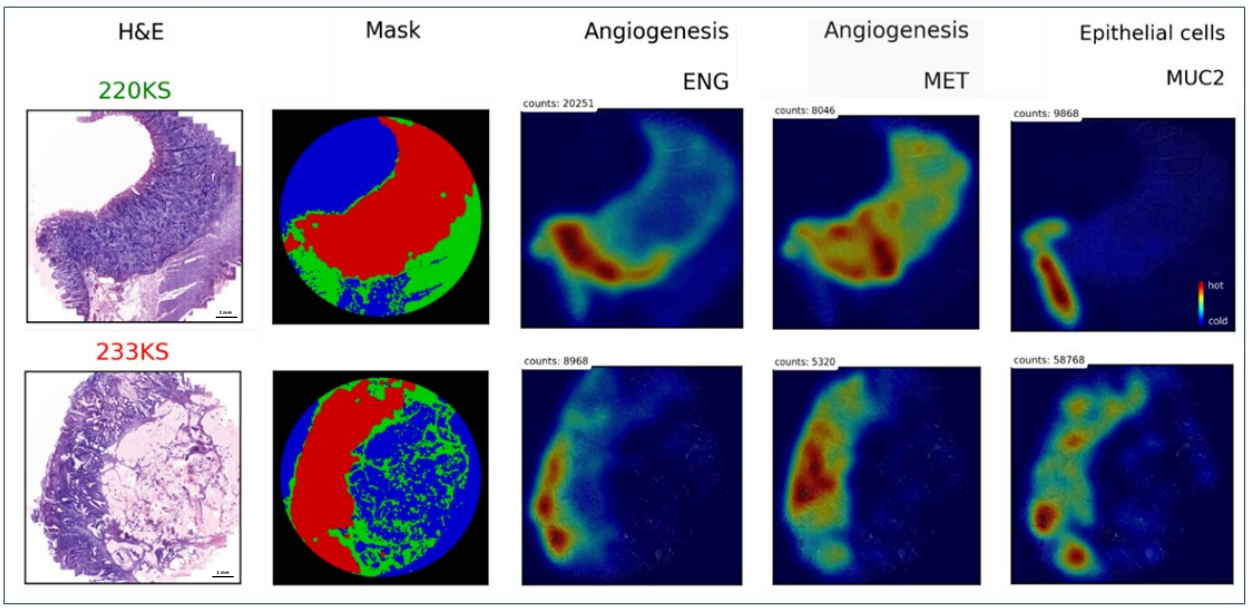


***Figure 26: Gaussian heatmap plots***

*Heatmap plots for the patients 220KS and 233KS can be observed for the transcripts ENG, MET and MUC2 to examine hotspots and expression patterns. ENG and MET are transcripts that are highly expressed in the neoplastic areas, whereas MUC2 is a gene expressed in non-neoplastic epithelial- and cancer cells.*

## 3.12. Automatic generation of neoplastic- and non-neoplastic tissue masks

For the automatic classification of neoplastic and non-neoplastic tissue structures of samples, an in-house developed tool, called GTC-tool, was used. First, virtually generated H&E images of each sample were created and given to a pathologist who classified neoplastic and non-neoplastic areas of the tissues based on morphology (Sallinger et al., 2023). The GTC-tool allowed for automatic identification of neoplastic tissue areas based on the gene expression of a set of 8 signature genes, *BIK, CCND1, CD44, EREG, ITGAV, MET, MYBL2* and *S100A4,* which were highly expressed in the tumor region (Sallinger et al., 2023). To define the non-neoplastic areas, the neoplastic areas were subtracted from the total tissue. Some areas had to be excluded from analysis due to high autofluorescence and damage/loss of tissue areas during the sequencing procedure (figure 27) (Sallinger et al., 2023). The overlap of both tissue masks (morphological-based and expression-based) was calculated for each patient and can be seen in figure 27d (patient 1=85.7%, patient 2=78.1%, patient 3=69.4%, patient 4=81.9%, patient 5=74.2%, patient 6=84.7%, patient 7=78.8%, patient 8=78.3%, patient 9=71.4% and patient 10=71.0%) (Sallinger et al., 2023). The morphological-based (figure 27f) and the expression-based (figure 27g) masks

were plotted on DAPI images to better evaluate the location of the masks within the tissues. The GTC-tool, additionally, allows for quantification of RNA transcripts by counting each single dRNA-HybISS transcript and nucleus in the respective area.

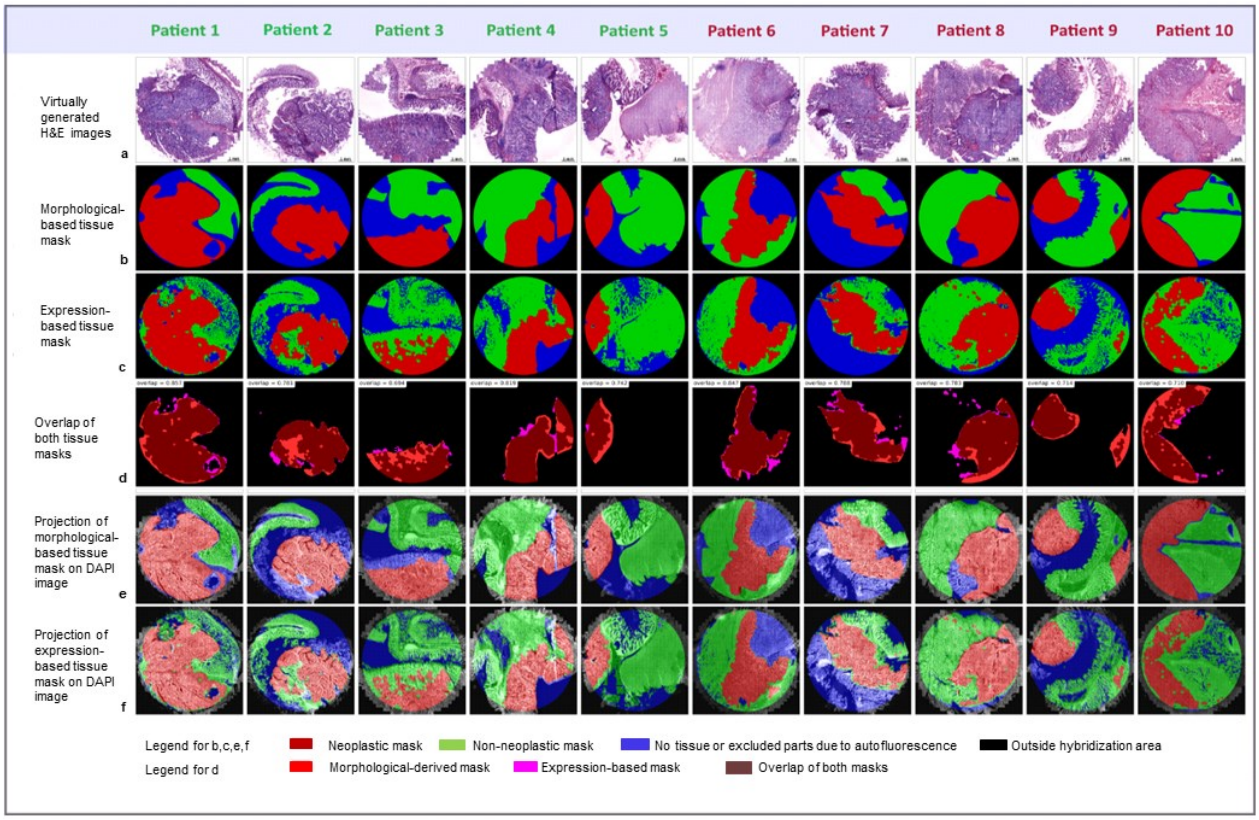


***Figure 27: Computational creation of expression-based tissue masks and comparison with morphological tissue masks classified by a pathologist.***

*a) Virtually generated H&E images of non-relapsed (patient 1-5) and relapsed patient (patient 6-10) samples (Sallinger et al., 2023). b) Neoplastic and non-neoplastic tissue masks classified based on morphological characteristics of the tissue samples (Sallinger et al., 2023). c) Neoplastic and non-neoplastic tissue masks generated based on the expression level of the in situ sequencing tumor gene signature (BIK, CCND1, CD44, EREG, ITGAV, MET, MYBL2 and S100A4) (Sallinger et al., 2023). d) Comparison of the morphological- and the expression-based tissue masks of neoplastic tissues, by generation of an overlap of both masks (Sallinger et al., 2023). Overlay of the e) morphological-based and the f) expression-based compartments with the respective DAPI images (Sallinger et al., 2023). Size bar is valid for all images. Adapted "Fig. 2", Sallinger et al., 2023, licensed under CC BY 4.0.*

## 3.13. Differentially expressed genes in neoplastic versus non-neoplastic tissues

For visualizing the spatial distribution, the detected transcripts were plotted on the expression-based tissue areas. The spatial distribution of 5 example transcripts *EREG*, *MET, BIK, MUC2, and*

*FABP1* and are depicted in figure 28. *EREG*, *MET and BIK* (figure 28b-d) are defined as genes of the tumor gene signature, whereas *MUC2* (figure 28e) is a gene that is mainly expressed in the epithelium of non-neoplastic tissues. *FABP1* (figure 28f), a highly expressed gene in colonic tissues, can be seen in neoplastic- and non-neoplastic tissues.

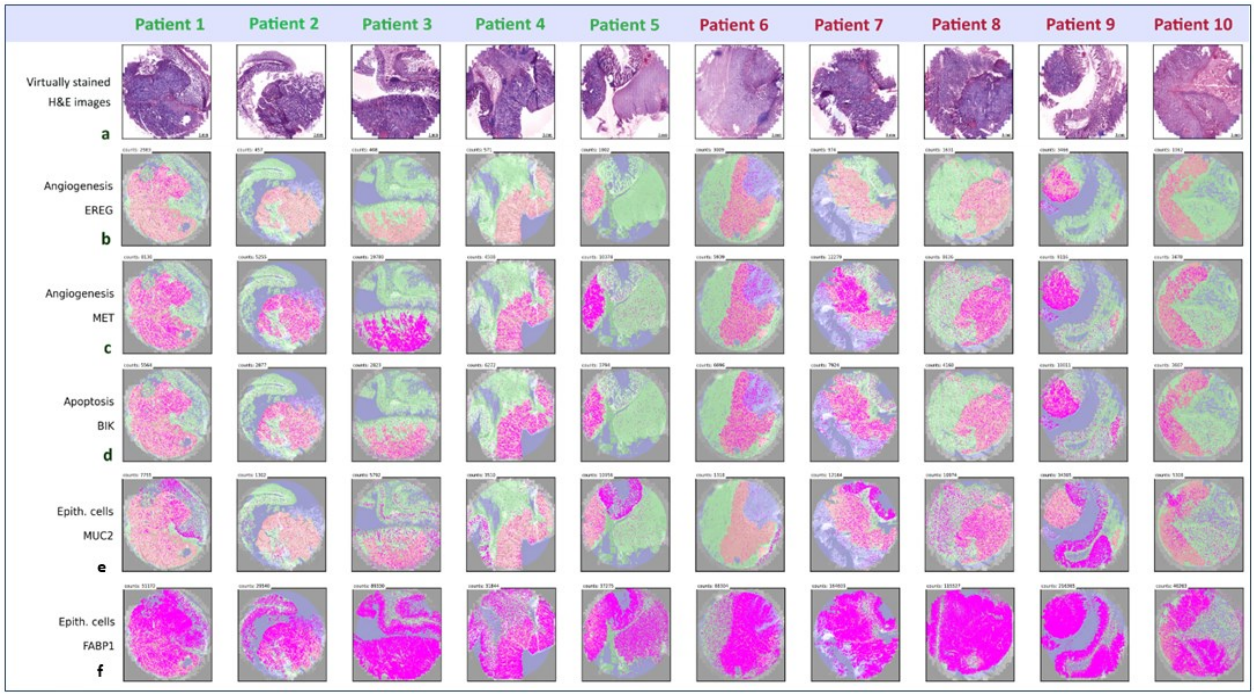


***Figure 28: Spatial distribution of 5 example transcripts out of 176 genes.*** *a) Virtually generated H&E images of non-relapsed (patient 1-5) and relapsed patient (patient 6-10) samples (Sallinger et al., 2023). Spatial distribution of b) EREG, c) MET, d) BIK, genes of the tumor gene signature, e) MUC2, a gene mainly expressed in the epithelium of non-neoplastic tissues and e) FABP1, a gene highly expressed in colonic tissues (Sallinger et al., 2023). Size bar is valid for all images. Adapted "Fig. 3", Sallinger et al., 2023, licensed under CC BY 4.0.*

The expression level for 10 colon cancer patients of each gene was studied by comparing the transcript counts normalized per cell in the neoplastic versus the non-neoplastic tissue regions (Sallinger et al., 2023). To identify significantly upregulated genes related to different biological processes, volcano plots with α=0.05 (=significance level) were generated (Sallinger et al., 2023). In total, 81 significantly upregulated genes were identified by using the morphological-based tissue masks (figure 29d, e), whereas 98 upregulated genes were identified in the expression-based tissue masks (figure 29c, d) (Sallinger et al., 2023). All significantly upregulated genes (81 genes) identified by the morphological-based mask approach could also be identified in the expression-based approach (Sallinger et al., 2023).

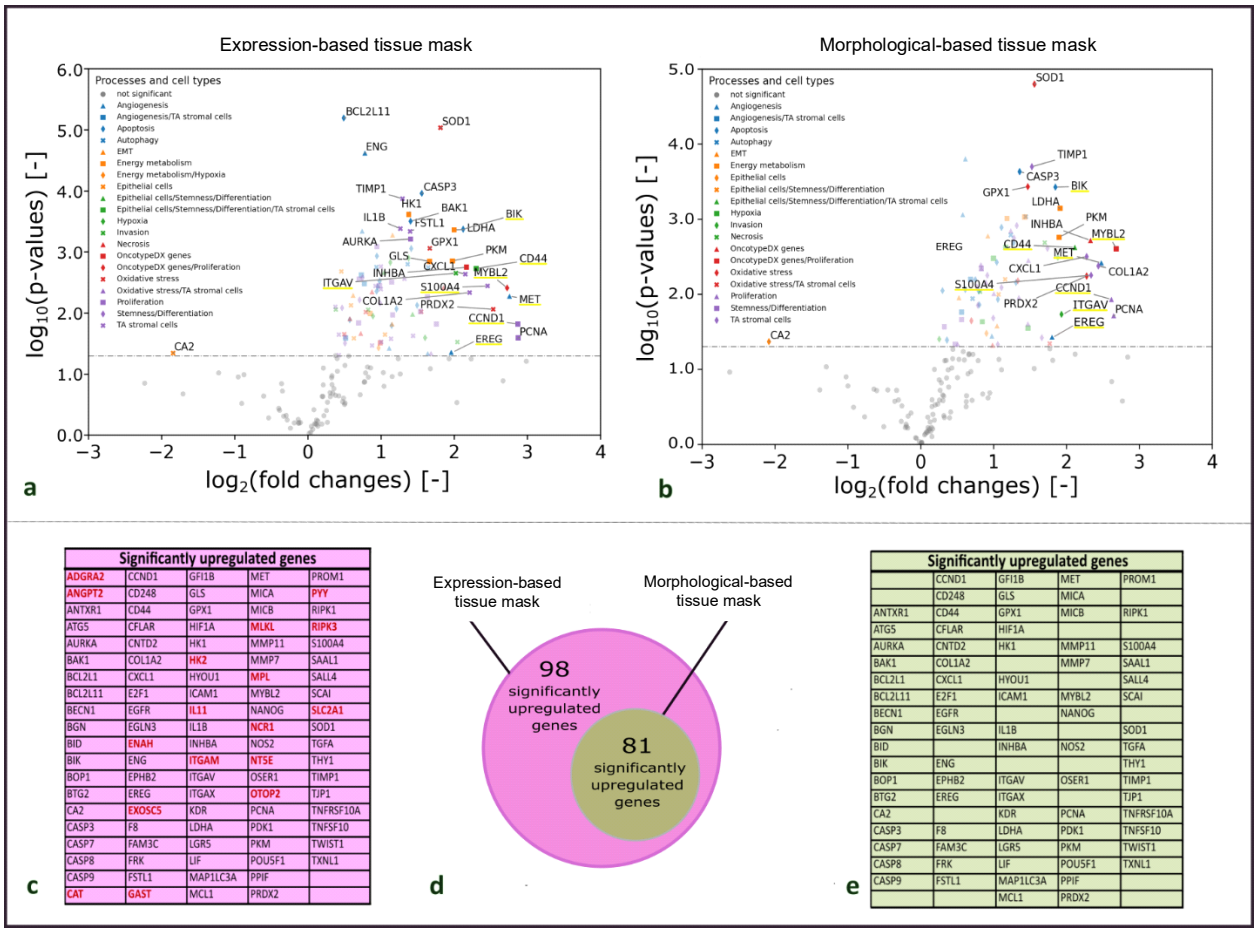


| Significantly upregulated genes | | | | |
|---|---|---|---|---|
| ADGRA2 | CCND1 | GFI1B | MET | PROM1 |
| ANGPT2 | CD248 | GLS | MICA | PYY |
| ANTXR1 | CD44 | GPX1 | MICB | RIPK1 |
| ATG5 | CFLAR | HIF1A | MLKL | RIPK3 |
| AURKA | CNTD2 | HK1 | MMP11 | S100A4 |
| BAK1 | COL1A2 | HK2 | MMP7 | SAAL1 |
| BCL2L1 | CXCL1 | HYOU1 | MPL | SALL4 |
| BCL2L11 | E2F1 | ICAM1 | MYBL2 | SCAI |
| BECN1 | EGFR | IL11 | NANOG | SLC2A1 |
| BGN | EGLN3 | IL1B | NCR1 | SOD1 |
| BID | ENAH | INHBA | NOS2 | TGFA |
| BIK | ENG | ITGAM | NT5E | THY1 |
| BOP1 | EPHB2 | ITGAV | OSER1 | TIMP1 |
| BTG2 | EREG | ITGAX | OTOP2 | TJP1 |
| CA2 | EXOSC5 | KDR | PCNA | TNFRSF10A |
| CASP3 | F8 | LDHA | PDK1 | TNFSF10 |
| CASP7 | FAM3C | LGR5 | PKM | TWIST1 |
| CASP8 | FRK | LIF | POU5F1 | TXNL1 |
| CASP9 | FSTL1 | MAP1LC3A | PPIF | |
| CAT | GAST | MCL1 | PRDX2 | |

| Significantly upregulated genes | | | | |
|---|---|---|---|---|
| | CCND1 | GFI1B | MET | PROM1 |
| | CD248 | GLS | MICA | |
| ANTXR1 | CD44 | GPX1 | MICB | RIPK1 |
| ATG5 | CFLAR | HIF1A | | |
| AURKA | CNTD2 | HK1 | MMP11 | S100A4 |
| BAK1 | COL1A2 | | MMP7 | SAAL1 |
| BCL2L1 | CXCL1 | HYOU1 | | SALL4 |
| BCL2L11 | E2F1 | ICAM1 | MYBL2 | SCAI |
| BECN1 | EGFR | | NANOG | |
| BGN | EGLN3 | IL1B | | SOD1 |
| BID | | INHBA | NOS2 | TGFA |
| BIK | ENG | | | THY1 |
| BOP1 | EPHB2 | ITGAV | OSER1 | TIMP1 |
| BTG2 | EREG | ITGAX | | TJP1 |
| CA2 | | KDR | PCNA | TNFRSF10A |
| CASP3 | F8 | LDHA | PDK1 | TNFSF10 |
| CASP7 | FAM3C | LGR5 | PKM | TWIST1 |
| CASP8 | FRK | LIF | POU5F1 | TXNL1 |
| CASP9 | FSTL1 | MAP1LC3A | PPIF | |
| | | MCL1 | PRDX2 | |

***Figure 29: Genes with a significant upregulation in the neoplastic tissue masks in comparison to the non-neoplastic tissue masks (Sallinger et al., 2023).***

*Generated volcano plots depicting upregulated genes in the a) expression-based tissue mask and the b) morphological-based tissue mask (Sallinger et al., 2023). High significant genes and/or genes with a high fold change between the neoplastic versus non-neoplastic tissue regions are labelled by name (Sallinger et al., 2023). Related biological processes can be seen on the left side of the plot marked with different symbols and colors. A two-sided paired t-test with a significance level α=0.05 is used for statistical testing. All significantly differentially expressed genes in c) the expression-based and in the e) morphological-based masks can be seen in the lists (Sallinger et al., 2023). Genes labelled in red were found to be significantly upregulated only in the expression-based tissue mask (Sallinger et al., 2023). d) Venn Diagram depicting the amount of genes upregulated in the expression-based and the morphological tissue mask (Sallinger et al., 2023). Adapted "Fig. 4", Sallinger et al., 2023, licensed under CC BY 4.0.*

By using the morphological-based approach these high fold change and/or high significantly increased expression genes were identified: angiogenesis- (*MET*), apoptosis- (*CASP3, BIK*), energy metabolism (*LDHA, PKM*) associated genes, oxidative stress- (*SOD1, GPX1, PRDX2*), proliferation- (*CCND1, PCNA, MYBL2*) and stemness (*CD44*) related genes, tumor associated stromal genes (*TIMP1, CXCL1, COL1A2, S100A4, CD44*) and Oncotype DX genes (*INHBA, MYBL2*) (figure 29b) (Sallinger et al., 2023).

By using the expression-based approach (figure 29a) the neoplastic tissue compartment included: angiogenesis- (*ENG, MET*), apoptosis- (*BCL2L11, ENG, CASP3, BAK, BIK*), energy metabolism- (*HK1, GLS, LDHA, PKM*) and invasion- (*ITGAV*) associated genes, oxidative stress (*SOD1, GPX1, PRDX2*), stemness (*CD44*) and proliferation related (*AURKA, CCND1, PCNA, MYBL2*) genes, tumor associated stromal genes (*IL1B, FSTL1, TIMP1, CXCL1, COL1A2, S100A4, CD44*) and Oncotype DX genes (*INHBA, MYBL2*) (Sallinger et al., 2023).

## 3.14. Upregulated genes in the neoplastic tissue regions of relapsed patients versus non-relapsed patients

A two-sided independent t-test with α=0.05 (=significance level) was performed to examine the differences of expression in the neoplastic tissue areas of 5 relapsed stage II colon cancer patients versus 5 non-relapsed patients (volcano plot of figure 30a) (Sallinger et al., 2023). Three genes indicated a high-significant increase in expression in relapsed patients compared to non-relapsed patients in the neoplastic tissue regions (Sallinger et al., 2023). The expression for the transcript *OTOP2* (figure 30b) showed 2.6 counts per 1000 cells for relapsed and 1.9 for non-relapsed patients (p-value=0.0042) (Sallinger et al., 2023). For *FGFR2* (figure 30c) significantly elevated expression levels for relapsed patients were indicated, with 4.9 counts per 1000 cells for relapsed and 3.1 counts per 1000 cells for non-relapsed patients (p-value= 0.0137) (Sallinger et al., 2023). The expression level of *MMP11* (figure 30d) indicated a significant upregulation with 49.2 counts per 1000 cells for relapsed compared to 16.4 counts per 1000 cells for non-relapsed patients (p-value=0.0415) (Sallinger et al., 2023). A list with the p-values of all transcripts can be found in the supplementary table 3.

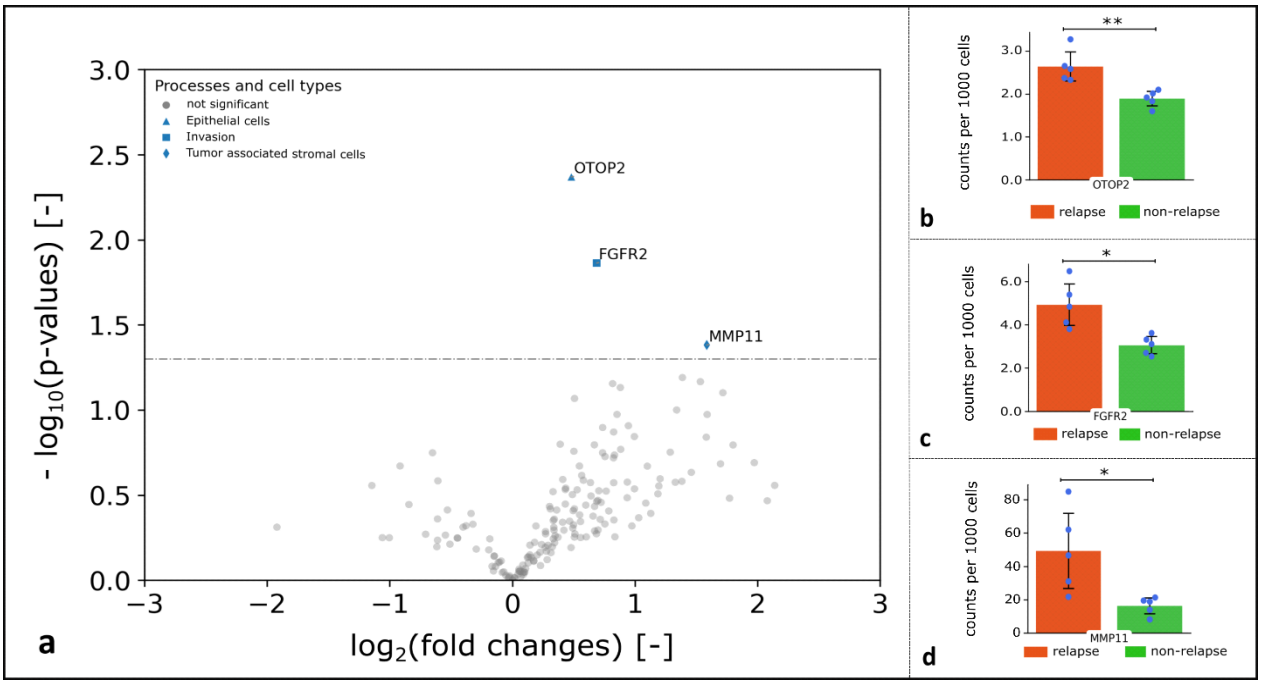


**Figure 30: Differently expressed genes in the neoplastic tissue regions of relapsed versus non-relapsed patients.**

*a) Volcano plot that identifies 3 differentially expressed genes in the neoplastic areas of relapsed patient samples versus non-relapsed patient samples (Sallinger et al., 2023). For statistical testing a two-sided independent t-test with a significance level α=0.05 is used. Expression level of b) OTOP2, c) FGFR2 and d) MMP11 in the neoplastic tissue regions of relapsed and non-relapsed patients, showing a significant upregulation of these transcripts in relapsed patients (Sallinger et al., 2023). Significant differences were highlighted with asterisks and bars (*p < 0.05 and **p < 0.005). "Fig. 5", Sallinger et al., 2023, licensed under CC BY 4.0.*

The heatmaps of the identified transcripts *OTOP2, FGFR2* and *MMP11* are depicted in figure 31. The heatmaps were plotted on the DAPI image which enables a better visualization of their hotspot locations.

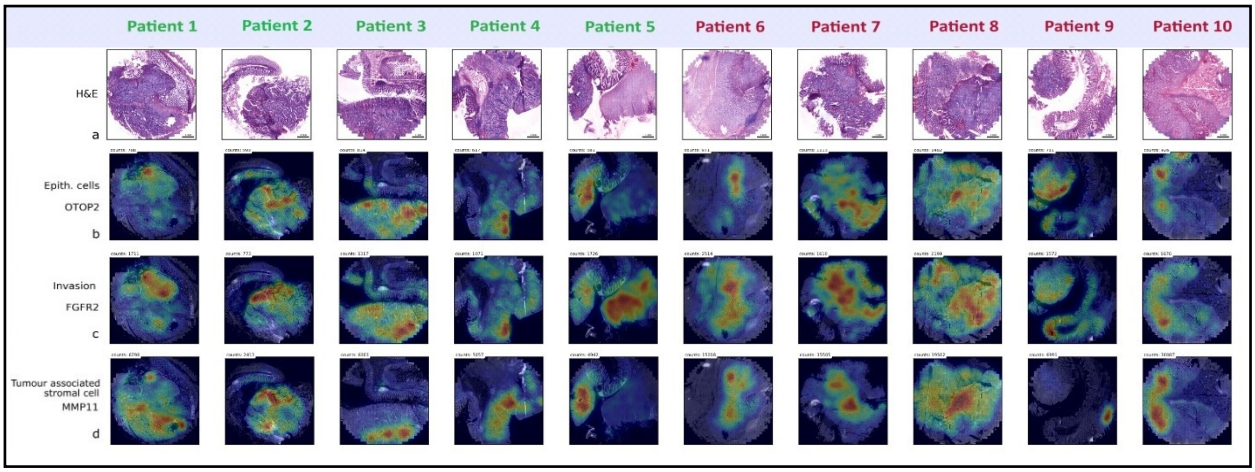


***Figure 31: Heatmaps of OTOP2, FGFR2 and MMP11.***

*a) Virtually generated H&E images of non-relapsed (patient 1-5) and relapsed patient (patient 6-10) samples (Sallinger et al., 2023). Heatmaps of a) OTOP2, b) FGFR2 and c) MMP11 indicate tumor heterogeneity (Sallinger et al., 2023). Each heatmap plot is normalized to its own maximum density value, whereby the heat bar color scale is valid for all heatmaps. Adapted "Fig. 6", Sallinger et al., 2023, licensed under CC BY 4.0.*

## 3.15. Spatial *in situ* sequencing analysis reveals advantages in comparison to bulk RNA expression analysis.

To compare spatial analysis versus bulk RNA sequencing we simulated bulk RNA expression by omitting the spatial tissue areas. Thereby we quantified the differences of gene expression between relapsed and non-relapsed patients (Sallinger et al., 2023). This resulted in a significant upregulation of *OTOP2* (p-value=0.0167) and *MMP11* (p-value=0.0177) but *FGFR2* did not indicate significant changes (p-value=0.1304) (figure 32) (Sallinger et al., 2023).

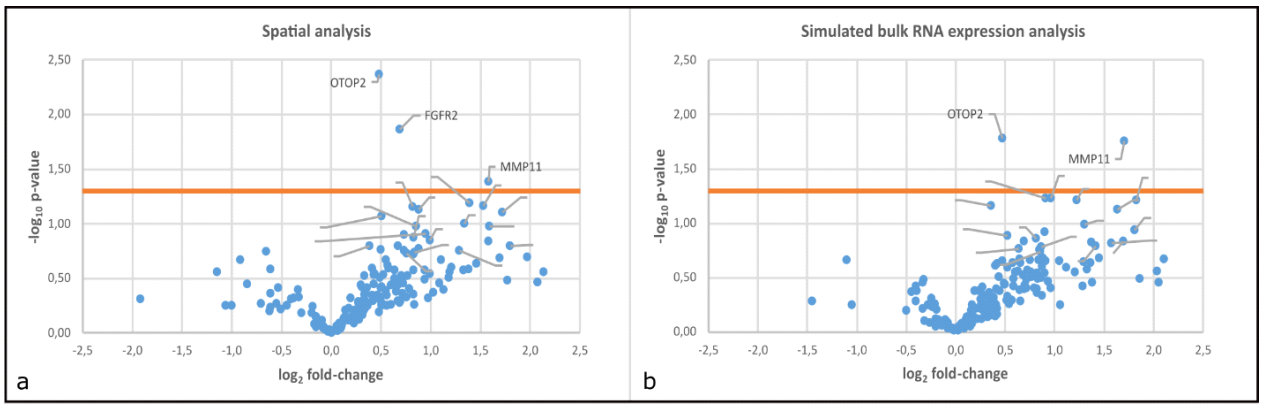


***Figure 32: Comparison between spatial analysis and stimulated bulk RNA expression analysis.***

*a) Volcano plot depict differentially expressed genes (OTOP2, FGFR2 and MMP11) in the neoplastic tissue region of*



FGFR2

*relapsed versus non-relapsed patients (Sallinger et al., 2023). b) Volcano plot that shows significantly upregulated genes (OTOP2 and MMP11) in the whole tissue sample (neoplastic and non-neoplastic tissues) of relapsed in comparison to non-relapsed patients (Sallinger et al., 2023). For statistical testing a two-sided independent t-test with a significance level α=0.05 is used, indicated by the orange threshold line. "Fig. S12", Sallinger et al., 2023, licensed under CC BY 4.0.*

## 3.16. DeNovo SSAM analysis allows for cell-phenotyping of colonic tissue structures based on dRNA-HybISS gene expression.

Colonic tissue was cell-phenotyped based on spatial gene expression data to automatically identify histological tissue structures in the sample. By using DeNovo SSAM, a colonic tissue sample was classified into several clusters, whereby cells in each cluster show high similarity in gene expression patterns. Figure 33 shows 5 different clusters. For cluster visualization, two plots for each cluster were generated examining the location of the identified cluster within the tissue architecture. Additionally, the gene expression profile and a t-SNE plot for each cluster was created to observe the relation of one cluster to the other clusters in a two-dimensional plot. Clusters located next to each other in the t-SNE plot indicate very similar expression profiles, whereas clusters with dissimilar expression profiles are located apart from each other. After manually annotating the clusters based on their position within the tissue, removing unspecific marker genes and combining clusters into subgroups (figure 34c), 16 different clusters were identified, shown in figure 34d: 6 muscle tissue clusters, 5 connective tissue clusters, one non-neoplastic epithelium clusters, 2 neoplastic epithelium clusters, one immune cell cluster and one lymphoid tissue cluster. Clusters with very similar expression profiles forming one big cluster in the t-SNE plot were labelled in a similar color in the cell type map (e.g: all 6 muscle cell clusters were labelled in a pinkish color, whereas connective tissue clusters have a blueish color) for a better visualization of the classified tissue structures.

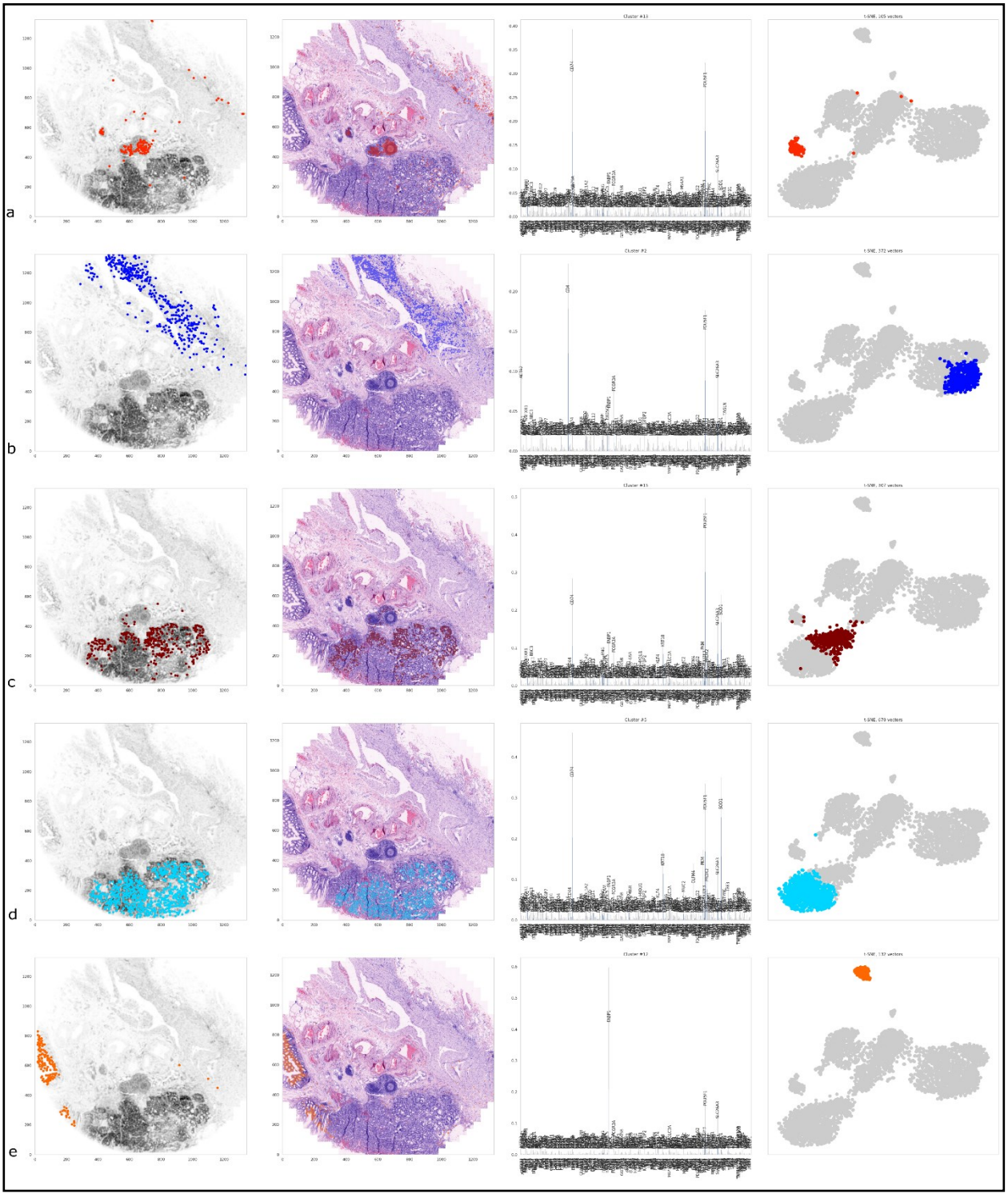


***Figure 33: 5 identified clusters by DeNovo SSAM analysis.***

*Each cluster was projected on a density plot and a virtual H&E staining to visualize the position of the clusters. Additionally, a gene expression pattern profile was generated for each cluster, in order to see which genes are upregulated in the cluster. For a better estimation of relations between the different clusters, t-SNE plots were created to show the location of each cluster in relation to the other clusters.*

*a) Shows the lymphoid tissue cluster and b) indicates a muscle tissue cluster, which is located next to the other muscle tissue clusters in the t-SNE plot. c) The invasive margin cluster is located in the neoplastic epithelium and is located next to the d) neoplastic epithelium cluster, both clusters form one big cluster in the t-SNE plot. e) Shows the non-neoplastic epithelium cluster, which forms a separate cluster very distinct from all other clusters. This work was performed in collaboration with Sebastian Tiesmeyer under the supervision of Naveed Ishaque (Digital Health Center, Berlin Institute of Health (BIH) at Charité - Universitätsmedizin Berlin, Germany)*

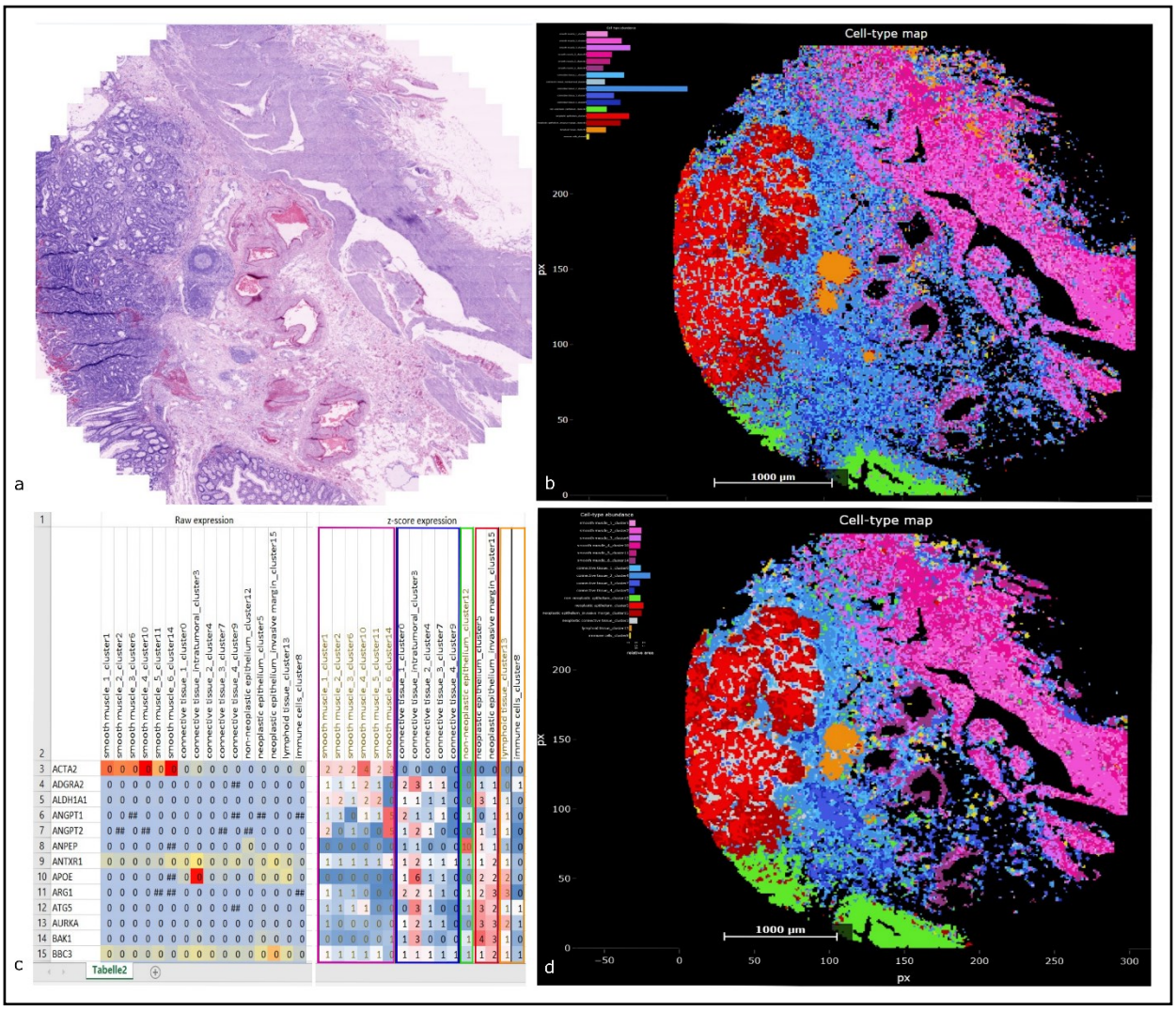


***Figure 34: Cell-phenotyping by DeNovo SSAM analysis***

*a) virtual H&E staining of samples b) Cell type map of the sample before optimization representing clusters that belong to the same tissue structure in similar colors e.g.: all muscle tissue clusters are depicted in a pinkish color. c) Shows the cell type/gene expression matrix that was optimized by removing unspecific markers from the matrix. d) Optimized cell type map of the tissue sample.*

## 3.17. Plasma sequencing with TSO500 kit

So far, the shedder study has included a total of 21 patients. Plasma samples, collected from these patients before tumor resection, and tissue samples were sequenced at the Institute of Human Genetics, Diagnostic & Research Center for Molecular BioMedicine, Medical University of Graz. Germline mutations of both plasma and tissue samples were matched to confirm their same origin. Based on the occurrence of the same somatic variants in the plasma and resected tissue, patients were labelled as either non/low shedders (33.3 %) which are depicted in green in table 14 or shedders (66.7 %) which can be seen in red in table 14.

***Table 14: Grouping of patients included into the shedder project study.***

*Parameters such as year of birth, gender, date of tumor resection, tumor location, TNM classification, histological characterisation and stage were collected from each patient and are depicted in the table. Patient 1-7 were classified as non/low-shedders and are labelled in green, whereas patient 8-21 were classified as shedders and are depicted in red. NA = not available*

| ID | Occurrence of somatic variants 0=No 1=Yes | Year of birth | Gender 0=Male 1=Female | Date of Tumor OP | Tumor Location | T | N | M | Histo | Stage |
|---|---|---|---|---|---|---|---|---|---|---|
| Patient 1 | 0 | 1942 | f | 01.09.2021 | C.ascendens | T3a | N0 | M0 | Adenocarcinoma | 2 |
| Patient 2 | 0 | 1962 | ? | 25.05.2021 | NA | T4a | N0 | M0 | NA | 2 |
| Patient 3 | 0 | 1953 | f | 17.05.2022 | C.transversum | T2 | N0 | M0 | Adenocarcinoma | 1 |
| Patient 4 | 0 | 1943 | m | 26.01.2022 | Rectum | T1 | N0 | M0 | Adenocarcinoma | 1 |
| Patient 5 | 0 | 1954 | m | 30.07.2021 | C.sigmoideum | T3a | N0 | M0 | Adenocarcinoma | 2 |
| Patient 6 | 0 | 1954 | m | 27.07.2021 | C.descendens | T2 | N0 | M0 | Adenocarcinoma | 1 |
| Patient 7 | 0 | 1952 | f | 19.07.2021 | C.ascendens | T2 | N0 | M0 | Adenocarcinoma | 1 |
| Patient 8 | 1 | ? | ? | 22.06.2021 | NA | T4a | N0 | M0 | NA | 2 |
| Patient 9 | 1 | 1949 | f | 10.01.2022 | C.sigmoideum | T3b | N0 | M0 | Adenocarcinoma | 2 |
| Patient 10 | 1 | 1953 | f | 05.04.2022 | C.ascendens | T4a | N0 | M0 | Adenocarcinoma | 2 |
| Patient 11 | 1 | 1951 | f | 24.03.2021 | C.ascendens | T3a | N0 | M0 | Adenocarcinoma | 2 |
| Patient 12 | 1 | 1946 | f | 24.08.2021 | Rectum | T3 | N0 | M0 | Adenocarcinoma | 2 |
| Patient 13 | 1 | ? | ? | 21.05.2021 | NA | T3a | N0 | M0 | NA | 2 |
| Patient 14 | 1 | 1953 | m | 11.05.2021 | C.sigmoideum | T2 | N0 | M0 | Adenocarcinoma | 1 |
| Patient 15 | 1 | 1964 | f | 31.05.2021 | C.sigmoideum | T3a | N0 | M0 | Adenocarcinoma | 2 |
| Patient 16 | 1 | NA | NA | 21.03.2022 | C.sigmoideum | T3 | N0 | M0 | Adenocarcinoma | 2 |
| Patient 17 | 1 | 1959 | m | 28.05.2021 | C.sigmoideum/ Rectum | T3b | N0 | M0 | Adenocarcinoma | 2 |
| Patient 18 | 1 | 1944 | m | 12.07.2021 | C.sigmoideum | T4 | N0 | M0 | Adenocarcinoma | 2 |
| Patient 19 | 1 | NA | NA | 06.05.2021 | NA | T3a | N0 | M0 | NA | 2 |
| Patient 20 | 1 | 1959 | f | 02.03.2022 | C.sigmoideum / Rectum | T2 | N0 | M0 | Adenocarcinoma | 1 |
| Patient 21 | 1 | 1973 | m | 28.06.2021 | C.ascendens | T2 | N0 | M0 | Adenocarcinoma | 1 |

## 3.18. dRNA-HybISS analysis of shedder samples

The first tissue samples have been *in situ* hybridized and analyzed. However, the analysis of additional samples is still ongoing. Since the dRNA-HybISS analysis is not yet complete, this thesis cannot present final results. Nonetheless, with the initial analyzed dRNA-HybISS samples, we have been optimizing the automated mask generation process, as we have used a broader gene panel for this study cohort (Pathway panel plus two Immune panels). Consequently, additionally to the neoplastic and non-neoplastic mask, a third tissue compartment representing stromal tissue within both neoplastic and non-neoplastic areas has been introduced, which is depicted in yellow in figure 35i.

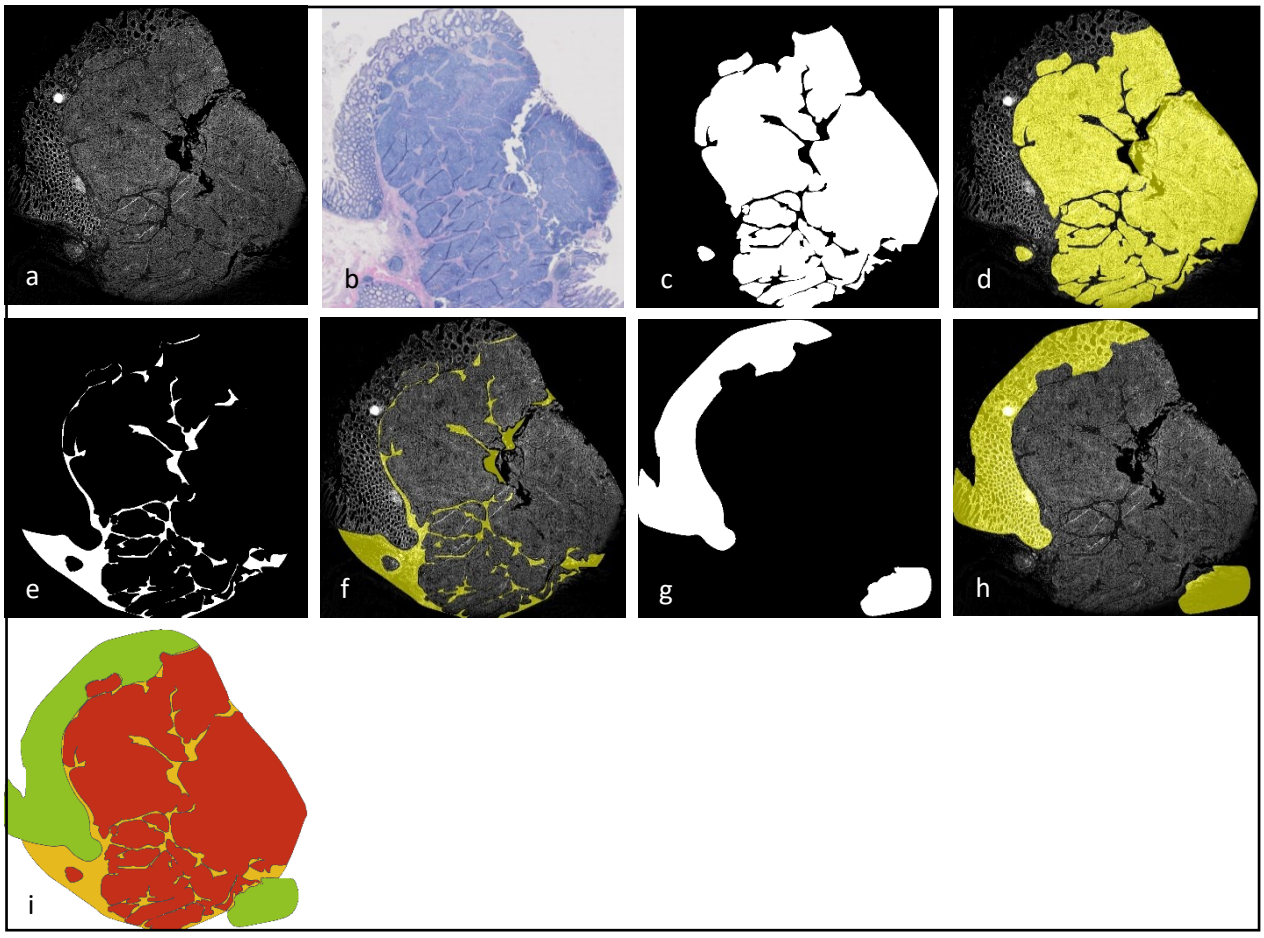


***Figure 35: Generation of automated masks for the shedder project.***

*a) displays the DAPI staining of nuclei, while b) illustrates the H&E staining of a consecutive section. c) represents the neoplastic tissue mask, merged with the DAPI staining in d). The stromal mask is shown in e) and overlaid on the DAPI staining in f). g) Represents the non-neoplastic mask, which is mapped on the DAPI staining in h). i) Depicts all three created masks: green indicates non-neoplastic tissue, red shows neoplastic tissue and displays stromal tissue areas.*

# 4. Discussion

## 4.1. Optimization of the dRNA-HybISS technology

### 4.1.1. Optimization of permeabilization

Prior to implementing dRNA-HybISS technology, it is crucial to conduct permeabilization tests tailored to specific tissue types. Therefore, various permeabilization conditions were carefully examined to obtain optimal outcomes for colonic tissue samples. The focus laid on optimizing the number of signals per unit area and enhancing the signal to background ratio.

In pursuit of this goal, several approaches, such as specified durations of enzymatic digestion using pepsin, were assessed. Additonally, permeabilization with citrate buffer, both in a cooking steamer and a microwave, were explored. These methods were chosen due to their established compatibility with dRNA-HybISS technology and were, furthermore, recommended by the company CARTANA.

For colonic tissue sections, the most promising results were observed when using citrate buffer in a cooking steamer for a duration of 45 minutes. Here, it is important to mention that the strict adherance to the recommended temperature (95-100°C) for citrate buffer in the microwave proved challenging, as a maximum temperature of only 93°C could be achieved. Moreover, there was a noticeable thermal variation ranging from 88°C to 93°C during microwave incubation.

In contrast, when utilizing the cooking steamer, however, the desired permeabilization temperature was consistently maintained at levels exceeding 95°C throughout the entire permeabilization process. This temperature stability of the cooking steamer proved to be advantageous for achieving optimal results with colonic tissue samples.

### 4.1.2. The optimal exposure time for each channel for the VS200

The VS200 slide scanner by Evident (Tokio, Japan) was subjected to a comprehensive performance comparison with the AxioObserver.Z1 by Zeiss (Jena, Germany) to optimize the imaging process of dRNA-HybISS-stained slides. The VS200 from Evident (Tokio, Japan) features clearly surpass those of the AxioObserver.Z1 (Zeiss, Jena, Germany), offering superior features and capabilities across various parameters, including scanning time, autofocusing precision, batch imaging efficiency, applicability to different tasks, and overall imaging quality.

To achieve the highest signal to background ratio for each channel, optimal exposure times were determined as follows: 50 ms for Atto488, 100 ms for Cy3 and 400 ms for Cy5 and Cy7.

It was consistently observed that fluorescent dyes with longer excitation wavelengths, such as Cy5 and Cy7, tended to require longer exposure times, whereas dyes with lower excitation wavelengths demonstrated a preference for shorter exposure times. A major advantage of utilizing high-wavelength dyes, like Cy5 and Cy7, is the noticeable reduction in the occurrence of autofluorescent structures. In contrast, low-wavelength dyes tend to exhibit a significant level of autofluorescence, which can be challenging to manage.

The determination of optimal exposure times is dependent on the specific microscope in use, the characteristics of the light source, and the properties of the integrated filters within the microscope. Consequently, these parameters must be thoroughly tested and optimized for each individual device to ensure optimal imaging outcomes. This process is essential to harness the full potential of the chosen imaging system and to obtain precise and reliable results in dRNA-HybISS -stained slide imaging.

### 4.1.3. Generation of a pseudo-general stain

The original protocol outlined by CARTANA introduces an additional staining step, involving the detection of all signals via the general stain sequence, prior to beginning with the sequencing cycles. While this approach has its advantages, it can also present challenges, particularly when dealing with tissues expected to yield a high number of signals. A notable challenge worth mentioning arises from the direct targeting of the general stain sequence. This tends to produce signals that are not only larger but also brighter, compared to those generated using the bridge probes and DOs. These differences in signal size and intensity can introduce problems during subsequent analysis, potentially leading to issues with densely packed individual signals that cannot be effectively separated from one another. The resulting signal overcrowding can lead to a necessary exclusion of these signals from the analysis, due to their enlarged size.

Moreover, there have been observations of stripping issues in specific samples, whereby the general stain signals were expected to be stripped before initiating the first sequencing cycle. These unexpected challenges can disrupt the sequencing process and pose a significant hurdle to achieve reliable results. An additional concern arises from the tissue damage that potentially could occur during each additional staining cycle. The process of repeatedly subjecting the tissue to sequencing cycles carries the risk of tissue loss or damage.

To circumvent the issues described above, a pseudo-general stain was, therefore, created by merging all four channels of the first sequencing cycle. This strategic adaptation not only minimizes lab work but also reduces the risk of overcrowding, tissue damage, and the exclusion of signals during analysis.

### 4.1.4. Background subtraction increases number of expected reads

Autofluorescence is of critical concern when working on the detection of fluorescently labelled signals within tissues. Various tissues contain endogenous fluorophores, including collagen, elastin, lipofuscin, nicotinamide adenine dinucleotide, and flavin adenine dinucleotides (Deal et al., 2018). These intrinsic fluorophores can either prove advantageous or present challenges, contingent upon the specific field of application.

Some researchers have utilized these features to their advantage such as Deal et al. (2018), who used the distinctive autofluorescence patterns to differentiate between neoplastic and non-neoplastic tissues (Deal et al., 2018). Similarly, DaCosta et al. (2005) observed significantly higher autofluorescence in adenomatous epithelial cells when compared to normal and hyperplastic epithelial cells (DaCosta et al., 2005). These findings have opened novel possibilities for tissue characterization and diagnosis (Deal et al., 2018; DaCosta et al., 2005). Furthermore, we have used the autofluorescent tissue properties of the FITC background image in combination with the DAPI image to generate virtual H&E stainings of the tissue samples. Particularly during the repeated stripping and rehybridization of tissues, we have noted a significant increase in FITC autofluorescence all over the tissue, to an extent that distinguishing FITC signals from the background becomes challenging. This issue was especially present in neoplastic areas, where true signals often indicated lower intensities than the FITC background. As a result, this leads to the detection of false-positive signals, causing errors in decoding. Thus, reducing or minimizing background intensity could enhance the number of expected reads. These reads would have been "lost" without background subtraction, due to incorrect base calling during the decoding process. To address this challenge, a background subtraction module was integrated into the CellProfiler (Broad Institute, MA, United States) pipeline. This module plays a central role in excluding highly fluorescent structures from the analysis, thus enhancing the accuracy of the results. Implementing this background subtraction module, necessitates an additional imaging cycle, during which the background of each channel is captured without the presence of any labelled signals. This supplementary step ensures that autofluorescent structures are effectively subtracted from the analysis.

The efficacy of this developed module was tested by comparing the output of a dRNA-HybISS analysis with and without background subtraction. The results with the application of background subtraction yielded an approximate 27% increase in expected reads.

This improvement underscores the potential of our developed background subtraction step, as it weakens the impact of autofluorescence and enhances the precision and reliability of dRNA-HybISS technologies.

### 4.1.5. Alignment of tiles

Ensuring precise tile alignment is an essential prerequisite for the successful execution of dRNA-HybISS analysis. Therefore, it is of great importance to verify the alignment efficacy for each performed sequencing cycle. The effectiveness of the alignment process is directly linked to the abundance of truly positive signals within a given tile. Put simply, the more true signals are present in a tile, the more accurately the alignment algorithm can manage to correctly align tiles with each other. However, certain challenges, particularly in border regions of samples or in tiles that encompass areas of damaged tissue, can arise. Tiles such as those pose specific alignment difficulties, as only a small area of the tile contains hybridized signals, making it challenging for the alignment algorithm to match them precisely.

Most signals within misaligned tiles are automatically excluded during the subsequent decoding process. Nonetheless, it is of extreme importance to eliminate misaligned tiles from any further analysis. This measure must be taken, as, in rare cases, false-positive signals can sporadically be detected in misaligned tiles. This stringent quality control process of alignment serves to enhance the accuracy and reliability of dRNA-HybISS analysis results.

## 4.2. Quality control of dRNA-HybISS data

In general, data pre-processing, involving steps such as normalization and quality control, is a foundational step in spatial transcriptomics data analysis. It is essential for refining data quality and ensuring that subsequent analyzes yield robust and reliable biological insights (Du et al., 2023). The overarching objective of quality control in the context of conventional spatial transcriptomics is to eliminate low-quality regions and genes from the data (Du et al., 2023). The criteria applied for quality control can be tailored and optimized to suit the specific characteristics of the tissue type under investigation, the precise research objectives, and additional considerations (Du et al., 2023). The criteria used for quality control can encompass several dimensions. For instance, genes expressed in fewer than a specified number of spots should be excluded from the analysis (Du et al., 2023). Similarly, spots with transcript counts falling below a defined threshold and spots demonstrating a high proportion of mitochondrial gene expression should be removed as part of the quality control process (Du et al., 2023).

With innovative approaches such as the dRNA-HybISS technology, however, the landscape of spatial transcriptomics is continually evolving. dRNA-HybISS, a relatively recent addition to the spatial transcriptomics “toolbox”, differs from more established techniques in several respects. Currently, there is no quality control in place to verify the efficacy of execution and the quality of RNA. Additionally, dRNA-HybISS methodology is based on targeted panels with a relative low

sensitivity, compared to other commercially available spatial transcriptomic approaches, which do not yield results on single cell resolution. This characteristic makes it challenging to introduce specific thresholds for spots with low transcript counts or to exclude spots with a high number of detected mitochondrial transcripts (Du et al., 2023).

Nevertheless, even in the absence of traditional quality control parameters, we assessed the efficacy of the dRNA-HybISS methodology through the quantification of expected decoded transcripts after decoding. This was conducted for each patient sample and the values were normalized to the total number of reads in each respective sample. The results of this assessment revealed a consistent range of values, falling within the range of 66-77 percent. None of the patient samples exhibited significant outliers below the threshold of 65 percent.

## 4.3. Cell segmentation and normalization

The process of cell segmentation plays a major role in the assignment of detected transcripts to their respective cells, and it represents an essential step in spatial transcriptomics data analysis. Over time, several segmentation methods have been developed, with notable contributions from pipelines such as pciSeq (Qian et al., n.d.), Scanpy (Wolf et al., 2018), JSTA (Littman et al., 2021), and Baysor (Petukhov et al., 2022). A universally accepted gold standard for cell segmentation, however, remains elusive. The efficiency of segmentation methodologies is highly dependent on the unique structural and density characteristics of the tissue under examination. Consequently, the selection and adaptation of the ideal segmentation approach must be conducted on a case-by-case basis, tailored to the specific tissue sample type in question. In our study, we opted for the Otsu segmentation methodology based on nucleic staining of cells and the subsequent expansion of detected nuclei. This formed the basis for our downstream analysis. In your study, the segmentation performance was evaluated by examining different fields of view within each sample. However, future experiments could benefit from using a pixel classifier like CellPose (Stringer et al., 2021). This approach could significantly enhance the accuracy and efficiency of cell segmentation compared to the currently used Otsu method (Stringer et al., 2021). CellPose can be applied to a wide range of cell types and imaging conditions without the need of retraining (Stringer et al., 2021). Additionally, it enables the identification of cell boundaries using typical cell shapes and sizes, rather than just intensity thresholds (Stringer et al., 2021). Integrating a pixel classifier into our future studies, could significantly improve the accuracy and reliability of cell segmentation, thereby enhancing the overall quality and interpretability of the results.

When it came to normalizing spatial transcriptomic datasets across samples, however, we encountered particular challenges. Existing normalization tools such as SCnorm (Bacher et al.,

2017) and scran (Lun et al., 2016) were originally designed and optimized for single-cell RNA studies and were not tailored to handle spatial dRNA-HybISS datasets at the single cell resolution. Considering these limitations, we decided to use the segmentation data generated based on nucleic staining of cells as an anchor point for normalizing the detected transcripts to the cell counts.

## 4.4. Automatic versus morphological tissue compartments

Classifying neoplastic tissues into their distinct histological sub-compartments, such as distinguishing between neoplastic and non-neoplastic areas, necessitates a profound understanding of histology and practical experience. While significant progress has been made in harnessing artificial intelligence (AI) tools for this purpose, the demand for large training datasets to ensure accurate identification of these tissue compartments (Xie et al., 2020) appears to be a limitation. In our study, we developed a novel approach that uses dRNA-HybISS generated data to define tissue compartments. This was achieved by utilizing the expression patterns of eight specific genes, which we have termed the "tumor gene signature." These genes exhibited high expression levels within the neoplastic regions of tissue samples. An advantage of this approach is its independence from histology. Here, spatial gene expression patterns serve as the guiding principle, allowing for the identification of tissue compartments without the explicit involvement of an expert histologist. Another advantage of our method is its adaptability and flexibility. It can be applied to other colorectal tissue samples without the prior need of large datasets for training purposes (Sallinger et al., 2023). Meylan et al. (2022) developed a similar approach based on the expression of 29 genes to identify tertiary lymphoid structures in renal tumors (Meylan et al., 2022; Sallinger et al., 2023). This demonstrates the broader applicability of gene expression-based methodologies across diverse tissue types and conditions. In comparing the performance of our expression-based tissue mask with the traditional morphological approach conducted by a pathologist, a more precise and granular representation of the neoplastic area in three patients could be observed (Sallinger et al., 2023).

Further validation of our approach was achieved by observing the gene expression profiles of neoplastic versus non-neoplastic tissue masks, using both the morphological and expression-based approach. A high degree of overlap was observed, with a total of 81 upregulated genes being identified by both the morphological-based tissue mask and the expression-based approach (Sallinger et al., 2023). The expression-based mask, furthermore, indicated 17 additional differentially expressed genes, shedding light on differential expression patterns that may have otherwise remained hidden (Sallinger et al., 2023).

The remarkable concordance between traditional histological assessments and gene expression-based methodologies shows the robustness and reliability of our approach, opening up new avenues for tissue analysis and classification in colorectal tissue samples and potentially other tissue types.

## 4.5. Relapse markers

In our study, we were the first to perform a dRNA-HybISS approach on CRC tissue samples to identify potential relapse markers. We identified *FGFR2, MMP11* and *OTOP2* as differentially upregulated genes in the neoplastic compartments in the relapse-subgroup of patients with stage II CRC (Sallinger et al., 2023). Interestingly, *MMP11* and *FGFR2* are used as druggable targets in other cancer types and could become predictive relapse markers in stage II CRC patients (Sallinger et al., 2023).

### *4.5.1. FGFR2*

Fibroblast growth factor receptor 2 (*FGFR2*) has emerged as a promising candidate for cancer therapy, given its notable overexpression in various solid tumors, including CRC (Li et al., 2019). This receptor has already been characterized to play a crucial role in tumorigenesis and progression of cancer, facilitating metastasis, and the formation of new blood vessels within tumors (Li et al., 2019).

The interaction between the ligand and its receptor activates multiple signalling pathways that are involved in proliferation, differentiation, and survival (Li et al., 2019; Matsuda, Ueda, et al., 2012). In CRC, elevated levels of *FGFR2* are associated with an increased risk of lymph node metastasis and advanced clinical stages, highlighting its significance in predicting disease prognosis (Li et al., 2019). Interestingly, erdafitinib and pemigatinib, two *FGFR* targeting agents, have previously been approved by the Food and Drug Administration for treating urothelial carcinoma and cholangiocarcinoma and various *FGFR* inhibitors are, furthermore, being tested in preclinical- and clinical studies (Krook et al., 2021; Sallinger et al., 2023). Due to this and the overexpression in various other tumors, *FGFR2* seems to be a promising target worth future evaluation in stage II CRC patients (Matsuda, Hagio, et al., 2012).

### *4.5.2. MMP11*

Matrix metalloproteinase 11 (*MMP11*) is known to play an essential role in the development, progression and metastasis of cancers as it is associated with various pathways that are involved in the development of tumors (Sallinger et al., 2023; Tian et al., 2015; Zhuang et al., 2021).

The study by Zhuang et al. (2019) unveiled a significant correlation between elevated *MMP11* expression and advanced tumor stages, as well as an unfavourable prognosis in breast cancer patients (Yang et al., 2019). *MMP11* was significantly overexpressed in breast cancer tissues and cell lines, where it enhanced proliferative capacity (Yang et al., 2019). Additionally, the study demonstrated that an *MMP11* inhibition could significantly impair cell proliferation and growth in breast cancer (Yang et al., 2019). Xenograft experiments confirmed the pro-tumorigenic effects of *MMP11* in breast cancer (Yang et al., 2019). *MMP11* was observed to play a key role in the development of lung cancer as elevated expression levels were observed in sera and tissues of patients (Yang et al., 2019). Furthermore, as anti-*MMP11* antibodies suppress the growth of cancers in vitro and in xenograft models, *MMP11* was identified as a potential target for antibody therapies (Yang et al., 2019). This research highlights the potential of *MMP11* in being a promising therapeutic target in lung cancer (Yang et al., 2019).

### *4.5.3. OTOP2*

In comparison to *FGFR2* and *MMP11*, less is known about the function of Otoperin 2 (*OTOP2*) regarding cancer development (Sallinger et al., 2023). The gene encodes a proton-selective channel, which transfers protons into the cytosol of cells (Sallinger et al., 2023; Tu et al., 2018). A new subtype of cells positive for *OTOP2* and *BEST4* in the intestinal crypts, responsible for the transportation of electrolytes, was identified by scRNAseq analysis (Parikh et al., 2019; Sallinger et al., 2023). In a study by Guo and Sun (2022) high expression levels of *OTOP2* in bulk CRC tissues were associated with a better overall survival (Guo & Sun, 2022; Sallinger et al., 2023). It is important to mention, however, that this study did not focus on stage II CRC patients and was performed on bulk tissue samples. Therefore, results of this study cannot be compared with results from our spatial approach focusing on stage II CRC patients.

## 4.6. Spatial analysis versus bulk analysis

To underscore the importance of spatial analysis and to indicate the distinctions between spatial analysis and bulk analysis, we simulated profiling of bulk RNA. For this simulation we combined the neoplastic and non-neoplastic tissue mask, emulating the profiling of bulk RNA expression.
While the results of the simulation indicated a significant upregulation of *OTOP2* and *MMP11* in both spatial and bulk analysis, the gene *FGFR2* showed no upregulation in the bulk analysis (Sallinger et al., 2023). An upregulation of *FGFR2* was only observed when we applied our spatial analysis approach (Sallinger et al., 2023). This highlights the importance of performing spatial analysis to yield novel findings which otherwise would easily have been overlooked within the context of bulk analysis techniques (Sallinger et al., 2023).

## 4.7. Cell-phenotyping based on dRNA-HybISS data

While spatial transcriptomic datasets hold immense promise in unveiling tissue organization at the cellular- and subcellular levels, the path to fully unlocking its potential is not without its challenges. One of the foremost hurdles lies in the downstream analysis of these datasets. These contain a complex network of spatially resolved gene expression information, which demands specialized tools and methodologies for interpretation. In response, an array of visualization and analysis tools for cell-phenotyping, clustering and cell-cell interactions has been developed, each bearing its own set of advantages and limitations. As discussed in the chapter of cell segmentation, one critical aspect in the analysis of dense tissue structures, such as neoplastic tissue, is the accurate segmentation of individual cells - a prerequisite for most cell-phenotyping approaches.
Here, we performed cell-phenotyping of dRNA-HybISS generated data by applying DeNovo SSAM which does not require prior cell segmentation. The outcome of this analysis was the identification of a total of 16 distinct clusters, each representing cells with highly similar gene expression patterns. After manual annotation of the clusters based on their position within the tissue, clusters for muscle tissue, connective tissue, neoplastic- and non-neoplastic epithelium, immune cells and lymphoid tissue were characterized. These identified clusters overlapped perfectly with the morphological structures observed in the traditional H&E staining, further validating the accuracy and specificity of the transcripts detected via dRNA-HybISS technology. These findings underscore the remarkable potential of spatial transcriptomic technologies, confirming their ability to capture and represent the complex spatial relationships and functional diversity within tissues.

## 4.8. Limitations and challenges of dRNA-HybISS

### *4.8.1. Detection efficiency*

The detection efficiency of the method with ~5% is, as already mentioned in the introduction, lower than in other FISH-based approaches such as MERFISH with ~80% for 140 genes and seqFISH+ with ~49% for 60 genes (K. H. Chen et al., 2015; Eng et al., 2019; Gyllborg et al., 2020; Lee et al., 2022; Moses & Pachter, 2022). However, as Hartman et al. have noted, direct comparison of these methods in terms of the number of molecules detected per cell is challenging (Hartman & Satija, n.d.). This complexity arises from variations in the gene panel compositions, used signal amplification systems, error correction mechanisms, and the presence of off-target artifacts across different technologies (Hartman & Satija, n.d.) To estimate the detection efficiency of the dRNA-HybISS approach used for analyzing CRC samples, we utilized our in-house developed GTC-tool, which is currently undergoing further development. A test version, GTC-tool 2, is being evaluated, that includes a new function to estimate the average number of transcripts per cell, although this function is still a work in progress. We performed analysis with GTC-tool 2 on a patient sample, generating preliminary data to determine the average number of transcripts detectable in our sample.

A figure generated with GTC-tool 2 has been included in the supplement. However, it's crucial to note that the first bar, representing cells with 0 transcripts, is not accurate. A significant number of these cells are located in the circular border region adjacent to the secure seal. The circular boarder area is depicted in supplementary figure 1. This area is consistently excluded from analysis by the GTC-tool, as tissue detachment often occurs due to the removal of the secure seal. While transcripts in this area have been excluded in GTC-tool 2, the cells have not, leading to an incorrect display of 0 transcripts for these cells. Despite this issue, which is expected to be resolved soon, the figure provides an initial estimate of detected transcripts per cell, ranging from 0 to 25. It should also be noted that detection efficiency varies across samples stored under different conditions. RNA degradation, even in FFPE tissues, plays a crucial role and can significantly affect the outcomes of experiments. Given that our samples are at least 10 years old, we expect that freshly prepared FFPE tissues would yield higher numbers of transcripts per cell.

### *4.8.2. Specificity and false positive reads*

The in situ padlock probe approach, as demonstrated by Krzywkowski and Nilsson (2018), is a highly specific method for analyzing DNA and RNA molecules, capable of detecting single nucleotide variants with high precision (Krzywkowski & Nilsson, 2018). This technique is effective

in differentiating between human and mouse cells in a co-culture, utilizing a single nucleotide variant in the conserved ACTB mRNA as a marker (Krzywkowski & Nilsson, 2018). In this approach, mRNA is reverse-transcribed to cDNA, which is then targeted by padlock probes (Krzywkowski & Nilsson, 2018). The employed dRNA-HybISS methodology used in our study is demonstrated to show the same level of specificity as the cDNA-based HybISS approach, as stated in the paper by Lee et al. (Lee et al., 2022). Unfortunately, the paper does not elaborate on how the specificity of the CARTANA method was tested. Similarly, in our application, no specific tests regarding specificity were performed. In future experiments, it is crucial to include control samples, such as padlocks that do not bind to mRNA transcripts present in human tissues but are found in other species, to evaluate the technique's specificity. Additionally, counting transcripts in areas without tissue proves challenging, as it is impossible to determine whether the presence of mRNA is due to contamination from the cutting process or if the probes have bound in the absence of RNA, generating false signals.

#### *4.8.3. Hybridization area*

In this study, we utilized hybridization spots with a diameter of 9 mm, allowing us to analyze a tissue area of 63.62 mm². This analysis typically takes around two weeks, with the potential to expand the analyzed area by using larger hybridization spots. Indeed, this would be of great significance when examining heterogeneity in tumors, especially in very large tumors. It would also be crucial to compare different adjacent sections to identify local differences within tumors However, this expansion would also increase the costs per slide, extend imaging times, and result in much larger output files.

#### *4.8.4. Selecting the GTC-tool for analysis*

A key advantage of the dRNA-HybISS approach highlighted in the thesis is its subcellular resolution. Although this technology can provide data at the single-cell levels, the performance of analysis tools for cell-phenotyping become challenging when the average number of transcripts per cell is low. In the relapse project, we decided to use only the pathway panel, excluding the immune panel, because it was not ready for implementation at that time due to overcrowding effects. The optimization of the immune panel involved identifying and quenching of genes with high expression levels, a process that took several months to complete. It is crucial to note that the pathway panel was not specifically designed for cell-phenotyping but rather to investigate various biological processes, such as apoptosis, angiogenesis, and proliferation, leading to challenges in cell-phenotyping due to the inclusion of few cell type-specific markers. Furthermore,

the relatively advanced age of the samples contributed to a lower average transcript count per cell.

Considering this, we decided to develop a tool that utilizes the spatial expression of specific markers to automatically create masks for different tissue compartments and compare the expression of genes in the generated masks. Additionally, cell-phenotyping analysis utilizing the pathway panel generated data is still under development, facing the above mentioned challenges. Preliminary results are presented in supplementary figure 1c.

## 4.9. Conclusion

Our primary objective of this thesis was to delve deeper into the complex biological mechanisms underpinning tumor dissemination in stage II colon cancer patients. To accomplish this, we designed a panel of 176 genes, encompassing a wide spectrum of biological processes, ranging from apoptosis and proliferation to angiogenesis, stemness, oxidative stress, hypoxia, invasion, and markers associated with the tumor microenvironment (TME) to examine the spatial tissue composition (Sallinger et al., 2023). Our chosen tool for this investigation was the novel dRNA-HybISS spatial transcriptomics technology, capable of preserving tissue architecture while providing insights into gene expression at single cell and subcellular resolutions.

The optimization of dRNA-HybISS technology for colonic tissue was a complex and comprehensive process, encompassing various aspects for an enhanced workflow. The optimization of permeabilization conditions and exposure times for different channels on the VS200 scanner, the introduction of a pseudo-general stain, and the implementation of background subtraction have all contributed to the refinement of dRNA-HybISS technology, leading to more precise and reliable results.

The importance of quality control in dRNA-HybISS data cannot be overstated, even in the absence of traditional quality control parameters. The evaluation of expected decoded transcripts normalized to total reads has provided confidence in the methodology's consistency and reliability. Cell segmentation and normalization strategies were adapted to suit the unique characteristics of the tissue samples, ensuring proper downstream analysis. The alignment of tiles was stringently controlled to enhance the accuracy of results. The novel approach of defining tissue compartments based on gene expression patterns, rather than relying on histological expertise, has demonstrated its robustness and shows potential for broader applications across tissue types and conditions, promising a more comprehensive understanding of tissue organization. Comparing spatial analysis to bulk analysis emphasized the importance of spatial analysis in uncovering novel findings which otherwise would easily have been overlooked.

By using this innovative methodology, we were able to identify three novel predictive biomarkers—*OTOP2, MMP11,* and *FGFR2*—that exhibited significant upregulation in the neoplastic regions of relapsed stage II colon cancer patients compared to non-relapsed patient samples (Sallinger et al., 2023). These findings offer promising prospects for targeted therapies and future research to enhance the understanding of CRC disease progression.

Moreover, the application of DeNovo SSAM for cell-phenotyping without prior cell segmentation has demonstrated the power of dRNA-HybISS technology in capturing complex spatial relationships and functional diversity within tissues. Tissue structures, such as muscle tissue,

connective tissue, non-neoplastic epithelium, neoplastic epithelium, immune cells and lymphoid tissues, comparable to the tissue characterisation of a histologist based on H&E staining, were identified. These promising preliminary results confirmed the high specificity of the dRNA-HybISS approach and shows its great potential in understanding tissue organization at the cellular and subcellular levels.

## 4.10. Outlook for the shedder project

The data presented in this thesis demonstrate that we successfully established the dRNA-HybISS approach and downstream data analysis to perform powerful spatial analyses of colorectal tissue. These tools hold the potential to create a better understanding of biological processes where spatial information is a crucial, but previously inaccessible factor. For example, the exact mechanism of ctDNA release into the blood circulation is still poorly understood but of high interest, since ctDNA-based assays are increasingly used in cancer research and the clinic.
In an ongoing study, we are aiming to investigate the spatial architecture among stage I and II CRC patients, distinguishing between those who are ctDNA-positive and ctDNA-negative.
To achieve this, we have, so far, enlisted a cohort of 21 patients who were diagnosed with stage I and II CRC. Sequencing was conducted on blood samples collected before tumor removal and on FFPE tissue samples obtained post-surgery. Somatic mutations were identified in the tumor tissue and used to categorize patients into two groups: shedders, characterized by the presence of variants in both plasma and tissue, and non/low shedders, characterized by minimal or no occurrence of the identified variants in plasma.

The dRNA-HybISS technology was employed for the spatial analysis on the first patient samples, utilizing the pathway gene panel along with two pre-designed immune panels from CARTANA. We were able to introduce a third mask that represents stromal tissue in both neoplastic and non-neoplastic tissue areas, facilitated by the additional use of two immune panels in this project. Data analysis is currently ongoing. Furthermore, we aim to trace the variants identified through sequencing back to their origins in the tissue sections using the cDNA padlock probe technology (El-Heliebi et al., 2017). This technique specifically allows for the detection of single nucleotide variants (El-Heliebi et al., 2017). As a subsequent step, we plan to investigate the tissue surrounding the detected variants to identify differences compared to the remaining neoplastic tissue through neighbourhood analysis.

## 4.11. Outlook for ISS technologies

Spatial transcriptomics has revolutionized our understanding of gene expression within complex biological systems, enabling the precise detection of mRNA transcripts across a vast number of tissues. This field has evolved from early techniques like smFISH to advanced spatially resolved transcriptomics methods, which include sequencing-based (Visium) and imaging-based approaches such as seqFISH, MERFISH, HybISS and dRNA-HybISS (K. H. Chen et al., 2015; Eng et al., 2019; Gyllborg et al., 2020; Lee et al., 2022). These methods have facilitated the creation of detailed molecular atlases, offering insights into the spatial architecture of tissues (Salas et al., 2024). The technologies mentioned above each come with their own set of strengths and weaknesses. For instance, MERFISH is capable of achieving 80% efficiency for 140 genes, yet this efficiency decreases to approximately 30% for analyses involving up to 10,000 genes (K. H. Chen et al., 2015). SeqFISH+ demonstrates an efficiency of about 49% for 60 genes (Eng et al., 2019). Whereas technologies such as HybISS (~1%) and dRNA-HybISS (~5%) bear much lower detection efficiencies but bringing advantages in comparison to the above mentioned techniques regarding the number of required probes per target which lead to a robust signal (Gyllborg et al., 2020; Lee et al., 2022). Whereas for FISH based technologies such as MERFISH and seqFISH a large number (50-100) of probes are used HybISS and dRNA-HybISS utilize 4-5 probes per target (K. H. Chen et al., 2015; Eng et al., 2019; Gyllborg et al., 2020; Lee et al., 2022). All advanced spatial transcriptomic approaches, including dRNA-HybISS, require extensive time for optimization in laboratory work, imaging processes, and analysis tools. This investment in time and resources is crucial for ensuring good results. Our team has extensive experience with *in situ* padlock technology, which played a crucial role in our decision to utilize dRNA-HybISS for this project, despite being aware of its limitations. One of the primary challenges with this technology is its lower detection efficiency of transcripts, which can be problematic for cell-phenotyping.

However, with the recently commercialized Xenium technology from CARTANA, we expect a significantly higher detection efficiency (Salas et al., 2024). The recently published paper in bioRxiv by Salas et al. (2024) indicated that across ten datasets, cells had an average of 229 reads, with 78.5% of these reads being allocated to specific cells (Salas et al., 2024). Our method uses 9 mm hybridization spots to examine a 63.62 mm² tissue area in about two weeks, with the option to increase this area at the cost of higher expenses and longer imaging times. The Xenium platform is capable of analysing an area of 235,235 mm² in just 4-5 working days (Salas et al., 2024). This efficiency is due to the automated nature of the Xenium system, where only library

preparation is performed manually, while hybridization, stripping, imaging, and decoding processes are fully automated. This streamlined workflow not only reduces the workload but also shortens the timeline of spatial transcriptomic analysis.

The integration of spatial transcriptomic approaches into clinical routine diagnostics remains uncertain, primarily due to high costs and the time-consuming nature. However, with platforms like MERFISH and Xenium, their application in precision medicine becomes more imaginable (Moses & Pachter, 2022). These technologies have the potential to revolutionize precision medicine by characterizing tissue architecture of individual patient samples to identify the most effective treatment options, thereby improving treatment outcomes. Tumors often indicate significant heterogeneity, and small, aggressive clones capable of potentially causing metastatic progression might be lost in bulk sequencing (Svedlund et al., 2019). Spatial transcriptomic analysis could offer a deeper insight into cellular environments and disease pathology and could enhance our understanding of disease progression.

# 5. Bibliography


Ahmed, M. (2020). Colon Cancer: A Clinician's Perspective in 2019. *Gastroenterology Research*, *13*(1), 1–10. https://doi.org/10.14740/gr1239

American Cancer Society. (2011). *Colorectal Cancer Facts & Figures 2011-2013*.

Argilés, G., Tabernero, J., Labianca, R., Hochhauser, D., Salazar, R., Iveson, T., Laurent-Puig, P., Quirke, P., Yoshino, T., Taieb, J., Martinelli, E., & Arnold, D. (2020). Localised colon cancer: ESMO Clinical Practice Guidelines for diagnosis, treatment and follow-up†. *Annals of Oncology*, *31*(10), 1291–1305. https://doi.org/10.1016/j.annonc.2020.06.022

Avid, D., Ieberman, A. L., Eiss, A. G. W., Ohn, J., Ond, H. B., Ennis, D., Hnen, J. A., Arewal, A. G., Regorio, G., Hejfec, C., Ffairs, A., Ooperative, C., Tudy, S., & Roup, G. (2000). *The New England Journal of Medicine USE OF COLONOSCOPY TO SCREEN ASYMPTOMATIC ADULTS FOR COLORECTAL CANCER Background and Methods The role of colonosco*.

Baxter, N. N., Kennedy, E. B., Bergsland, E., Berlin, J., George, T. J., Gill, S., Gold, P. J., Hantel, A., Jones, L., Lieu, C., Mahmoud, N., Morris, A. M., Ruiz-Garcia, E., Nancy You, Y., & Meyerhardt, J. A. (2021). Adjuvant Therapy for Stage II Colon Cancer: ASCO Guideline Update. *J Clin Oncol*, *40*, 892–910. https://doi.org/10.1200/JCO.21

Cardoso, R., Guo, F., Heisser, T., De Schutter, H., Van Damme, N., Christina Nilbert, M., Christensen, J., Bouvier, A.-M., eronique Bouvier, V., Launoy, G., Woronoff, A.-S., elanie Cariou, M., Robaszkiewicz, M., Delafosse, P., Poncet, F., Walsh, P. M., Senore, C., Rosso, S., EPP Lemmens, V., … Brenner, H. (2022). Overall and stage-specific survival of patients with screen-detected colorectal cancer in European countries: A population-based study in 9 countries. *The Lancet Regional Health - Europe*, *21*, 100458. https://doi.org/10.1016/j

Chen, K., Collins, G., Wang, H., & Toh, J. W. T. (2021). Pathological features and prognostication in colorectal cancer. *Current Oncology*, *28*(6), 5356–5383. https://doi.org/10.3390/curroncol28060447

Chen, K. H., Boettiger, A. N., Moffitt, J. R., Wang, S., & Zhuang, X. (2015b). Spatially resolved, highly multiplexed RNA profiling in single cells. *Science*, *348*(6233). https://doi.org/10.1126/science.aaa6090

Church, D. N., Midgley, R., & Kerr, D. J. (2013). Stage II colon cancer. In *Chinese Clinical Oncology* (Vol. 2, Issue 2). AME Publishing Company. https://doi.org/10.3978/j.issn.2304-3865.2013.03.03

Dacosta, R. S., Andersson, H., Cirocco, M., Marcon, N. E., & Wilson, B. C. (2005). Autofluorescence characterisation of isolated whole crypts and primary cultured human epithelial cells from normal, hyperplastic, and adenomatous colonic mucosa. *Journal of Clinical Pathology*, *58*(7), 766–774. https://doi.org/10.1136/jcp.2004.023804

Deal, J., Mayes, S., Browning, C., Hill, S., Rider, P., Boudreaux, C., Rich, T. C., & Leavesley, S. J. (2018). Identifying molecular contributors to autofluorescence of neoplastic and normal colon sections using excitation-scanning hyperspectral imaging. *Journal of Biomedical Optics*, *24*(02), 1. https://doi.org/10.1117/1.jbo.24.2.021207

Desch, C. E., Benson, A. B., Somerfield, M. R., Flynn, P. J., Krause, C., Loprinzi, C. L., Minsky, B. D., Pfister, D. G., Virgo, K. S., & Petrelli, N. J. (2005). Colorectal cancer surveillance: 2005 Update of an American Society of Clinical Oncology practice guideline. *Journal of Clinical Oncology*, *23*(33), 8512–8519. https://doi.org/10.1200/JCO.2005.04.0063

Dong, Y. X. (2014). Review of Otsu segmentation algorithm. *Advanced Materials Research*, *989–994*, 1959–1961. https://doi.org/10.4028/www.scientific.net/AMR.989-994.1959

El-Heliebi, A., Kashofer, K., Fuchs, J., Jahn, S. W., Viertler, C., Matak, A., Sedlmayr, P., & Hoefler, G. (2017). Visualization of tumor heterogeneity by in situ padlock probe technology in colorectal cancer. *Histochemistry and Cell Biology*, *148*(2), 105–115. https://doi.org/10.1007/s00418-017-1557-5

Eng, C. H. L., Lawson, M., Zhu, Q., Dries, R., Koulena, N., Takei, Y., Yun, J., Cronin, C., Karp, C., Yuan, G. C., & Cai, L. (2019). Transcriptome-scale super-resolved imaging in tissues by RNA seqFISH+. *Nature*, *568*(7751), 235–239. https://doi.org/10.1038/s41586-019-1049-y

Femino Andrea M., & Fay Fredric S. (1998). Visualization of Single RNA Transcripts in Situ. *Science*, *280*, 585–589.

Filice, M., & Ruiz-Cabello, J. (2019). *Nucleic Acid Nanotheranostics: Biomedical Applications*.

Giacomelli MG. (2016). Virtual Hematoxylin and Eosin Transillumination Microscopy Using Epi-Fluorescence Imaging. *PLOS ONE* , *11*.

Goh, J. J. L., Chou, N., Seow, W. Y., Ha, N., Cheng, C. P. P., Chang, Y. C., Zhao, Z. W., & Chen, K. H. (2020). Highly specific multiplexed RNA imaging in tissues with split-FISH. *Nature Methods*, *17*(7), 689–693. https://doi.org/10.1038/s41592-020-0858-0

Guo, S., & Sun, Y. (2022). OTOP2, Inversely Modulated by miR-3148, Inhibits CRC Cell Migration, Proliferation and Epithelial–Mesenchymal Transition: Evidence from Bioinformatics Data Mining and Experimental Verification. *Cancer Management and Research*, *14*, 1371–1384. https://doi.org/10.2147/CMAR.S345299

Gyllborg, D., Langseth, C. M., Qian, X., Choi, E., Salas, S. M., Hilscher, M. M., Lein, E. S., & Nilsson, M. (2020). Hybridization-based in situ sequencing (HybISS) for spatially resolved transcriptomics in human and mouse brain tissue. *Nucleic Acids Research*, *48*(19), E112. https://doi.org/10.1093/nar/gkaa792

Hartman, A., & Satija, R. (n.d.). *Comparative analysis of multiplexed in situ gene expression profiling technologies*. https://doi.org/10.1101/2024.01.11.575135

Joe V. Selby. (1992). *A case control study of screening sigmoidoscopy and mortality from colorectal cancer*.

Johnson, C. D., Chen, M.-H., Toledano, A. Y., Heiken, J. P., Dachman, A., Kuo, M. D., Menias, C. O., Siewert, B., Cheema, J. I., Obregon, R. G., Fidler, J. L., Zimmerman, P., Horton, K. M., Coakley, K., Iyer, R. B., Hara, A. K., Halvorsen, R. A., Casola, G., Yee, J., … Limburg, P. J. (2008). Accuracy of CT Colonography for Detection of Large Adenomas and Cancers. *New England Journal of Medicine*, *359*(12), 1207–1217. https://doi.org/10.1056/nejmoa0800996

Kamentsky, L., Jones, T. R., Fraser, A., Bray, M. A., Logan, D. J., Madden, K. L., Ljosa, V., Rueden, C., Eliceiri, K. W., & Carpenter, A. E. (2011). Improved structure, function and compatibility for cellprofiler: Modular high-throughput image analysis software. *Bioinformatics*, *27*(8), 1179–1180. https://doi.org/10.1093/bioinformatics/btr095

Kobayashi, H., Mochizuki, H., Sugihara, K., Morita, T., Kotake, K., Teramoto, T., Kameoka, S., Saito, Y., Takahashi, K., Hase, K., Oya, M., Maeda, K., Hirai, T., Kameyama, M., Shirouzu, K., & Muto, T. (2007). Characteristics of recurrence and surveillance tools after curative resection for colorectal cancer: A multicenter study. *Surgery*, *141*(1), 67–75. https://doi.org/10.1016/j.surg.2006.07.020

Kopetz, S., Tabernero, J., Rosenberg, R., Jiang, Z.-Q., Moreno, V., Bachleitner-Hofmann, T., Lanza, G., Stork-Sloots, L., Maru, D., Simon, I., Capellà, G., & Salazar, R. (2015). Genomic Classifier ColoPrint Predicts Recurrence in Stage II Colorectal Cancer Patients More Accurately Than Clinical Factors. *The Oncologist*, *20*(2), 127–133. https://doi.org/10.1634/theoncologist.2014-0325

Krook, M. A., Reeser, J. W., Ernst, G., Barker, H., Wilberding, M., Li, G., Chen, H. Z., & Roychowdhury, S. (2021). Fibroblast growth factor receptors in cancer: genetic alterations, diagnostics, therapeutic targets and mechanisms of resistance. In *British Journal of Cancer* (Vol. 124, Issue 5, pp. 880–892). Springer Nature. https://doi.org/10.1038/s41416-020-01157-0

Krzywkowski, T., & Nilsson, M. (2018). Padlock probes to detect single nucleotide polymorphisms. In *Methods in Molecular Biology* (Vol. 1649, pp. 209–229). Humana Press Inc. https://doi.org/10.1007/978-1-4939-7213-5_14

Lee, H., Marco Salas, S., Gyllborg, D., & Nilsson, M. (2022). Direct RNA targeted in situ sequencing for transcriptomic profiling in tissue. *Scientific Reports*, *12*(1). https://doi.org/10.1038/s41598-022-11534-9

Lein, E., Borm, L. E., & Linnarsson, S. (n.d.). *The promise of spatial transcriptomics for neuroscience in the era of molecular cell typing*. https://www.science.org

Lewis, C., Xun, P., & He, K. (2016). Effects of adjuvant chemotherapy on recurrence, survival, and quality of life in stage II colon cancer patients: a 24-month follow-up. *Supportive Care in Cancer*, *24*(4), 1463–1471. https://doi.org/10.1007/s00520-015-2931-2

Li, P., Huang, T., Zou, Q., Liu, D., Wang, Y., Tan, X., Wei, Y., & Qiu, H. (2019). FGFR2 Promotes Expression of PD-L1 in Colorectal Cancer via the JAK/STAT3 Signaling Pathway. *The Journal of Immunology*, *202*(10), 3065–3075. https://doi.org/10.4049/jimmunol.1801199

Lochhead, P., Chan, A. T., Giovannucci, E., Fuchs, C. S., Wu, K., Nishihara, R., O'Brien, M., & Ogino, S. (2014). Progress and opportunities in molecular pathological epidemiology of colorectal premalignant lesions. *American Journal of Gastroenterology*, *109*(8), 1205–1214. https://doi.org/10.1038/ajg.2014.153

Lubeck, E., Coskun, A. F., Zhiyentayev, T., Ahmad, M., & Cai, L. (2014). Single-cell in situ RNA profiling by sequential hybridization. In *Nature Methods* (Vol. 11, Issue 4, pp. 360–361). Nature Publishing Group. https://doi.org/10.1038/nmeth.2892

Lüllmann-Rauch, R., & Asan, E. (2015). *Taschenlehrbuch Histologie* (5th ed.). Georg Thieme Verlag.

Magoulopoulou, A., Salas, S. M., Tiklová, K., Samuelsson, E. R., Hilscher, M. M., & Nilsson, M. (2023). *Padlock Probe-Based Targeted In Situ Sequencing: Overview of Methods and Applications*. https://doi.org/10.1146/annurev-genom-102722

Mahul B. Amin, & Stephen B. Edge. (2017). *AJCC Cancer Staging Manual* (Springer, Ed.). Springer.

Mariotto, A. B., Robin Yabroff, K., Shao, Y., Feuer, E. J., & Brown, M. L. (2011). Projections of the cost of cancer care in the United States: 2010-2020. *Journal of the National Cancer Institute*, *103*(2), 117–128. https://doi.org/10.1093/jnci/djq495

Mármol, I., Sánchez-de-Diego, C., Dieste, A. P., Cerrada, E., & Yoldi, M. J. R. (2017). Colorectal carcinoma: A general overview and future perspectives in colorectal cancer. In *International Journal of Molecular Sciences* (Vol. 18, Issue 1). MDPI AG. https://doi.org/10.3390/ijms18010197

Matsuda, Y., Hagio, M., Seya, T., & Ishiwata, T. (2012). Fibroblast growth factor receptor 2 IIIc as a therapeutic target for colorectal cancer cells. *Molecular Cancer Therapeutics*, *11*(9), 2010–2020. https://doi.org/10.1158/1535-7163.MCT-12-0243

Matsuda, Y., Ueda, J., & Ishiwata, T. (2012). Fibroblast growth factor receptor 2: Expression, roles, and potential as a novel molecular target for colorectal cancer. In *Pathology Research International* (Vol. 2012). https://doi.org/10.1155/2012/574768

Meylan, M., Petitprez, F., Becht, E., Bougoüin, A., Pupier, G., Calvez, A., Giglioli, I., Verkarre, V., Lacroix, G., Verneau, J., Sun, C. M., Laurent-Puig, P., Vano, Y. A., Elaïdi, R., Méjean, A., Sanchez-Salas, R., Barret, E., Cathelineau, X., Oudard, S., … Fridman, W. H. (2022). Tertiary lymphoid structures generate and propagate anti-tumor antibody-producing plasma cells in renal cell cancer. *Immunity*, *55*(3), 527-541.e5. https://doi.org/10.1016/j.immuni.2022.02.001

Morley-Bunker, A., Pearson, J., Currie, M. J., Morrin, H., Whitehead, M. R., Eglinton, T., & Walker, L. C. (2019). Assessment of intra-tumoural colorectal cancer prognostic biomarkers using RNA in situ hybridisation. In *Oncotarget* (Vol. 10, Issue 14). www.oncotarget.com

Moses, L., & Pachter, L. (2022). Museum of spatial transcriptomics. In *Nature Methods* (Vol. 19, Issue 5, pp. 534–546). Nature Research. https://doi.org/10.1038/s41592-022-01409-2

Pagès, F., Mlecnik, B., Marliot, F., Bindea, G., Ou, F. S., Bifulco, C., Lugli, A., Zlobec, I., Rau, T. T., Berger, M. D., Nagtegaal, I. D., Vink-Börger, E., Hartmann, A., Geppert, C., Kolwelter, J., Merkel, S., Grützmann, R., Van den Eynde, M., Jouret-Mourin, A., … Galon, J. (2018). International validation of the consensus Immunoscore for the classification of colon cancer: a prognostic and accuracy study. *The Lancet*, *391*(10135), 2128–2139. https://doi.org/10.1016/S0140-6736(18)30789-X

Parikh, K., Antanaviciute, A., Fawkner-Corbett, D., Jagielowicz, M., Aulicino, A., Lagerholm, C., Davis, S., Kinchen, J., Chen, H. H., Alham, N. K., Ashley, N., Johnson, E., Hublitz, P., Bao, L., Lukomska, J., Andev, R. S., Björklund, E., Kessler, B. M., Fischer, R., … Simmons, A. (2019). Colonic epithelial cell diversity in health and inflammatory bowel disease. *Nature*, *567*(7746), 49–55. https://doi.org/10.1038/s41586-019-0992-y

Park, J., Choi, W., Tiesmeyer, S., Long, B., Borm, L. E., Garren, E., Nguyen, T. N., Tasic, B., Codeluppi, S., Graf, T., Schlesner, M., Stegle, O., Eils, R., & Ishaque, N. (2021). Cell segmentation-free inference of

cell types from in situ transcriptomics data. *Nature Communications*, *12*(1). https://doi.org/10.1038/s41467-021-23807-4

Rebuzzi, S. E., Pesola, G., Martelli, V., & Sobrero, A. F. (2020). Adjuvant chemotherapy for stage II colon cancer. In *Cancers* (Vol. 12, Issue 9, pp. 1–12). MDPI AG. https://doi.org/10.3390/cancers12092584

Reinert, T., Henriksen, T. V., Christensen, E., Sharma, S., Salari, R., Sethi, H., Knudsen, M., Nordentoft, I., Wu, H. T., Tin, A. S., Heilskov Rasmussen, M., Vang, S., Shchegrova, S., Frydendahl Boll Johansen, A., Srinivasan, R., Assaf, Z., Balcioglu, M., Olson, A., Dashner, S., … Andersen, C. L. (2019). Analysis of Plasma Cell-Free DNA by Ultradeep Sequencing in Patients with Stages i to III Colorectal Cancer. *JAMA Oncology*, *5*(8), 1124–1131. https://doi.org/10.1001/jamaoncol.2019.0528

Rosen RD, & Sapra A. (2023, February 13). *TNM Classification*. StatPearls. https://www.ncbi.nlm.nih.gov/books/NBK553187/

Ryuk, J. P., Choi, G. S., Park, J. S., Kim, H. J., Park, S. Y., Yoon, G. S., Jun, S. H., & Kwon, Y. C. (2014). Predictive factors and the prognosis of recurrence of colorectal cancer within 2 years after curative resection. *Annals of Surgical Treatment and Research*, *86*(3), 143–151. https://doi.org/10.4174/astr.2014.86.3.143

Safieddine, A., Coleno, E., Lionneton, F., Traboulsi, A. M., Salloum, S., Lecellier, C. H., Gostan, T., Georget, V., Hassen-Khodja, C., Imbert, A., Mueller, F., Walter, T., Peter, M., & Bertrand, E. (2023). HT-smFISH: a cost-effective and flexible workflow for high-throughput single-molecule RNA imaging. *Nature Protocols*, *18*(1), 157–187. https://doi.org/10.1038/s41596-022-00750-2

Salas, S. M., Czarnewski, P., Kuemmerle, L. B., Helgadottir, S., Matsson-Langseth, C., Tismeyer, S., Avenel, C., Rehman, H., Tiklova, K., Andersson, A., Chatzinikolaou, M., Theis, F. J., Luecken, M. D., Wählby, C., Ishaque, N., & Nilsson, M. (n.d.). *Optimizing Xenium In Situ data utility by quality assessment and best practice analysis workflows*. https://doi.org/10.1101/2023.02.13.528102

Sallinger, K., Gruber, M., Müller, C. T., Bonstingl, L., Pritz, E., Pankratz, K., Gerger, A., Smolle, M. A., Aigelsreiter, A., Surova, O., Svedlund, J., Nilsson, M., Kroneis, T., & El-Heliebi, A. (2023). Spatial tumour gene signature discriminates neoplastic from non-neoplastic compartments in colon cancer: unravelling predictive biomarkers for relapse. *Journal of Translational Medicine*, *21*(1). https://doi.org/10.1186/s12967-023-04384-0

Simon, K. (2016). Colorectal cancer development and advances in screening. In *Clinical Interventions in Aging* (Vol. 11, pp. 967–976). Dove Medical Press Ltd. https://doi.org/10.2147/CIA.S109285

Stirling, D. R., Swain-Bowden, M. J., Lucas, A. M., Carpenter, A. E., Cimini, B. A., & Goodman, A. (2021). CellProfiler 4: improvements in speed, utility and usability. *BMC Bioinformatics*, *22*(1). https://doi.org/10.1186/s12859-021-04344-9

Stringer, C., Wang, T., Michaelos, M., & Pachitariu, M. (2021). Cellpose: a generalist algorithm for cellular segmentation. *Nature Methods*, *18*(1), 100–106. https://doi.org/10.1038/s41592-020-01018-x

Su, Y., Tian, X., Gao, R., Guo, W., Chen, C., Chen, C., Jia, D., Li, H., & Lv, X. (2022). Colon cancer diagnosis and staging classification based on machine learning and bioinformatics analysis. *Computers in Biology and Medicine*, *145*. https://doi.org/10.1016/j.compbiomed.2022.105409

Sung, H., Ferlay, J., Siegel, R. L., Laversanne, M., Soerjomataram, I., Jemal, A., & Bray, F. (2021). Global Cancer Statistics 2020: GLOBOCAN Estimates of Incidence and Mortality Worldwide for 36 Cancers in 185 Countries. *CA: A Cancer Journal for Clinicians*, *71*(3), 209–249. https://doi.org/10.3322/caac.21660

Svedlund, J., Strell, C., Qian, X., Zilkens, K. J. C., Tobin, N. P., Bergh, J., Sieuwerts, A. M., & Nilsson, M. (2019a). Generation of in situ sequencing based OncoMaps to spatially resolve gene expression profiles of diagnostic and prognostic markers in breast cancer. *EBioMedicine*, *48*, 212–223. https://doi.org/10.1016/j.ebiom.2019.09.009

Svedlund, J., Strell, C., Qian, X., Zilkens, K. J. C., Tobin, N. P., Bergh, J., Sieuwerts, A. M., & Nilsson, M. (2019b). Generation of in situ sequencing based OncoMaps to spatially resolve gene expression profiles of diagnostic and prognostic markers in breast cancer. *EBioMedicine*, *48*, 212–223. https://doi.org/10.1016/j.ebiom.2019.09.009

Tian, X., Ye, C., Yang, Y., Guan, X., Dong, B., Zhao, M., & Hao, C. (2015). Expression of CD147 and matrix metalloproteinase-11 in colorectal cancer and their relationship to clinicopathological features. *Journal of Translational Medicine*, *13*(1). https://doi.org/10.1186/s12967-015-0702-y

Tie, J., Cohen, J. D., Lahouel, K., Lo, S. N., Wang, Y., Kosmider, S., Wong, R., Shapiro, J., Lee, M., Harris, S., Khattak, A., Burge, M., Harris, M., Lynam, J., Nott, L., Day, F., Hayes, T., McLachlan, S.-A., Lee, B., … Gibbs, P. (2022). Circulating Tumor DNA Analysis Guiding Adjuvant Therapy in Stage II Colon Cancer. *New England Journal of Medicine*, *386*(24), 2261–2272. https://doi.org/10.1056/nejmoa2200075

Tsai, H. L., Chu, K. S., Huang, Y. H., Su, Y. C., Wu, J. Y., Kuo, C. H., Chen, C. W., & Wang, J. Y. (2009). Predictive factors of early relapse in UICC stage I-III colorectal cancer patients after curative resection. *Journal of Surgical Oncology*, *100*(8), 736–743. https://doi.org/10.1002/jso.21404

Tu, Y. H., Cooper, A. J., Teng, B., Chang, R. B., Artiga, D. J., Turner, H. N., Mulhall, E. M., Ye, W., Smith, A. D., & Liman, E. R. (2018). An evolutionarily conserved gene family encodes proton-selective ion channels. *Science*, *359*(6379), 1047–1050. https://doi.org/10.1126/science.aao3264

Vuik, F. E. R., Nieuwenburg, S. A. V., Bardou, M., Lansdorp-Vogelaar, I., Dinis-Ribeiro, M., Bento, M. J., Zadnik, V., Pellisé, M., Esteban, L., Kaminski, M. F., Suchanek, S., Ngo, O., Májek, O., Leja, M., Kuipers, E. J., & Spaander, M. C. W. (2019). Increasing incidence of colorectal cancer in young adults in Europe over the last 25 years. *Gut*. https://doi.org/10.1136/gutjnl-2018-317592

Wang, N., Li, X., Wang, R., & Ding, Z. (2021). Spatial transcriptomics and proteomics technologies for deconvoluting the tumor microenvironment. In *Biotechnology Journal* (Vol. 16, Issue 9). John Wiley and Sons Inc. https://doi.org/10.1002/biot.202100041

Weitz, J., Koch, M., Debus, J., Höhler, T., Galle, P. R., & Büchler, M. W. (2005). Colorectal cancer. *Lancet*, *365*(9454), 153–165. https://doi.org/10.1016/S0140-6736(05)17706-X

Xie, Y. H., Chen, Y. X., & Fang, J. Y. (2020). Comprehensive review of targeted therapy for colorectal cancer. In *Signal Transduction and Targeted Therapy* (Vol. 5, Issue 1). Springer Nature. https://doi.org/10.1038/s41392-020-0116-z

Xu, L., Wang, R., Ziegelbauer, J., Wu, W. W., Shen, R.-F., Juhl, H., Zhang, Y., Pelosof, L., & Rosenberg, A. S. (2017). *Transcriptome analysis of human colorectal cancer biopsies reveals extensive expression*

*correlations among genes related to cell proliferation, lipid metabolism, immune response and collagen catabolism*. www.impactjournals.com/oncotarget

Yamanaka, T., Oki, E., Yamazaki, K., Yamaguchi, K., Muro, K., Uetake, H., Sato, T., Nishina, T., Ikeda, M., Kato, T., Kanazawa, A., Kusumoto, T., Chao, C., Lopatin, M., Krishnakumar, J., Bailey, H., Akagi, K., Ochiai, A., Ohtsu, A., … Yoshino, T. (2016). 12-Gene Recurrence Score assay stratifies the recurrence risk in stage II/III colon cancer with surgery alone: The sunrise study. *Journal of Clinical Oncology*, *34*(24), 2906–2913. https://doi.org/10.1200/JCO.2016.67.0414

Yang, H., Jiang, P., Liu, D., Wang, H. Q., Deng, Q., Niu, X., Lu, L., Dai, H., Wang, H., & Yang, W. (2019). Matrix Metalloproteinase 11 Is a Potential Therapeutic Target in Lung Adenocarcinoma. *Molecular Therapy - Oncolytics*, *14*, 82–93. https://doi.org/10.1016/j.omto.2019.03.012

Zhuang, Y., Li, X., Zhan, P., Pi, G., & Wen, G. (2021). MMP11 promotes the proliferation and progression of breast cancer through stabilizing Smad2 protein. *Oncology Reports*, *45*(4). https://doi.org/10.3892/or.2021.7967

# 6. Appendix

## 6.1. dRNA-HybISS optimization protocols

### 6.1.1. Optimization protocol for the detection of *Malat1*

Protocol "D101 HS Library Preparation Kit Protocol FFPE sample" from CARTANA was used

| | |
|---|---|
| **11.08.2020** | **16KS_Optimization 1_Library Preperation on FFPE samples with CARTANA kit and protocol** |

**(1)** first try of the library prep kit from CARTANA | **(2)** Optimize the conditions for the permeabilization (3)testing ISS on tissue |

| | |
|---|---|
| **Goal:** | **detect Malat1 (long non coding RNA) on CRC tissue with the Cartana kit for library preperation** |
| **64KS** | **CRC tissue - Permeabilization: slide was incubated with 0.5mg/ml pepsin in PS at 37^C for 30mins** |
| **65KS** | **CRC tissue - Permeabilization: slide was incubated with 0.5mg/ml pepsin in PS at 37^C for 10mins** |
| **66KS** | **CRC tissue - Permeabilization: slide was incubated Citrate buffer at 93°C for 45mins in a microwave** |
| **67KS** | **CRC tissue - Permeabilization: slide was incubated Citrate buffer at 93°C for 45mins in a cooking steamer** |



## HS Library Preparation on FFPE samples

### Step 1: Dehydration and Permeabilization

1. **Deparaffinization:**
   a. Bake sections in 60°C oven for **one hour** to prepare for deparaffinization.
   b. Incubate slides in fresh **xylene** for **7 min** at room temperature (if using a xylene substitute, increase incubation to **15 min**).
   c. Repeat Step 1.1.b. with fresh **xylene** and incubate for **7 min** at room temperature (if using a xylene substitute, increase the incubation to **15 min**).
2. **Rehydration:**
   a. Incubate slides in **100% EtOH** for **5 min** at room temperature.
   b. Incubate slides in **70% EtOH** for **5 min** at room temperature.
   c. Incubate slides in **DEPC treated MQ $H_2O$** for **2 min** at room temperature.
3. Wash slides in **WB1** for **1 min**.
4. **Permeabilization:**
   Incubate slides in 0.5 mg/mL pepsin in PS at room temperature for **5-60 min**.
   OR
   Incubate slides in Citrate Buffer pH 6.0 for **30 min** at **95-99°C** in a steamer or on a hot plate (refer to HS Library Preparation Kit Tips and Guidelines (D082) for additional information).

   These conditions might require optimization depending on sample types and fixation conditions

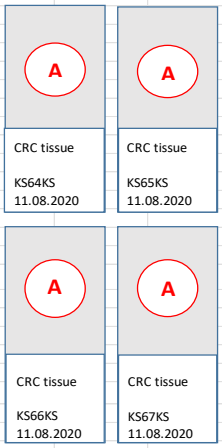


5. Wash slides twice in fresh **WB1** (different containers) at room temperature.
6. **Ethanol series:** dip slides into 70% EtOH for **2 min**, and then 100% EtOH for **2 min**.
7. Air dry the samples for **5 min**.
8. Apply **SecureSeal™** chambers over each tissue section (or draw a Pap pen barrier around them, see General Guidelines above).

### Step 2: Probe Hybridization

9. **Rehydration:** Thaw **WB3**, make sure there is no precipitate in the mix (if so, incubate briefly at 37°C and vortex again).
10. Add 100 µL **WB3** to each SecureSeal™ chamber while preparing Step 2.11 (do not incubate in WB3 longer than 10 minutes).
11. Prepare the Reaction Mix 1. Below are volumes for one SecureSeal™ chamber:
    a. Thaw **RM1**. Vortex briefly and spin down.
    b. Mix in an RNase free Eppendorf tube:
       80.0 µL **RM1**
       20.0 µL **Probes**
    c. Mix gently by pipetting up and down.
12. Remove WB3 and add 100 µL **RM1-mix** to each tissue section. Place the slides in a RNAse free humidity chamber and incubate **overnight** at 37°C.

## Step 3: Probe Ligation

13. Thaw **WB4,** mix and vortex gently.
14. Aspirate and discard the **RM1-mix** from the SecureSeal™ chamber and wash twice with 100 µL **WB2**.
15. Apply 100 µL of **WB4** to each section and incubate at 37°C for **30 min**.
16. Wash three times with 100 µL **WB2**, but leave the last wash inside until step 3.17 is prepared.
17. Prepare Reaction Mix 2. Below are volumes for one SecureSeal™ chamber:
    a. Thaw **RM2**, Vortex and spin-down.
    b. Mix in an RNase free Eppendorf tube:
       92.5 µL **RM2**
       2.5 µL **Enzyme 1**
       5.0 µL **Enzyme 2**
    c. Mix gently by pipetting up and down and quickly spin down.
18. Remove **WB2** and add 100 µL of **RM2-mix** to each tissue section. Place the slides in a RNAse free humidity chamber and incubate at 37°C for **2 hours.**
19. Wash twice with 100 µL **WB2** but leave the last wash inside the secure seal until step 4.20a is prepared.

## Step 4: Amplification

20. Prepare the Amplification mix.
    ⚠ It is recommended to precisely follow these steps, and to proceed swiftly since any delay may reduce performance
    Below are volumes for one SecureSeal™ chamber:
    a. Thaw **RM3**. Vortex and spin down. Transfer to an Eppendorf tube:
       90 µL **RM3**
    b. Remove **WB2** from the Secure seals.
    c. Transfer 10 µL of **Enzyme 3** to the Eppendorf tube containing **RM3**
    d. Mix gently.
21. Add 100 µL **RM3-mix** to each tissue section. Place the slides in a RNAse free humidity chamber and incubate **overnight** at 30°C.

## Step 5: Fluorescent Labeling

1. Wash three times with 100 µL **WB2**.
2. Prepare the Labeling Mix (**LM**) (which includes DAPI for nuclei counterstaining). Below are volumes for one SecureSeal™ chamber:
   a. Thaw **LM**. Vortex and spin down.
   b. Add 100 µL **LM** to each SecureSeal™ chamber.
3. Incubate at room temperature for **30 min** kept in the dark.
4. Wash three times with 100 µL **WB2**.
5. Remove SecureSeal™ chambers by dipping the slides for 20 seconds in 70% EtOH (make sure to fill each chamber) and then carefully remove the seal by pulling from the corner with a tweezer.
6. **Ethanol series:** dip slides into 70% EtOH solution for **2 min**, and then 100% EtOH for **2 min**.
7. Air dry the samples for ~5 min protecting in the dark.
8. Apply 10 µL Mounting Medium to the center of each section and carefully apply a cover slip (see General Guidelines above).

## 6.1.2. Optimization protocol for the dectection of *RPLP0*

Protocol "D101 HS Library Preparation Kit Protocol FFPE sample" from CARTANA was used

| | |
|---|---|
| **11.08.2020** | **16KS_Optimization 1_Library Preperation on FFPE samples with CARTANA kit and protocol** |

**(1)** first try of the library prep kit from CARTANA | **(2)** Optimize the conditions for the permeabilization (3)testing ISS on tissue |

| | |
|---|---|
| **Goal:** | **detect RPLP0 (low expressing gene) on CRC tissue with the Cartana kit for library preperation** |
| **68KS** | **CRC tissue - Permeabilization: slide was incubated with 0.5mg/ml pepsin in PS at 37^C for 30mins** |
| **69KS** | **CRC tissue - Permeabilization: slide was incubated with 0.5mg/ml pepsin in PS at 37^C for 10mins** |
| **70KS** | **CRC tissue - Permeabilization: slide was incubated Citrate buffer at 93°C for 45mins in a microwave** |
| **71KS** | **CRC tissue - Permeabilization: slide was incubated Citrate buffer at 93°C for 45mins in a cooking steamer** |



### HS Library Preparation on FFPE samples

#### Step 1: Dehydration and Permeabilization

1. **Deparaffinization:**
   a. Bake sections in 60°C oven for **one hour** to prepare for deparaffinization.
   b. Incubate slides in fresh **xylene** for **7 min** at room temperature (if using a xylene substitute, increase incubation to **15 min**).
   c. Repeat Step 1.1.b. with fresh **xylene** and incubate for **7 min** at room temperature (if using a xylene substitute, increase the incubation to **15 min**).
2. **Rehydration:**
   a. Incubate slides in **100% EtOH** for **5 min** at room temperature.
   b. Incubate slides in **70% EtOH** for **5 min** at room temperature.
   c. Incubate slides in **DEPC treated MQ $H_2O$** for **2 min** at room temperature.
3. Wash slides in **WB1** for **1 min**.
4. **Permeabilization:**
   Incubate slides in 0.5 mg/mL pepsin in PS at room temperature for **5-60 min**.
   OR
   Incubate slides in Citrate Buffer pH 6.0 for **30 min** at **95-99°C** in a steamer or on a hot plate (refer to HS Library Preparation Kit Tips and Guidelines (D082) for additional information).

Fo
Fo
Fo
Fo

⚠ These conditions might require optimization depending on sample types and fixation conditions

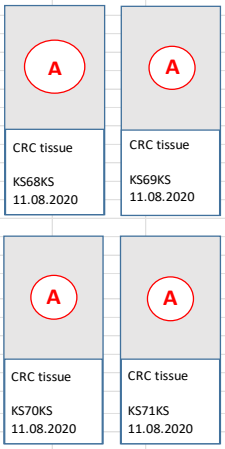


5. Wash slides twice in fresh **WB1** (different containers) at room temperature.
6. **Ethanol series:** dip slides into 70% EtOH for **2 min**, and then 100% EtOH for **2 min**.
7. Air dry the samples for **5 min**.
8. Apply **SecureSeal™** chambers over each tissue section (or draw a Pap pen barrier around them, see General Guidelines above).

#### Step 2: Probe Hybridization

9. **Rehydration:** Thaw **WB3**, make sure there is no precipitate in the mix (if so, incubate briefly at 37°C and vortex again).
10. Add 100 µL **WB3** to each SecureSeal™ chamber while preparing Step 2.11 (do not incubate in WB3 longer than 10 minutes).
11. Prepare the Reaction Mix 1. Below are volumes for one SecureSeal™ chamber:
    a. Thaw **RM1**. Vortex briefly and spin down.
    b. Mix in an RNase free Eppendorf tube:
       80.0 µL **RM1**
       20.0 µL **Probes**
    c. Mix gently by pipetting up and down.
12. Remove WB3 and add 100 µL **RM1-mix** to each tissue section. Place the slides in a RNAse free humidity chamber and incubate **overnight** at 37°C.

# 6.2. Protocol for testing the exposure times

**15.02.2021** **32KS_Exposure time test for Olymous**

**(1)** strip and rehybridize detection olgios | **(2)** Find best exposure time for each channel

**Stripping:**

Dip slide in 70 % EtOH and remove coverslip
EtOH series 70%, 85% & 100% for 2 minutes
Air dry samples for 5 min protecting in the dark.
mount secure seals (eg.: 50 µl ) per spot or use a pap pen
Add 50 µl 1xDEPC-PBS-Tween to each section for a 1 min wash, then remove 1xDEPC-PB
Next steps should be carried out in a laminar flow hood:
Add 50 µl 100% Formamide, incubate for 1 min at room temperature.
Repeat this step two more times.
Cover section with 50 µl 1xDEPC-PBS-Tween and incubate at room temperature.
Repeat this step one more time.

before stripping

| Transcript | | backbone |
|---|---|---|
| Nuclei | DAPI | |
| AR-V7 | TR | Lin16 |
| AR-FL | cy3 | Lin33 |
| PSA | Atto488 | B2DO |
| EPCAM | cy7 | Neu_18 |
| KRT8 | cy5 | Lei17 |

after stripping

| Backbone | Detectio | channel |
|---|---|---|
| Lei17 | | |
| Lei17 | D0033 | Cy7 |
| Lei17 | D0041 | Cy3 |
| Lei17 | D0032 | Atto488 |
| Lei17 | D0036 | Atto425 |
| Lei17 | D0043 | Cy5 |
| Lei17 | D0042 | TR |

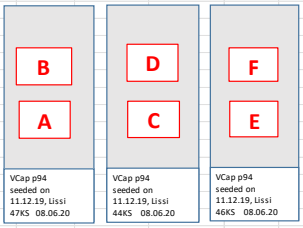


| | | | | | | | | A | B | C |
|---|---|---|---|---|---|---|---|---|---|---|
| | Master Mix folds: | | | | | | | 1 | 1 | |
| **Number** | **Detection probe hybridisation** | **channel** | **stock** | | **final** | | **1x [µl]** | **MM** | | |
| | 2xHyb buffer | | 2 | x | 1 | x | 25 | 25 | 25 | 25 |
| D0033 | Lei_17_Cy7 | Cy7 | 10 | µM | 0,1 | µM | 0,5 | 0,5 | | |
| D0041 | Lei_17_Cy3 | Cy3 | 10 | µM | 0,1 | µM | | | 0,5 | |
| D0032 | Lei_17_Atto488 | Atto488 | 10 | µM | 0,1 | µM | | | | 0,5 |
| D0036 | Lei_17_Atto425 | Atto425 | 10 | µM | 0,1 | µM | | | | |
| D0043 | Lei_17_Cy5 | Cy5 | 10 | µM | 0,1 | µM | | | | |
| D0042 | Lei_17_TR | TR | 10 | µM | 0,1 | µM | | | | |
| | DAPI (vortex before use!) | | 100 | µg/ml | 2 | µg/ml | 1 | 1 | 1 | 1 |
| | DEPC $H_20$ | | | | | | 23,5 | 23,5 | 23,5 | 23,5 |
| | **Volume** | | | | 50 | | 50 | 50 | 50 | 50 |
| | each sample (1x) | | | | | | | | | |

| | | | | | | | | D | E | F |
|---|---|---|---|---|---|---|---|---|---|---|
| | Master Mix folds: | | | | | | | 1 | 1 | |
| **Number** | **Detection probe hybridisation** | **channel** | **stock** | | **final** | | **1x [µl]** | | | |
| | 2xHyb buffer | | 2 | x | 1 | x | 25 | 25 | 25 | 25 |
| D0033 | Lei_17_Cy7 | Cy7 | 10 | µM | 0,1 | µM | 0,5 | | | |
| D0041 | Lei_17_Cy3 | Cy3 | 10 | µM | 0,1 | µM | | | | |
| D0032 | Lei_17_Atto488 | Atto488 | 10 | µM | 0,1 | µM | | | | |
| D0036 | Lei_17_Atto425 | Atto425 | 10 | µM | 0,1 | µM | | 0,5 | | |
| D0043 | Lei_17_Cy5 | Cy5 | 10 | µM | 0,1 | µM | | | 0,5 | |
| D0042 | Lei_17_TR | TR | 10 | µM | 0,1 | µM | | | | 0,5 |
| | DAPI (vortex before use!) | | 100 | µg/ml | 2 | µg/ml | 1 | 1 | 1 | 1 |
| | DEPC $H_20$ | | | | | | 23,5 | 23,5 | 23,5 | 23,5 |
| | **Volume** | | | | 50 | | 50 | 50 | 50 | 50 |
| | each sample (1x) | | | | | | | | | |

**From now on protect slides from light**
Apply tapes
37°C for 30min
2 washes 1xDEPC-PBS-Tween for 2 min each

ensure that the position of cells is marked by crystal pen, then remove the seal

EtOH series (2min in 70, 85 and 98%)
Air dry the slides (5-10min)
For Slides
Mount with 20-60µl slow fade Gold Antifdade reagent
24x55 mm coverslip

# 6.3. Protocol for H&E staining

## 6.3.1. Protocol for H&E staining I

**20.06.2022** **Exp63KS_Cutting CRC tissue and H+E staining to localize the tumor site**

**(1)** Cutting CRC tissue and H+E staining to localize the tumor site

Protocol by Katja Sallinger. Adapted from CARTANA

5 tissue blocks (early CRC tissue) were cut with the microtome with a diameter of 5 µm.

1 slide from each block was cut for H+E staining the rest of the slides were stored at -80°C

From each block 5 slides were cut for Stefan Kühberger und will perform NGS of the tumor tissue. (Humangenetik)

**2x 4 cosecutive slides were cut of each block:** On the first slide ISS with the Immune panel will be perfromed

On the second slide ISS with the Katja panel will be performed.

And the third slide will be used for the mutation detection.

The following tissue blocks were used:

| |
|---|
| eCRC-5 |
| eCRC-7 |
| eCRC-8 |
| eCRC-9 |
| eCRC-13 |
| WEST1 |
| EL2 |
| EL3 |
| EL4 |
| EL5 |
| EL6 |

DDetails to the tissue blocks can be found under: C:\Users\Kitty\Nextcloud\Forschungsgruppe El-Heliebi\In situ Sequencing for all\CRC patient samples

H/E staining was performing as it is described in the protocol at our institue:

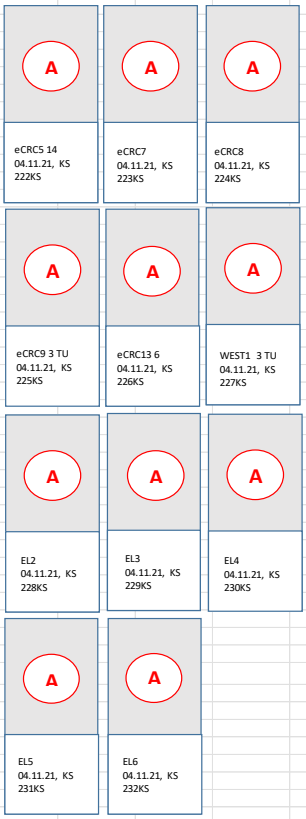


Medizinische Universität Graz | Gottfried Schatz Forschungszentrum | Lehrstuhl für Zellbiologie, Histologie und Embryologie

**HE Färbung - Paraffinschnitt**

| | | |
|---|---|---|
| Erstellt von: | Astrid Blaschitz, Sabine Richter | am: 05.11.2014 |
| Überarbeitet von: | Monika Siwetz | am: 07.06.2021 |

| **FÄRBEREIHE im Raum FI02I19 / 355D** | |
|---|---|
| **Entparaffinieren / Entwässern** | |
| HistoLab Clear 1a, 1b | Je 5 min (gesamt 10 min) |
| HistoLab Clear 2a, 2b | Je 5 min (gesamt 10 min) |
| HistoLab Clear /100% Ethanol 1:1 | Schwenken, auf Papierhandtüchern abrinnen lassen |
| 100% Ethanol | Schwenken, auf Papierhandtüchern abrinnen lassen |
| 96% Ethanol | Schwenken, auf Papierhandtüchern abrinnen lassen |
| 70% Ethanol | Schwenken, auf Papierhandtüchern abrinnen lassen |
| 50% Ethanol | Schwenken, auf Papierhandtüchern abrinnen lassen |
| A. dest. | 3 Chargen |
| **Färben** | |
| Saures Hämalaun.nach Mayer (selbst hergestellt lt. Romeis) | 10 min |
| A.dest. | 2 – 3 x wechseln bis keine Farbe herausgeht |
| Ammoniumwasser ($NH_3$) Wasser 2,5 ml Ammoniak / 1l A. dest. | einige Sekunden - bis Kerne blau |
| A.dest. | 2 x wechseln |
| Eosin gelblich 1 % (selbst hergestellt) | 5 sec – 60 min |
| 96% Ethanol 1 | Kurz differenzieren |
| 96% Ethanol 2 | Kurz differenzieren |
| 100% Ethanol | Kurz |
| HistoLab Clear /100% Ethanol 1:1 | Kurz |
| HistoLab Clear 2b | mindestens 10 min |
| permanent eindeckeln | trocknen lassen |

Verwendete Objektträgerständer über die absteigende Alkoholreihe ins A.dest. bringen. Ständer unter A.dest. Leitung gründlich spülen, zum Trocknen auf das Tablett neben dem Abzug stellen. Saubere und trockene Ständer in den Abzug zurückräumen. A.dest.-Küvetten entleeren, gut spülen und mit frischem A.dest. auffüllen.
Verschmutzte Alkohole (96% Ethanol 1 und 2) in Abfallkanister entsorgen.

HE Färbeprotokoll für Paraffinschnitt.docx Seite 1/1

## 6.3.2. Protocol for H&E staining II

**30.08.2022** **Exp65KS_Cutting CRC tissue and H+E staining to localize the tumor site**

**(1)** Cutting CRC tissue and H+E staining to localize the tumor site

Protocol by Katja Sallinger. Adapted from CARTANA

5 tissue blocks (early CRC tissue) were cut with the microtome with a diameter of 5 µm.

1 slide from each block was cut for H+E staining the rest of the slides were stored at -80°C

From each block 5 slides were cut for Stefan Kühberger und will perform NGS of the tumor tissue. (Humangenetik)

**2x 4 cosecutive slides were cut of each block:** On the first slide ISS with the Immune panel will be perfromed

On the second slide ISS with the Katja panel will be performed.

And the third slide will be used for the mutation detection.

The following tissue blocks were used:

| |
|---|
| eCRC28 |
| eCRC32 |
| eCRC33 |
| eCRC37 |
| el.eCRC-12 |
| el.eCRC-13 |
| West.eCRC3 |
| West.eCRC7 |
| West.eCRC8 |
| West.eCRC12 |
| West.eCRC16 |
| West.eCRC17 |

DDetails to the tissue blocks can be found under: C:\Users\Kitty\Nextcloud\Forschungsgruppe El-Heliebi\In situ Sequencing for all\CRC patient samples

H/E staining was performing as it is described in the protocol at our institue:

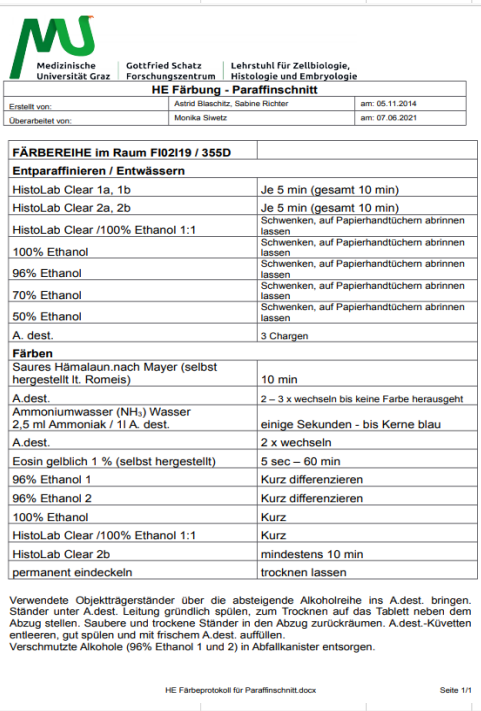

Medizinische Universität Graz | Gottfried Schatz Forschungszentrum | Lehrstuhl für Zellbiologie, Histologie und Embryologie

**HE Färbung - Paraffinschnitt**

| | | |
|---|---|---|
| Erstellt von: | Astrid Blaschitz, Sabine Richter | am: 05.11.2014 |
| Überarbeitet von: | Monika Siwetz | am: 07.06.2021 |

| **FÄRBEREIHE im Raum FI02I19 / 355D** | |
|---|---|
| **Entparaffinieren / Entwässern** | |
| HistoLab Clear 1a, 1b | Je 5 min (gesamt 10 min) |
| HistoLab Clear 2a, 2b | Je 5 min (gesamt 10 min) |
| HistoLab Clear /100% Ethanol 1:1 | Schwenken, auf Papierhandtüchern abrinnen lassen |
| 100% Ethanol | Schwenken, auf Papierhandtüchern abrinnen lassen |
| 96% Ethanol | Schwenken, auf Papierhandtüchern abrinnen lassen |
| 70% Ethanol | Schwenken, auf Papierhandtüchern abrinnen lassen |
| 50% Ethanol | Schwenken, auf Papierhandtüchern abrinnen lassen |
| A. dest. | 3 Chargen |
| **Färben** | |
| Saures Hämalaun nach Mayer (selbst hergestellt lt. Romeis) | 10 min |
| A.dest. | 2 – 3 x wechseln bis keine Farbe herausgeht |
| Ammoniumwasser ($NH_3$) Wasser 2,5 ml Ammoniak / 1l A. dest. | einige Sekunden - bis Kerne blau |
| A.dest. | 2 x wechseln |
| Eosin gelblich 1 % (selbst hergestellt) | 5 sec – 60 min |
| 96% Ethanol 1 | Kurz differenzieren |
| 96% Ethanol 2 | Kurz differenzieren |
| 100% Ethanol | Kurz |
| HistoLab Clear /100% Ethanol 1:1 | Kurz |
| HistoLab Clear 2b | mindestens 10 min |
| permanent eindeckeln | trocknen lassen |

Verwendete Objektträgerständer über die absteigende Alkoholreihe ins A.dest. bringen. Ständer unter A.dest. Leitung gründlich spülen, zum Trocknen auf das Tablett neben dem Abzug stellen. Saubere und trockene Ständer in den Abzug zurückräumen. A.dest.-Küvetten entleeren, gut spülen und mit frischem A.dest. auffüllen.
Verschmutzte Alkohole (96% Ethanol 1 und 2) in Abfallkanister entsorgen.

HE Färbeprotokoll für Paraffinschnitt.docx Seite 1/1

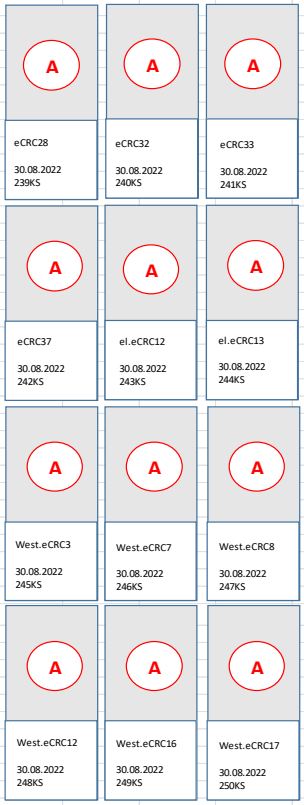

# 6.4. dRNA-HybISS fusion protocols

## 6.4.1. dRNA-HybISS fusion protocols I

**30.12.2021** **Exp54KS_In Situ sequencing on Fusion sildes with Katja panel_part 1**

**(1)** perform ISS with CARTANA Katja panel on Fusion slides
Protocol by Katja Sallinger. Adapted from CARTANA

**experiment design & protocol: Katja Sallinger**
**lab work: Karin and Lissi**
**scanning: Karin and Lissi (Katja assist)**
**data analysis: Katja Sallinger**

scanning instructions:
* XY-shift calibration: not necessary - spectrasplit filters are **NOT** used when performing sequencing!!!
* switch channel before moving XY
* avoid overexposure in all channels including DAPI
* scan ~ 8mm diameter spot, 40x objective, EFI

* save scans here >>> W:\Images\Katja Sallinger\exp54KS
* file names >>> slideID
* convert to TIFF: 2x2 binning, no tiling

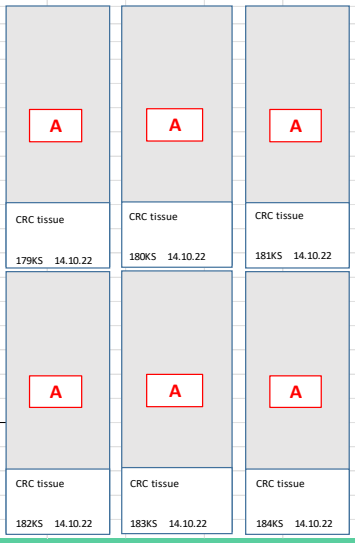


**Comments:**
no QP (quenching of some genes) necessary with Katja panel!
please start with AP2 cycle when performing the sequencing cycles and perform AP1 after AP6!

**DAY 1**

**Step 1: Dehydration and Permeabilization**

A..Katja panel

**Deparaffinization:**
Bake sections in 60°C oven for one hour to prepare for deparaffinization
Incubate slides in Tissue clear 1A for 5 mins
Incubate slides in Tissue clear 1B for 5 mins
Incubate slides in Tissue clear 2A for 5 mins
Incubate slides in Tissue clear 2B for 5 mins

**tick when done:**

| AP2 | AP3 | AP4 | AP5 | AP6 | AP1 | BG | LM |
|---|---|---|---|---|---|---|---|
| | | | | | | | |

**Rehydration:**
Incubate slides in 100% EtOH for 2 mins
Incubate slides in 95% EtOH for 2 mins
Incubate slides in 70% EtOH for 2 mins
Incubate slides in DEPC-H2O for 2 mins
Incubate slides in DEPC-PBS for 2 mins

**Permeabilization:**
Incubate slides in citrate buffer pH=6 for 45 mins in a steamer (95-99°C)
Incubate slides in DEPC-H2O for 5 mins
Incubate slides in DEPC-PBS for 2 mins
EtOH series 70%, 85% & 100% for 2 minutes
mount secure seals (eg.: 50 µl ) per spot

**Step 2: Probe Hybridization**

Rehydration: Thaw WB3 and add 50 µl WB3 to each secure seal chamber while preparing the next steps, but do not incubate in WB3 longer than 10 minutes!!
(if performing the optimization step:
Prepare the reaction mix 1: Thaw RM1 and mix in an Rnase free Eppi: 40 µl RM1 and 10µl of the probes. Mix gently by pippeting up and down.)
**if preparing the gene panel:**

| | | | | spot A | spot B |
|---|---|---|---|---|---|
| Master Mix folds: | | | | 6 | 0 |
| **Prehybridization 1** | **concentration** | | **1x [µl]** | **MM1** | **MM1** |
| Placenta gene panel | 20 | x | 2,5 | | 0,00 |
| Immune panel I1A 0.1 | 20 | x | 2,5 | | 0,00 |
| Immune panel I2B 0.1 | 20 | x | 2,5 | | 0,00 |
| Katja gene panel | 20 | x | 2,5 | 15,00 | |
| **Buffer A** | | | | **120,00** | **0,00** |
| Final Volume | **20** | | **20** | **120,00** | **0,00** |
| each sample (1x) | | | | | |

Mix gently by pippeting up and down.

Prepare the reaction mix 1:
Thaw RM1 and mix in an Rnase free Eppi:

| | | spot A | spot B |
|---|---|---|---|
| Master Mix folds: | | 6 | 0 |
| **Prehybridization 2** | **1x [µl]** | **MM1** | **MM1** |
| RM1 | 30 | 180,00 | 0,00 |
| diluted gene panels | 20 | 120,00 | 0,00 |
| **Final Volume** | **50** | **300,00** | **0,00** |
| each sample (1x) | 50 | | |

Mix gently by pippeting up and down.
Remove WB3 and add 50 µl RM1-mix to each tissue section.
Place slides in a RNAse free humidity chamber and incubate overnight at 37°C.

## DAY 2

### Step 3: Probe Ligation

Thaw WB4, mix and vortex gently
Aspirate and discard RM1-mix from secure seal chamber and wash twice with 50 µl WB2
Apply 50µl of WB4 to each section and incubate at 37°C for 30 mins.
Wash three times with WB2, but leave the last wash inside until the next reaction mix is prepared.
Prepare reaction mix 2:
Thaw RM2, Vortex and spin down.

| | | spots |
|---|---|---|
| Master Mix folds: | | 6 |
| **Prehybridization 1** | **1x [µl]** | **MM1** |
| RM2 | 46,25 | 277,50 |
| Enzyme 1 | 1,25 | 7,50 |
| Enzyme 2 | 2,5 | 15,00 |
| **Final Volume** | **50** | **300,00** |
| each sample (1x) | **50** | |

Mix gently by pippeting up and down and spin down.
Remove WB2 and add 50 µl of the RM2-mix to each section.
Place slides in a RNAse free humidity chamber and incubate for 2 hours at 37°C.
Wash two times with WB2, but leave the last wash inside until the next reaction mix is prepared.

### Step 4: Amplification

Prepare reaction mix 3:
Thaw RM3. Vortex and spin down.

| | | spots |
|---|---|---|
| Master Mix folds: | | 6 |
| **Prehybridization 1** | **1x [µl]** | **MM1** |
| RM3 | 45 | 270,00 |
| Enzyme 3 | 5 | 30,00 |
| **Final Volume** | **50** | **300,00** |
| each sample (1x) | **50** | |

Remove WB2 from the secure seal.
Transfer 5 µl (per reaction) of Enzyme 3 to the Eppi with RM3.
Mix gently.
Add 50 µl RM3-mix to each section.
Place slides in a RNAse free humidity chamber and incubate overnight at 30°C.

## DAY 3

### Step 5: Fluorescent labeling

Wash three times with 50 µl WB2.
Prepare the labeling mix (LM):
Thaw LM. Vortex and spin down
Add 50 µl to each secure seal
Incubate at room temperature for 30 mins kept in the dark.
Wash three times with 50 µl WB2.
Remove secure seal chambers.
EtOH series 70%, 85% & 100% for 2 minutes
Air dry samples for 5 min protecting in the dark.
Apply 5-10 µl mounting medium to the center of each section and apply cover slip.

## DAY 4

### Step 6: Stripping

Put slide in DEPC-PBS till coverslip falls off.
EtOH series 70%, 85% & 100% for 2 minutes .
Air dry samples for 5 min protecting in the dark.
mount secure seals (eg.: 50 µl ) per spot or use a pap pen
Add 50 µl WB2 to each section for a 1 min wash, then remove WB2.
Next steps should be carried out in a laminar flow hood:
Add 50 µl 100% Formamide, incubate for 1 min at room temperature.
Repeat this step two more times.
Cover section with 50 µl WB2 and incubate at room temperature.
Repeat this step one more time.

### Step 7: Quenching: not performed

### Step 8: Hybridization and Quenching Sequencing

For each section prepare AP mix in an Eppi and mix gently by slow vortexing:

| | | spot A | spot B |
|---|---|---|---|
| Master Mix folds: | | 6 | |
| **Prehybridization 1** | **1x [µl]** | **MM1** | |
| Buffer A | 45 | 270,00 | |
| Apx | 5 | 30,00 | |
| QP | 0,5 | 0,00 | |
| **Final Volume** | **50** | **300,00** | |
| each sample (1x) | **50** | | |

(it is essential to document which AP is used in each sequencing cycle.)

(Incubate the AP-QP Mix at 37°C for 15mins.(
Remove WB2 from each section and add AP mix
Place slide at 37°C for 1 hour.
Remove AP mix and quickly wash twice with 50 µlWB2 for 1 min.

**Now work in the dark!!!**
For each section prepare SP mix in an Eppi and mix gently by slow vortexing:

| | | spots |
|---|---|---|
| Master Mix folds: | | 6 |
| **Prehybridization 1** | **1x [µl]** | **MM1** |
| Buffer A | 45 | 270,00 |
| SPx | 5 | 30,00 |
| **Final Volume** | **50** | **300,00** |
| each sample (1x) | **50** | |

(SP mix is the same for all sequencing cycles but needs to be prepared fresh for each cycle.)
Remove WB2 from each section and add SP mix
Place slide at 37°C for 30 mins.
Remove SP mix and quickly wash twice with 50 µlWB2 for 1 min.
EtOH series 70%, 85% & 100% for 2 minutes
Air dry samples for 5 min protecting in the dark.
Apply 5-10 µl mounting medium to the center of each section and apply cover slip.

Repeat Step 6-8 with appropriate AP mix until all six cycles have been performed.

## 6.4.2. dRNA-HybISS fusion protocol II

**07.02.2022** **Exp55KS_In Situ sequencing on Fusion sildes with Katja panel_part 2**

**(1)** perform ISS with CARTANA Katja panel on Fusion slides

Protocol by Katja Sallinger. Adapted from CARTANA

**experiment design & protocol: Katja Sallinger**

**lab work: Karin and Lissi**

**scanning: Karin and Lissi (Katja assist)**

**data analysis: Katja Sallinger**

scanning instructions:

* XY-shift calibration: not necessary - spectrasplit filters are **NOT** used when performing sequencing!!!

* switch channel before moving XY

* avoid overexposure in all channels including DAPI

* scan ~ 8mm diameter spot, 40x objective, EFI

* save scans here >>> W:\Images\Katja Sallinger\exp54KS

* file names >>> slideID

* convert to TIFF: 2x2 binning, no tiling

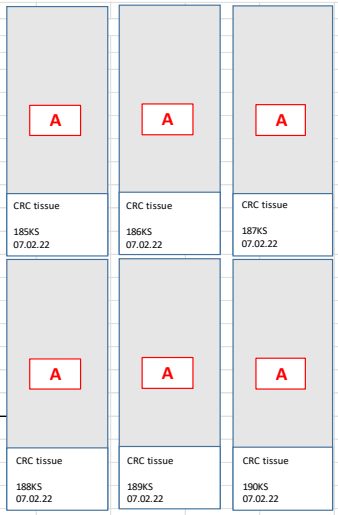


**Comments:**

no QP (quenching of some genes) necessary with Katja panel!

please start with AP2 cycle when performing the sequencing cycles and perform AP1 after AP6!

**DAY 1**

### Step 1: Dehydration and Permeabilization

A..Katja panel

**Deparaffinization:**

Bake sections in 60°C oven for one hour to prepare for deparaffinization

Incubate slides in Tissue clear 1A for 5 mins

Incubate slides in Tissue clear 1B for 5 mins

Incubate slides in Tissue clear 2A for 5 mins

Incubate slides in Tissue clear 2B for 5 mins

**tick when done:**

| **Rehydration:** | AP2 | AP3 | AP4 | AP5 | AP6 | AP1 | BG | LM |
|---|---|---|---|---|---|---|---|---|
| Incubate slides in 100% EtOH for 2 mins | | | | | | | | |
| Incubate slides in 95% EtOH for 2 mins | | | | | | | | |
| Incubate slides in 70% EtOH for 2 mins | | | | | | | | |
| Incubate slides in DEPC-H2O for 2 mins | | | | | | | | |
| Incubate slides in DEPC-PBS for 2 mins | | | | | | | | |

**Permeabilization:**

Incubate slides in citrate buffer pH=6 for 45 mins in a steamer (95-99°C)

Incubate slides in DEPC-H2O for 5 mins

Incubate slides in DEPC-PBS for 2 mins

EtOH series 70%, 85% & 100% for 2 minutes

mount secure seals (eg.: 50 µl ) per spot

### Step 2: Probe Hybridization

Rehydration: Thaw WB3 and add 50 µl WB3 to each secure seal chamber while preparing the next steps, but do not incubate in WB3 longer than 10 minutes!!

(if performing the optimization step:

Prepare the reaction mix 1: Thaw RM1 and mix in an Rnase free Eppi: 40 µl RM1 and 10µl of the probes. Mix gently by pippeting up and down.)

**if preparing the gene panel:**

| | | | | spot A | spot B |
|---|---|---|---|---|---|
| Master Mix folds: | | | | 6 | 0 |
| **Prehybridization 1** | **concentration** | | **1x [µl]** | **MM1** | **MM1** |
| Placenta gene panel | 20 | x | 2,5 | | 0,00 |
| Immune panel I1A 0.1 | 20 | x | 2,5 | | 0,00 |
| Immune panel I2B 0.1 | 20 | x | 2,5 | | 0,00 |
| Katja gene panel | 20 | x | 2,5 | 15,00 | |
| **Buffer A** | | | | **120,00** | **0,00** |
| Final Volume | **20** | | **20** | **120,00** | **0,00** |
| each sample (1x) | | | | | |

Mix gently by pippeting up and down.

Prepare the reaction mix 1:

Thaw RM1 and mix in an Rnase free Eppi:

| | | spot A | spot B |
|---|---|---|---|
| Master Mix folds: | | 6 | 0 |
| **Prehybridization 2** | **1x [µl]** | **MM1** | **MM1** |
| RM1 | 30 | 180,00 | 0,00 |
| diluted gene panels | 20 | 120,00 | 0,00 |
| **Final Volume** | **50** | **300,00** | **0,00** |
| each sample (1x) | 50 | | |

Mix gently by pippeting up and down.

Remove WB3 and add 50 µl RM1-mix to each tissue section.

Place slides in a RNAse free humidity chamber and incubate overnight at 37°C.

## DAY 2

### Step 3: Probe Ligation

Thaw WB4, mix and vortex gently
Aspirate and discard RM1-mix from secure seal chamber and wash twice with 50 µl WB2
Apply 50µl of WB4 to each section and incubate at 37°C for 30 mins.
Wash three times with WB2, but leave the last wash inside until the next reaction mix is prepared.
Prepare reaction mix 2:
Thaw RM2, Vortex and spin down.

| | | spots |
|---|---|---|
| Master Mix folds: | | 6 |
| **Prehybridization 1** | **1x [µl]** | **MM1** |
| RM2 | 46,25 | 277,50 |
| Enzyme 1 | 1,25 | 7,50 |
| Enzyme 2 | 2,5 | 15,00 |
| **Final Volume** | **50** | **300,00** |
| each sample (1x) | **50** | |

Mix gently by pippeting up and down and spin down.
Remove WB2 and add 50 µl of the RM2-mix to each section.
Place slides in a RNAse free humidity chamber and incubate for 2 hours at 37°C.
Wash two times with WB2, but leave the last wash inside until the next reaction mix is prepared.

### Step 4: Amplification

Prepare reaction mix 3:
Thaw RM3. Vortex and spin down.

| | | spots |
|---|---|---|
| Master Mix folds: | | 6 |
| **Prehybridization 1** | **1x [µl]** | **MM1** |
| RM3 | 45 | 270,00 |
| Enzyme 3 | 5 | 30,00 |
| **Final Volume** | **50** | **300,00** |
| each sample (1x) | **50** | |

Remove WB2 from the secure seal.
Transfer 5 µl (per reaction) of Enzyme 3 to the Eppi with RM3.
Mix gently.
Add 50 µl RM3-mix to each section.
Place slides in a RNAse free humidity chamber and incubate overnight at 30°C.

## DAY 3

### Step 5: Fluorescent labeling

Wash three times with 50 µl WB2.
Prepare the labeling mix (LM):
Thaw LM. Vortex and spin down
Add 50 µl to each secure seal
Incubate at room temperature for 30 mins kept in the dark.
Wash three times with 50 µl WB2.
Remove secure seal chambers.
EtOH series 70%, 85% & 100% for 2 minutes
Air dry samples for 5 min protecting in the dark.
Apply 5-10 µl mounting medium to the center of each section and apply cover slip.

## DAY 4

### Step 6: Stripping

Put slide in DEPC-PBS till coverslip falls off.
EtOH series 70%, 85% & 100% for 2 minutes .
Air dry samples for 5 min protecting in the dark.
mount secure seals (eg.: 50 µl ) per spot or use a pap pen
Add 50 µl WB2 to each section for a 1 min wash, then remove WB2.
Next steps should be carried out in a laminar flow hood:
Add 50 µl 100% Formamide, incubate for 1 min at room temperature.
Repeat this step two more times.
Cover section with 50 µl WB2 and incubate at room temperature.
Repeat this step one more time.

### Step 7: Quenching: not performed

### Step 8: Hybridization and Quenching Sequencing

For each section prepare AP mix in an Eppi and mix gently by slow vortexing:

| | | spot A | spot B |
|---|---|---|---|
| Master Mix folds: | | 6 | |
| **Prehybridization 1** | **1x [µl]** | **MM1** | |
| Buffer A | 45 | 270,00 | |
| Apx | 5 | 30,00 | |
| QP | 0,5 | 0,00 | |
| **Final Volume** | **50** | **300,00** | |
| each sample (1x) | **50** | | |

(it is essential to document which AP is used in each sequencing cycle.)

(Incubate the AP-QP Mix at 37°C for 15mins.(
Remove WB2 from each section and add AP mix
Place slide at 37°C for 1 hour.
Remove AP mix and quickly wash twice with 50 µlWB2 for 1 min.

**Now work in the dark!!!**
For each section prepare SP mix in an Eppi and mix gently by slow vortexing:

| | | spots |
|---|---|---|
| Master Mix folds: | | 6 |
| **Prehybridization 1** | **1x [µl]** | **MM1** |
| Buffer A | 45 | 270,00 |
| SPx | 5 | 30,00 |
| **Final Volume** | **50** | **300,00** |
| each sample (1x) | **50** | |

(SP mix is the same for all sequencing cycles but needs to be prepared fresh for each cycle.)
Remove WB2 from each section and add SP mix
Place slide at 37°C for 30 mins.
Remove SP mix and quickly wash twice with 50 µlWB2 for 1 min.
EtOH series 70%, 85% & 100% for 2 minutes
Air dry samples for 5 min protecting in the dark.
Apply 5-10 µl mounting medium to the center of each section and apply cover slip.

Repeat Step 6-8 with appropriate AP mix until all six cycles have been performed.

## 6.4.3. dRNA-HybISS fusion protocol III

**31.03.2022** **Exp57KS_In Situ sequencing on Fusion sildes with Katja panel_part 3**

**(1)** perform ISS with CARTANA Katja panel on Fusion slides

Protocol by Katja Sallinger. Adapted from CARTANA

**experiment design & protocol: Katja Sallinger**

**lab work: Karin and Lissi**

**scanning: Karin and Lissi (Katja assist)**

**data analysis: Katja Sallinger**

scanning instructions:

* XY-shift calibration: not necessary - spectrasplit filters are **NOT** used when performing sequencing!!!

* switch channel before moving XY

* avoid overexposure in all channels including DAPI

* scan ~ 8mm diameter spot, 40x objective, EFI

* save scans here >>> W:\Images\Katja Sallinger\exp54KS

* file names >>> slideID

* convert to TIFF: 2x2 binning, no tiling

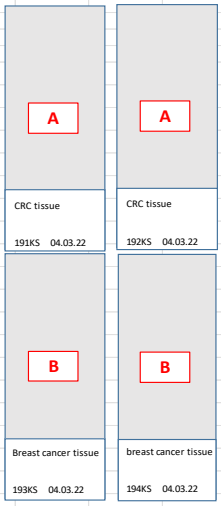


**Comments:**

no QP (quenching of some genes) necessary with Katja panel!

please start with AP2 cycle when performing the sequencing cycles and perform AP1 after AP6!

**DAY 1**

### Step 1: Dehydration and Permeabilization

A.. Katja panel
B... Immunepanel 1A+2B

**Deparaffinization:**

Bake sections in 60°C oven for one hour to prepare for deparaffinization

Incubate slides in Tissue clear 1A for 5 mins

Incubate slides in Tissue clear 1B for 5 mins

Incubate slides in Tissue clear 2A for 5 mins

Incubate slides in Tissue clear 2B for 5 mins

**tick when done:**

| **Rehydration:** | AP1 | AP2 | AP3 | AP4 | AP5 | AP6 | BG | LM |
|---|---|---|---|---|---|---|---|---|
| Incubate slides in 100% EtOH for 2 mins | | | | | | | | |
| Incubate slides in 95% EtOH for 2 mins | | | | | | | | |
| Incubate slides in 70% EtOH for 2 mins | | | | | | | | |
| Incubate slides in DEPC-H2O for 2 mins | | | | | | | | |
| Incubate slides in DEPC-PBS for 2 mins | | | | | | | | |

**Permeabilization:**

Incubate slides in citrate buffer pH=6 for 45 mins in a steamer (95-99°C)

Incubate slides in DEPC-H2O for 5 mins

Incubate slides in DEPC-PBS for 2 mins

EtOH series 70%, 85% & 100% for 2 minutes

mount secure seals (eg.: 50 µl ) per spot

### Step 2: Probe Hybridization

Rehydration: Thaw WB3 and add 50 µl WB3 to each secure seal chamber while preparing the next steps, but do not incubate in WB3 longer than 10 minutes!!

(if performing the optimization step:

Prepare the reaction mix 1: Thaw RM1 and mix in an Rnase free Eppi: 40 µl RM1 and 10µl of the probes. Mix gently by pippeting up and down.)

**if preparing the gene panel:**

| | | | | spot A | spot B |
|---|---|---|---|---|---|
| Master Mix folds: | | | | 2 | 2 |
| **Prehybridization 1** | **concentration** | | **1x [µl]** | **MM1** | **MM1** |
| Placenta gene panel | 20 | x | 2,5 | | 0,00 |
| Immune panel I1A 0.1 | 20 | x | 2,5 | | 5,00 |
| Immune panel I2B 0.1 | 20 | x | 2,5 | | 5,00 |
| Katja gene panel | 20 | x | 2,5 | 5,00 | 5,00 |
| **Buffer A** | | | | **35,00** | **25,00** |
| Final Volume | **20** | | **20** | **40,00** | **40,00** |
| each sample (1x) | | | | | |

Mix gently by pippeting up and down.

Prepare the reaction mix 1:

Thaw RM1 and mix in an Rnase free Eppi:

| | | spot A | spot B |
|---|---|---|---|
| Master Mix folds: | | 2 | 2 |
| **Prehybridization 2** | **1x [µl]** | **MM1** | **MM1** |
| RM1 | 30 | 60,00 | 60,00 |
| diluted gene panels | 20 | 40,00 | 40,00 |
| **Final Volume** | **50** | **100,00** | **100,00** |
| each sample (1x) | 50 | | |

Mix gently by pippeting up and down.

Remove WB3 and add 50 µl RM1-mix to each tissue section.

Place slides in a RNAse free humidity chamber and incubate overnight at 37°C.

## DAY 2

### Step 3: Probe Ligation

Thaw WB4, mix and vortex gently
Aspirate and discard RM1-mix from secure seal chamber and wash twice with 50 µl WB2
Apply 50µl of WB4 to each section and incubate at 37°C for 30 mins.
Wash three times with WB2, but leave the last wash inside until the next reaction mix is prepared.
Prepare reaction mix 2:
Thaw RM2, Vortex and spin down.

| | | spots |
|---|---|---|
| Master Mix folds: | | 6 |
| **Prehybridization 1** | **1x [µl]** | **MM1** |
| RM2 | 46,25 | 277,50 |
| Enzyme 1 | 1,25 | 7,50 |
| Enzyme 2 | 2,5 | 15,00 |
| **Final Volume** | **50** | **300,00** |
| each sample (1x) | **50** | |

Mix gently by pippeting up and down and spin down.
Remove WB2 and add 50 µl of the RM2-mix to each section.
Place slides in a RNAse free humidity chamber and incubate for 2 hours at 37°C.
Wash two times with WB2, but leave the last wash inside until the next reaction mix is prepared.

### Step 4: Amplification

Prepare reaction mix 3:
Thaw RM3. Vortex and spin down.

| | | spots |
|---|---|---|
| Master Mix folds: | | 6 |
| **Prehybridization 1** | **1x [µl]** | **MM1** |
| RM3 | 45 | 270,00 |
| Enzyme 3 | 5 | 30,00 |
| **Final Volume** | **50** | **300,00** |
| each sample (1x) | **50** | |

Remove WB2 from the secure seal.
Transfer 5 µl (per reaction) of Enzyme 3 to the Eppi with RM3.
Mix gently.
Add 50 µl RM3-mix to each section.
Place slides in a RNAse free humidity chamber and incubate overnight at 30°C.

## DAY 3

### Step 5: Fluorescent labeling

Wash three times with 50 µl WB2.
Prepare the labeling mix (LM):
Thaw LM. Vortex and spin down
Add 50 µl to each secure seal
Incubate at room temperature for 30 mins kept in the dark.
Wash three times with 50 µl WB2.
Remove secure seal chambers.
EtOH series 70%, 85% & 100% for 2 minutes
Air dry samples for 5 min protecting in the dark.
Apply 5-10 µl mounting medium to the center of each section and apply cover slip.

## DAY 4

### Step 6: Stripping

Put slide in DEPC-PBS till coverslip falls off.
EtOH series 70%, 85% & 100% for 2 minutes .
Air dry samples for 5 min protecting in the dark.
mount secure seals (eg.: 50 µl ) per spot or use a pap pen
Add 50 µl WB2 to each section for a 1 min wash, then remove WB2.
Next steps should be carried out in a laminar flow hood:
Add 50 µl 100% Formamide, incubate for 1 min at room temperature.
Repeat this step two more times.
Cover section with 50 µl WB2 and incubate at room temperature.
Repeat this step one more time.

### Step 7: Quenching: not performed

### Step 8: Hybridization and Quenching Sequencing

For each section prepare AP mix in an Eppi and mix gently by slow vortexing:

| | | spot A | spot B |
|---|---|---|---|
| Master Mix folds: | | 6 | |
| **Prehybridization 1** | **1x [µl]** | **MM1** | |
| Buffer A | 45 | 270,00 | |
| Apx | 5 | 30,00 | |
| QP | 0,5 | 0,00 | |
| **Final Volume** | **50** | **300,00** | |
| each sample (1x) | **50** | | |

(it is essential to document which AP is used in each sequencing cycle.)

(Incubate the AP-QP Mix at 37°C for 15mins.(
Remove WB2 from each section and add AP mix
Place slide at 37°C for 1 hour.
Remove AP mix and quickly wash twice with 50 µlWB2 for 1 min.

**Now work in the dark!!!**
For each section prepare SP mix in an Eppi and mix gently by slow vortexing:

| | | spots |
|---|---|---|
| Master Mix folds: | | 6 |
| **Prehybridization 1** | **1x [µl]** | **MM1** |
| Buffer A | 45 | 270,00 |
| SPx | 5 | 30,00 |
| **Final Volume** | **50** | **300,00** |
| each sample (1x) | **50** | |

(SP mix is the same for all sequencing cycles but needs to be prepared fresh for each cycle.)
Remove WB2 from each section and add SP mix
Place slide at 37°C for 30 mins.
Remove SP mix and quickly wash twice with 50 µlWB2 for 1 min.
EtOH series 70%, 85% & 100% for 2 minutes
Air dry samples for 5 min protecting in the dark.
Apply 5-10 µl mounting medium to the center of each section and apply cover slip.

Repeat Step 6-8 with appropriate AP mix until all six cycles have been performed.

# 6.5. dRNA-HybISS shedder project protocols

## 6.5.1. dRNA-HybISS shedder project protocol I

**17.05.2022** **Exp61KS_In Situ sequencing on early CRC with all panels on one slide**

**(1)** perform ISS with CARTANA Katja panel +immunepanels +krt18 on early CRC slides

Protocol by Katja Sallinger. Adapted from CARTANA

**experiment design & protocol: Katja Sallinger**

**lab work: Christin**

**scanning: Christin and Lissi (Katja assist)**

**data analysis: Katja Sallinger**

scanning instructions:

* XY-shift calibration: not necessary - spectrasplit filters are **NOT** used when performing sequencing!!!

* switch channel before moving XY

* avoid overexposure in all channels including DAPI

* scan ~ 8mm diameter spot, 40x objective, EFI

* save scans here >>> W:\Images\Katja Sallinger\exp61KS

* file names >>> slideID

* convert to TIFF: 2x2 binning, no tiling

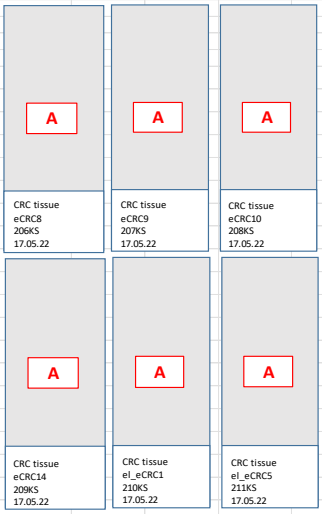


**Comments:**

maybe we need to quench krt18!

For spot A use the old CARTANA kit (which is working)

For spot B use the "new" CARTANA kit, which will probably not work!

**DAY 1**

**Step 1: Dehydration and Permeabilization**

A..Katja panel+immunepanel+krt18 B

| | |
|---|---|
| eCRC8 | Box31, Position 46, Slidenr 18 |
| eCRC9 | Box32, Position 11, Slidenr 17 |
| eCRC10 | Box29, Position 35, Slidenr 2 |
| eCRC14 | Box30, Position 5, Slidenr 6 |
| el-eCRC1 | Box29, Position 23, Slidenr 4 |
| el-eCRC5 | Box33, Position 37, Slidenr 11 |

**Deparaffinization:**

Bake sections in 60°C oven for one hour to prepare for deparaffinization

Incubate slides in Tissue clear 1A for 5 mins

Incubate slides in Tissue clear 1B for 5 mins

Incubate slides in Tissue clear 2A for 5 mins

Incubate slides in Tissue clear 2B for 5 mins

**tick when done:**

| AP1 | AP2 | AP3 | AP4 | AP5 | AP6 | BG | LM |
|---|---|---|---|---|---|---|---|
| | | | | | | | |

**Rehydration:**

Incubate slides in 100% EtOH for 2 mins

Incubate slides in 95% EtOH for 2 mins

Incubate slides in 70% EtOH for 2 mins

Incubate slides in DEPC-H2O for 2 mins

Incubate slides in DEPC-PBS for 2 mins

**Permeabilization:**

Incubate slides in citrate buffer pH=6 for 45 mins in a steamer (95-99°C)

Incubate slides in DEPC-H2O for 5 mins

Incubate slides in DEPC-PBS for 2 mins

EtOH series 70%, 85% & 100% for 2 minutes

mount secure seals (eg.: 50 µl ) per spot

**Step 2: Probe Hybridization**

Rehydration: Thaw WB3 and add 50 µl WB3 to each secure seal chamber while preparing the next steps, but do not incubate in WB3 longer than 10 minutes!!

(if performing the optimization step:

Prepare the reaction mix 1: Thaw RM1 and mix in an Rnase free Eppi: 40 µl RM1 and 10µl of the probes. Mix gently by pippeting up and down.)

**if preparing the gene panel:**

| | | | spot A | |
|---|---|---|---|---|
| Master Mix folds: | | | 6 | |
| **Prehybridization 1** | **concentration** | **1x [µl]** | **MM1** | |
| KRT18 | 20 x | 2,5 | 15,00 | |
| Immune panel I1A 0.1 | 20 x | 2,5 | 15,00 | |
| Immune panel I2B 0.1 | 20 x | 2,5 | 15,00 | |
| Katja gene panel | 20 x | 2,5 | 15,00 | |
| **Buffer A** | | | **60,00** | |
| Final Volume | **20** | **20** | **120,00** | |
| each sample (1x) | | | | |

Mix gently by pippeting up and down.

Prepare the reaction mix 1:

Thaw RM1 and mix in an Rnase free Eppi:

| | | spot A | |
|---|---|---|---|
| Master Mix folds: | | 6 | |
| **Prehybridization 2** | **1x [µl]** | **MM1** | |
| RM1 | 30 | 180,00 | |
| diluted gene panels | 20 | 120,00 | |
| **Final Volume** | **50** | **300,00** | |
| each sample (1x) | 50 | | |

Mix gently by pippeting up and down.

Remove WB3 and add 50 µl RM1-mix to each tissue section.

Place slides in a RNAse free humidity chamber and incubate overnight at 37°C.

## DAY 2

### Step 3: Probe Ligation

Thaw WB4, mix and vortex gently
Aspirate and discard RM1-mix from secure seal chamber and wash twice with 50 µl WB2
Apply 50µl of WB4 to each section and incubate at 37°C for 30 mins.
Wash three times with WB2, but leave the last wash inside until the next reaction mix is prepared.
Prepare reaction mix 2:
Thaw RM2, Vortex and spin down.

| | | spots |
|---|---|---|
| Master Mix folds: | | 6 |
| **Prehybridization 1** | **1x [µl]** | **MM1** |
| RM2 | 46,25 | 277,50 |
| Enzyme 1 | 1,25 | 7,50 |
| Enzyme 2 | 2,5 | 15,00 |
| **Final Volume** | **50** | **300,00** |
| each sample (1x) | **50** | |

Mix gently by pippeting up and down and spin down.
Remove WB2 and add 50 µl of the RM2-mix to each section.
Place slides in a RNAse free humidity chamber and incubate for 2 hours at 37°C.
Wash two times with WB2, but leave the last wash inside until the next reaction mix is prepared.

### Step 4: Amplification

Prepare reaction mix 3:
Thaw RM3. Vortex and spin down.

| | | spots |
|---|---|---|
| Master Mix folds: | | 6 |
| **Prehybridization 1** | **1x [µl]** | **MM1** |
| RM3 | 45 | 270,00 |
| Enzyme 3 | 5 | 30,00 |
| **Final Volume** | **50** | **300,00** |
| each sample (1x) | **50** | |

Remove WB2 from the secure seal.
Transfer 5 µl (per reaction) of Enzyme 3 to the Eppi with RM3.
Mix gently.
Add 50 µl RM3-mix to each section.
Place slides in a RNAse free humidity chamber and incubate overnight at 30°C.

## DAY 3

### Step 5: Fluorescent labeling

Wash three times with 50 µl WB2.
Prepare the labeling mix (LM):
Thaw LM. Vortex and spin down
Add 50 µl to each secure seal
Incubate at room temperature for 30 mins kept in the dark.
Wash three times with 50 µl WB2.
Remove secure seal chambers.
EtOH series 70%, 85% & 100% for 2 minutes
Air dry samples for 5 min protecting in the dark.
Apply 5-10 µl mounting medium to the center of each section and apply cover slip.

## DAY 4

### Step 6: Stripping

Put slide in DEPC-PBS till coverslip falls off.
EtOH series 70%, 85% & 100% for 2 minutes .
Air dry samples for 5 min protecting in the dark.
mount secure seals (eg.: 50 µl ) per spot or use a pap pen
Add 50 µl WB2 to each section for a 1 min wash, then remove WB2.
Next steps should be carried out in a laminar flow hood:
Add 50 µl 100% Formamide, incubate for 1 min at room temperature.
Repeat this step two more times.
Cover section with 50 µl WB2 and incubate at room temperature.
Repeat this step one more time.

### Step 7: Quenching: not performed

### Step 8: Hybridization and Quenching Sequencing

For each section prepare AP mix in an Eppi and mix gently by slow vortexing:

| | | spot A | spot B |
|---|---|---|---|
| Master Mix folds: | | 6 | |
| **Prehybridization 1** | **1x [µl]** | **MM1** | |
| Buffer A | 45 | 270,00 | |
| Apx | 5 | 30,00 | |
| QP | 0,5 | 0,00 | |
| **Final Volume** | **50** | **300,00** | |
| each sample (1x) | **50** | | |

(it is essential to document which AP is used in each sequencing cycle.)

(Incubate the AP-QP Mix at 37°C for 15mins.(
Remove WB2 from each section and add AP mix
Place slide at 37°C for 1 hour.
Remove AP mix and quickly wash twice with 50 µlWB2 for 1 min.

**Now work in the dark!!!**
For each section prepare SP mix in an Eppi and mix gently by slow vortexing:

| | | spots |
|---|---|---|
| Master Mix folds: | | 6 |
| **Prehybridization 1** | **1x [µl]** | **MM1** |
| Buffer A | 45 | 270,00 |
| SPx | 5 | 30,00 |
| **Final Volume** | **50** | **300,00** |
| each sample (1x) | **50** | |

(SP mix is the same for all sequencing cycles but needs to be prepared fresh for each cycle.)
Remove WB2 from each section and add SP mix
Place slide at 37°C for 30 mins.
Remove SP mix and quickly wash twice with 50 µlWB2 for 1 min.
EtOH series 70%, 85% & 100% for 2 minutes
Air dry samples for 5 min protecting in the dark.
Apply 5-10 µl mounting medium to the center of each section and apply cover slip.

Repeat Step 6-8 with appropriate AP mix until all six cycles have been performed.

## 6.5.2. dRNA-HybISS shedder project protocol II

**10.08.2022** **Exp64KS_In Situ sequencing on early CRC with all panels on one slide**

**(1)** perform ISS with CARTANA Katja panel +immunepanels +krt18 on early CRC slides **(2)** exchange Enzyme 3 with Phi Polymerase from damaged ISS kit

Protocol by Katja Sallinger. Adapted from CARTANA

**experiment design & protocol: Katja Sallinger**

**lab work: Christin**

**scanning: Christin and Lissi (Katja assist)**

**data analysis: Katja Sallinger**

scanning instructions:

* XY-shift calibration: not necessary - spectrasplit filters are **NOT** used when performing sequencing!!!

* switch channel before moving XY

* avoid overexposure in all channels including DAPI

* scan ~ 8mm diameter spot, 40x objective, EFI

* save scans here >>> W:\Images\Katja Sallinger\exp64KS

* file names >>> slideID

* convert to TIFF: 2x2 binning, no tiling

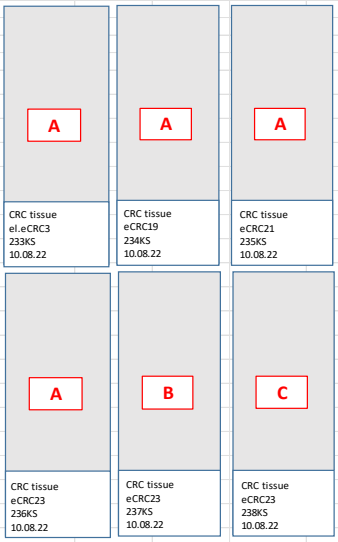


**Comments:**

maybe we need to quench krt18!

For spot A use the old CARTANA kit (which is working)

For spot B use the "new" CARTANA kit, which will probably not work!

**DAY 1**

**Step 1: Dehydration and Permeabilization**

A..Katja panel+immunepanel+krt18 B, good ISS library prep kit

B..Katja panel+immunepanel+krt18 B, damaged ISS library prep kit

C..Katja panel+immunepanel+krt18 B, damaged ISS library prep kit + Phi Pol insted of Enzyme 3

**Deparaffinization:**

Bake sections in 60°C oven for one hour to prepare for deparaffinization

Incubate slides in Tissue clear 1A for 5 mins

Incubate slides in Tissue clear 1B for 5 mins

Incubate slides in Tissue clear 2A for 5 mins

Incubate slides in Tissue clear 2B for 5 mins

| | |
|---|---|
| el.CRC3 | Box33, Position 13, Slidenr 15 |
| eCRC19 | Box38, Position 4, Slidenr 10 |
| eCRC21 | Box38, Position 8, Slidenr 6 |
| eCRC23 | Box38, Position 27, Slidenr 10 |
| eCRC23 | Box38, Position 28, Slidenr 11 |
| eCRC23 | Box38, Position 29, Slidenr 12 |

**tick when done:**

| AP1 | AP2 | AP3 | AP4 | AP5 | AP6 | BG | LM |
|---|---|---|---|---|---|---|---|
| | | | | | | | |

**Rehydration:**

Incubate slides in 100% EtOH for 2 mins

Incubate slides in 95% EtOH for 2 mins

Incubate slides in 70% EtOH for 2 mins

Incubate slides in DEPC-H2O for 2 mins

Incubate slides in DEPC-PBS for 2 mins

**Permeabilization:**

Incubate slides in citrate buffer pH=6 for 45 mins in a steamer (95-99°C)

Incubate slides in DEPC-H2O for 5 mins

Incubate slides in DEPC-PBS for 2 mins

EtOH series 70%, 85% & 100% for 2 minutes

mount secure seals (eg.: 50 µl ) per spot

**Step 2: Probe Hybridization**

Rehydration: Thaw WB3 and add 50 µl WB3 to each secure seal chamber while preparing the next steps, but do not incubate in WB3 longer than 10 minutes!!

(if performing the optimization step:

Prepare the reaction mix 1: Thaw RM1 and mix in an Rnase free Eppi: 40 µl RM1 and 10µl of the probes. Mix gently by pippeting up and down.)

**if preparing the gene panel:**

| | | | | spot A | spot B+C |
|---|---|---|---|---|---|
| Master Mix folds: | | | | 4 | 2 |
| **Prehybridization 1** | **concentration** | | **1x [µl]** | **MM1** | **MM2** |
| KRT18 | 20 | x | 2,5 | 10,00 | 5,00 |
| Immune panel I1A 0.1 | 20 | x | 2,5 | 10,00 | 5,00 |
| Immune panel I2B 0.1 | 20 | x | 2,5 | 10,00 | 5,00 |
| Katja gene panel | 20 | x | 2,5 | 10,00 | 5,00 |
| **Buffer A** | | | | **40,00** | **20,00** |
| Final Volume | **20** | | **20** | **80,00** | **40,00** |
| each sample (1x) | | | | | |

Mix gently by pippeting up and down.

Prepare the reaction mix 1:

Thaw RM1 and mix in an Rnase free Eppi:

| | | spot A | spot B+C |
|---|---|---|---|
| Master Mix folds: | | 4 | 2 |
| **Prehybridization 2** | **1x [µl]** | **MM1** | **MM2** |
| RM1 | 30 | 120,00 | 60,00 |
| diluted gene panels | 20 | 80,00 | 40,00 |
| **Final Volume** | **50** | **200,00** | **100,00** |
| each sample (1x) | 50 | | |

Mix gently by pippeting up and down.

Remove WB3 and add 50 µl RM1-mix to each tissue section.

Place slides in a RNAse free humidity chamber and incubate overnight at 37°C.

## DAY 2

### Step 3: Probe Ligation

Thaw WB4, mix and vortex gently
Aspirate and discard RM1-mix from secure seal chamber and wash twice with 50 µl WB2
Apply 50µl of WB4 to each section and incubate at 37°C for 30 mins.
Wash three times with WB2, but leave the last wash inside until the next reaction mix is prepared.
Prepare reaction mix 2:
Thaw RM2, Vortex and spin down.

| | | spots |
|---|---|---|
| Master Mix folds: | | 6 |
| **Prehybridization 1** | **1x [µl]** | **MM1** |
| RM2 | 46,25 | 277,50 |
| Enzyme 1 | 1,25 | 7,50 |
| Enzyme 2 | 2,5 | 15,00 |
| **Final Volume** | **50** | **300,00** |
| each sample (1x) | **50** | |

Mix gently by pippeting up and down and spin down.
Remove WB2 and add 50 µl of the RM2-mix to each section.
Place slides in a RNAse free humidity chamber and incubate for 2 hours at 37°C.
Wash two times with WB2, but leave the last wash inside until the next reaction mix is prepared.

### Step 4: Amplification

Prepare reaction mix 3:
Thaw RM3. Vortex and spin down.

| | | spots |
|---|---|---|
| Master Mix folds: | | 6 |
| **Prehybridization 1** | **1x [µl]** | **MM1** |
| RM3 | 45 | 270,00 |
| Enzyme 3 | 5 | 30,00 |
| **Final Volume** | **50** | **300,00** |
| each sample (1x) | **50** | |

Remove WB2 from the secure seal.
Transfer 5 µl (per reaction) of Enzyme 3 to the Eppi with RM3.
Mix gently.
Add 50 µl RM3-mix to each section.
Place slides in a RNAse free humidity chamber and incubate overnight at 30°C.

## DAY 3

### Step 5: Fluorescent labeling

Wash three times with 50 µl WB2.
Prepare the labeling mix (LM):
Thaw LM. Vortex and spin down
Add 50 µl to each secure seal
Incubate at room temperature for 30 mins kept in the dark.
Wash three times with 50 µl WB2.
Remove secure seal chambers.
EtOH series 70%, 85% & 100% for 2 minutes
Air dry samples for 5 min protecting in the dark.
Apply 5-10 µl mounting medium to the center of each section and apply cover slip.

## DAY 4

### Step 6: Stripping

Put slide in DEPC-PBS till coverslip falls off.
EtOH series 70%, 85% & 100% for 2 minutes .
Air dry samples for 5 min protecting in the dark.
mount secure seals (eg.: 50 µl ) per spot or use a pap pen
Add 50 µl WB2 to each section for a 1 min wash, then remove WB2.
Next steps should be carried out in a laminar flow hood:
Add 50 µl 100% Formamide, incubate for 1 min at room temperature.
Repeat this step two more times.
Cover section with 50 µl WB2 and incubate at room temperature.
Repeat this step one more time.

### Step 7: Quenching: not performed

### Step 8: Hybridization and Quenching Sequencing

For each section prepare AP mix in an Eppi and mix gently by slow vortexing:

| | | spot A | spot B |
|---|---|---|---|
| Master Mix folds: | | 6 | |
| **Prehybridization 1** | **1x [µl]** | **MM1** | |
| Buffer A | 45 | 270,00 | |
| Apx | 5 | 30,00 | |
| QP | 0,5 | 0,00 | |
| **Final Volume** | **50** | **300,00** | |
| each sample (1x) | **50** | | |

(it is essential to document which AP is used in each sequencing cycle.)

(Incubate the AP-QP Mix at 37°C for 15mins.(
Remove WB2 from each section and add AP mix
Place slide at 37°C for 1 hour.
Remove AP mix and quickly wash twice with 50 µlWB2 for 1 min.

**Now work in the dark!!!**
For each section prepare SP mix in an Eppi and mix gently by slow vortexing:

| | | spots |
|---|---|---|
| Master Mix folds: | | 6 |
| **Prehybridization 1** | **1x [µl]** | **MM1** |
| Buffer A | 45 | 270,00 |
| SPx | 5 | 30,00 |
| **Final Volume** | **50** | **300,00** |
| each sample (1x) | **50** | |

(SP mix is the same for all sequencing cycles but needs to be prepared fresh for each cycle.)
Remove WB2 from each section and add SP mix
Place slide at 37°C for 30 mins.
Remove SP mix and quickly wash twice with 50 µlWB2 for 1 min.
EtOH series 70%, 85% & 100% for 2 minutes
Air dry samples for 5 min protecting in the dark.
Apply 5-10 µl mounting medium to the center of each section and apply cover slip.

Repeat Step 6-8 with appropriate AP mix until all six cycles have been performed.

## 6.5.3. dRNA-HybISS shedder project protocol III

**31.08.2022** **Exp66KS_In Situ sequencing on early CRC and glioblastoma**

**(1)** perform ISS with CARTANA Katja panel +immunepanels +krt18 on early CRC slides (2) perform ISS with CARTANA neuropanel 1+2 ??and
Protocol by Katja Sallinger. Adapted from CARTANA

**experiment design & protocol: Katja Sallinger**

**lab work: Christin**

**scanning: Christin and Lissi (Katja assist)**

**data analysis: Katja Sallinger**

scanning instructions:

* XY-shift calibration: not necessary - spectrasplit filters are **NOT** used when performing sequencing!!!

* switch channel before moving XY

* avoid overexposure in all channels including DAPI

* scan ~ 8mm diameter spot, 40x objective, EFI

* save scans here >>> W:\Images\Katja Sallinger\exp66KS

* file names >>> slideID

* convert to TIFF: 2x2 binning, no tiling

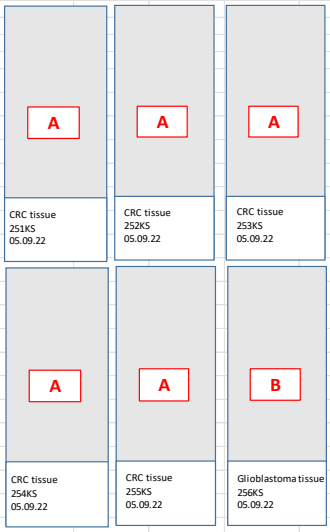


**Comments:**
choose slides as instructed by Stefan!
Decide together with Amin if you want to use only 2 neuropanels for glioblastoma or if you want to add the immunepanels

**DAY 1**

**Step 1: Dehydration and Permeabilization**

A..Katja panel+immunepanel+krt18
B..Neuropanel Gerneral N1C + CNS xx and ? Immunepanel?

| | | |
|---|---|---|
| **Deparaffinization:** | | |
| Bake sections in 60°C oven for one hour to prepare for deparaffinization | xxxx | Box47, Position xx, Slidenr xx |
| Incubate slides in Tissue clear 1A for 5 mins | xxxx | Box47, Position xx, Slidenr xx |
| Incubate slides in Tissue clear 1B for 5 mins | xxxx | Box47, Position xx, Slidenr xx |
| Incubate slides in Tissue clear 2A for 5 mins | xxxx | Box47, Position xx, Slidenr xx |
| Incubate slides in Tissue clear 2B for 5 mins | xxxx | Boxxx, Position xx, Slidenr xx |

**tick when done:**

| AP1 | AP2 | AP3 | AP4 | AP5 | AP6 | BG | LM |
|---|---|---|---|---|---|---|---|
| | | | | | | | |

| |
|---|
| **Rehydration:** |
| Incubate slides in 100% EtOH for 2 mins |
| Incubate slides in 95% EtOH for 2 mins |
| Incubate slides in 70% EtOH for 2 mins |
| Incubate slides in DEPC-H2O for 2 mins |
| Incubate slides in DEPC-PBS for 2 mins |
| **Permeabilization:** |
| Incubate slides in citrate buffer pH=6 for 45 mins in a steamer (95-99°C) |
| Incubate slides in DEPC-H2O for 5 mins |
| Incubate slides in DEPC-PBS for 2 mins |
| EtOH series 70%, 85% & 100% for 2 minutes |
| mount secure seals (eg.: 50 µl ) per spot |

**Step 2: Probe Hybridization**

Rehydration: Thaw WB3 and add 50 µl WB3 to each secure seal chamber while preparing the next steps, but do not incubate in WB3 longer than 10 minutes!!
(if performing the optimization step:
Prepare the reaction mix 1: Thaw RM1 and mix in an Rnase free Eppi: 40 µl RM1 and 10µl of the probes. Mix gently by pippeting up and down.)
**if preparing the gene panel:**

| | | | | spot A | spot B |
|---|---|---|---|---|---|
| Master Mix folds: | | | | 5 | 1 |
| **Prehybridization 1** | **concentration** | | **1x [µl]** | **MM1** | **MM2** |
| KRT18 | 20 | x | 2,5 | 12,50 | |
| Immune panel I1A 0.1 | 20 | x | 2,5 | 12,50 | 2,50 |
| Immune panel I2B 0.1 | 20 | x | 2,5 | 12,50 | 2,50 |
| Katja gene panel | 20 | x | 2,5 | 12,50 | |
| Neuropanel General N1C | 20 | x | 2,5 | | 2,50 |
| Neuropanel CNS xxx | 20 | x | 2,5 | | 2,50 |
| **Buffer A** | | | | **50,00** | **10,00** |
| Final Volume | **20** | | **20** | **100,00** | **20,00** |
| each sample (1x) | | | | | |

Mix gently by pippeting up and down.

Prepare the reaction mix 1:
Thaw RM1 and mix in an Rnase free Eppi:

| | | spot A | spot B |
|---|---|---|---|
| Master Mix folds: | | 5 | 1 |
| **Prehybridization 2** | **1x [µl]** | **MM1** | **MM2** |
| RM1 | 30 | 150,00 | 30,00 |
| diluted gene panels | 20 | 100,00 | 20,00 |
| **Final Volume** | **50** | **250,00** | **50,00** |
| each sample (1x) | 50 | | |

Mix gently by pippeting up and down.
Remove WB3 and add 50 µl RM1-mix to each tissue section.
Place slides in a RNAse free humidity chamber and incubate overnight at 37°C.

## DAY 2

### Step 3: Probe Ligation

Thaw WB4, mix and vortex gently
Aspirate and discard RM1-mix from secure seal chamber and wash twice with 50 µl WB2
Apply 50µl of WB4 to each section and incubate at 37°C for 30 mins.
Wash three times with WB2, but leave the last wash inside until the next reaction mix is prepared.
Prepare reaction mix 2:
Thaw RM2, Vortex and spin down.

| | | spots |
|---|---|---|
| Master Mix folds: | | 6 |
| **Prehybridization 1** | **1x [µl]** | **MM1** |
| RM2 | 46,25 | 277,50 |
| Enzyme 1 | 1,25 | 7,50 |
| Enzyme 2 | 2,5 | 15,00 |
| **Final Volume** | **50** | **300,00** |
| each sample (1x) | **50** | |

Mix gently by pippeting up and down and spin down.
Remove WB2 and add 50 µl of the RM2-mix to each section.
Place slides in a RNAse free humidity chamber and incubate for 2 hours at 37°C.
Wash two times with WB2, but leave the last wash inside until the next reaction mix is prepared.

### Step 4: Amplification

Prepare reaction mix 3:
Thaw RM3. Vortex and spin down.

| | | spots |
|---|---|---|
| Master Mix folds: | | 6 |
| **Prehybridization 1** | **1x [µl]** | **MM1** |
| RM3 | 45 | 270,00 |
| Enzyme 3 | 5 | 30,00 |
| **Final Volume** | **50** | **300,00** |
| each sample (1x) | **50** | |

Remove WB2 from the secure seal.
Transfer 5 µl (per reaction) of Enzyme 3 to the Eppi with RM3.
Mix gently.
Add 50 µl RM3-mix to each section.
Place slides in a RNAse free humidity chamber and incubate overnight at 30°C.

## DAY 3

### Step 5: Fluorescent labeling

Wash three times with 50 µl WB2.
Prepare the labeling mix (LM):
Thaw LM. Vortex and spin down
Add 50 µl to each secure seal
Incubate at room temperature for 30 mins kept in the dark.
Wash three times with 50 µl WB2.
Remove secure seal chambers.
EtOH series 70%, 85% & 100% for 2 minutes
Air dry samples for 5 min protecting in the dark.
Apply 5-10 µl mounting medium to the center of each section and apply cover slip.

## DAY 4

### Step 6: Stripping

Put slide in DEPC-PBS till coverslip falls off.
EtOH series 70%, 85% & 100% for 2 minutes .
Air dry samples for 5 min protecting in the dark.
mount secure seals (eg.: 50 µl ) per spot or use a pap pen
Add 50 µl WB2 to each section for a 1 min wash, then remove WB2.
Next steps should be carried out in a laminar flow hood:
Add 50 µl 100% Formamide, incubate for 1 min at room temperature.
Repeat this step two more times.
Cover section with 50 µl WB2 and incubate at room temperature.
Repeat this step one more time.

### Step 7: Quenching: not performed

### Step 8: Hybridization and Quenching Sequencing

For each section prepare AP mix in an Eppi and mix gently by slow vortexing:

| | | spot A | spot B |
|---|---|---|---|
| Master Mix folds: | | 6 | |
| **Prehybridization 1** | **1x [µl]** | **MM1** | |
| Buffer A | 45 | 270,00 | |
| Apx | 5 | 30,00 | |
| QP | 0,5 | 0,00 | |
| **Final Volume** | **50** | **300,00** | |
| each sample (1x) | **50** | | |

(it is essential to document which AP is used in each sequencing cycle.)

(Incubate the AP-QP Mix at 37°C for 15mins.(
Remove WB2 from each section and add AP mix
Place slide at 37°C for 1 hour.
Remove AP mix and quickly wash twice with 50 µlWB2 for 1 min.

**Now work in the dark!!!**
For each section prepare SP mix in an Eppi and mix gently by slow vortexing:

| | | spots |
|---|---|---|
| Master Mix folds: | | 6 |
| **Prehybridization 1** | **1x [µl]** | **MM1** |
| Buffer A | 45 | 270,00 |
| SPx | 5 | 30,00 |
| **Final Volume** | **50** | **300,00** |
| each sample (1x) | **50** | |

(SP mix is the same for all sequencing cycles but needs to be prepared fresh for each cycle.)
Remove WB2 from each section and add SP mix
Place slide at 37°C for 30 mins.
Remove SP mix and quickly wash twice with 50 µlWB2 for 1 min.
EtOH series 70%, 85% & 100% for 2 minutes
Air dry samples for 5 min protecting in the dark.
Apply 5-10 µl mounting medium to the center of each section and apply cover slip.

Repeat Step 6-8 with appropriate AP mix until all six cycles have been performed.

## 6.5.4. dRNA-HybISS shedder project protocol IV

**07.10.2022** **Exp67KS_In Situ sequencing on early CRC and test tumor sample**

**(1)** perform ISS with CARTANA pathway gene panel +immunepanels +krt18 on early CRC slides (2) perform ISS with CARTANA test tumor panel and immunepanel

Protocol by Katja Sallinger. Adapted from CARTANA

**experiment design & protocol: Katja Sallinger**

**lab work: Christin**

**scanning: Christin (Katja assist)**

**data analysis: Katja Sallinger**

scanning instructions:

* XY-shift calibration: not necessary - spectrasplit filters are **NOT** used when performing sequencing!!!
* switch channel before moving XY
* avoid overexposure in all channels including DAPI
* scan ~ 8mm diameter spot, 40x objective, EFI

* save scans here >>> W:\Images\Katja Sallinger\exp67KS
* file names >>> slideID
* convert to TIFF: 2x2 binning, no tiling

**Comments:**

choose slides as instructed by Stefan!

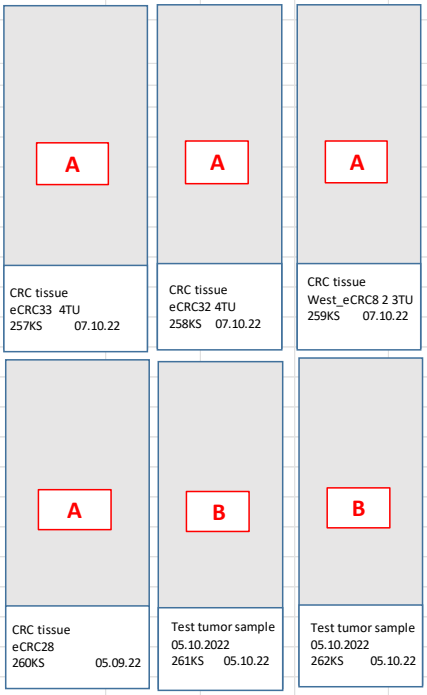


**DAY 1**

**Step 1: Dehydration and Permeabilization**

A..Pathway gene panel +immunepanels+krt18
B..Test tumor panel + Immunepanels

**Deparaffinization:**

Bake sections in 60°C oven for one hour to prepare for deparaffinization
Incubate slides in Tissue clear 1A for 5 mins
Incubate slides in Tissue clear 1B for 5 mins
Incubate slides in Tissue clear 2A for 5 mins
Incubate slides in Tissue clear 2B for 5 mins

**Rehydration:**

Incubate slides in 100% EtOH for 2 mins
Incubate slides in 95% EtOH for 2 mins
Incubate slides in 70% EtOH for 2 mins
Incubate slides in DEPC-H2O for 2 mins
Incubate slides in DEPC-PBS for 2 mins

**Permeabilization:**

Incubate slides in citrate buffer pH=6 for 45 mins in a steamer (95-99°C)
Incubate slides in DEPC-H2O for 5 mins
Incubate slides in DEPC-PBS for 2 mins
EtOH series 70%, 85% & 100% for 2 minutes
mount secure seals (eg.: 50 µl ) per spot

## Step 2: Probe Hybridization

Rehydration: Thaw WB3 and add 50 µl WB3 to each secure seal chamber while preparing the next steps, but do not incubate in WB3 longer than 10 minutes!!
(if performing the optimization step:
Prepare the reaction mix 1: Thaw RM1 and mix in an Rnase free Eppi: 40 µl RM1 and 10µl of the probes. Mix gently by pippeting up and down.)
**if preparing the gene panel:**

| | | | | spot A | spot B |
|---|---|---|---|---|---|
| Master Mix folds: | | | | 4 | 2 |
| **Prehybridization 1** | **concentration** | | **1x [µl]** | **MM1** | **MM2** |
| KRT18 | 20 | **x** | 2,5 | 10,00 | |
| Immune panel I1A 0.1 | 20 | **x** | 2,5 | 10,00 | 5,00 |
| Immune panel I2B 0.1 | 20 | **x** | 2,5 | 10,00 | 5,00 |
| Pathway gene panel | 20 | **x** | 2,5 | 10,00 | |
| Test tumor panel | 20 | **x** | 2,5 | | 5,00 |
| **Buffer A** | | | | **40,00** | **25,00** |
| Final Volume | **20** | | **20** | **80,00** | **40,00** |
| each sample (1x) | | | | | |

Mix gently by pippeting up and down.

Prepare the reaction mix 1:
Thaw RM1 and mix in an Rnase free Eppi:

| | | spot A | |
|---|---|---|---|
| Master Mix folds: | | 4 | 2 |
| **Prehybridization 2** | **1x [µl]** | **MM1** | **MM2** |
| RM1 | 30 | 120,00 | 60,00 |
| diluted gene panels | 20 | 80,00 | 40,00 |
| **Final Volume** | **50** | **200,00** | **100,00** |
| each sample (1x) | 50 | | |

Mix gently by pippeting up and down.
Remove WB3 and add 50 µl RM1-mix to each tissue section.
Place slides in a RNAse free humidity chamber and incubate overnight at 37°C.

## DAY 2

## Step 3: Probe Ligation

Thaw WB4, mix and vortex gently
Aspirate and discard RM1-mix from secure seal chamber and wash twice with 50 µl WB2
Apply 50µl of WB4 to each section and incubate at 37°C for 30 mins.
Wash three times with WB2, but leave the last wash inside until the next reaction mix is prepared.
Prepare reaction mix 2:
Thaw RM2, Vortex and spin down.

| | | spot A |
|---|---|---|
| Master Mix folds: | | 6 |
| **Prehybridization 1** | **1x [µl]** | **MM1** |
| RM2 | 46,25 | 277,50 |
| Enzyme 1 | 1,25 | 7,50 |
| Enzyme 2 | 2,5 | 15,00 |
| **Final Volume** | **50** | **300,00** |
| each sample (1x) | **50** | |

Mix gently by pippeting up and down and spin down.
Remove WB2 and add 50 µl of the RM2-mix to each section.
Place slides in a RNAse free humidity chamber and incubate for 2 hours at 37°C.
Wash two times with WB2, but leave the last wash inside until the next reaction mix is prepared.

## Step 4: Amplification

Prepare reaction mix 3:
Thaw RM3. Vortex and spin down.

| | | spot A |
|---|---|---|
| Master Mix folds: | | 6 |
| **Prehybridization 1** | **1x [µl]** | **MM1** |
| RM3 | 45 | 270,00 |
| Enzyme 3 | 5 | 30,00 |
| **Final Volume** | **50** | **300,00** |
| each sample (1x) | **50** | |

Remove WB2 from the secure seal.
Transfer 5 µl (per reaction) of Enzyme 3 to the Eppi with RM3.
Mix gently.
Add 50 µl RM3-mix to each section.
Place slides in a RNAse free humidity chamber and incubate overnight at 30°C.

## DAY 3

### Step 5: Fluorescent labeling

Wash three times with 50 µl WB2.
Prepare the labeling mix (LM):
Thaw LM. Vortex and spin down
Add 50 µl to each secure seal
Incubate at room temperature for 30 mins kept in the dark.
Wash three times with 50 µl WB2.
Remove secure seal chambers.
EtOH series 70%, 85% & 100% for 2 minutes
Air dry samples for 5 min protecting in the dark.
Apply 5-10 µl mounting medium to the center of each section and apply cover slip.

## DAY 4

### Step 6: Stripping

Put slide in DEPC-PBS till coverslip falls off.
EtOH series 70%, 85% & 100% for 2 minutes .
Air dry samples for 5 min protecting in the dark.
mount secure seals (eg.: 50 µl ) per spot or use a pap pen
Add 50 µl WB2 to each section for a 1 min wash, then remove WB2.
Next steps should be carried out in a laminar flow hood:
Add 50 µl 100% Formamide, incubate for 1 min at room temperature.
Repeat this step two more times.
Cover section with 50 µl WB2 and incubate at room temperature.
Repeat this step one more time.

### Step 7: Quenching: not performed

### Step 8: Hybridization and Quenching Sequencing

For each section prepare AP mix in an Eppi and mix gently by slow vortexing:

| | | spot A+B |
|---|---|---|
| Master Mix folds: | | 6 |
| **Prehybridization 1** | **1x [µl]** | **MM1** |
| Buffer A | 44,5 | 267,00 |
| Apx | 5 | 30,00 |
| QP IGKC | 0,5 | 3,00 |
| **Final Volume** | **50** | **300,00** |
| each sample (1x) | **50** | |

(it is essential to document which AP is used in each sequencing cycle.)

(Incubate the AP-QP Mix at 37°C for 15mins.(
Remove WB2 from each section and add AP mix
Place slide at 37°C for 1 hour.
Remove AP mix and quickly wash twice with 50 µlWB2 for 1 min.

**Now work in the dark!!!**
For each section prepare SP mix in an Eppi and mix gently by slow vortexing:

| | | spots |
|---|---|---|
| Master Mix folds: | | 6 |
| **Prehybridization 1** | **1x [µl]** | **MM1** |
| Buffer A | 45 | 270,00 |
| SPx | 5 | 30,00 |
| **Final Volume** | **50** | **300,00** |
| each sample (1x) | **50** | |

(SP mix is the same for all sequencing cycles but needs to be prepared fresh for each cycle.)
Remove WB2 from each section and add SP mix
Place slide at 37°C for 30 mins.
Remove SP mix and quickly wash twice with 50 µlWB2 for 1 min.
Apply 5-10 µl mounting medium to the center of each section and apply cover slip directly after WB2.

Repeat Step 6-8 with appropriate AP mix until all six cycles have been performed.

## 6.6. CellProfiler pipelines

### 6.6.1. CellProfiler pipeline for the calculation of the multiplication factor

To calculate the multiplication factor, the CellProfiler version 4 was used (Stirling et al., 2021).

```
CellProfiler Pipeline: http://www.cellprofiler.org

Version:4

DateRevision:421

GitHash:

ModuleCount:28

HasImagePlaneDetails:False


LoadData:[module_num:1|svn_version:'Unknown'|variable_revision_number:6|show_window:True|notes:['Load the data into the CellProfiler pipeline', 'And select the number of rows you want to process']|batch_state:array([], dtype=uint8)|enabled:True|wants_pause:False]

    Input data file location:Elsewhere...|W:\\Analysis\\Katja Sallinger\\exp60KS\\203KS_AP1\\Cellprofiler

    Name of the file:InputForCP.csv

    Load images based on this data?:Yes

    Base image location:Default Input Folder|

    Process just a range of rows?:Yes

    Rows to process:1,169

    Group images by metadata?:No

    Select metadata tags for grouping:Position

    Rescale intensities?:No


IdentifyPrimaryObjects:[module_num:2|svn_version:'Unknown'|variable_revision_number:15|show_window:True|notes:['This module identifies cytoplasma from FITC staining.', '', 'In that case no adjustment is necessary!!!', '', '(ADJUST the threshold correction factor and lower and upper bounds on threshold, to get the best results for identification and declumping of cytoplasma!)']|batch_state:array([], dtype=uint8)|enabled:True|wants_pause:False]

    Select the input image:DO4

    Name the primary objects to be identified:Cytoplasma_object
```

Typical diameter of objects, in pixel units (Min,Max):10,100000

Discard objects outside the diameter range?:No

Discard objects touching the border of the image?:No

Method to distinguish clumped objects:Intensity

Method to draw dividing lines between clumped objects:Intensity

Size of smoothing filter:0

Suppress local maxima that are closer than this minimum allowed distance:10

Speed up by using lower-resolution image to find local maxima?:Yes

Fill holes in identified objects?:After declumping only

Automatically calculate size of smoothing filter for declumping?:Yes

Automatically calculate minimum allowed distance between local maxima?:Yes

Handling of objects if excessive number of objects identified:Continue

Maximum number of objects:500

Use advanced settings?:Yes

Threshold setting version:12

Threshold strategy:Global

Thresholding method:Minimum Cross-Entropy

Threshold smoothing scale:0

Threshold correction factor:0.1

Lower and upper bounds on threshold:0.01,0.8

Manual threshold:0.0

Select the measurement to threshold with:None

Two-class or three-class thresholding?:Two classes

Log transform before thresholding?:No

Assign pixels in the middle intensity class to the foreground or the background?:Foreground

Size of adaptive window:50

Lower outlier fraction:0.05

Upper outlier fraction:0.05

Averaging method:Mean

Variance method:Standard deviation

# of deviations:2.0

Thresholding method:Otsu

ExpandOrShrinkObjects:[module_num:3|svn_version:'Unknown'|variable_revision_number:2|show_window:True|notes:['The identified cells are often too small. ', 'Therefore, this module is used to expand the cell border by 7 pixels.']|batch_state:array([], dtype=uint8)|enabled:True|wants_pause:False]

Select the input objects:Cytoplasma_object

Name the output objects:Cytoplasma_expanded_object

Select the operation:Expand objects by a specified number of pixels

Number of pixels by which to expand or shrink:7

Fill holes in objects so that all objects shrink to a single point?:No

ImageMath:[module_num:4|svn_version:'Unknown'|variable_revision_number:5|show_window:False|notes:['With this module the background of channels is subtracted.', '', 'Adjust the "Multiply the second image by" for each channel.']|batch_state:array([], dtype=uint8)|enabled:True|wants_pause:False]

Operation:Subtract

Raise the power of the result by:1.0

Multiply the result by:1.0

Add to result:0.0

Set values less than 0 equal to 0?:No

Set values greater than 1 equal to 1?:No

Replace invalid values with 0?:Yes

Ignore the image masks?:No

Name the output image:DO1_subtracted

Image or measurement?:Image

Select the first image:DO1

Multiply the first image by:1.0

Measurement:

Image or measurement?:Image

Select the second image:BGDO1

Multiply the second image by:0.8

Measurement:

ImageMath:[module_num:5|svn_version:'Unknown'|variable_revision_number:5|show_window:False|notes:['With this module the background of channels is subtracted.', '', 'Adjust the "Multiply the second image by" for each channel.']|batch_state:array([], dtype=uint8)|enabled:True|wants_pause:False]

Operation:Subtract

Raise the power of the result by:1.0

Multiply the result by:1.0

Add to result:0.0

Set values less than 0 equal to 0?:No

Set values greater than 1 equal to 1?:No

Replace invalid values with 0?:Yes

Ignore the image masks?:No

Name the output image:DO2_subtracted

Image or measurement?:Image

Select the first image:DO2

Multiply the first image by:1.0

Measurement:

Image or measurement?:Image

Select the second image:BGDO2

Multiply the second image by:0.8

Measurement:

ImageMath:[module_num:6|svn_version:'Unknown'|variable_revision_number:5|show_window:False|notes:['With this module the background of channels is subtracted.', '', 'Adjust the "Multiply the second image by" for each channel.']|batch_state:array([], dtype=uint8)|enabled:True|wants_pause:False]

Operation:Subtract

Raise the power of the result by:1.0

Multiply the result by:1.0

Add to result:0.0

Set values less than 0 equal to 0?:No

Set values greater than 1 equal to 1?:No

Replace invalid values with 0?:Yes

Ignore the image masks?:No

Name the output image:DO3_subtracted

Image or measurement?:Image

Select the first image:DO3

Multiply the first image by:1.0

Measurement:

Image or measurement?:Image

Select the second image:BGDO3

Multiply the second image by:1.4

Measurement:

ImageMath:[module_num:7|svn_version:'Unknown'|variable_revision_number:5|show_window:False|notes:['With this module the background of channels is subtracted.', '', 'Adjust the "Multiply the second image by" for each channel.']|batch_state:array([], dtype=uint8)|enabled:True|wants_pause:False]

Operation:Subtract

Raise the power of the result by:1.0

Multiply the result by:1.0

Add to result:0.0

Set values less than 0 equal to 0?:No

Set values greater than 1 equal to 1?:No

Replace invalid values with 0?:Yes

Ignore the image masks?:No

Name the output image:DO4_subtracted

Image or measurement?:Image

Select the first image:DO4

Multiply the first image by:1.0

Measurement:

Image or measurement?:Image

Select the second image:BGDO4

Multiply the second image by:0.9

Measurement:

EnhanceOrSuppressFeatures:[module_num:8|svn_version:'Unknown'|variable_revision_number:7|show_window:False|notes:['This enhances the blobs/spots in the Cy7 channel. It simple makes it more bright and reduces the background.', '', 'Speckles with a feature size of 10 pixels are enhanced. This image processing tool improves the subsequent identification of RCPs using the module identify primary objects.']|batch_state:array([], dtype=uint8)|enabled:True|wants_pause:False]

Select the input image:DO1_subtracted

Name the output image:Enhanced_cy7

Select the operation:Enhance

Feature size:10

Feature type:Speckles

Range of hole sizes:1,10

Smoothing scale:2.0

Shear angle:0.0

Decay:0.95

Enhancement method:Tubeness

Speed and accuracy:Fast

Rescale result image:Yes

EnhanceOrSuppressFeatures:[module_num:9|svn_version:'Unknown'|variable_revision_number:7|show_window:False|notes:['This enhances the blobs/spots in the Cy3 channel. It simple makes it more bright and reduces the background.', '', 'Speckles with a feature size of 10 pixels are enhanced. This image processing tool improves the subsequent identification of RCPs using the module identify primary objects.']|batch_state:array([], dtype=uint8)|enabled:True|wants_pause:False]

Select the input image:DO2_subtracted

Name the output image:Enhanced_cy3

Select the operation:Enhance

Feature size:10

Feature type:Speckles

Range of hole sizes:1,10

Smoothing scale:2.0

Shear angle:0.0

Decay:0.95

Enhancement method:Tubeness

Speed and accuracy:Fast

Rescale result image:Yes

EnhanceOrSuppressFeatures:[module_num:10|svn_version:'Unknown'|variable_revision_number:7|show_window:False|notes:['This enhances the blobs/spots in the Cy5 channel. It simple makes it more bright and reduces the background.', '', 'Speckles with a feature size of 10 pixels are enhanced. This image processing tool improves the subsequent identification of RCPs using the module identify primary objects.']|batch_state:array([], dtype=uint8)|enabled:True|wants_pause:False]

Select the input image:DO3_subtracted

Name the output image:Enhanced_cy5

Select the operation:Enhance

Feature size:10

Feature type:Speckles

Range of hole sizes:1,10

Smoothing scale:2.0

Shear angle:0.0

Decay:0.95

Enhancement method:Tubeness

Speed and accuracy:Fast

Rescale result image:Yes

EnhanceOrSuppressFeatures:[module_num:11|svn_version:'Unknown'|variable_revision_number:7|show_window:False|notes:['This enhances the blobs/spots in the FITC channel. It simple makes it more bright and reduces the background.', '', 'Speckles with a feature size of 10 pixels are enhanced. This image processing tool improves the subsequent identification of RCPs using the module identify primary objects.']|batch_state:array([], dtype=uint8)|enabled:True|wants_pause:False]

Select the input image:DO4_subtracted

Name the output image:Enhanced_fitc

Select the operation:Enhance

Feature size:10

Feature type:Speckles

Range of hole sizes:1,10

Smoothing scale:2.0

Shear angle:0.0

Decay:0.95

Enhancement method:Tubeness

Speed and accuracy:Fast

Rescale result image:Yes

IdentifyPrimaryObjects:[module_num:12|svn_version:'Unknown'|variable_revision_number:15|show_window:False|notes:['This identifes the Cy7-labelled blobs/spots (after they were enchanced). ', '', 'ADJUST threshold correction factor, lower and upper bounds on threshold, and size of smoothing filter for each spot.', 'To find the best settings, go to the test mode and choose an image set with high density of Cy7 spots. ', 'Make sure that the background fluorescence between neighboring spots / the "halos" of very bright spots are not identified as fitc objects. If necessary, increase the size of the smoothing filter and/or change the lower and upper bounds on threshold.', 'If small / low intensity spots are not identified as objects, change the lower bounds on threshold. The calculated threshold is displayed in the "display" window in the test mode. If this calculated threshold is too high, you can decrease the threshold correction factor - the calculated threshold will be closer to your lower bound on threshold.']|batch_state:array([], dtype=uint8)|enabled:True|wants_pause:False]

Select the input image:Enhanced_cy7

Name the primary objects to be identified:cy7_objects

Typical diameter of objects, in pixel units (Min,Max):2,12

Discard objects outside the diameter range?:Yes

Discard objects touching the border of the image?:Yes

Method to distinguish clumped objects:Intensity

Method to draw dividing lines between clumped objects:Intensity

Size of smoothing filter:4

Suppress local maxima that are closer than this minimum allowed distance:7.0

Speed up by using lower-resolution image to find local maxima?:Yes

Fill holes in identified objects?:After both thresholding and declumping

Automatically calculate size of smoothing filter for declumping?:No

Automatically calculate minimum allowed distance between local maxima?:Yes

Handling of objects if excessive number of objects identified:Continue

Maximum number of objects:500

Use advanced settings?:Yes

Threshold setting version:12

Threshold strategy:Global

Thresholding method:Minimum Cross-Entropy

Threshold smoothing scale:1.3488

Threshold correction factor:0.3

Lower and upper bounds on threshold:0.002,1.0

Manual threshold:0.0

Select the measurement to threshold with:None

Two-class or three-class thresholding?:Two classes

Log transform before thresholding?:No

Assign pixels in the middle intensity class to the foreground or the background?:Foreground

Size of adaptive window:50

Lower outlier fraction:0.05

Upper outlier fraction:0.05

Averaging method:Mean

Variance method:Standard deviation

# of deviations:2.0

Thresholding method:Otsu

IdentifyPrimaryObjects:[module_num:13|svn_version:'Unknown'|variable_revision_number:15|show_window:False|notes:['This identifes the Cy3-labelled blobs/spots (after they were enchanced). ', '', 'ADJUST threshold correction factor, lower and upper bounds on threshold, and size of smoothing filter for each spot.', 'To find the best settings, go to the test mode and choose an image set with high density of Cy3 spots. ', 'Make sure that the background fluorescence between neighboring spots / the "halos" of very

bright spots are not identified as fitc objects. If necessary, increase the size of the smoothing filter and/or change the lower and upper bounds on threshold.', 'If small / low intensity spots are not identified as objects, change the lower bounds on threshold. The calculated threshold is displayed in the "display" window in the test mode. If this calculated threshold is too high, you can decrease the threshold correction factor - the calculated threshold will be closer to your lower bound on threshold.']|batch_state:array([], dtype=uint8)|enabled:True|wants_pause:False]

Select the input image:Enhanced_cy3

Name the primary objects to be identified:cy3_objects

Typical diameter of objects, in pixel units (Min,Max):2,12

Discard objects outside the diameter range?:Yes

Discard objects touching the border of the image?:Yes

Method to distinguish clumped objects:Intensity

Method to draw dividing lines between clumped objects:Intensity

Size of smoothing filter:5

Suppress local maxima that are closer than this minimum allowed distance:7.0

Speed up by using lower-resolution image to find local maxima?:Yes

Fill holes in identified objects?:After both thresholding and declumping

Automatically calculate size of smoothing filter for declumping?:No

Automatically calculate minimum allowed distance between local maxima?:Yes

Handling of objects if excessive number of objects identified:Continue

Maximum number of objects:500

Use advanced settings?:Yes

Threshold setting version:12

Threshold strategy:Global

Thresholding method:Minimum Cross-Entropy

Threshold smoothing scale:1.3488

Threshold correction factor:0.3

Lower and upper bounds on threshold:0.004,1.0

Manual threshold:0.0

Select the measurement to threshold with:None

Two-class or three-class thresholding?:Two classes

Log transform before thresholding?:No

Assign pixels in the middle intensity class to the foreground or the background?:Foreground

Size of adaptive window:50

Lower outlier fraction:0.05

Upper outlier fraction:0.05

Averaging method:Mean

Variance method:Standard deviation

# of deviations:2.0

Thresholding method:Otsu

IdentifyPrimaryObjects:[module_num:14|svn_version:'Unknown'|variable_revision_number:15|show_window:False|notes:['This identifes the Cy5-labelled blobs/spots (after they were enchanced). ', '', 'ADJUST threshold correction factor, lower and upper bounds on threshold, and size of smoothing filter for each spot.', 'To find the best settings, go to the test mode and choose an image set with high density of Cy5 spots. ', 'Make sure that the background fluorescence between neighboring spots / the "halos" of very bright spots are not identified as fitc objects. If necessary, increase the size of the smoothing filter and/or change the lower and upper bounds on threshold.', 'If small / low intensity spots are not identified as objects, change the lower bounds on threshold. The calculated threshold is displayed in the "display" window in the test mode. If this calculated threshold is too high, you can decrease the threshold correction factor - the calculated threshold will be closer to your lower bound on threshold.']|batch_state:array([], dtype=uint8)|enabled:True|wants_pause:False]

Select the input image:Enhanced_cy5

Name the primary objects to be identified:cy5_objects

Typical diameter of objects, in pixel units (Min,Max):3,12

Discard objects outside the diameter range?:Yes

Discard objects touching the border of the image?:Yes

Method to distinguish clumped objects:Intensity

Method to draw dividing lines between clumped objects:Intensity

Size of smoothing filter:4

Suppress local maxima that are closer than this minimum allowed distance:7.0

Speed up by using lower-resolution image to find local maxima?:Yes

Fill holes in identified objects?:After both thresholding and declumping

Automatically calculate size of smoothing filter for declumping?:No

Automatically calculate minimum allowed distance between local maxima?:Yes

Handling of objects if excessive number of objects identified:Continue

Maximum number of objects:500

Use advanced settings?:Yes

Threshold setting version:12

Threshold strategy:Global

Thresholding method:Minimum Cross-Entropy

Threshold smoothing scale:1.3488

Threshold correction factor:0.3

Lower and upper bounds on threshold:0.004,1.0

Manual threshold:0.0

Select the measurement to threshold with:None

Two-class or three-class thresholding?:Two classes

Log transform before thresholding?:No

Assign pixels in the middle intensity class to the foreground or the background?:Foreground

Size of adaptive window:50

Lower outlier fraction:0.05

Upper outlier fraction:0.05

Averaging method:Mean

Variance method:Standard deviation

# of deviations:2.0

Thresholding method:Otsu

IdentifyPrimaryObjects:[module_num:15|svn_version:'Unknown'|variable_revision_number:15|show_window:False|notes:['This identifes the FITC-labelled blobs/spots (after they were enchanced). ', '', 'ADJUST threshold correction factor, lower and upper bounds on threshold, and size of smoothing filter for each spot.', 'To find the best settings, go to the test mode and choose an image set with high density of FITC spots. ', 'Make sure that the background fluorescence between neighboring spots / the "halos" of very bright spots are not identified as fitc objects. If necessary, increase the size of the smoothing filter and/or change the lower and upper bounds on threshold.', 'If small / low intensity spots are not identified as objects, change the lower bounds on threshold. The calculated threshold is displayed in the "display" window in the test mode. If this calculated threshold is too high, you can decrease the

threshold correction factor - the calculated threshold will be closer to your lower bound on threshold.']|batch_state:array([], dtype=uint8)|enabled:True|wants_pause:False]

Select the input image:Enhanced_fitc

Name the primary objects to be identified:fitc_objects

Typical diameter of objects, in pixel units (Min,Max):2,12

Discard objects outside the diameter range?:Yes

Discard objects touching the border of the image?:Yes

Method to distinguish clumped objects:Intensity

Method to draw dividing lines between clumped objects:Intensity

Size of smoothing filter:4

Suppress local maxima that are closer than this minimum allowed distance:7.0

Speed up by using lower-resolution image to find local maxima?:Yes

Fill holes in identified objects?:After both thresholding and declumping

Automatically calculate size of smoothing filter for declumping?:No

Automatically calculate minimum allowed distance between local maxima?:Yes

Handling of objects if excessive number of objects identified:Continue

Maximum number of objects:500

Use advanced settings?:Yes

Threshold setting version:12

Threshold strategy:Global

Thresholding method:Otsu

Threshold smoothing scale:1.3488

Threshold correction factor:0.3

Lower and upper bounds on threshold:0.002,1.0

Manual threshold:0.0

Select the measurement to threshold with:None

Two-class or three-class thresholding?:Two classes

Log transform before thresholding?:No

Assign pixels in the middle intensity class to the foreground or the background?:Foreground

Size of adaptive window:50

Lower outlier fraction:0.05

Upper outlier fraction:0.05

Averaging method:Mean

Variance method:Standard deviation

# of deviations:2.0

Thresholding method:Otsu

OverlayOutlines:[module_num:16|svn_version:'Unknown'|variable_revision_number:4|show_window:False|notes:[]|batch_state:array([], dtype=uint8)|enabled:False|wants_pause:False]

Display outlines on a blank image?:No

Select image on which to display outlines:DO1

Name the output image:Overlay_objects_Cy7

Outline display mode:Color

Select method to determine brightness of outlines:Max of image

How to outline:Inner

Select outline color:blue

Select objects to display:Cytoplasma_expanded_object

Select outline color:#800080

Select objects to display:cy7_objects

OverlayOutlines:[module_num:17|svn_version:'Unknown'|variable_revision_number:4|show_window:False|notes:[]|batch_state:array([], dtype=uint8)|enabled:False|wants_pause:False]

Display outlines on a blank image?:No

Select image on which to display outlines:DO2

Name the output image:Overlay_objects_Cy3

Outline display mode:Color

Select method to determine brightness of outlines:Max of image

How to outline:Inner

Select outline color:blue

Select objects to display:Cytoplasma_expanded_object

Select outline color:#FF8040

Select objects to display:cy3_objects

OverlayOutlines:[module_num:18|svn_version:'Unknown'|variable_revision_number:4|show_window:False|notes:[]|batch_state:array([], dtype=uint8)|enabled:False|wants_pause:False]

Display outlines on a blank image?:No

Select image on which to display outlines:DO3

Name the output image:Overlay_objects_Cy5

Outline display mode:Color

Select method to determine brightness of outlines:Max of image

How to outline:Inner

Select outline color:blue

Select objects to display:Cytoplasma_expanded_object

Select outline color:red

Select objects to display:cy5_objects

OverlayOutlines:[module_num:19|svn_version:'Unknown'|variable_revision_number:4|show_window:False|notes:['Visualization of results: show object outlines of parents (cell border) and children (FITC, Cy3, and Cy5 blobs) on nucleus_raw_image']|batch_state:array([], dtype=uint8)|enabled:False|wants_pause:False]

Display outlines on a blank image?:No

Select image on which to display outlines:DO4

Name the output image:Overlay_objects_FITC

Outline display mode:Color

Select method to determine brightness of outlines:Max of image

How to outline:Inner

Select outline color:blue

Select objects to display:Cytoplasma_expanded_object

Select outline color:green

Select objects to display:fitc_objects

MeasureObjectIntensity:[module_num:20|svn_version:'Unknown'|variable_revision_number:4|show_window:False|notes:['Measure intensity of cy7 objects']|batch_state:array([], dtype=uint8)|enabled:True|wants_pause:False]

Select images to measure:DO1_subtracted

Select objects to measure:cy7_objects

MeasureObjectIntensity:[module_num:21|svn_version:'Unknown'|variable_revision_number:4|show_window:False|notes:['Measure intensity of cy3 objects']|batch_state:array([], dtype=uint8)|enabled:True|wants_pause:False]

Select images to measure:DO2_subtracted

Select objects to measure:cy3_objects

MeasureObjectIntensity:[module_num:22|svn_version:'Unknown'|variable_revision_number:4|show_window:False|notes:['Measure intensity of cy5 objects']|batch_state:array([], dtype=uint8)|enabled:True|wants_pause:False]

Select images to measure:DO3_subtracted

Select objects to measure:cy5_objects

MeasureObjectIntensity:[module_num:23|svn_version:'Unknown'|variable_revision_number:4|show_window:False|notes:['Measure intensity of fitc objects']|batch_state:array([], dtype=uint8)|enabled:True|wants_pause:False]

Select images to measure:DO4_subtracted

Select objects to measure:fitc_objects

SaveImages:[module_num:24|svn_version:'Unknown'|variable_revision_number:16|show_window:False|notes:['save the image showing object outlines of parents (cell border) and children on nucleus_raw_image', '', '!!! CHANGE OUTPUT FOLDER']|batch_state:array([], dtype=uint8)|enabled:False|wants_pause:False]

Select the type of image to save:Image

Select the image to save:Overlay_objects_Cy3

Select method for constructing file names:Sequential numbers

Select image name for file prefix:None

Enter file prefix:Overlay_objects_Cy3

Number of digits:0

Append a suffix to the image file name?:No

Text to append to the image name:

Saved file format:tiff

Output file location:Elsewhere...|W:\\Analysis\\Katja Sallinger\\34KS\\Intensity calculation\\Cellprofiler results 2\\images

Image bit depth:8-bit integer

Overwrite existing files without warning?:Yes

When to save:Every cycle

Record the file and path information to the saved image?:No

Create subfolders in the output folder?:No

Base image folder:Elsewhere...|

How to save the series:T (Time)

Save with lossless compression?:No

SaveImages:[module_num:25|svn_version:'Unknown'|variable_revision_number:16|show_window:False|notes:['save the image showing all object outlines on nucleus_raw_image.', '', '!!! CHANGE OUTPUT FOLDER']|batch_state:array([], dtype=uint8)|enabled:False|wants_pause:False]

Select the type of image to save:Image

Select the image to save:Overlay_objects_Cy5

Select method for constructing file names:Sequential numbers

Select image name for file prefix:None

Enter file prefix:overlay_objects_Cy5

Number of digits:0

Append a suffix to the image file name?:No

Text to append to the image name:

Saved file format:tiff

Output file location:Elsewhere...|W:\\Analysis\\Katja Sallinger\\34KS\\Intensity calculation\\Cellprofiler results 2\\images

Image bit depth:8-bit integer

Overwrite existing files without warning?:No

When to save:Every cycle

Record the file and path information to the saved image?:No

Create subfolders in the output folder?:No

Base image folder:Elsewhere...|

How to save the series:T (Time)

Save with lossless compression?:No

SaveImages:[module_num:26|svn_version:'Unknown'|variable_revision_number:16|show_window:False|notes:[]|batch_state:array([], dtype=uint8)|enabled:False|wants_pause:False]

Select the type of image to save:Image

Select the image to save:Overlay_objects_Cy7

Select method for constructing file names:Sequential numbers

Select image name for file prefix:None

Enter file prefix:overlay_objects_Cy7

Number of digits:0

Append a suffix to the image file name?:No

Text to append to the image name:

Saved file format:tiff

Output file location:Elsewhere...|W:\\Analysis\\Katja Sallinger\\34KS\\Intensity calculation\\Cellprofiler results 2\\images

Image bit depth:8-bit integer

Overwrite existing files without warning?:No

When to save:Every cycle

Record the file and path information to the saved image?:No

Create subfolders in the output folder?:No

Base image folder:Elsewhere...|

How to save the series:T (Time)

Save with lossless compression?:No

SaveImages:[module_num:27|svn_version:'Unknown'|variable_revision_number:16|show_window:False|notes:[]|batch_state:array([], dtype=uint8)|enabled:False|wants_pause:False]

Select the type of image to save:Image

Select the image to save:Overlay_objects_FITC

Select method for constructing file names:Sequential numbers

Select image name for file prefix:None

Enter file prefix:overlay_objects_FITC

Number of digits:0

Append a suffix to the image file name?:No

Text to append to the image name:

Saved file format:tiff

Output file location:Elsewhere...|W:\\Analysis\\Katja Sallinger\\34KS\\Intensity calculation\\Cellprofiler results 2\\images

Image bit depth:8-bit integer

Overwrite existing files without warning?:No

When to save:Every cycle

Record the file and path information to the saved image?:No

Create subfolders in the output folder?:No

Base image folder:Elsewhere...|

How to save the series:T (Time)

Save with lossless compression?:No

ExportToSpreadsheet:[module_num:28|svn_version:'Unknown'|variable_revision_number:13|show_window:False|notes:['Data will be saved in the chosen file location', '', 'Additionally it can be selected, which parameters are going to be saved! THis can be chosen under: Press button to select measurments']|batch_state:array([], dtype=uint8)|enabled:True|wants_pause:False]

Select the column delimiter:Tab

Add image metadata columns to your object data file?:No

Add image file and folder names to your object data file?:No

Select the measurements to export:Yes

Calculate the per-image mean values for object measurements?:Yes

Calculate the per-image median values for object measurements?:No

Calculate the per-image standard deviation values for object measurements?:No

Output file location:Elsewhere...|W:\\Analysis\\Katja Sallinger\\exp60KS\\203KS_AP1\\Multiplication factor

Create a GenePattern GCT file?:No

Select source of sample row name:Metadata

Select the image to use as the identifier:None

Select the metadata to use as the identifier:None

Export all measurement types?:No

Press button to select measurements:fitc_objects|Intensity_MedianIntensity_DO4_subtracted,fitc_objects|Intensity_MeanIntensity_DO4_subtracted,fitc_objects|Intensity_MaxIntensity_DO4_subtracted,cy7_objects|Intensity_MaxIntensity_DO1_subtracted,cy7_objects|Intensity_MeanIntensity_DO1_subtracted,cy7_objects|Intensity_MedianIntensity_DO1_subtracted,cy3_objects|Intensity_MeanIntensity_DO2_subtracted,cy3_objects|Intensity_MedianIntensity_DO2_subtracted,cy3_objects|Intensity_MaxIntensity_DO2_subtracted,cy5_objects|Intensity_MaxIntensity_DO3_subtracted,cy5_objects|Intensity_MeanIntensity_DO3_subtracted,cy5_objects|Intensity_MedianIntensity_DO3_subtracted

Representation of Nan/Inf:NaN

Add a prefix to file names?:Yes

Filename prefix:Intensity calculation_cycle1

Overwrite existing files without warning?:Yes

Data to export:Image

Combine these object measurements with those of the previous object?:No

File name:DATA.csv

Use the object name for the file name?:Yes

Data to export:cy3_objects

Combine these object measurements with those of the previous object?:No

File name:DATA.csv

Use the object name for the file name?:Yes

Data to export:Cytoplasma_expanded_object

Combine these object measurements with those of the previous object?:No

File name:DATA.csv

Use the object name for the file name?:Yes

Data to export:fitc_objects

Combine these object measurements with those of the previous object?:Yes

File name:DATA.csv

Use the object name for the file name?:Yes

Data to export:cy5_objects

Combine these object measurements with those of the previous object?:Yes

File name:DATA.csv

Use the object name for the file name?:Yes

Data to export:cy7_objects

Combine these object measurements with those of the previous object?:Yes

File name:DATA.csv

Use the object name for the file name?:Yes

### 6.6.2. Parts of the CellProfiler pipeline for dRNA-HybISS image analysis

To perform dRNA-HybISS image analysis the CellProfiler version 2 was used (Kamentsky et al., 2011).

CellProfiler Pipeline: http://www.cellprofiler.org

Version:2

DateRevision:20140723174500

GitHash:6c2d896

ModuleCount:74

HasImagePlaneDetails:False

.

.

.

ImageMath:[module_num:25|svn_version:\'Unknown\'|variable_revision_number:4|show_window:False|notes:\x5B\'For a second, more exact alignment, a Pseudo-Anchor stain of each cycle is generated and aligned with the Pseudo-General Stain of cycle one.\', \'Before generating the Pseudo-Anchor stain for each cycle, the background of each channel must be subtracted from all channels.\', \'This is done for each channel separatly. Additonaly, the multiplication factor, that was calculated before in a separate pipeline must be included for each channel. \', \'DO1= Cy7 of cycle\'\x5D|batch_state:array(\x5B\x5D, dtype=uint8)|enabled:True|wants_pause:False]

Operation:Subtract

Raise the power of the result by:1.0

Multiply the result by:10

Add to result:0.0

Set values less than 0 equal to 0?:Yes

Set values greater than 1 equal to 1?:Yes

Ignore the image masks?:No

Name the output image:DO1_subtracted

Image or measurement?:Image

Select the first image:DO1

Multiply the first image by:1.0

Measurement:

Image or measurement?:Image

Select the second image:BGDO1

Multiply the second image by:0

Measurement:

ImageMath:[module_num:26|svn_version:\'Unknown\'|variable_revision_number:4|show_window:False|notes:\x5B\'For a second, more exact alignment, a Pseudo-Anchor stain of each cycle is generated and aligned with the Pseudo-General Stain of cycle one.\', \'Before generating the Pseudo-Anchor stain for each cycle, the background of each channel must be subtracted from all channels.\', \'This is done for each channel separatly. Additonaly, the multiplication factor, that was calculated before in a separate pipeline must be included for each channel. \'\x5D|batch_state:array(\x5B\x5D, dtype=uint8)|enabled:True|wants_pause:False]

Operation:Subtract

Raise the power of the result by:1.0

Multiply the result by:5

Add to result:0.0

Set values less than 0 equal to 0?:Yes

Set values greater than 1 equal to 1?:Yes

Ignore the image masks?:No

Name the output image:DO2_subtracted

Image or measurement?:Image

Select the first image:DO2

Multiply the first image by:1

Measurement:

Image or measurement?:Image

Select the second image:BGDO2

Multiply the second image by:0

Measurement:

ImageMath:[module_num:27|svn_version:\'Unknown\'|variable_revision_number:4|show_window:False|notes:\x5B\'For a second, more exact alignment, a Pseudo-Anchor stain of each cycle is generated and aligned with the Pseudo-General Stain of cycle one.\', \'Before generating the Pseudo-Anchor stain for each cycle, the background of each channel must be subtracted from all channels.\', \'This is done for each channel separatly. Additonaly, the multiplication factor, that was calculated before in a separate pipeline must be included for each channel. \'\x5D|batch_state:array(\x5B\x5D, dtype=uint8)|enabled:True|wants_pause:False]

Operation:Subtract

Raise the power of the result by:1.0

Multiply the result by:8

Add to result:0.0

Set values less than 0 equal to 0?:Yes

Set values greater than 1 equal to 1?:Yes

Ignore the image masks?:No

Name the output image:DO3_subtracted

Image or measurement?:Image

:DO3

:1.0

Measurement:

Image or measurement?:Image

:BGDO3

:0

Measurement:

ImageMath:[module_num:28|svn_version:\'Unknown\'|variable_revision_number:4|show_window:False|notes:\x5B\'For a second, more exact alignment, a Pseudo-Anchor stain of each cycle is generated and aligned with the Pseudo-General Stain of cycle one.\', \'Before generating the Pseudo-Anchor stain for each cycle, the background of each channel must be subtracted from all channels.\', \'This is done for each channel separatly. Additonaly, the multiplication factor, that was calculated before in a separate pipeline must be included for each channel. \'\x5D|batch_state:array(\x5B\x5D, dtype=uint8)|enabled:True|wants_pause:False]

Operation:Subtract

Raise the power of the result by:1.0

Multiply the result by:5

Add to result:0.0

Set values less than 0 equal to 0?:Yes

Set values greater than 1 equal to 1?:Yes

Ignore the image masks?:No

Name the output image:DO4_subtracted

Image or measurement?:Image

:Extra_CHO4

:1.0

Measurement:

Image or measurement?:Image

:BGDO4

:0

Measurement:

EnhanceOrSuppressFeatures:[module_num:29|svn_version:\'Unknown\'|variable_revision_number:4|show_window:False|notes:\x5B\'Signales (speckles) with a feature size of 10 are enhanced.\', \'This, again, is done for each channel separatly.\'\x5D|batch_state:array(\x5B\x5D, dtype=uint8)|enabled:True|wants_pause:False]

Select the input image:DO1_subtracted

Name the output image:Enhanced_A

Select the operation:Enhance

Feature size:10

Feature type:Speckles

Range of hole sizes:1,10

Smoothing scale:2.0

Shear angle:0

Decay:.95

Enhancement method:Line structures

EnhanceOrSuppressFeatures:[module_num:30|svn_version:\'Unknown\'|variable_revision_number:4|show_window:False|notes:\x5B\'Signales (speckles) with a feature size of 10 are enhanced.\', \'This, again, is done for each channel separatly.\'\x5D|batch_state:array(\x5B\x5D, dtype=uint8)|enabled:True|wants_pause:False]

Select the input image:DO2_subtracted

Name the output image:Enhanced_C

Select the operation:Enhance

Feature size:10

Feature type:Speckles

Range of hole sizes:1,10

Smoothing scale:2.0

Shear angle:0

Decay:.95

Enhancement method:Line structures

EnhanceOrSuppressFeatures:[module_num:31|svn_version:\'Unknown\'|variable_revision_number:4|show_window:False|notes:\x5B\'Signales (speckles) with a feature size of 10 are enhanced.\', \'This, again, is done for each channel separatly.\'\x5D|batch_state:array(\x5B\x5D, dtype=uint8)|enabled:True|wants_pause:False]

Select the input image:DO3_subtracted

Name the output image:Enhanced_G

Select the operation:Enhance

Feature size:10

Feature type:Speckles

Range of hole sizes:1,10

Smoothing scale:2.0

Shear angle:0

Decay:.95

Enhancement method:Line structures

EnhanceOrSuppressFeatures:[module_num:32|svn_version:\'Unknown\'|variable_revision_number:4|show_window:False|notes:\x5B\'Signales (speckles) with a feature size of 10 are enhanced.\', \'This, again, is done for each channel separatly.\'\x5D|batch_state:array(\x5B\x5D, dtype=uint8)|enabled:True|wants_pause:False]

Select the input image:DO4_subtracted

Name the output image:Enhanced_T

Select the operation:Enhance

Feature size:10

Feature type:Speckles

Range of hole sizes:1,10

Smoothing scale:2.0

Shear angle:0

Decay:.95

Enhancement method:Line structures

EnhanceOrSuppressFeatures:[module_num:33|svn_version:\'Unknown\'|variable_revision_number:4|show_window:False|notes:\x5B\x5D|batch_state:array(\x5B\x5D, dtype=uint8)|enabled:False|wants_pause:False]

Select the input image:Spec_blob

Name the output image:Enhanced_SpecBlob

Select the operation:Enhance

Feature size:10

Feature type:Speckles

Range of hole sizes:1,10

Smoothing scale:2.0

Shear angle:0

Decay:.95

Enhancement method:Line structures

## 6.7. Preliminary data: Detection efficiency

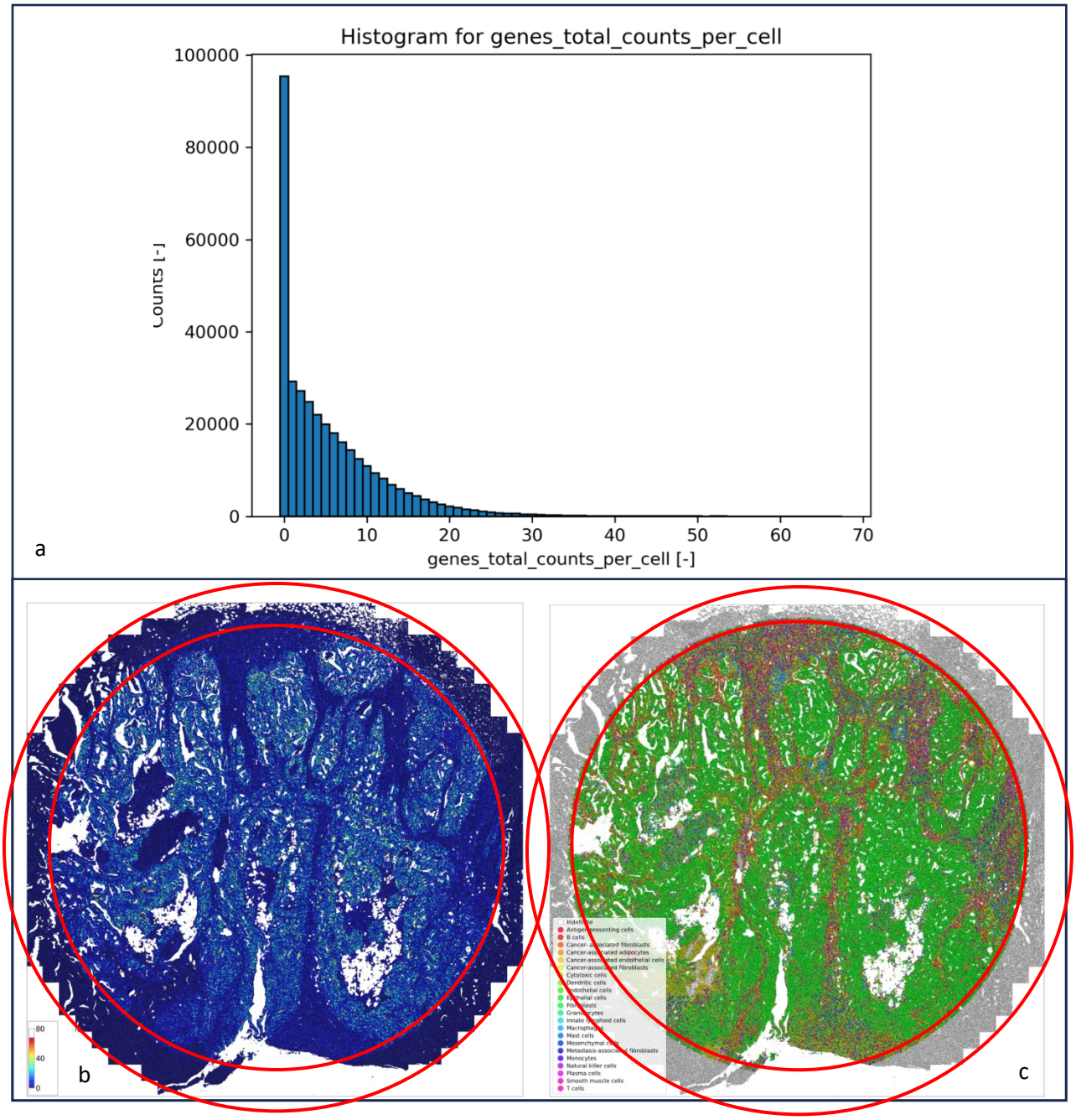


***Supplementary figure 1: Detection efficiency of one patient sample calculated by GTC-tool 2.***

*a) depicts a barplot of the total transcript counts per cell ranging from 0-25. It's crucial to mention the overrepresentation of cells with 0 transcripts, primarily situated in the circular border adjacent to the secure seal (highlighted in red in figures b (dark blue cells) and c (grey cells)).This area is consistently excluded from analysis by the GTC-tool, due to potential tissue detachment from seal removal. While transcripts in this area have been excluded in GTC-tool 2, the cells have not, leading to an incorrect display of 0 transcripts for these cells. b) shows the total counts per cell varying from 0, represented in dark blue, to approximately 25, shown in light blue. c) shows preliminary data of cell-phenotyping analysis, which is still under development, using the pathway panel.*

## 6.8. Gene panels for dRNA-HybISS analysis

### 6.8.1. Immune panel I: Immune General I1A 0.2

***Supplementary table 1: Immune panel I***

| Celltype/function | Gene (according to Human protein atlas [1,2]) | ENS number (derived from Ensembl genome browser) |
|---|---|---|
| hematopoietic lineage | PTPRC | ENSG00000081237 |
| hematopoietic stem cells and endothelial cells | CD34 | ENSG00000174059 |
| antigen presenting cells (APC) | CD40 | ENSG00000101017 |
| antigen presenting cells (APC) | CD80 | ENSG00000121594 |
| macrophages and monocytes | FCGR1A | ENSG00000150337 |
| monocytes | S100A8 | ENSG00000143546 |
| CD14+ monocytes | CD14 | ENSG00000170458 |
| CD16+ monocytes | FCGR3A | ENSG00000203747 |
| mast cells | MS4A2 | ENSG00000149534 |
| mast cells | TPSAB1 | ENSG00000172236 |
| macrophages | APOE | ENSG00000130203 |
| macrophages | C1QA | ENSG00000173372 |
| macrophages | C1QB | ENSG00000173369 |
| macrophages | CD163 | ENSG00000177575 |
| macrophages | CD68 | ENSG00000129226 |
| resident macrophages | FOLR2 | ENSG00000165457 |
| granulocytes | CEACAM8 | ENSG00000124469 |
| neutrohpils and eosinophils | FUT4 | ENSG00000196371 |
| dendritic cells (DC) | CD209 | ENSG00000090659 |
| dendritic cells (DC) | ITGAX | ENSG00000140678 |
| type 1 dendritic cells (DC1) | CLEC9A | ENSG00000197992 |
| type 2 dendritic cells (DC2) | CD1C | ENSG00000158481 |
| type 2 dendritic cells (DC2) | CLEC10A | ENSG00000132514 |
| IDO1+ myeloid dendritic cells (mDC) | IDO1 | ENSG00000131203 |
| innate lymphoid cells (ILC) | LST1 | ENSG00000204482 |
| natural killer (NK) cells | CD7 | ENSG00000173762 |
| natural killer (NK) cells | KLRC2 | ENSG00000205809 |
| natural killer (NK) cells | KLRD1 | ENSG00000134539 |
| natural killer (NK) cells | TYROBP | ENSG00000011600 |
| natural killer (NK) cells/ NKT cells | NKG7 | ENSG00000105374 |
| T cells | CD3D | ENSG00000167286 |
| T cells | CD3E | ENSG00000198851 |
| T cells | CD3G | ENSG00000160654 |
| T cells, T cell activation | CD28 | ENSG00000178562 |

| | | |
|---|---|---|
| CD4+ T cells | CD4 | ENSG00000010610 |
| CD8+ T cells | CD8A | ENSG00000153563 |
| CD8+ T cells | CD8B | ENSG00000172116 |
| human Th1 effector | IL2RA | ENSG00000134460 |
| mucosal-associated invariant T cells (MAIT) | KLRB1 | ENSG00000111796 |
| regulatory T cells (Treg) | FOXP3 | ENSG00000049768 |
| type 1 T helper cells (Th1) | CXCR3 | ENSG00000186810 |
| type 2 T helper cells (Th2) | CCR4 | ENSG00000183813 |
| mucosal-targeted plasma cells | JCHAIN | ENSG00000132465 |
| memory cells | GPR183 | ENSG00000169508 |
| B cells | CD19 | ENSG00000177455 |
| B cells | CD79A | ENSG00000105369 |
| B cells | CD79B | ENSG00000007312 |
| B cells | MS4A1 | ENSG00000156738 |
| plasma cells | IGKC | ENSG00000211592 |

### 6.8.2. Immune panel II: Immune Oncology I2B 0.2

***Supplementary table 2: Immune panel II***

| Celltype/function | Gene (according to Human protein atlas) | ENS number (derived from Ensembl genome browser) |
|---|---|---|
| endothelial cells | PECAM1 | ENSG00000261371 |
| epithelial cells | EPCAM | ENSG00000119888 |
| epithelial cells | CDH1 | ENSG00000039068 |
| fibroblasts | COL6A1 | ENSG00000142156 |
| mesenchymal cells | VIM | ENSG00000026025 |
| smooth muscle cells | ACTA2 | ENSG00000107796 |
| angiogenesis | PDGFRA | ENSG00000134853 |
| angiogenesis | PDGFRB | ENSG00000113721 |
| angiogenesis | VEGFA | ENSG00000112715 |
| apoptosis | BCL2 | ENSG00000171791 |
| apoptosis | CTSD | ENSG00000117984 |
| apoptosis | FAS | ENSG00000026103 |
| epithelial to mesenchymal transition (EMT) | CDH2 | ENSG00000170558 |
| epithelial to mesenchymal transition (EMT) | SNAI1 | ENSG00000124216 |
| epithelial to mesenchymal transition (EMT) | SNAI2 | ENSG00000019549 |
| epithelial to mesenchymal transition (EMT) | ZEB2 | ENSG00000169554 |
| extracellular matrix (ECM) remodeling | MMP9 | ENSG00000100985 |
| cancer-associated fibroblasts | FAP | ENSG00000078098 |
| metastasis-associated fibroblasts | CXCR4 | ENSG00000121966 |
| co-stimulatory checkpoint molecule, activated T cells | ICOS | ENSG00000163600 |
| immune checkpoint | CD27 | ENSG00000139193 |
| immune checkpoint | CTLA4 | ENSG00000163599 |
| immune checkpoint | PDCD1 | ENSG00000188389 |
| immune checkpoint | TIGIT | ENSG00000181847 |

| | | |
|---|---|---|
| Immune checkpoint, stimulate or inhibit cytotoxic activity of NK cells | KLRC1 | ENSG00000134545 |
| immune checkpoint, T cell activation | LAG3 | ENSG00000089692 |
| immune checkpoint, Th1 response, exhausted T cells | HAVCR2 | ENSG00000135077 |
| PD-1 ligand | CD274 | ENSG00000120217 |
| PD-1 ligand 2 | PDCD1LG2 | ENSG00000197646 |
| TIGIT co-stimulatory molecule | CD226 | ENSG00000150637 |
| anti-inflammation, Treg and monocyte effector, immunosupression | IL10 | ENSG00000136634 |
| chemotactic for immune cells | CCL5 | ENSG00000271503 |
| induced by inflammatory stimuli, immune cell recruiting signal | CCL2 | ENSG00000108691 |
| cytotoxic cells | GNLY | ENSG00000115523 |
| cytotoxic cells | GZMA | ENSG00000145649 |
| cytotoxic cells | GZMB | ENSG00000100453 |
| cytotoxic cells | GZMH | ENSG00000100450 |
| cytotoxic cells | GZMK | ENSG00000113088 |
| cytotoxic cells | PRF1 | ENSG00000180644 |
| cell cycle | STMN1 | ENSG00000117632 |
| proliferation | MKI67 | ENSG00000148773 |
| self-renewal | MYC | ENSG00000136997 |
| cell survival | CD74 | ENSG00000019582 |
| immune escape, diverse functions | CD24 | ENSG00000272398 |
| immunosuppression | ARG1 | ENSG00000118520 |
| immunosuppression | ENTPD1 | ENSG00000138185 |
| macropahges, myeloid-derived suppressor cells (MDSC) | CSF1R | ENSG00000182578 |
| T cell recruiting signal | CXCL10 | ENSG00000169245 |
| T cell recruiting signal | CXCL11 | ENSG00000169248 |
| T cell recruiting signal | CXCL9 | ENSG00000138755 |
| Treg effector, immunosupression | TGFB1 | ENSG00000105329 |
| T cell exhaustion | CD244 | ENSG00000122223 |
| T cell exhaustion | CD38 | ENSG00000004468 |

## 6.9. P-values of statistical testing of relapsed versus non-relapsed patients

***Supplementary table 3: The resulting p-values for the statistical testing of relapse and non-relapse patients with the neoplastic tissue compartments.***

| genes | p-value | mean relapse patients | mean non-relapse patients |
|---|---|---|---|
| ADGRA2 | 0.4380 | 0.0017 | 0.0013 |
| ALDH1A1 | 0.9271 | 0.0021 | 0.0019 |
| ANGPT1 | 0.9514 | 0.0010 | 0.0010 |
| ANGPT2 | 0.2625 | 0.0104 | 0.0040 |
| ANPEP | 0.5374 | 0.0021 | 0.0034 |
| ANTXR1 | 0.5995 | 0.0764 | 0.0673 |
| ATG5 | 0.4726 | 0.0041 | 0.0029 |
| AURKA | 0.7366 | 0.0092 | 0.0083 |
| BAK1 | 0.9219 | 0.0087 | 0.0084 |
| BBC3 | 0.8933 | 0.0893 | 0.0937 |
| BCL2L1 | 0.1268 | 0.0601 | 0.0360 |
| BCL2L11 | 0.7712 | 0.0039 | 0.0041 |
| BECN1 | 0.6856 | 0.0043 | 0.0036 |
| BEST4 | 0.3816 | 0.0058 | 0.0046 |
| BGN | 0.5344 | 0.0093 | 0.0065 |
| BID | 0.2140 | 0.0429 | 0.0200 |
| BIK | 0.4501 | 0.0260 | 0.0188 |
| BMI1 | 0.3415 | 0.0084 | 0.0020 |
| BOP1 | 0.8287 | 0.0327 | 0.0366 |
| BTG2 | 0.1062 | 0.0519 | 0.0287 |
| BTLA | 0.4055 | 0.0005 | 0.0006 |
| CA1 | 0.3870 | 0.0022 | 0.0017 |
| CA2 | 0.5645 | 0.0012 | 0.0017 |
| CASP3 | 0.0700 | 0.0100 | 0.0057 |
| CASP7 | 0.0682 | 0.0609 | 0.0210 |

| | | | |
|---|---|---|---|
| CASP8 | 0.5583 | 0.0034 | 0.0024 |
| CASP9 | 0.2590 | 0.0041 | 0.0028 |
| CAT | 0.8154 | 0.0054 | 0.0050 |
| CCND1 | 0.8206 | 0.0243 | 0.0207 |
| CCNE1 | 0.5620 | 0.0411 | 0.0279 |
| CD248 | 0.4689 | 0.0030 | 0.0037 |
| CD44 | 0.9015 | 0.0186 | 0.0196 |
| CD80 | 0.6438 | 0.0001 | 0.0001 |
| CD83 | 0.5719 | 0.0016 | 0.0018 |
| CD86 | 0.0738 | 0.0011 | 0.0006 |
| CDH5 | 0.2937 | 0.0026 | 0.0019 |
| CFLAR | 0.2040 | 0.0032 | 0.0008 |
| CHGA | 0.1433 | 0.0076 | 0.0038 |
| CNTD2 | 0.5664 | 0.0091 | 0.0124 |
| COL1A2 | 0.6891 | 0.1772 | 0.1424 |
| CSPG4 | 0.3571 | 0.0077 | 0.0057 |
| CXCL1 | 0.2984 | 0.0069 | 0.0042 |
| CXCL12 | 0.8857 | 0.0076 | 0.0073 |
| CXCL8 | 0.4133 | 0.0058 | 0.0039 |
| DCLK1 | 0.2134 | 0.0012 | 0.0008 |
| DCN | 0.7197 | 0.0016 | 0.0018 |
| E2F1 | 0.8938 | 0.0094 | 0.0088 |
| EGFR | 0.3622 | 0.0165 | 0.0109 |
| EGLN3 | 0.2134 | 0.0066 | 0.0125 |
| ENAH | 0.2609 | 0.0263 | 0.0400 |
| ENG | 0.6169 | 0.0630 | 0.0534 |
| ENTPD1 | 0.4883 | 0.0013 | 0.0049 |
| EPHB2 | 0.1347 | 0.0030 | 0.0017 |
| EREG | 0.2798 | 0.0085 | 0.0037 |
| EXOSC5 | 0.5477 | 0.0307 | 0.0241 |
| F8 | 0.5569 | 0.0041 | 0.0027 |
| FABP1 | 0.1063 | 0.3312 | 0.1101 |
| FABP4 | 0.2537 | 0.0015 | 0.0006 |

| | | | |
|---|---|---|---|
| FAM3C | 0.5082 | 0.0042 | 0.0033 |
| FGFR2 | 0.0137 | 0.0049 | 0.0031 |
| FLT4 | 0.3144 | 0.0252 | 0.0179 |
| FN1 | 0.2072 | 0.0830 | 0.0256 |
| FOXC2 | 0.1784 | 0.0009 | 0.0006 |
| FRK | 0.7101 | 0.0015 | 0.0014 |
| FSTL1 | 0.7359 | 0.0068 | 0.0063 |
| GADD45B | 0.3688 | 0.0076 | 0.0062 |
| GAST | 0.0856 | 0.0046 | 0.0032 |
| GFI1B | 0.4393 | 0.0023 | 0.0014 |
| GIP | 0.1603 | 0.0011 | 0.0007 |
| GLS | 0.5713 | 0.0131 | 0.0104 |
| GLUD1 | 0.6640 | 0.0028 | 0.0032 |
| GPX1 | 0.6236 | 0.0280 | 0.0229 |
| GRB7 | 0.2775 | 0.0115 | 0.0026 |
| GSR | 0.6764 | 0.0213 | 0.0176 |
| GUCA2B | 0.2908 | 0.0024 | 0.0012 |
| HIF1A | 0.7241 | 0.0043 | 0.0048 |
| HIF3A | 0.1704 | 0.0037 | 0.0020 |
| HK1 | 0.4892 | 0.0145 | 0.0115 |
| HK2 | 0.5087 | 0.0157 | 0.0117 |
| HMGB1 | 0.3301 | 0.0080 | 0.0023 |
| HYOU1 | 0.4569 | 0.0457 | 0.0344 |
| ICAM1 | 0.7122 | 0.0051 | 0.0044 |
| IDO2 | 0.1770 | 0.0009 | 0.0004 |
| IGFBP2 | 0.7922 | 0.0483 | 0.0441 |
| IL11 | 0.3020 | 0.0034 | 0.0027 |
| IL1B | 0.1749 | 0.0265 | 0.0187 |
| IL6 | 0.3527 | 0.0019 | 0.0009 |
| IL7R | 0.4805 | 0.0017 | 0.0015 |
| INHBA | 0.9982 | 0.0038 | 0.0038 |
| ITGAM | 0.8851 | 0.0022 | 0.0021 |
| ITGAV | 0.6371 | 0.0158 | 0.0126 |

| | | | |
|---|---|---|---|
| ITGAX | 0.3278 | 0.0010 | 0.0005 |
| KDR | 0.7293 | 0.0027 | 0.0024 |
| KIT | 0.4801 | 0.0010 | 0.0005 |
| KLF4 | 0.1445 | 0.2326 | 0.0777 |
| KLRK1 | 0.8630 | 0.0007 | 0.0007 |
| L1CAM | 0.1590 | 0.0040 | 0.0031 |
| LAMC2 | 0.5822 | 0.0051 | 0.0078 |
| LDHA | 0.1784 | 0.0052 | 0.0081 |
| LGR5 | 0.7745 | 0.0043 | 0.0038 |
| LIF | 0.3691 | 0.0055 | 0.0034 |
| MAP1LC3A | 0.6020 | 0.0214 | 0.0168 |
| MCL1 | 0.3200 | 0.0178 | 0.0114 |
| MCM2 | 0.4943 | 0.0118 | 0.0084 |
| MET | 0.4367 | 0.0327 | 0.0499 |
| MICA | 0.4789 | 0.0023 | 0.0030 |
| MICB | 0.2659 | 0.0157 | 0.0062 |
| MIEN1 | 0.1606 | 0.0099 | 0.0029 |
| MLKL | 0.9694 | 0.0375 | 0.0370 |
| MLN | 0.2325 | 0.0053 | 0.0019 |
| MMP11 | 0.0415 | 0.0492 | 0.0164 |
| MMP2 | 0.8319 | 0.0019 | 0.0021 |
| MMP7 | 0.8832 | 0.0061 | 0.0068 |
| MPL | 0.1839 | 0.0010 | 0.0006 |
| MUC2 | 0.2674 | 0.0124 | 0.0080 |
| MUC5AC | 0.2946 | 0.0008 | 0.0005 |
| MYBL2 | 0.4202 | 0.0091 | 0.0057 |
| NANOG | 0.2675 | 0.0042 | 0.0024 |
| NCAM1 | 0.6225 | 0.0117 | 0.0106 |
| NCR1 | 0.7844 | 0.0010 | 0.0010 |
| NOS1 | 0.4461 | 0.0129 | 0.0102 |
| NOS2 | 0.6146 | 0.0076 | 0.0109 |
| NT5E | 0.8994 | 0.0027 | 0.0025 |
| NTS | 0.3922 | 0.0013 | 0.0008 |

| | | | |
|---|---|---|---|
| OLFM4 | 0.6367 | 0.0911 | 0.1395 |
| OSER1 | 0.4527 | 0.0102 | 0.0069 |
| OTOP2 | 0.0043 | 0.0026 | 0.0019 |
| PCNA | 0.5341 | 0.0125 | 0.0077 |
| PDGFA | 0.1237 | 0.0302 | 0.0157 |
| PDK1 | 0.4882 | 0.0024 | 0.0032 |
| PKM | 0.7688 | 0.0922 | 0.0817 |
| PLXDC1 | 0.5181 | 0.0062 | 0.0051 |
| POU2F3 | 0.5070 | 0.1033 | 0.0636 |
| POU5F1 | 0.5592 | 0.5020 | 0.3878 |
| PPIF | 0.3442 | 0.0056 | 0.0035 |
| PRDX2 | 0.7580 | 0.1062 | 0.0872 |
| PRF1 | 0.2779 | 0.0005 | 0.0011 |
| PROM1 | 0.0792 | 0.0086 | 0.0026 |
| PYY | 0.3809 | 0.0027 | 0.0019 |
| RIPK1 | 0.7866 | 0.0047 | 0.0051 |
| RIPK3 | 0.2560 | 0.0153 | 0.0115 |
| RPS6KB1 | 0.5633 | 0.0004 | 0.0008 |
| S100A4 | 0.0645 | 0.0308 | 0.0118 |
| SAAL1 | 0.3395 | 0.0018 | 0.0011 |
| SALL4 | 0.6568 | 0.0019 | 0.0023 |
| SCAI | 0.1913 | 0.0047 | 0.0026 |
| SLC26A3 | 0.9402 | 0.1045 | 0.1083 |
| SLC2A1 | 0.3493 | 0.0006 | 0.0004 |
| SOD1 | 0.9646 | 0.0983 | 0.0971 |
| SOX2 | 0.8878 | 0.0138 | 0.0131 |
| SPDEF | 0.2998 | 0.0039 | 0.0023 |
| SST | 0.5133 | 0.0011 | 0.0007 |
| TAGLN | 0.1000 | 0.0039 | 0.0015 |
| TBXT | 0.4052 | 0.0027 | 0.0012 |
| TEK | 0.9708 | 0.0005 | 0.0005 |
| TFF1 | 0.5438 | 0.0092 | 0.0134 |
| TFF3 | 0.4431 | 0.0703 | 0.0396 |

| | | | |
|---|---|---|---|
| TGFA | 0.1879 | 0.0057 | 0.0034 |
| TGFB3 | 0.9421 | 0.0032 | 0.0033 |
| THY1 | 0.6415 | 0.0036 | 0.0030 |
| TIAM1 | 0.2424 | 0.0009 | 0.0006 |
| TIE1 | 0.2877 | 0.0013 | 0.0010 |
| TIMP1 | 0.9941 | 0.0257 | 0.0256 |
| TJP1 | 0.4679 | 0.0133 | 0.0079 |
| TNC | 0.8990 | 0.0073 | 0.0068 |
| TNF | 0.5561 | 0.0010 | 0.0006 |
| TNFRSF10A | 0.4299 | 0.0071 | 0.0035 |
| TNFRSF10B | 0.3869 | 0.0028 | 0.0041 |
| TNFSF10 | 0.8549 | 0.0077 | 0.0071 |
| TRPM5 | 0.3110 | 0.0058 | 0.0025 |
| TWIST1 | 0.5346 | 0.0256 | 0.0212 |
| TXNL1 | 0.3908 | 0.0069 | 0.0049 |
| URGCP | 0.5626 | 0.0002 | 0.0004 |
| VCAM1 | 0.9583 | 0.0007 | 0.0007 |
| ZEB1 | 0.2654 | 0.0014 | 0.0007 |
| ZGLP1 | 0.3593 | 0.0026 | 0.0046 |

## 6.10. List of materials

***Supplementary table 4: List of reagents, buffers, solutions, and kits***

| Reagents, buffer, solutions, kits | Company / Catalog number |
|---|---|
| AP mix (1-6) | CARTANA Stockholm, Sweden, now 10x Genomics, Pleasanton, California, |
| Buffer A | CARTANA Stockholm, Sweden, now 10x Genomics, Pleasanton, California, |
| DEPC | Sigma-Aldrich, Vienna, Austria / D5758 |
| Distilled Water (Gibco) | Thermo Fisher Scientific, Waltham, MA, USA / 1523014 |
| Enzyme 1 | CARTANA Stockholm, Sweden, now 10x Genomics, Pleasanton, California, |
| Enzyme 2 | CARTANA Stockholm, Sweden, now 10x Genomics, Pleasanton, California, |
| Enzyme 3 | CARTANA Stockholm, Sweden, now 10x Genomics, Pleasanton, California, |
| Eosin | (Merck, Darmstadt, Germany) |
| Ethanol | Sigma-Aldrich, Vienna, Austria / 1.0083.5000 |
| Formamide 100% | Sigma-Aldrich, Vienna, Austria / F9037 |
| Histolab-Clear (Tissue clear) | Sanova Pharma, Vienna, Austria / 11070 |
| Immune panel I1A | CARTANA Stockholm, Sweden, now 10x Genomics, Pleasanton, California, |
| Immune panel I1B | CARTANA Stockholm, Sweden, now 10x Genomics, Pleasanton, California, |
| Mayer's hematoxylin | Merck, Darmstadt, Germany |
| Nuclease-Free Water | Thermo Fisher Scientific, Waltham, MA, USA / AM9930 |
| Pathway gene panel (designed at the Division of Cell Biology, Histology and Embryology, Gottfried Schatz Research Centre, Medical University of Graz, Graz, Austria, in collaboration with Olga Surova and Jessica Svedlund, Science for Life Laboratory, Department of Biochemistry and Biophysics, Stockholm University, 17165, Solna, Sweden) | CARTANA Stockholm, Sweden, now 10x Genomics, Pleasanton, California, |
| RM1 | CARTANA Stockholm, Sweden, now 10x Genomics, Pleasanton, California, |
| RM2 | CARTANA Stockholm, Sweden, now 10x Genomics, Pleasanton, California, |
| RM3 | CARTANA Stockholm, Sweden, now 10x Genomics, Pleasanton, California, |
| SlowFade Gold Antifade Mountant | Thermo Fisher Scientific, Waltham, MA, USA / S36936 |
| SP mix | CARTANA Stockholm, Sweden, now 10x Genomics, Pleasanton, California, |
| Tissue-Tek Glass tissue mount | Sakura Finetek, Umkirch, Germany / 94-1408N |

| | |
|---|---|
| Tween-20 | Sigma-Aldrich, Vienna, Austria / 822184 |
| WB 2 | CARTANA Stockholm, Sweden, now 10x Genomics, Pleasanton, California, |
| WB 3 | CARTANA Stockholm, Sweden, now 10x Genomics, Pleasanton, California, |
| WB 4 | CARTANA Stockholm, Sweden, now 10x Genomics, Pleasanton, California, |
| **Consumables** | **Company / Catalog number** |
| Centrifuge Tubes (15 ml) | VWR, Vienna, Austria / 525-0401 |
| ep Dualfilter T.I.P.S., 0.1-10 µl | Eppendorf Austria, Vienna, Austria / 0030077504 |
| ep Dualfilter T.I.P.S., 2-200 µl | Eppendorf Austria, Vienna, Austria / 0030077555 |
| ep Dualfilter T.I.P.S., 50-1000 µl | Eppendorf Austria, Vienna, Austria / 0030077571 |
| Eppendorf Tubes 3810X, 1.5 ml | Eppendorf Austria, Vienna, Austria / 0030125150 |
| epT.I.P.S. Standard, 0.1-10 µl | Eppendorf Austria, Vienna, Austria / 0030000811 |
| epT.I.P.S. Standard, 0.1-10 µl | Eppendorf Austria, Vienna, Austria / 0030000811 |
| epT.I.P.S. Standard, 2-200 µl | Eppendorf Austria, Vienna, Austria / 0030000870 |
| epT.I.P.S. Standard, 50-1000 µl | Eppendorf Austria, Vienna, Austria / 0030000919 |
| Microwave | Miele, Gütersloh, Deutschland |
| ReadyProbe Hydrophobic Barrier Pap Pen | Thermo Fisher Scientific, Waltham, MA, USA / R3777 |
| Secure-Seal hybridization chamber gasket, 9 mm diameter, 0.8 mm deep | Thermo Fisher Scientific, Waltham, MA, USA /S24732 |
| SuperFrost plus microscope slides | Thermo Fisher Scientific, Waltham, MA, USA / J1800AMNT |
| **Fluorescence microscope equipment** | **Company / Catalog number** |
| Slide scanner (Slideview VS200) | Evident, Tokio, Japan |
| LED source | Excelitas Technologies, X-Cite Xylis, Mississauga, Canada |
| Fluorescence filter cubes (pentafilter, excitations: 352-404 nm, 460-488 nm, 542-566 nm, 626-644 nm, 721-749 nm; emissions 416-452 nm, 500-530 nm, 579-611 nm, 665-705 nm, 767-849 nm) | AHF Analysetechnik, Tübingen, Deutschland |
| sCMOS camera (2304 × 2304, ORCA-Fusion C14440-20UP, 16bit) | Hamamatsu, Shizuoka, Japan / C15440-20UP |
| Olympus universal-plan super apochromat 40× (0.95 NA/air) | Evident, Tokio, Japan / N2246700 |
| **Software and online tools** | **Company** |
| CellProfiler image analysis software (V 2.1.1 & V 4.2.1) | Broad Institute of MIT and Harvard, Cambridge, MA, USA |
| MATLBAB (V R2020b) | MathWorks, Portola Valley, California, USA |
| Olympus VS200 Desktop Version | Evident, Tokio, Japan |